# HETEROGENEOUS CATALYSIS

## OF

# INORGANIC SUBSTITUTION REACTIONS

A Thesis submitted for the degree of

Doctor of Philosophy

of the

University of London

by

Mary Doreen Archer

Physical Chemistry Department,

Imperial College,

London, S.W.7.

October 1968.

## ABSTRACT

This research was suggested by scattered references
in the literature, surveyed in this thesis, to the
catalytic effects which many solids have upon homogeneous
substitution reactions. A systematic investigation of
the heterogeneous catalysis of slow inorganic substitution
reactions was accordingly undertaken.

The aquation of the acidopentamminecobalt(III) ions,
$[Co(NH_3)_5X]^{2+}$ (X=Cl or Br), was studied at 25°C and pH
2 or 3. Preliminary studies were carried out with a wide
variety of solids, such as metals and non-metallic elements,
insoluble salts and silicates.

The insoluble salts of silver(I) and mercury(II)
were found to be the most effective catalysts, which was
not unexpected, as Ag(I) and Hg(II) in solution induce
aquation of $[Co(NH_3)_5X]^{2+}$. Catalysis by silver bromide
and mercuric sulphide was studied quantitatively as a
function of the mass of catalyst and the concentration of
$[Co(NH_3)_5X]^{2+}$. The rate of the catalytic reaction was
controlled by equilibrium adsorption of $[Co(NH_3)_5X]^{2+}$
prior to reaction.

Platinum was also a catalyst for the aquation reaction,
and a platinum rotating disc was used to study reaction
kinetics in conditions of controlled diffusion, according
to the Levich equation, to the catalyst surface. Again,
the catalysis was surface-controlled, and subsidiary

experiments showed that the platinum potential affected catalytic efficiency.

A diffusion-controlled redox reaction between $[Co(NH_3)_5X]^{2+}$ and solid silver was discovered, and studied at 25°C and 0°C using a silver rotating disc.

Attempts were made to find a heterogeneous catalyst for the monoanation of hexaquochromium(III) by thiocyanate: although platinum, mercury and some heavy metal sulphides were found to be slight catalysts, the effects were too small for quantitative investigation. It was concluded that for a surface-controlled catalytic process to have a striking effect, the number of molecules reacting homogeneously must not be much greater than the number reacting heterogeneously: this restricts work to dilute solutions.

# ACKNOWLEDGEMENTS

## SYMBOLS AND ABBREVIATIONS.

| | |
|---|---|
| A | area |
| ads | adsorbed |
| c | molarity |
| D | optical density |
| $D_i$ | diffusion coefficient of species i |
| E | electromotive force |
| F | Faraday's constant |
| G | Gibbs free energy |
| H | Enthalpy |
| h | Planck's constant |
| het | heterogeneous |
| hom | homogeneous |
| I | ionic strength |
| K | equilibrium constant |
| k | velocity constant |
| $N_0$ | Avogadro's number |
| R | universal gas constant |
| T | absolute temperature |
| t | time |
| V | volume |
| $z_i$ | no. of units of electronic charge on ion i |

| | |
|---|---|
| $\delta$ | thickness of Nernst diffusion layer |
| $\epsilon$ | molar extinction coefficient |
| $\eta$ | viscosity |
| $\theta_i$ | degree of coverage of surface by species i |
| $\lambda$ | equivalent conductance |
| $\mu$ | micron ($m\mu$ = millimicron) |
| $\nu$ | rate of reaction |
| $\nu_s$ | kinematic viscosity |
| $\sigma$ | sticking probability |
| $\tau$ | time interval |
| $\omega$ | speed of rotation |

# CONTENTS.

CHAPTER                                          Page.

PART I


INTRODUCTION

# CHAPTER I : GENERAL CONSIDERATION OF CATALYTIC PHENOMENA.

A catalyst is a substance which increases the rate of a chemical reaction, without itself being chemically changed in the process, and without affecting the position of chemical equilibrium. Homogeneous and heterogeneous catalytic processes are extremely common in both gas-phase and liquid-phase systems. Catalysts are very widely used in industrial and laboratory preparative chemistry, and the extensive fundamental study of catalysis that has been carried out in this century perhaps reflects the practical importance of catalysts.

Work in the past has dealt mainly with heterogeneous catalysis of gas reactions and homogeneous catalysis of liquid reactions. The subject of this thesis, the heterogeneous catalysis of reactions occurring in solution, is practically a novel topic. The present work is restricted to catalysis at solid surfaces. Catalysis and reaction kinetics at liquid interfaces have been reviewed by Davies (1).

A catalyst acts by providing a reaction path of lower energy than is otherwise available to the reactants. In simple terms, it reduces the heat of activation, $\Delta H_a$, for the reaction, thus increasing the velocity constant, k, according to the Van't Hoff equation

$$\frac{d \ln k}{dT} = \frac{\Delta H_a}{RT^2} \qquad (1.1)$$

In the more detailed analysis of the theory of absolute reaction rates, since the rate at which activated complexes cross the energy barrier to reaction is the universal frequency $RT/N_0 h$, it is the steady-state concentration of activated complexes which determines the rate of reaction. A catalyst therefore acts by reducing the free energy of activation, $\Delta G^{\ddagger}$, for the reaction.

Clearly the catalytic reaction will become more significant the greater the reduction in $\Delta G^{\ddagger}$ and, in the case of heterogeneous catalysis, the larger the surface area. It has been shown by Thomas and Thomas (2) that for the rates of the heterogeneous and homogeneous reactions in a system containing a catalyst of surface area $100 m^2$ in 1 ml. to be equal, $\Delta G^{\ddagger}_{het}$ must be less by 16-17 kcal $mole^{-1}$ than $\Delta G^{\ddagger}_{hom}$ at room temperature. This disparity in $\Delta G^{\ddagger}$ must rise as the reaction temperature rises to maintain parity of rates.

Both homogeneous and heterogeneous catalysts contain molecular or atomic or ionic species which interact physically with the reacting species, weakening chemical bonds in such a way as to lower $\Delta G^{\ddagger}$ and increase the rate of reaction. In the case of heterogeneous catalysis,

the concentration of reacting species at the interface is likely to be enhanced, and this also increases the rate of reaction by a numerical effect. The study of physical adsorption of substances at interfaces, and especially at the surface of finely divided solids, is therefore a valuable complement to the study of hetero-geneous catalysis, at least of surface-controlled processes. (A surface-controlled process is one in which the rate of overall reaction is determined by some process other than diffusion of reactants to the catalyst surface: the slowest step may be the adsorption of reactants onto the surface, the rate of the reaction itself on the surface, or the desorption of products from the surface.) Chemisorption is not usually the precursor to heterogeneous catalysis in mild conditions, as such sorption is normally irreversible except under drastic treatment.

The effect of finely divided solid catalysts on the rates of non-ionic processes occurring in the gas and liquid phases is often most striking. Hydrogen and oxygen, for example, react imperceptibly slowly without a catalyst, but can form an explosive mixture in the presence of platinum black. The efficient catalytic cracking of vaporised or partly vaporised crude petroleum on solid acids, such as synthetic silica, has produced the vast petrochemical industry. On the surface of a heterogeneous

catalyst, even covalent molecules must be polarised, and ionic intermediates may be produced.

The situation with ionic processes occurring in polar solution is rather different. A catalyst is not required to generate ionic intermediates, but merely to interact with ions already present. This implies that the catalytic species, either homogeneous or heterogeneous, must either interact specifically with the reacting ions, or that it must electrostatically lower the free energy of the ions more than the solvent does.

Beck (3) has classified the various catalytic phenomena that are observed in the catalysis of complex formation reactions, which of course includes the substitution reactions of inorganic complexes with which this thesis is concerned, as shown in Table I. Beck's classification is printed in capitals, and that section of the Table investigated in the research reported in this thesis is outlined.

As the surfaces of insoluble ionic salts or metals in the massive state both carry more surface charge than the surfaces of molecular solids, it is probable that the former type of solid will be intrinsically a better heterogeneous catalyst for ionic processes occurring in solution than the latter. This tendency may, however, be masked by the very high specific surface areas of

TABLE I : CATALYSIS OF COMPLEX FORMATION REACTIONS (based on Ref. 3).

CATALYSIS OF COMPLEX FORMATION REACTIONS

**COORDINATION CATALYSIS**
(formation of complex
preceded by temporary
formation of another
complex)

**REDOX CATALYSIS**

**HETEROGENEOUS CATALYSIS**

LIGAND
ATALYSIS
e.g.
effect
of OH
on
$Cr^{3+}$+ SCN
eaction)

CATION
CATALYSIS
(e.g.heavy
metal ions
catalyse
aquation
of several
halo
complexes)

COORDINATION
CHAIN
REACTIONS
(Interchange
of chelating
ligands
greatly
accelerated
by free
ligand
through
chain
mechanism).

ELECTRON
TRANSFER
CATALYSIS
(e.g.Cr(II)
catalyses
certain
reactions
of Cr(III)
complexes)

INDUCED
COMPLEX
FORMATION
(formation
of
complex is
accelerated
by simulta-
neous
redox
reaction)

Heterogeneous
catalysis of
redox reactions.
A widely
occurring
phenomenon,
proceeding via
electron
transfer
through the
catalyst.
See Ravnø and
Spiro (4a)

ADSORPTION
EFFECTS.
(In general
adsorption
loosens
bonding in
reactant
complex)

SOLUBILISA
-TION
EFFECTS.
(e.g.
detergent
increase
the
solubility
of some
ligands)

9.

some "molecular" solids, like charcoal and silica.

The electric double layer at the surface of the former type of heterogeneous catalyst can polarise intermediates and reactants, and in some cases, reaction products appear which differ from those formed homogeneously. This is often the case with catalytic hydrogenation of organic compounds on metals such as platinum. Thus Hoijtink (5) rationalises the hydrogenation products of anthracene derivatives by the hypothesis that the catalyst causes heterolysis of $H_2$ molecules:

$$\tfrac{1}{2}(x+y)H_2 + Cat \rightleftharpoons CatH_x^{y-} + yH^+_{solvated} \qquad (1.2)$$
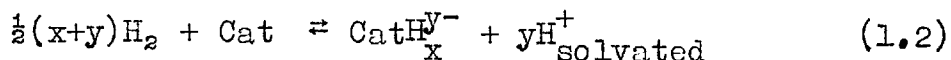
The catalyst, negative with respect to the solution, transfers one or two electrons to the organic substance, and then addition of $H^+$ usually occurs within the electric double layer. This means that the overall orientation of the hydrogen addition may be affected by the double layer and by the electron deficiency of the metal catalyst. Similarly, even if the heterogeneous catalyst does not alter the course of an inorganic substitution reaction, it may well alter the stereochemistry.

To return to the general consideration of the subject of this thesis, it is known from numerous types of experiment that ions do adsorb on a wide variety of solid surfaces. These experiments include those in the fields

of electrophoresis, polarography, electrocapillarity, colloid chemistry and ion-exchange chromatography, although the latter is strictly a bulk, not a surface, phenomenon. It seems not unlikely that surfaces which adsorb ions could also catalyse ionic processes such as redox reactions and the substitution reactions of ionic complexes, especially such of these processes as occur rather slowly in homogeneous solution because their energy of activation is high. Some of the literature references to such catalytic processes, usually dismissed in the past as annoying side reactions, are given in the next chapter. This survey is almost certainly incomplete, as the references generally occur in papers whose titles do not mention catalysis.

A brief survey of other ionic processes which bear relevance to the central theme is also given in the next chapter.

# CHAPTER II : SURVEY OF LITERATURE REFERENCES TO THE HETEROGENEOUS CATALYSIS OF IONIC PROCESSES IN SOLUTION, AND RELATED TOPICS.

II.1.  Heterogeneous catalysis of substitution reactions.

The present study is restricted to inert complexes
of the transition metal ions.  As pointed out by Taube (6),
the d electron structure of the central metal ion partly
determines the lability of a transition metal complex.
In general the labile complexes are, in valence bond
terminology, either of the outer orbital type or of the
inner orbital type with at least one vacant lower energy d
orbital;  inert complexes are those in which no d orbitals
are vacant, although some may be singly occupied.  In
crystal field terminology, the greater the crystal field
stabilisation of the complex, the greater the activation
energy required to pass to a transition state of different
stereochemistry, and so the more inert is the complex.
Thus, inert complexes include those of low-spin Co(III)
($d^6$) and Cr(III) ($d^3$) in the first transition series and
those of Rh(III) ($d^6$), Ru(III) ($d^5$) and Pt(IV) ($d^6$) in
subsequent transition series:  more metal ions in the
later series are low-spin, and hence form inert complexes,
than in the first transition series.  There is, of course,
no necessary connection between thermodynamic stability

and kinetic inertness in homogeneous solution. There
may be more basis for such a connection for the hetero-
geneously catalysed reaction of an inert complex. Thus,
the extent of bond weakening induced in the reacting
complex by adsorption should be greater the less stable
the complex. The more the incipient bond rupture in
the reactant complex is thus enhanced, the more effective
should be the collision of the incoming ligand with the
adsorbed complex compared with the same collision in
bulk solution.

Clearly, heterogeneous catalysis of ligand substi-
tution reactions will only be observable for inert
complexes, and it is therefore not surprising that the
majority of the examples that follow are for Co(III)
complexes, whose reaction kinetics have been extremely
thoroughly investigated. Moreover, the phenomenon of
heterogeneous catalysis is most likely to be observed
with solids of large specific surface area. This is why
many of the literature examples cite charcoal and platinum
black as heterogeneous catalysts, although there are
occasional references to the catalytic effects of other
powdered solids.

II.1.1:  Heterogeneous catalysis of ligand substitution
 reactions of cobalt(III) complexes.


The kinetics of the aquation and other types of
substitution reaction of the Co(III) ammines have been
extensively investigated.  The general reaction is of
the type

$$[Co^{III}(NH_3)_nX_{6-n}] + Y \rightleftharpoons [Co^{III}(NH_3)_nX_{5-n}Y] + X \quad (2.1)$$
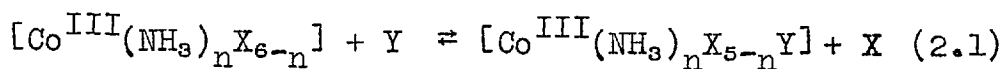
where n may be 1-6, and the ammonia ligands may be replaced
by the appropriate number of ammine derivatives.

Bjerrum (7a) noted several examples of the hetero-
geneous catalysis of cobaltammine reactions by mercury
and charcoal, and determined the equilibrium constant
for the reaction

$$[Co(NH_3)_6]^{3+} + H_2O \rightleftharpoons [Co(NH_3)_5OH]^{2+} + NH_4^+ \quad (2.2)$$
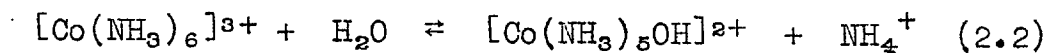
in ammoniacal ammonium salt solutions using carefully
purified active carbon as catalyst.  A common preparative
method for cobalt hexammine salts is based on the rapid
establishment of equilibrium (2.2) in the presence of
charcoal (8).  Bjerrum also reported (7b) some minor
experiments showing that the reverse of reaction (2.2)
was catalysed by a bright platinum electrode, by mercury
and, strongly, by colloidal palladium, provided a trace

of Co(II) ions was present.

It may be mentioned here that, in the course of the present work, decolourising charcoal was found to reduce the complex $[Co(NH_3)_5Br]^{2+}$ stoichiometrically to Co(II) at low concentrations. However, no mention of possible redox reactions is made in Bjerrum's work, although the significance of trace amounts of Co(II) is mentioned in more recent work with carbon referred to in this section. The reasons for this are possibly two-fold. The charcoal used in the present work was not so carefully purified as that used by Bjerrum, and could have contained a sorbed reducing impurity. Moreover, Bjerrum worked with much higher concentrations of Co(III) complexes than were used in the present work, so that, even had the entire catalyst surface been oxidised by a redox reaction, the amount of Co(II) formed would have been insignificant in comparison with the amount of Co(III) present.

It is clear from Bjerrum's work that charcoal is an excellent catalyst for the inter conversion of various Co(III) ammine complexes, despite the unconsidered possibility that a slight redox reaction may also occur. Bjerrum points out (7c) that $[Co(NH_3)_5Cl]^{2+}$ cannot be formed when $[Co(NH_3)_6]Cl_3$ is shaken with carbon or silica gel in slightly basic solution, as concluded by Schwartz and Krönig (9), since $[Co(NH_3)_5Cl]^{2+}$ is rapidly hydrolysed in basic solution. Despite their wrong assumption as to

the nature of the product, Schwartz and Krönig did consider the possibility of a redox reaction with the charcoal, but were unable to detect any Co(II) with the relatively insensitive means at their disposal in 1923. It is worth mentioning, however, that Bjerrum (7c) found a considerable increase in the catalytic action of carbon by the addition of cobaltous salt in an atmosphere of nitrogen. A possible explanation of this, that Co(II) lowers the potential of the charcoal surface, is proposed in Part III.

Carbon has also been found to catalyse the reaction of Co(III) ammines with ethylenediaminetetraacetic acid (10), and the very striking catalysis by carbon of the racemisation of several optically active Co(III) complexes has been investigated: Erdman and Douglas (11) found that [Co(EDTA)]$^-$ was racemised very rapidly by wood charcoal, and less rapidly by sugar charcoal, which has a smaller specific surface area. Some reduction of the Co(III) complex occurred with the wood charcoal, but very little with the sugar charcoal.

Isomerisation (12) and racemisation (13) of cobalt(III)ethylenediamine complexes is markedly catalysed by active charcoal, and again, small amounts of Co(II) are formed. [Pt(en)$_3$]$^{4+}$ is less readily racemised, while [Rh(en)$_3$]$^{3+}$ is stable to charcoal treatment even on boiling for some time (14). As Pt(IV) is less readily

reduced than Co(III), while Rh(III) is reduced only
with difficulty, this suggests that the charcoal is
involved in an intermediate redox process. Dwyer and
Sargeson (15) suggest that the charcoal converts small
amounts of the low-spin $[Co(en)_3]^{3+}$ into a high-spin
state, which is then reduced to high-spin $[Co(en)_3]^{2+}$.
This complex exists as a racemic mixture because of its
lability, and it catalyses the racemisation of $[Co(en)_3]^{3+}$
by an electron transfer process. This mechanism explains
the increase in catalytic action of carbon that Bjerrum
observed (7c) on addition of Co(II) to his systems.

Bailar and Work (16) found that Raney nickel and
silica gel, as well as activated charcoal, catalysed
many reactions involving the coordination of nitrogen to
cobalt and chromium, immaterial of whether the nitrogen
was part of a nitro group, a primary amine or ammonia.
These workers recommended a new preparative method for
$[Cr(en)_3]Cl_3$, using charcoal as a catalyst for the reaction
of hydrated chromic chloride and aqueous ethylenediamine.

The preparation of the six-coordinated chelated ion
$[Co(EDTA)]^-$ from $[Co(NH_3)_6]^{3+}$, $[Co(en)_2Cl_2]^+$ and $[Co(Ox)_3]^{3-}$
in the presence of EDTA and carbon-supported palladium was
reported by Schwarzenbach (17).

Various interactions of cobalt(III) complexes with
platinum, usually in the form of an electrode, have been
reported in the literature. Lamb and Larson (18), in

an attempt to determine the redox potentials of various cobalt(III) ammines, found that the aquation of $[Co(NH_3)_6]^{3+}$, $[Co(NH_3)_5H_2O]^{3+}$ and $[Co(NH_3)_4(H_2O)_2]^{3+}$ was catalysed by smooth, but more markedly by platinised, platinum electrodes.

Brönsted and Livingston (19) measured the rate of the bimolecular reaction between $[Co(NH_3)_5Br]^{2+}$ and $OH^-$ by a conductance method, but recorded that the cobaltammines in the system appeared to be somewhat unstable in the presence of platinum electrodes. A similar reaction, the aquation of halobis(dimethylglyoxime)aquocobalt(III),

$$[Co(H_2O)(DG)_2X] + H_2O \rightarrow [Co(H_2O)_2(DG)_2]^+ + X^-, \quad (2.3)$$
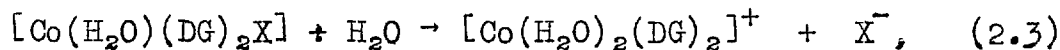
is also catalysed by platinum (20).

Catalysis of substitution reactions by electrodes of other materials has not frequently been observed, but Stranks (21) reported that $[Co(en)_2Cl_2]^+$ interacted with an Ag-AgCl electrode, but did not give details. Certain polarographic observations on the rate of reduction of $[Co(NH_3)_5X]^{2+}$ at a dropping mercury electrode have been explained by the hypothesis that the exchange

$$[Co(NH_3)_5X]^{2+} + Cl^- \rightleftharpoons [Co(NH_3)_5Cl]^{2+} + X^- \quad (2.4)$$
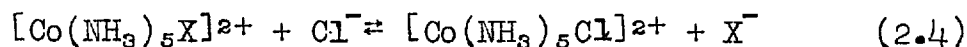
is efficiently catalysed by the mercury surface (22). All electrode reactions are, of course, heterogeneous reactions at charged surfaces, and the material of the

electrode is frequently designed to catalyse the electrode reaction. Usually, however, this is a redox, rather than a substitution, process.

There is an isolated reference to the catalytic effect of barium oxide and silver oxide on the aquation of $[Co(NH_3)_5Cl]^{2+}$ to $[Co(NH_3)_5H_2O]^{3+}$ by Jørgenson (23), but this could have been the homogeneous effect of $Ba^{2+}$ and $Ag^+$, rather than heterogeneous catalysis.

II.1.2: Heterogeneous catalysis of other ligand substitution reactions.

Not many literature references to the heterogeneous catalysis of the substitution reactions of metal complexes other than those of Co(III) have been discovered during the present work, which was mainly concerned with Co(III) complexes.

Waind (24) reported that the exchange reaction

$$[PtF_6]^{2-} + 6I^- \rightleftharpoons [PtI_6]^{2-} + 6F^- \qquad (2.5)$$
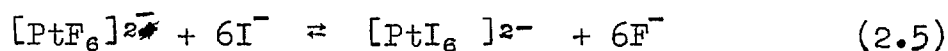
was catalysed by platinum black, but not by charcoal, and Zhukov and Shipulina (25) found that activated charcoal caused several complexes of Pt(IV) with chloride and ethylenediamine ligands to lose some chloride, which was presumably replaced by water.

Burwell (26) and others investigated the adsorption and reaction of various labile and inert coordination complexes on silica gel, and found inhibition of some substitution reactions. This is, of course, in a way, as revealing as positive heterogeneous catalysis. Silica gel in water behaves as a weak acid ion exchanger, with $\equiv$Si-O$^-$ and $\ast$Si(OH)$_2^-$ anionic sites. The negative charge carried by the surface was thought to be the reason why the pH-independent hydrolyses of [Co(en)$_2$NO$_2$Cl]$^+$ and [Pt(dien)Br]$^+$ were only one-fifth as fast on silica gel as in solution. These workers saw "no sign whatever that silica gel can catalyse solvolytic reactions". It might be thought that a negatively charged surface would facilitate the expulsion of a halide ion from a positively charged complex adsorbed on the surface. This was not the case, Burwell et al. suggested, because the silica gel modified the structure of the water near the interface, though why this would inhibit the reaction they did not say.

Finally, it may be mentioned that the heterogeneous catalysis of organic substitution reactions is also a well-established phenomenon. Walton (27) investigated the effect of many solids on the reaction

$$EtI + Ag^+ + H_2O \rightarrow EtOH + AgI \downarrow + H^+ \qquad (2.6)$$
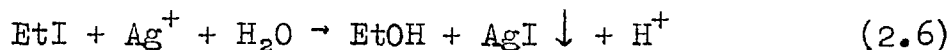
and found the silver halides and charcoal to be very effective catalysts and other substances, such as powdered

Pt, Pd, Ag and Au, to be moderate catalysts.

The catalysis of reaction (2.6) by silver iodide
and charcoal was investigated quantitatively in
subsequent work (28), and it was concluded that a
Langmuir-Hinshelwood mechanism, with adsorption of both
EtI and $Ag^+$ onto the catalyst, was operating.

Walton's thesis (27) also contains an extensive
compilation of literature references to the hetero-
geneous catalysis of the hydrolysis of alkyl halides
and α-halo-acids.

Kolthoff (29), in an early systematic investigation
into the catalytic effects of charcoal, found that the
bromination of phenol was inhibited when both reactants
were sorbed on charcoal, but the iodination of hydroquinone
was greatly assisted. This superficial contradiction
invites further study of the reactions: catalytic
efficiency might well be dependent on the mobility and
polarisability of the adsorbed reactants.

II.2.   Topics related to the heterogeneous catalysis
  of substitution reactions.

II.2.1:   Catalysis by ion exchange resins.


    Ion exchange resins are insoluble substances that
have been synthesised especially to absorb and exchange
ions.   It is therefore not surprising that cation exchange
resins are able to catalyse the substitution reactions of
some cationic complex ions.

    Indelli and Bonora (30) found that the acid hydrolysis
of $[Cr(H_2O)_5N_3]^{2+}$ was catalysed by several cation exchangers,
the most effective being Dowex 50 in the $H^+$ form.   In a
system of unit ionic strength and pH 1 at 30°C, Swaddle
and King (31) found the first order aquation rate constant
of the complex to be $2.66 \times 10^{-7}$ sec$^{-1}$:   this value
increases as the pH decreases.   In the presence of Dowex
50 in the acid form, Indelli and Bonora found a value of
$115 \times 10^{-7}$ sec$^{-1}$.   The rate enhancement might well be due
to the very high $H^+$ "concentration" in the resin beads.
The amount of resin used and the particle size had little
effect on this value.   Resins in the $Na^+$ form were much
less effective than those in the $H^+$ form.   The action was
fairly specific,   Dowex 50 being much the most effective.
$HN_3$ is a weak acid and Indelli and Bonora therefore
suggested the mechanism shown

$$N_3^- \quad H_2O$$
$$[Cr(H_2O)_5]^{3+}$$
$$H^+$$
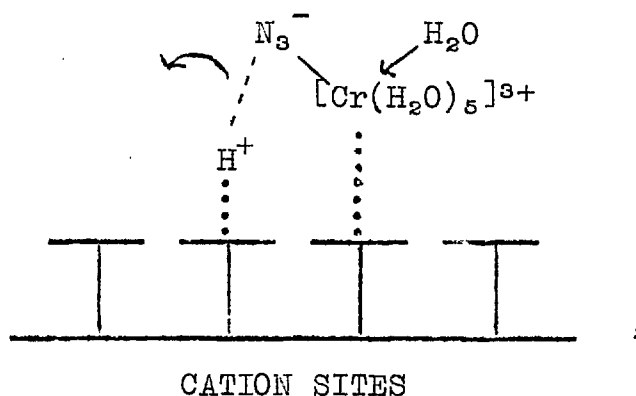
CATION SITES

in which the spacing of the cation sites in the resin
is critical for the catalytic ability.

Cation exchangers in the acid form are more effective
catalysts for the hydrolysis of several simple esters
than aqueous $H^+$. According to Davies and Thomas (32),
this is due to preferential sorption of ester on the resin.
(The heterogeneous catalysis is somewhat retarded by the
products, which are also sorbed.) In organic solution,
however, the esters are negatively sorbed, and the ion
exchange resin is then a less efficient catalyst for the
ester hydrolysis than $H^+$ in the bulk medium.


II.2.2: Catalysis by polyelectrolytes.


Polymer solutions are macroscopically homogeneous
systems, but because of the size of the molecules, there
is an intrinsic heterogeneity in such systems, somewhere
between the heterogeneity of a colloidal dispersion and
the true homogeneity of a simple solution. Polyanions
and polycations in solution present long (on a molecular

scale), flexible surfaces, along which charges are spaced at regular intervals. The analogy with ion exchange resins, electrode surfaces and indeed with all interfaces, which are normally electrostatically charged, is obvious. As would be expected from this analogy, it has been found that polyelectrolytes can catalyse ionic reactions in solution.

In the vicinity of a poly-anion or -cation, the electrostatic potential energy gradient is very high, and counter ions (i.e. ions of charge opposite to the charge of the polyion) are strongly attracted. A polyion should therefore strongly catalyse any reaction between two types of counter ion, and could also, by a bond weakening effect, increase the unimolecular reaction rate of one type of counter ion. Enzymes, for example, particularly those of low specificity, whose only probable interaction with the substrate is electrostatic, are polyion catalysts (33).

The theory of the effect of polyelectrolytes on the rates of reaction of simple ions in solution has been developed as a means of characterising the distribution of electrostatic potential round the polyions (33). The theory successfully accounted for the inhibition of the hydroxide ion hydrolysis of uni- or di-positive cationic esters in the presence of partially ionised polycarboxylic resins (34).

The predicted catalytic effect of polyions has been observed for reactions of some bulky organic reagents (35-39), but in some of these cases, at least (38,39), the hydrophobic nature of the reactants is important as well as their electrostatic attraction to the polyion. Recently, a system free from this complication has been investigated, and the results will be summarised here in some detail, as they illustrate many of the salient points of the nature of the heterogeneous and quasi-heterogeneous catalysis of ionic processes.

Vogel and Morawetz (40) found that the polyanions polyvinylsulphonate (PVS) and polymethacryloxyethyl-sulphonate (PMES)

$$\left[ \begin{array}{c} SO_3^- \\ | \\ -CH-CH_2- \end{array} \right]_n \qquad \left[ \begin{array}{c} OC_2H_4SO_3^- \\ | \\ -CHMe-CH- \end{array} \right]_n$$

PVS                              PMES
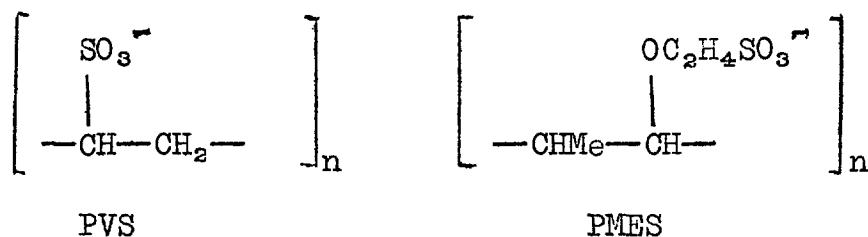
were extremely effective catalysts for the reaction between $Hg^{2+}$ and $[Co(NH_3)_5Cl]^{2+}$:

$$Hg^{2+} + [Co(NH_3)_5Cl]^{2+} + H_2O \xrightarrow[\text{solution}]{\text{in acid}} [Co(NH_3)_5H_2O]^{3+} + [HgCl]^+ \quad (2.7)$$
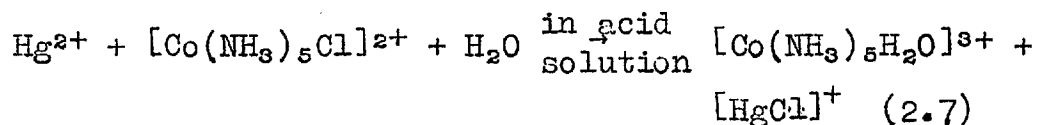
The course of the reaction was followed spectrophotometrically at very high dilutions of the reagents. This is probably one reason why such enormous catalytic effects were found. In systems containing $5 \times 10^{-6}$ M $[Co(NH_3)_5Cl]^{2+}$,

$5 \times 10^{-5}$ M $Hg^{2+}$, and $5 \times 10^{-5}$ M polyanion, PMES accelerated reaction (2.6) by a factor of 24,700, and PVS by 176,000. These concentrations are such that there is neither so much polyanion that the adsorbed reactant ions have small chance of being adsorbed as near neighbours, nor so little that the "heterogeneous" reaction occurring at the polyion surface is swamped by the slow, homogeneous reaction, so that there is little observable effect on the reaction rate. Vogel and Morawetz found that as the polyion concentration was increased from zero, while other variables were unchanged, the reaction rate at first increased, and then decreased sharply. The decrease is due to the "dilution" of adsorbed reactant ions over more polymer domains.

Addition of simple salts reduced the effect of the polyions on the reaction rate, since the added cations competed with $[Co(NH_3)_5Cl]^{2+}$ and $Hg^{2+}$ for polyion sites. Addition of more $Hg^{2+}$ also reduced the effectiveness of the catalytic reaction, because, once the polyions were saturated with reagent ions, further $Hg^{2+}$ addition displaced bound $[Co(NH_3)_5Cl]^{2+}$, and the reaction rate decreased.

Polyion catalysis is very closely related to catalysis by micelles, which are ordered aggregates of large organic ions in solution. For example, micelles of the cationic

surfactants $[C_{16}H_{33}N(CH_3)_3]^+Br^-$ and $[C_{12}H_{25}N(CH_3)_3]^+Cl^-$ catalyse the reaction between the two anions bromoacetate and thiosulphate to form bromide (41). Anionic and cationic detergents above the critical micelle concentration increase the rate of fading of cationic and anionic dyes respectively (42).

II.2.3:  Catalysis by heterogeneous buffer systems.

Bell and Prue (43) found that heterogeneous or partly heterogeneous systems such as zinc hydroxide : zinc sulphate in molar proportion 3:1, and 1:1 quinine : quinine sulphate in potassium sulphate solution, acted as acid-base buffers in aqueous solution.  In the first system, as zinc hydroxide is sparingly soluble, the value of $[OH^-]$ in the $3Zn(OH)_2:ZnSO_4$ system is determined by the value of $[Zn^{2+}]$, from the soluble zinc sulphate.  In the second system, the solution is simultaneously saturated with the sparingly soluble quinine sulphate and with quinine, which is basic.  The concentration of sulphate, from the potassium sulphate, therefore controls the pH of the solution.  Use of heterogeneous buffers reduces the homogeneous concentration of buffering species, which are inevitably weak acids or bases and may have undesirable side effects.

Bell and Prue used these buffer systems to study two base-catalysed reactions in media of constant pH:

(i) With quinine buffer (pH≈8), the alkaline hydrolysis of the esters $CH_2ClCOOMe$ and $HCOOEt$. (Initial concentration of ester was 0.025M in the presence of not more than 6 g. buffer).

(ii) With zinc buffer (pH≈7.16), the base catalysed iodination of acetone. (Acetone concentration was 0.07M: amount of buffer used not stated).

In neither of these systems was there any indication of heterogeneous catalysis on the surface of the solid phase, although Bell and Prue considered the possibility, and were surprised to find none.

In the light of the present research, the reason for this seems clear. Unless the heterogeneous reaction is diffusion controlled, if the number of species reacting homogeneously is very much greater than the number that can be adsorbed on the limited catalyst surface to react heterogeneously, then the heterogeneous reaction is swamped and its effect on the overall kinetics is negligible. This has long been obvious from work on hetero-catalysed gas reactions. This in practice restricts work in solution to low concentrations, of less than about $10^{-3}M$. Bell and Prue's work does not satisfy these requirements, so the existence of heterogeneous catalysis of reactions (i) and (ii) remains unproven, rather than disproved.

II.2.4:  Heterogeneous catalysis of solution phase
redox reactions.


The heterogeneous catalysis of substitution reactions
such as those given in Sections II.1.1. and II.1.2. must
be due to a chemical attraction of the catalyst surface
for the reacting ions, which results in rate enhancement
by concentration enhancement (for reaction orders higher
than one) and by encouraging heterolysis through bond
weakening.

The mechanism of the heterogeneous catalysis of
inorganic redox reactions is not always so specific, as
shown by Spiro and Ravnø (4b) for platinum.  For seventy
aqueous catalytic studies from the literature and their
own work, and with only one definite exception, they
concluded that the platinum catalyst acted simply as an
electron conductor.  This has now been quantitatively
substantiated for one reaction (44).  In such cases, there
is little relevance to the catalysis of substitution
reactions.  The role of the heterogeneous redox catalyst
cannot be so simple, however, for solids that are not
electronic conductors.  Manganese dioxide is a case in
point.  The reduction of permanganates in alkaline or
neutral solution to $MnO_2$ often proceeds autocatalytically,
and $MnO_2$ is known to catalyse other redox processes such
as the decomposition of hydrogen peroxide, probably via

a free radical mechanism (45), and the reduction by
Cr(II) of perchlorate (46). The reaction intermediates
in such reactions probably involve valence states of
manganese other than four, and there is an analogy with
the charcoal catalysed substitution reactions of Co(III)
discussed in Section II.1.1.

II.2.5:  Homogeneous catalysis by metal ions of inorganic
  substitution reactions, and related topics.

It is well-known that metal ions with an affinity
for halide accelerate the aquation reactions of many inert
halide complexes. The accelerating effect of the ions
$Ag^+$, $Hg^{2+}$ and $Tl^{3+}$ on the aquation of $[Co(NH_3)_5X]^{2+}$
(X=Cl, Br, I) is a case in point (47). The role of the
metal ion is not, strictly speaking, catalytic, as stable
complexes are formed between the metal ion and released
halide or pseudo-halide:

$$[Co(NH_3)_5Cl]^{2+} + Ag^+ + H_2O \rightarrow [Co(NH_3)_5H_2O]^{3+} + AgCl \downarrow \quad (2.8)$$

$$[Cr(NH_3)_5Cl]^{2+} + Hg^{2+} + H_2O \rightarrow [Cr(NH_3)_5H_2O]^{3+} + HgCl^+ \quad (2.9)$$
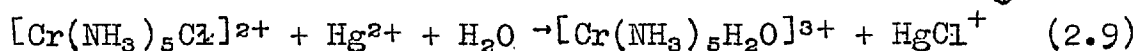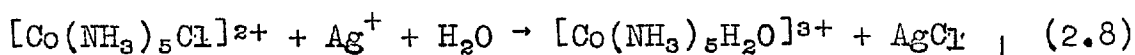
However, if metal ions such as $Ag^+$ and $Hg^{2+}$ could,
while bound on the surface of an insoluble salt, induce
aquation and similar reactions without being able to form
permanent complexes with the released ligand, the

phenomenon would be genuine heterogeneous catalysis.
A survey of literature references to homogeneous
"metal ion catalysis" was therefore a useful guide in
the present work as to which solids might act as hetero-
geneous catalysts for substitution reactions.  The
survey is reproduced in Tables II, III and IV on pages
29, 30 and 31.

As is seen from these Tables, $Hg^{2+}$ is the metal
ion most effective in removing coordinated halide or
pseudo-halide ions.  This probably reflects the very
high stability of the $Hg(II)$-halide complexes:  the
step-wise stability constants, $K_1$, for the equilibrium

$$M^{n+} + Cl^- \rightleftharpoons MCl^{(n-1)+} \qquad (2.10)$$
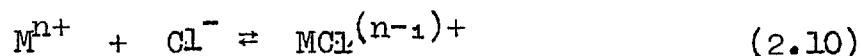
for various metal ions in aqueous media at $25°C$ are
reproduced below (48):

| Metal ion : | $Hg_2^{2+}$ | $Pb^{2+}$ | $Ag^+$ | $Tl^{3+}$ | $Hg^{2+}$ |
|---|---|---|---|---|---|
| $\log K_1$ : | <1.3 | 1.6±0.1 | 3.4±0.1 | ~6.2 | 7.0±0.2 |

## TABLE II : METAL ION ASSISTED AQUATION REACTIONS OF COBALT(III) COMPLEXES

| Metal ion. | Induced aquation reaction. | Remarks. | Ref. |
|---|---|---|---|
| $Ag^+$, $Hg^{2+}$, $Tl^{3+}$ | $[Co(NH_3)_5X]^{2+} \rightarrow [Co(NH_3)_5H_2O]^{3+}$  $X=Cl,Br,I$ | $Hg^{2+}$ is more effective than $Ag^+$ or $Tl^{3+}$.  Evidence for $[Co(NH_3)_5]^{3+}$ intermediate with $Hg^{2+}$, but not $Ag^+$ or $Tl^{3+}$. | (47,99) |
| $Hg^{2+}$ | $[Co(en)_2(H_2O)X]^{2+} \rightarrow [Co(en)_2(H_2O)_2]^{3+}$  $[Co(en)_2(N_3)X]^+ \rightarrow [Co(en)_2(N_3)(H_2O)]^{2+}$ | | (49) |
| $Ag^+$, $Hg^{2+}$ | $[Co(EDTA)Br]^{2-} \rightarrow [Co(EDTA)]^-$ | Spontaneous reaction quite fast, and induced reaction instantaneous. | (17) |
| $Ag^+$, $Pb^{2+}$, $Hg^{2+}$ | $[Co(NH_3)_5CO_3]^+ \rightarrow [Co(NH_3)_5H_2O]^{3+}$ | Induced reaction very rapid.  O-C fission, i.e. $CO_2$ removed. | (50) |
| $Ba^{2+}$, $Ni^{2+}$, $Cu^{2+}$, $Co^{2+}$ | " | Induced reaction less rapid.  Co-O fission.  These metal ions polarise $CO_3^{2-}$ group less than $Ag^+$, $Pb^{2+}$ and $Hg^{2+}$. | (50) |
| $Hg^{2+}$ | $[CoA_4XCl]^{n+} \rightarrow [CoA_4XH_2O]^{(n+1)+}$  A = amine derivative.  X = $NH_3$, $H_2O$ | Excellent correlation between rates of spontaneous and induced aquation reactions. | (123) |

| Metal ion. | Induced aquation reaction. | Remarks. | Ref. |
|---|---|---|---|
| $Hg^{2+}$ | $[Cr(NH_3)_5Cl]^{2+} \rightarrow [Cr(NH_3)_5H_2O]^{3+}$ | | (51) |
| $Ag^+$ | $[Cr(H_2O)_4Cl_2]^+ \rightarrow [Cr(H_2O)_5Cl]^{2+}$ | | (52) |
| $Ag^+, Hg^{2+}$ | $[Cr(H_2O)_5Cl]^{2+} \rightarrow [Cr(H_2O)_6]^{3+}$ | $Hg^{2+}$, $[HgCl]^+$ and $[HgCl_2]^o$ all effective. $[HgCl_3]^-$ and $[HgCl_4]^{2-}$ ineffective. | (52,53) |
| $Hg^{2+}$ | $[Cr(H_2O)_5CN]^{2+} \rightarrow [Cr(H_2O)_6]^{3+}$ | | (54) |
| $Ag^+, Hg^{2+}$ | $[Cr(NH_3)_5NCS]^{2+} \rightarrow [Cr(NH_3)_5H_2O]^{3+}$ | $Hg^{2+}$ especially effective. Neither $Hg^{2+}$ nor $Ag^+$ catalyse aquation of analogous complex $[Co(NH_3)_5SCN]^{2+}$, probably because of the extreme kinetic inertness of this ion. cf. spontaneous aquation rate constants: $[Cr(NH_3)_5NCS]^{2+}$ : $1.0 \times 10^{-7} sec^{-1}$ $[Co(NH_3)_5SCN]^{2+}$ : $4.0 \times 10^{-10} sec^{-1}$ | (56) (55) |
| $Hg^{2+}$ | $[Cr(CH_2Cl)(H_2O)_5]^{3+} \rightarrow [Cr(H_2O)_6]^{3+}$ and similar reactions. | $[HgCH_2Cl]^{2+}$ formed. $Ag^+$ has no action in cold, but reaction occurs on warming. | (57) |
| $Al^{3+}$ | $[Cr(Ox)_3]^{3-} \rightarrow [Cr(Ox)_2(H_2O)_2]^-$ etc. Ox = oxalate. | Example of interation between unpolarisable ("hard") metal ion and ligand. | (3a) |
| $Fe^{3+}$ | $[Cr(NCS)_6]^{3-} \rightarrow [Cr(NCS)_5H_2O]^{2-}$ | $Fe^{3+}-SCN^-$ complexes are very stable. | (58) |

## TABLE IV : METAL ION ASSISTED AQUATION REACTIONS OF OTHER INERT COMPLEXES

| Metal ion. | Induced aquation reaction. | Remarks. | Ref. |
|---|---|---|---|
| $Hg^{2+}$ | $[Fe(CN)_6]^{4-} \rightarrow [Fe(CN)_5H_2O]^{3-}$ etc. | Effectiveness of $Hg^{2+}$ studied in presence of various amounts of halide, X . $Hg^{2+}, [HgX]^+$ and $[HgX_2]^0$ approximately equally effective. $[HgX_3]$ and $[HgX_4]^{2-}$ completely inactive. | (3a) |
| $Fe^{3+}$ | $[AsF_5H_2O]^0 \rightarrow [AsF_4(H_2O)_2]^+$ etc. | Example of interaction between unpolarisable ("hard") metal ion and ligand. | (3a) |

Metal ions are, of course, catalysts for many solution processes other than the substitution reactions mentioned above. They accelerate a wide variety of organic reactions (59), and catalyse a great many redox reactions, for example. There seems no reason why metal ions bound on the surface of insoluble salts should not act as heterogeneous catalysts for such processes. It should be noted, however, that homogeneous metal ions involved in such reactions can alter the position of equilibrium, whereas, as heterogeneous catalysts, they cannot. This implies that, heterogeneously, they must catalyse the back as well as the forward reaction, whereas, homogeneously, they need have no effect on the back reaction.

Finally, it may be mentioned that anions, as well as cations, can affect the rates of substitution reactions. This effect is comparatively slight, and is due to ion-pair formation between cationic complexes and the anion, which affects the lability of the complex (60, 61, 62).

CHAPTER III :  CHOICE OF SUBSTITUTION REACTIONS TO BE
STUDIED FOR HETEROGENEOUS CATALYTIC EFFECTS.

More is known about the reaction kinetics of Co(III)
and Cr(III) complexes than about those of any other metal
ions, and the choice was therefore made from among the
substitution reactions of these two ions.  The possi-
bility of studying some of the reactions of ions of the
second and third transition series was considered, but
rejected as these reactions are usually too slow to study
except at higher temperatures, when side reactions and
decomposition tend also to occur;  moreover they often do
not proceed to completion except under forcing conditions.

A ligand substitution reaction that is to be studied
for possible heterogeneous effects should have, for
greatest convenience and accuracy, the following
characteristics:

(i) The homogeneous reaction should occur in a matter
of hours or days at a convenient temperature.

(ii) The course of the reaction should be easily followed
at quite high dilutions by an analytical method that
does not provide a possible catalyst for the reaction.
(Titration of released halide by $Ag^+$ or $Hg^{2+}$, for
example, is obviously unsuitable, as is the use of
an Ag/AgX electrode.)

(iii) The product(s) of the reaction should not be
affected by the heterogeneous catalyst at least
during the course of the experiments.

(iv) Autocatalytic reactions should be avoided: the
homogeneous mechanism should be as simple as
possible.

(v) The reaction should proceed to completion, or only
that portion of it free from a simultaneously
occurring back reaction should be studied. Although
a back reaction is not an insuperable obstacle, its
occurrence means that the position of equilibrium
in each experiment must be determined in order to
calculate the actual rate of the forward reaction.

(vi) Substitution reactions involving monodentate ligands
are more suitable than those involving polydentate
ligands, for which ring-opening and bridge-building
reactions are an additional mechanistic complication.

(vii) As most ligand-substitution reactions are pH-
dependent, pH changes during the course of experi-
ment should be avoided. If hydrogen ions are
produced or consumed during the reactions, this
means a buffer must be used. As buffers contain
weak acids or bases, they are likely to interact
with catalyst surfaces, as well as to affect the
homogeneous kinetics, so their use is to be avoided.

(viii) In general, only exothermic reactions are subject

## TABLE V : UNCATALYSED AQUATION OF $[ML_5X]^{2+}$ IONS.

| M | L | X | $k_{25°C}(sec^{-1})$ | $\Delta H^{\ddagger}$ kcal/mole. | Reaction conditions. | Ref. |
|---|---|---|---|---|---|---|
| Cr | $H_2O$ | I | $8.4 \times 10^{-5}$ | 23 | I=1 * | (64) |
| | | Br | $4.3 \times 10^{-6}$ | 24 | I=1 | (65) |
| | | Cl | $2.8 \times 10^{-7}$ | 24 | I=1 | (64) |
| | | NCS | $9.1 \times 10^{-9}$ | 28 | I=0.15 | (66) |
| | | F | $6.2 \times 10^{-10}$ | 29 | I=1 | (64) |
| | | $N_3$ | $5.6 \times 10^{-8}$ | 32 | I=1 | (31) |
| Cr | $NH_3$ | I | $1.0 \times 10^{-3}$ | 21 | pH=1.1, I=0.1 | (67) |
| | | Br | $1.0 \times 10^{-4}$ | 21 | pH=1.1, I=0.1 | (67) |
| | | Cl | $9.3 \times 10^{-6}$ | 22 | pH=1.1, I=0.1 | (67,68) |
| | | NCS | $1.0 \times 10^{-7}$ | 25 | pH=1.1 | (56) |
| Co | $NH_3$ | I | $8.3 \times 10^{-6}$ | 19 | pH=3, I=1 | (69) |
| | | Br | $6.7 \times 10^{-6}$ | 24 | pH=1 | (70) |
| | | Cl | $1.7 \times 10^{-6}$ | 23 | pH=1 | (70) |
| | | $NO_3$ | $2.6 \times 10^{-5}$ | 25 | pH=2-4 | (19) |
| | | NCS | $4.0 \times 10^{-10}$ | 30 | pH=1-2.7 | (56) |
| | | F | $8.7 \times 10^{-8}$ | 21 | – | (71) |
| | | $N_3$ | $2.1 \times 10^{-9}$ | 34 | – | (72) |

* I = ionic strength.

to heterogeneous catalysis. A reaction with a considerable heat of activation should therefore be chosen.

In Table V, on page 35, are reported the kinetic data for the spontaneous aquation of some complex ions of the type $[ML_5X]^{2+}$, where M is Co(III) or Cr(III), L is $H_2O$ or $NH_3$, and X is the mononegative labile ligand. Table V is taken from the compilation by Monacelli (63) of various literature values. Monacelli showed that there is a strong correlation within each series of the aquation rate and the base strength of $X^-$. All the aquations follow first order kinetics: the first order rate constants are designated k.

The aquation reactions of $[Co(NH_3)_5Cl]^{2+}$ and $[Co(NH_3)_5Br]^{2+}$ were selected for study, because these reactions fulfilled criteria (i)-(viii), and because the literature observations on them cited in Chapter II held out hope of observing heterogeneous effects. This hope was indeed realised, and experiments on the aquation of $[Co(NH_3)_5Cl]^{2+}$ and $[Co(NH_3)_5Br]^{2+}$ in the presence of various heterogeneous catalysts is described in Part III.

As a heterogeneous catalyst for the reaction

$$[ML_5X]^{2+} + H_2O \rightarrow [ML_5H_2O]^{3+} + X^- \qquad (3.1)$$
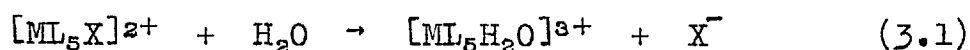
must also be a catalyst for the reverse, anation, reaction, it was decided that such a reaction should also be studied. Anation reactions which fulfil criteria

(i)-(viii) are few, and the most suitable was considered
to be the monoanation of hexaquochromium(III) by
thiocyanate,

$$[Cr(H_2O)_6]^{3+} + SCN^- \rightarrow [Cr(H_2O)_5NCS]^{2+} + H_2O, \quad (3.2)$$
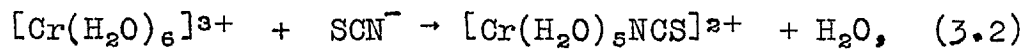
and experiments on this system, which were not very
fruitful, are discussed in Part II.

PART II


HETEROGENEOUS CATALYSIS OF CHROMIUM(III) REACTIONS

# CHAPTER IV : HETEROGENEOUS CATALYSIS OF THE ANATION

## REACTION $[Cr(H_2O)_6]^{3+} + SCN^- \rightarrow [Cr(H_2O)_5NCS]^{2+} + H_2O$     (4.1)
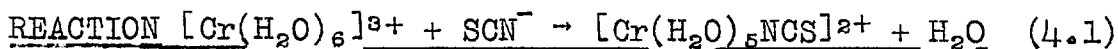
IV.1: The homogeneous reaction.

Bjerrum (73) showed the existence of complexes of the type $[Cr(NCS)_n(H_2O)_{6-n}]^{(3-n)+}$ (n=0-6), and developed classical methods for separating the six complexes. They are fairly inert in acid solution, and rapidly hydrolysed in alkaline solution.

The homogeneous reaction (4.1) in acid solution has been investigated by Postmus and King (74a) and by Poulsen, Bjerrum and Poulsen (58). Their results are only in fair agreement, and are summarised in Table VI, together with other relevant data.

The reaction is first order in $[Cr^{3+}]$ and in $[SCN^-]$, up to the highest thiocyanate concentration studied, 0.1M. At this concentration, the net rate of reaction (4.1) is still only 4% of the rate of water exchange by $[Cr(H_2O)_6]^{3+}$ (75), so there is competition between $H_2O$ and $SCN^-$ for an intermediate of the type $H_2O \ldots [Cr(H_2O)_5]^{3+}$.

Hydroxide ion labilises substitution by thiocyanate: the fraction of the anation that occurs by paths 2 and 3 (equation (4.2) ) is somewhat greater than the fraction of Cr(III) existing as $[Cr(H_2O)_5OH]^{2+}$ and $[Cr(H_2O)_4(OH)_2]^+$ (74a).

# TABLE VI : DATA AT 25°C FOR REACTION (4.1),

$$Cr^{3+} + SCN^- \rightarrow [CrNCS]^{2+} + H_2O,$$

## IN ACID SOLUTION.

| Analytical procedure. | (74) Spectrophotometric estimation of $[CrNCS]^{2+}$ <br> (58) Estimation of free $SCN^-$ by titration with $Ag^+$. |
|---|---|
| Anation rate law. | From reference (74a): <br><br> $$\frac{d}{dt}[CrNCS]^{2+} = \left\{ k_1^1 + k_2^1 [H^+]^{-1} + k_3^1 [H^+]^{-2} \right\}[Cr^{3+}][SCN^-] \quad (4.2)$$ <br><br> $$= k_2 [Cr^{3+}][SCN^-] \text{ M per unit time} \quad (4.2a)$$ <br><br> $k_2$ is the observed second order rate constant. <br><br> The 3 terms correspond to 3 different reaction paths: path 1 predominates at pH<3. <br><br> $k_1^1, k_2^1$ and $k_3^1$ are dependent on the ionic strength, I. ($\Delta z^2$ for reaction (4.1) is -6). <br><br> $k_1^1 = 1.12 \times 10^{-5} \text{ M}^{-1}\text{sec}^{-1}$ at I = 0 <br><br> $k_2^1 = 7.2 \times 10^{-9} \text{ sec}^{-1}$ at I = 0.3M <br> $\phantom{k_2^1 =} 7.4 \times 10^{-9} \text{ sec}^{-1}$ at I = 0 <br><br> $k_3^1 \approx 4.2 \times 10^{-12} \text{ M sec}^{-1}$ <br><br> For I $\leq$ 0.3M, <br><br> $$\log k_1^1 = \log 1.12 \times 10^{-5} - \frac{3.037 I^{\frac{1}{2}}}{1 + 2.475 I^{\frac{1}{2}}} \quad (4.3)$$ <br><br> From reference (58): <br><br> $k_2 = 6.2 \times 10^{-6} \text{ M}^{-1} \text{ sec}^{-1}$ at I = 1.0M $\}$ for $[H^+]$ <br> $\phantom{xxxxxxxxxxxxxxxxxxxxxxxxxxxxxxxxx}$ 0.02M- <br> $k_2 = 3.1 \times 10^{-5} \text{ M}^{-1} \text{ sec}^{-1}$ at I = 0 $\}$ 0.10M. <br><br> (These values are respectively 4- and 2-fold higher than values calculated from equation (4.2), which however was not tested for I>0.3M). |

## TABLE VI (contd.)

| | | |
|---|---|---|
| Enthalpy of reaction | $\Delta H^o = 2.13$ kcal mole$^{-1}$ at $I = 0$ | (74a) |
| | $\Delta H^o = -1.4$ " " at $I = 1.02M$ | (58) |
| Enthalpy of activation | $\Delta H_1^{\ddagger} = 25.7$ " " at $I = 0.08M$ | (74a) (path 1) |
| | $\Delta H_2^{\ddagger} = 32.8$ " " at $I = 0.08M$ | (74a) (path 2) |
| | $\Delta H_1^{\ddagger} = 26.0$ " " at $I = 0$ | (74a) (path 1) |
| | $\Delta H^{\ddagger} = 25.0$ " " at $I = 1.02M$ | (58) |
| | $\Delta H^{\ddagger} = 21.4$ " " at $I = 0.12M$ | (58) |
| Stability constant of $[CrNCS]^{2+}$ | $K_1 = 1230$ M$^{-1}$   at $I = 0$ | (74a) |
| | $K_1 = 200$ M$^{-1}$   at $I = 0.5$ | (74a) |
| | $K_1 = 74$ M$^{-1}$   at $I = 1.0M$ | (58) |
| Stability constant of outer sphere complex, $\dfrac{[Cr(H_2O)_6]^{3+}}{[SCN^-]}$ | $K_1^{out} = 0.1$ M$^{-1}$<br><br>(i.e. extent of association negligible<br><br>in dilute solutions). | (77) |
| Acid dissociation constant of $[Cr(H_2O)_6]^{3+}$ | $K_{a1} = 1.58 \times 10^{-4}$ M | (76) |
| | $K_{a1} = 1.5 \times 10^{-4}$ M | (66) |
| Rate of formation of $[Cr(NCS)_2]^+$ | No literature data. | |
| Stepwise stability constant of $[Cr(NCS)_2]^+$ | $K_2 = 130$ M$^{-1}$ | (58) |
| Rate of aquation of $[Cr(H_2O)_5NCS]^{2+}$ | 1st. order rate constant = $9 \times 10^{-9}$ sec$^{-1}$ for $[H^+] > 0.05M$ and $I = 0.3-1.0M$ | (74a) |

Both $[Cr(H_2O)_6]^{3+}$ and $[Cr(H_2O)_5NCS]^{2+}$ are octahedral, high-spin complexes. Thiocyanate is an ambident ligand, which tends to form isothiocyanates (N-attached) with class (a) metal ions and thiocyanates (S-attached) with class (b) metal ions (78). Class (a) metal ions are those which form their most stable complexes in water with the first ligand atom of each periodic group, i.e. N, O, F. Class (b) metal ions are those which form their most stable complex with the second or a subsequent ligand atom in each periodic group (79). Class (a) ions are more electro-positive than class (b) ions, and form their most stable complexes with unpolarisable, electronegative ligands.

$Cr^{3+}$ is a class (a) ion (80), and there is abundant evidence in the literature that it complexes to the linear thiocyanate ion through the N atom. This has been established for various thiocyanatochromium(III) ammines by X-ray crystallography (81,82,83) and by examination of C-N stretching frequencies by IR spectroscopy (81,84), and also for the compound $[\pi-(C_5H_5)Cr(NO)_2(NCS)]^0$ by IR spectroscopy (85).

No aquothiocyanato complexes seem to have been examined, but Cr-N bonding can be considered a virtual certainty in the ion $[Cr(H_2O)_5NCS]^{2+}$.

IV.2:    Experimental procedure.

IV.2.1: Preparation of reagents.

All solutions were made up in doubly distilled water, the second distillation being from alkaline permanganate solution in an all-glass apparatus.

(i) Perchloric acid solutions were made up by suitable dilution of AR grade perchloric acid supplied by British Drug Houses Ltd. The solutions were standardised by titration with sodium carbonate, using methyl orange as indicator.

(ii) GPR grade sodium thiocyanate was recrystallised twice from conductivity water, and dried in a desiccator in vacuum. Solutions were made up roughly by weight (the solid is deliquescent) and standardised by titration with silver nitrate, using eosin as adsorption indicator. The stock solution was stored in the dark and kept for not longer than a fortnight, to avoid possible deterioration.

(iii) Considerable difficulty was experienced in preparing a stock solution of pure chromic perchlorate.

The method employed by Poulsen, Bjerrum and
Poulsen (58), dissolution of freshly precipitated
chromic hydroxide in perchloric acid, produced greenish
solutions. The simple $[Cr(H_2O)_6]^{3+}$ ion is violet, and
the green species were found by ion-exchange and
spectrophotometric (86) experiments to be partly
hydrolysed polynuclear species of Cr(III). These were
troublesome to separate from the solution, and they
interfered with the spectrophotometric procedure for
following the reaction with thiocyanate.

The reduction of chromium trioxide dissolved in
perchloric acid by formic acid or hydrogen peroxide
was found to produce pure $[Cr(H_2O)_6]^{3+}$. Stock solutions
approximately 0.5M in $Cr(ClO_4)_3$ and 0.5M in $HClO_4$ were
prepared by modification of the method of Phipps and
Plane (77):

To prepare 1 litre of stock solution, 50g. (0.5 moles)
chromium trioxide were added to 2.0 moles perchloric
acid and 0.8 moles hydrogen peroxide in less than 1 litre
of water, and the whole heated gently on a water-bath to
start the reaction

$$2 \ CrO_3 + 3H_2O_2 + 6H^+ \rightarrow 2 \ Cr^{3+} + 3O_2 + 6H_2O \qquad (4.4)$$
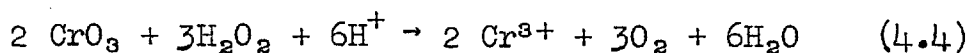
The solution was stirred without heating for at least
12 hours, after which time the reduction of orange
dichromate to violet Cr(III) was complete. Excess hydrogen
peroxide was destroyed by heating gently with powdered

platinum. The platinum was then filtered off, and the solution made up to 1 litre.

The stock solutions were analysed for chromium by oxidation with hydrogen peroxide of a diluted alkaline aliquot to chromate. The excess hydrogen peroxide was destroyed by heating, and chromate estimated spectrophotometrically at the 372mμ absorbance peak, at which $\varepsilon_{CrO_4^{2-}}$ was found to be $4.89 \times 10^3$.

The acid in the chromium(III) perchlorate solutions was estimated by a modification of the method of King and Neptune (87). Chromium(III) was converted to the inert oxalate complex by dissolving 15g. potassium oxalate (an excess) in 25ml. aliquots of solution. Acid was then estimated by potentiometric titration against sodium hydroxide, using a Radiometer pH meter, a glass electrode and a reference calomel electrode. Local excess of base, which hydrolysed the chromium(III) oxalate complexes, was avoided. The pH at the end point was about 7-8.


IV.2.2: Spectrophotometric data.


The anation reaction (4.1) was followed spectrophotometrically at the intense ultra-violet absorbance peak of the product ion at 292mμ.

The spectra in the region 200-700mμ of the sodium thiocyanate and chromium(III) perchlorate solutions used

in these experiments are shown in Figure 1. They agree well with spectral data in the literature, as shown in Table VII, which also gives literature data for the ion $[Cr(H_2O)_5NCS]^{2+}$.

All spectral measurements were made with a Unicam SP.500 spectrophotometer or a Hitachi Perkin-Elmer 139 spectrophotometer, using matched silica cells of path length 0.5cm. or 1.0cm.

IV.2.3: Kinetic runs.

Suitable volumes of chromium(III) perchlorate solution, and extra perchloric acid if required, were placed in a 500ml. volumetric flask, and the volume of solution made up to about 450ml. with doubly distilled water. This solution, and some sodium thiocyanate stock solution, were equilibrated separately in a water tank thermostatted at $25.0\pm0.05^{\circ}C$. At time $t_0$, a known volume of thiocyanate was added to the volumetric flask, the volume made up to 500ml. and the flask shaken.

Initial concentrations in the reacting solutions were in the ranges:

| | | | |
|---|---|---|---|
| $[Cr(H_2O)_6]^{3+}$ | $2.5 \times 10^{-2}$ | – | $5.0 \times 10^{-2}$ M |
| $[SCN^-]$ | $3.6 \times 10^{-2}$ | – | $5.2 \times 10^{-2}$ M |
| $[H^+]$ | $2.5 \times 10^{-2}$ | – | $8.0 \times 10^{-2}$ M |
| Ionic strength | 0.22 | – | 0.44 M |

# FIGURE I: UV-VISIBLE SPECTRA OF THE IONS $[Cr(H_2O)_6]^{3+}$ AND $[Cr(H_2O)_5NCS]^{2+}$.



Molar extinction coefficient ($\epsilon$)

$\epsilon_{292} = 2.90 \times 10^3$

$[Cr(H_2O)_5NCS]^{2+}$

$[SCN]^-$

$[Cr(H_2O)_6]^{3+}$

Wavelength (m$\mu$)
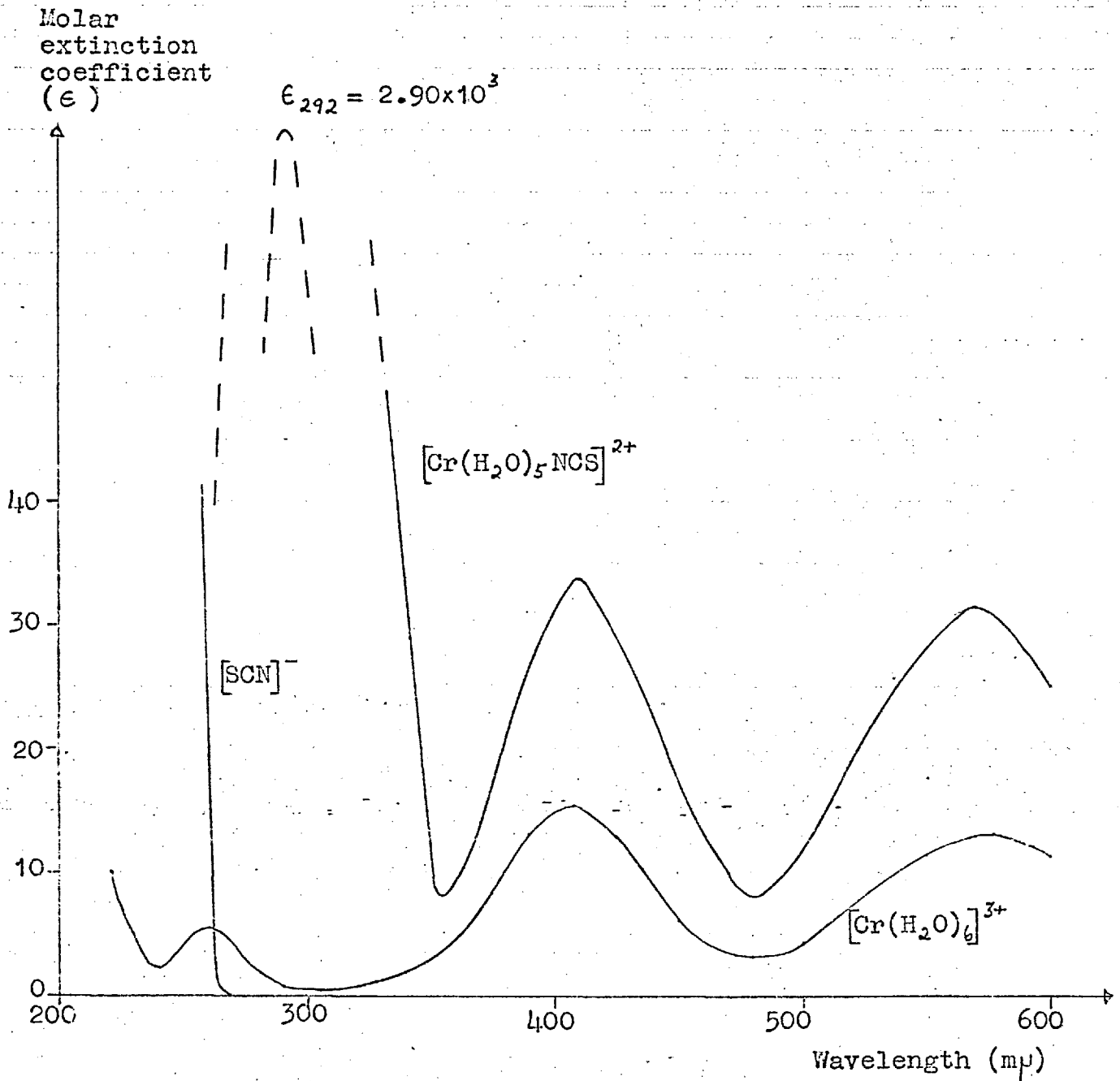
TABLE VII :   SPECTROPHOTOMETRIC DATA FOR THE IONS
$[Cr(H_2O)_6]^{3+}$,  $[Cr(H_2O)_5NCS]^{2+}$ and $SCN^-$.

| | Spectral maxima. | $\epsilon$ | Reference |
|---|---|---|---|
| $[Cr(H_2O)_6]^{3+}$ | 575mμ | 13.3 | Present work |
| | 570 | 13.4 | (86) |
| | 575 | 13.9 | (88) |
| | 408 | 15.5 | Present work |
| | 408 | 15.6 | (86) |
| | 407 | 16.1 | (88) |
| | 292 | 0.7 | Present work |
| | 292 | 0.7 | (74b) |
| $[Cr(H_2O)_5NCS]^{2+}$ | 570mμ | 31.5 | (89) |
| | 410 | 33.7 | (89) |
| | 292 | $2.90 \times 10^3$ | (74b) |
| $SCN^-$ | Onset of general absorbance below 260mμ | | Present work |
| | " | " | (90) |

The reaction at 25.0°C was followed for 4-5 hours
at the spectral maximum of the product ion $[Cr(H_2O)_5NCS]^{2+}$.
During this time, about 0.2% of the chromium(III) reacted
and caused the optical density, D, at 292mμ, to increase
by about 0.3 units per cm. cell length, from an initially
low value due to the $Cr^{3+}$ and $SCN^-$. As the change in
$[Cr^{3+}]$ and $[SCN^-]$ during each run was small, plots of
$D_{292}$ against time were linear, and the rate constant, $k_2$
in equation (4.2a), was calculated from the slope of the
plots by the equation

$$k_2 = \frac{\text{Increase in } D_{292} \text{ per cm. cell length per unit time}}{\varepsilon \text{ product } [Cr(H_2O)_6]^{3+}_{t=0} \quad [SCN^-]_{t=0}} \qquad (4.5)$$

The position of equilibrium in the $Cr^{3+}$ - $SCN^-$
solutions used in these experiments can be calculated by
standard algebraic methods, from knowledge of the stability
constants. Ignoring the formation of complexes with more
than two thiocyanate ligands, it was calculated that at
equilibrium, roughly one-third of the total Cr(III) was
present as $[Cr(H_2O)_6]^{3+}$, one-third as $[Cr(H_2O)_5NCS]^{2+}$ and
one-third as $[Cr(H_2O)_4(NCS)_2]^+$.

The back reaction, the aquation of $[Cr(H_2O)_5NCS]^{2+}$,
can be ignored in these experiments, as shown by the data
of Table VI, pages 40-41. There are no literature data
on the rate of reaction of $[Cr(H_2O)_5NCS]^{2+}$ with $NCS^-$:
it was assumed that this reaction was also negligible.

Measurements at 292mμ were made using water as a

reference liquid. The literature value of $\varepsilon$ product, $2.90 \times 10^3$ (74b), was used in equation (4.5).

The shape of the 292m$\mu$ product peak is not reported in the literature. To observe the developing shape during a run, thiocyanate solution was used as reference liquid to avoid the onset of thiocyanate absorbance below 260m$\mu$ obscuring the 292m$\mu$ peak. During each run, the shape of this peak, and the visible spectrum between 300m$\mu$ and 600m$\mu$ were checked. The latter was changed negligibly by 0.2% of the anation reaction, and any distortion therefore indicated that another reaction was occurring.

The hydrogen ion concentration, $2.5 \times 10^{-2}$ - $8.0 \times 10^{-2}$ M, was such that path 1 (equation (4.2), page 40) was the predominant reaction path: only ~2.5% of the reaction occurs by path 2 when $[H^+] = 2.5 \times 10^{-2}$ M, and the contribution of path 3 is negligible. Higher concentration of acid were not used as thiocyanate deteriorates in media of pH<1. Even so, reaction mixtures left over a period of days invariably smelt of hydrogen sulphide.

Although $k_2$ varies with ionic strength, no background electrolyte was used, as it was thought that heterogeneous catalytic effects might thereby have been modified or suppressed. Experimentally determined values of $k_2$ varied between $1.64 \times 10^{-6}$ and $2.23 \times 10^{-6}$ M$^{-1}$sec$^{-1}$, according to $[H^+]$ and I. Heterogeneous runs were therefore always compared with homogeneous runs under identical conditions.

The change in ionic strength during each run was negligible.

Experimental values of $k_2$ were reproducible to $\pm 0.5\%$. Agreement with values calculated from Postmus' and King's expressions (4.2) and (4.3) was sometimes no better than $\pm 25\%$, but these workers used background electrolyte and lower concentrations of $Cr^{3+}$ and $SCN^-$.

Experiment showed that the homogeneous reaction was not subject to photochemical effects, so all experiments were carried out in normal laboratory lighting.

Heterogeneous runs were performed by immediately pouring the 500ml. solution prepared at time $t_0$ into a 500ml. conical flask containing a weighed amount of solid and a magnetic stirrer encased in Teflon. The conical flask was placed in the thermostat at 25°C, and the system stirred during the run to form a slurry of solid and reacting solution.

Small aliquots ($<$3ml.) were removed with a plain pipette from the reaction vessels at roughly 25 minute intervals and $D_{292}$ measured. Heterogeneous samples were centrifuged for 30-40 sec. at top speed in a Gallenkamp Junior Centrifuge. Samples were not returned to the reaction vessels, which were stoppered except during removal of aliquots for analysis. By removing a small quantity of solid with each heterogeneous aliquot, the amount of solid per unit volume remained roughly unchanged,

and therefore no sampling correction was applied to these heterogeneous results. Despite use of the centrifuge, heterogeneous plots tended to be rather more scattered than homogeneous ones, but they were clearly linear.

IV.3: Experimental results.

Kinetic data for two typical homogeneous runs are tabulated in Table VIII, and plotted in Figure II.

The effects of various solid substances on the rate of the anation reaction were investigated, and the results are summarised in Table IX, page 55, Table X, page 56 and Figure III, page 57. Arbitrary quantities of each substance were used: in the case of powdered substances, the quantity taken was related to the apparent fineness of the powder, so that comparison might be made between samples with, very roughly, the same overall surface area.

Table IX lists the solids with no effect on the anation reaction. It was found that insoluble silver salts and silver itself were without effect, although they had a pronounced effect on the aquation rate of $[Co(NH_3)_5X]^{2+}$ (see Part III). Similarly, HgS, and the mercuric halides, although the latter are rather soluble, had no effect, although $[Hg^{2+}]$ in both the homogeneous and heterogeneous

## TABLE VIII : TYPICAL KINETIC DATA FOR THE REACTION

$$[Cr(H_2O)_6]^{3+} + SCN^- \rightarrow [Cr(H_2O)_5NCS]^{2+} + H_2O$$
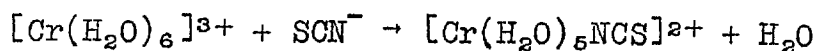
### IN ACID MEDIA AT 25.0°C.

| RUN 1. | | RUN 2. | |
|---|---|---|---|
| $[Cr(H_2O)_6]_0^{3+}$ = 4.944x10⁻² M | | $[Cr(H_2O)_6]_0^{3+}$ = 4.945x10⁻² M | |
| $[CNS^-]_0$ = 4.721x10⁻² M | | $[CNS^-]_0$ = 3.636x10⁻² M | |
| $[H^+]$ = 8.096x10⁻² M | | $[H^+]$ = 4.933x10⁻² M | |
| I = 0.4428 M | | I = 0.3841 M | |
| TIME | $D_{292m\mu}$* | TIME | $D_{292m\mu}$ |
| 0 min. | 0.047(extrap.) | 0 min. | 0.044(extrap.) |
| 37 " | 0.0808 | 40 " | 0.0656 |
| 59 " | 0.0990 | 64 " | 0.0763 |
| 84 " | 0.1250 | 96 " | 0.0933 |
| 111 " | 0.1500 | 128 " | 0.1103 |
| 139 " | 0.1738 | 153 " | 0.1248 |
| 166 " | 0.1982 | 181 " | 0.1390 |
| 210 " | 0.2360 | 207 " | 0.1522 |
| 238 " | 0.2625 | 239 " | 0.1700 |
| 266 " | 0.2860 | 263 " | 0.1842 |
| 293 " | 0.3100 | 286 " | 0.1950 |
| 336 " | 0.3480 | 306 " | 0.2105 |
| 364 " | 0.3750 | 330 " | 0.2180 |
| | | 355 " | 0.2305 |
| Experimental $k_2$=2.20x10⁻⁶ M⁻¹sec⁻¹ | | Experimental $k_2$=1.69x10⁻⁶ M⁻¹sec⁻¹ | |
| Calc.from equation (4.2), $k_2$=2.02x10⁻⁶ M⁻¹sec⁻¹ | | Calc.from equation (4.2), $k_2$=2.19x10⁻⁶ M⁻¹sec⁻¹ | |

*Optical measurements taken in cells of path length 1.0cm. against a water blank.

# FIGURE II: TYPICAL PLOTS OF $D_{292}$ vs. TIME

## (Data from Table VII)

Percentage of reaction that has occurred in

Run 1 = 0.23%

Run 2 = 0.13%
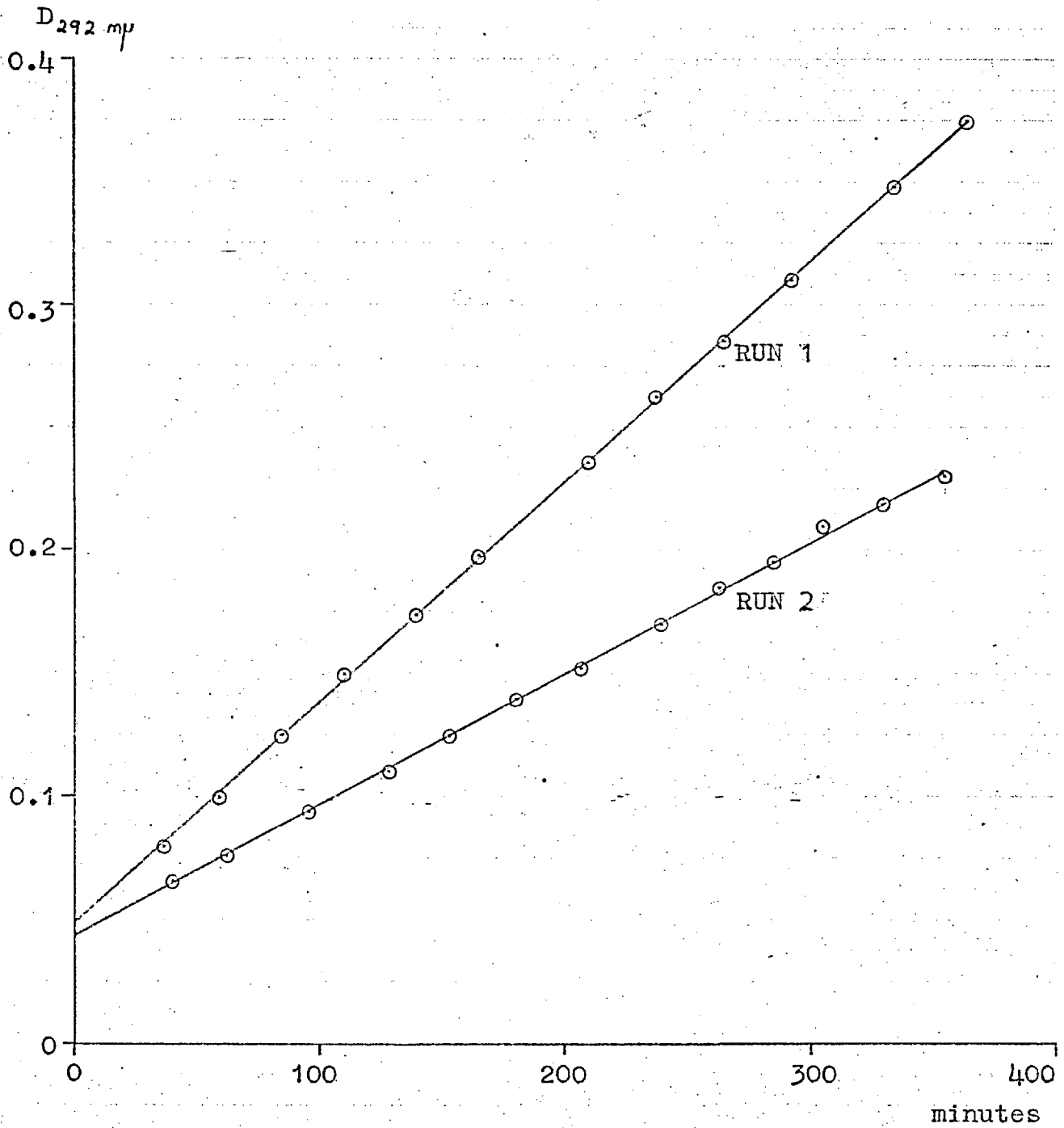
## TABLE IX : SOLIDS WITH NO EFFECT ON THE RATE AND COURSE OF THE ANATION REACTION (4.1).

| Solid | Quantity | Source |
|---|---|---|
| Pd powder | 0.4g. | Johnson Matthey. |
| Au powder | 0.85g. | "          " |
| Ag powder | 0.65g. | "          " |
| Ag foil | Surface area 39cm² | "          " |
| AgSCN | 0.65g. | Freshly precipitated |
| $Ag_2S$ | 1.6g. | "          " |
| AgI | 0.65g. | B.D.H. |
| Si | 1.2g. | B.D.H.;purified from iron in laboratory. |
| $SiO_2$ | 0.25g. | |
| S | 1.5g. | Freshly precipitated |
| Activated de-colourising charcoal. | 0.65g. | Hopkin and Williams. |
| HgS | 1.0g. | B.D.H. |
| TlI | 0.75g. | " |
| CuBr | 0.4g. | " |
| $BaSO_4$ | 1.3g. | " |
| Crushed pyrex glass. | 2.0g. | |
| Stainless steel turnings. | 0.5g. | |

## TABLE X : SOLIDS WITH AN EFFECT ON THE ANATION REACTION.

| Solid[*] | Mass used in 500ml. | Overall $k_2, M^{-1}sec^{-1}$ | Homogeneous $k_2, M^{-1}sec^{-1}$ | Remarks | Conclusion |
|---|---|---|---|---|---|
| CdS | 0.10g. | $2.25 \times 10^{-6}$ | $2.15 \times 10^{-6}$ | | Slight catalyst. |
| PbS | 0.84g. | $2.85 \times 10^{-6}$ | $2.15 \times 10^{-6}$ | $D_0$ at 292m$\mu$ rather high due to slight solubility of PbS. | Slight catalyst. $[Pb^{2+}]$ in solution is limited by $[SCN^-]$ |
| $HgCl_2, HgBr_2, HgI_2$ | ~0.5g. | $2.18 \times 10^{-6}$ | $2.18 \times 10^{-6}$ | Some solid dissolves giving slightly high $D_0$, but no other effect. | $[Hg^{2+}]$ in solution is limited by $[SCN^-]$. $[Hg^{2+}]$ not a homogeneous or a heterogeneous catalyst. |
| $Hg_2Cl_2, Hg_2Br_2, Hg_2I_2$ | $\leq$0.01g.<br><br>eg.0.1g. $Hg_2Br_2$ | <br><br>$8.46 \times 10^{-6}$ | <br><br>$1.64 \times 10^{-6}$ | Apparent 5-10 fold increase in reaction rate. | $SCN^-$ induces disproportionation of $Hg_2^{2+}$. Apparent rate constant decreases when surface reaction complete. |
| Pt powder. | 2.15g. | $2.51 \times 10^{-6}$ | $2.23 \times 10^{-6}$ | | Slight catalyst. |
| Hg(re-distilled) | 27.5g. | $2.09 \times 10^{-6}$ | $1.69 \times 10^{-6}$ | | Slight catalyst. |

[*] All compounds supplied by BDH; Pt supplied by Johnson Matthey.

FIGURE III: KINETIC PLOTS FOR REACTION (4.1) IN THE PRESENCE OF CATALYSTS (see Table X).
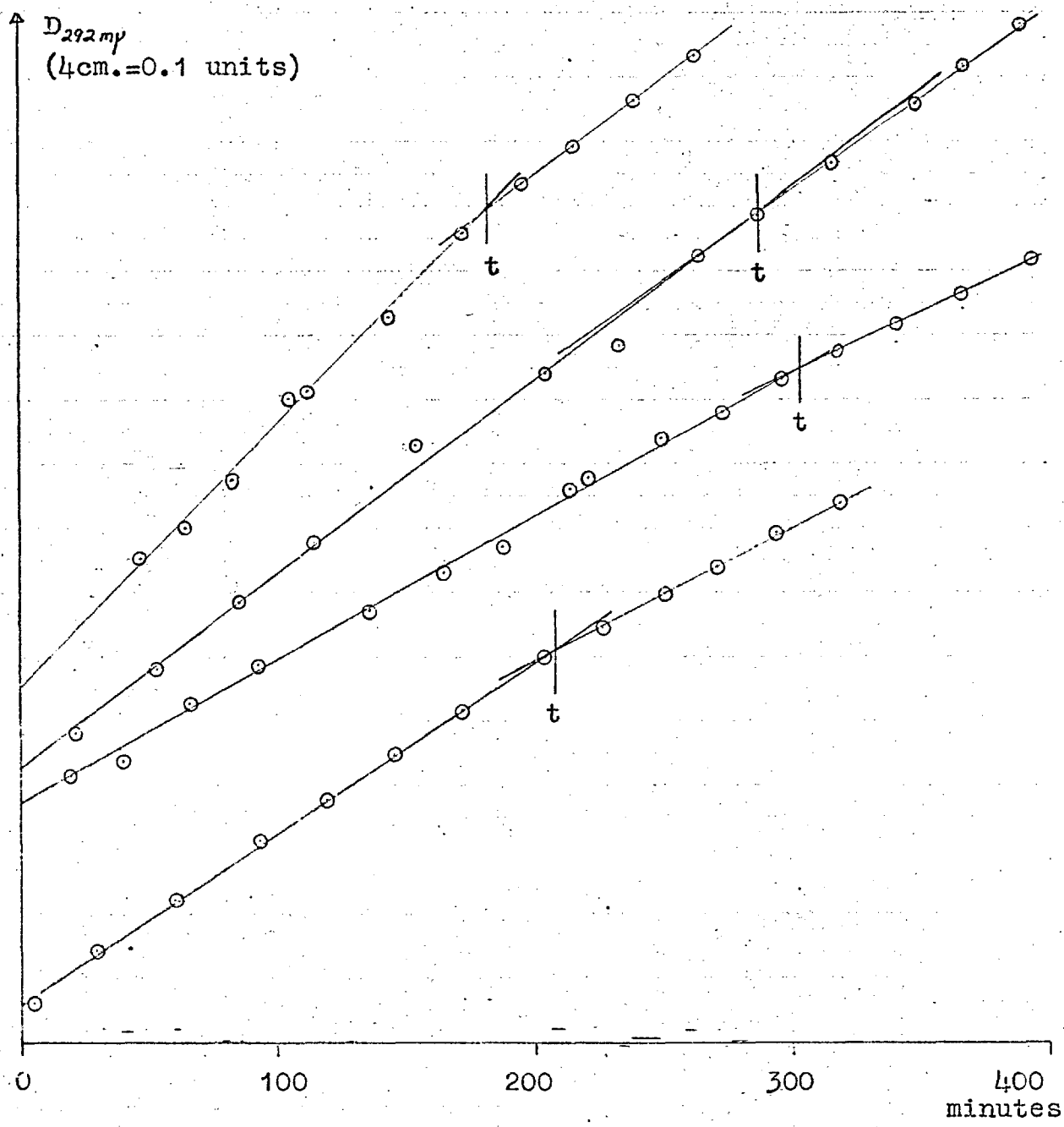
| Molar conc. | $10^2 \left[Cr^{3+}\right]$ | $10^2 \left[SCN^-\right]$ | $10^2 \left[H^+\right]$ | Ionic strength |
|---|---|---|---|---|
| a) Hg | 4.959 | 3.636 | 4.933 | 0.3841 |
| b) Pt powder | 2.479 | 5.023 | 2.467 | 0.2236 |
| c) CdS<br>d) PbS | 4.008 | 5.042 | 3.850 | 0.3294 |

At time t, the heterogeneous catalyst is removed.

states was found to be a catalyst for the aquation of $[Co(NH_3)_5X]^{2+}$. Charcoal has long been known as an effective catalyst for the interconversion of various cobaltammines (see Chapter II) but it had no effect on the anation reaction.

Insoluble salts of the ions $Hg(II)$, $Tl(I)$ and $Cu(I)$, all of which complex with thiocyanate in homogeneous solution, were also without effect.

Contamination of commercially supplied silicon and silica with iron was discovered by the appearance of the characteristic $[FeSCN]^{2+}$ absorbance peak at $450m\mu$ (91) during runs, and confirmed by spot tests. After thorough washing in perchloric acid to remove iron, silicon and silica were found not to be catalysts.

Surprisingly, stainless steel turnings did not produce $[FeSCN]^{2+}$ complexes: their surface was presumably passivated.

Table X lists the solids which had an effect on the anation reaction. Re-distilled mercury, platinum powder, CdS and PbS were found to be heterogeneous catalysts. The appearance of the $[Cr(H_2O)_5NCS]^{2+}$ absorbance peak at $292m\mu$ was followed for each, no side effects were observed, and the rate returned to the homogeneous value on removing the catalyst. Figure III illustrates runs carried out in the presence of these solids.

One square inch of shiny or of platinised platinum foil had no catalytic effect, presumably because their surface areas were too small. The effect of a platinum rotating disc, of active surface area of about 30cm² was also investigated. It was found that thiocyanate caused corrosion of the stainless steel former of the disc, which became discoloured in a few pin-holes around previously invisible holes in the protective Araldite coating on the former: $[FeSCN]^{2+}$ appeared in solution. Use of the disc was therefore discontinued.

Mercury was rather a slight catalyst, despite the fact that vigorous stirring during the run caused it to separate into a great many small droplets. Chrono-coulometric measurements have shown that thiocyanate and mercuric thiocyanate are adsorbed on a mercury electrode (92).

The mercurous halides were at first thought to be excellent catalysts for the anation reaction. However, the product peak at 292mµ was distorted in their presence, and it was discovered from subsidiary experiments that thiocyanate in solution induces a slow disproportionation of insoluble mercurous compounds to Hg(II) and Hg(0). Induced disproportionation of Hg(I) in solution was found to be very rapid by comparison, but the net result was the same. A greyish precipitate, a mixture of mercury and mercuric thiocyanate, was formed, and a rather broad

and ill-defined absorbance peak with a maximum at
about 280m$\mu$ appeared. This was due to the formation
of intensely absorbing, very stable Hg(II)-SCN$^-$ complexes
in low concentration in solution (93). Formation of
these complexes was thought to be the reason why the
slightly soluble mercuric halides gave rise to high
$D_0$ values at 292m$\mu$.

It is possible that mercurous salts are hetero-
geneous catalysts for the anation reaction, but because
of the slowness and irreproducibility of the induced
disproportionation, experiments to prove or to disprove
catalysis could not be devised.

IV.4:    Discussion of results.


IV.4.1:    Discussion of the nature of the heterogeneous
           catalysts.


Cadmium and lead sulphides, platinum and mercury
were found to be catalysts for the reaction between $Cr^{3+}$
and $SCN^-$.  Figure III, page 57, illustrates the kinetic
data summarised for these substances in Table X.  Mercuric
and silver halides and sulphides, among other substances,
were non-catalysts.

Very tentative and qualitative rationalisation of
these observations is possible by use of Pearson's SHAB
(soft and hard acids and bases) hypothesis (94).  This is
an extension of the Ahrland-Chatt classification of metal
ions as (a)- or (b)-type.  Pearson divides bases and
acids (i.e. electron donors and acceptors) into those
that are non-polarisable, or "hard", and those that are
polarisable, or "soft".  The SHAB principle is that acids
and bases of the same class react together more quickly,
and form more stable complexes, than do acids and bases
of different classes:  this is rationalised by elementary
considerations of bonding compatibility.  These requirements
may not be very rigorous, however, as all Lewis-type
interactions are composed of some electrostatic ("hard")
and some covalent ("soft") contributions, and "hardness"

and "softness" are not mutually exclusive. For example, an electrostatic interaction must always exist between donor and acceptor if ions are involved.

As discussed in the next section, it is necessary that a catalyst should adsorb both $Cr^{3+}$ and $SCN^-$ to some extent to catalyse the anation reaction.

Chromium(III) is a "hard" or (a)-class metal ion, as the order of stability of the aqueous complexes formed with halide is F>Cl>Br>I (48,79). However, the differences in stability are comparatively slight, and $Cr^{3+}$ is not so typically (a)-class as, say, $Li^+$ or $Mg^{2+}$ (80). Transition metal ions with less than 5d electrons are (a)-class because they do not have enough polarisable electrons on a high energy level to exhibit (b)-character (95).

Thiocyanate has an electronic structure described in valence bond terminology:

$$S = C = N^\ominus \rightleftharpoons {}^\ominus S - C \equiv N$$
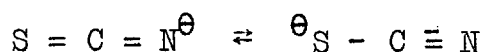
Nitrogen is more electronegative than sulphur, and the permanent dipole on the N atom is larger. The lone pair on sulphur is more easily polarised than the lone pair on nitrogen. Thiocyanate therefore complexes to (b)-class metal ions, such as Pt(II), Pd(II), Ag(I) and Hg(II), through S, and (a)-class metal ions, such as Cr(III), and even Zn(II), Cd(II) and Ni(II), through N (96). Thiocyanate also readily forms bridges between Ag(I), Pd(II), Pt(II), Hg(II) and Tl(I) ions, so the different-

iation between the S and N atoms is not great (96).

According to the SHAB hypothesis, a catalyst for the anation reaction should possess sites which adsorb both $Cr^{3+}$ and $SCN^-$. The catalyst should therefore possess "hard", or fairly hard, base sites for adsorption of $Cr^{3+}$. If $SCN^-$ is adsorbed by the S end, or with the linear molecule parallel to the surface so that $\pi$-orbital overlap occurs, the catalyst requires "soft" acid sites, but if the N end is adsorbed, fairly "hard" acid sites are required.

It is proposed that the catalysts for the $Cr^{3+} - SCN^-$ reaction possess the two kinds of site required.

Both cation and anion sites in the non-catalysts HgS, TlI, CuBr, $Ag_2S$, AgI and AgSCN(?) are soft, and these substances are non-catalysts. Both sites in $BaSO_4$ are extremely hard ($Ba^{2+}$ does not form ammine complexes in aqueous solution) and this substance is also a non-catalyst.

Cadmium(II) and lead(II), however, have rather weak (b)-character, because the full d-electron shells are rather well shielded by the outer two s electrons (80). (Lead(IV) shows more pronounced (b)-character than lead(II)). CdS and PbS could be catalysts by adsorbing $Cr^{3+}$ on sulphide sites, and thiocyanate through N on metal ion sites. A cis-attack of thiocyanate on $Cr^{3+}$ could then follow. However, sulphide is rather "soft" and does not complex with $Cr^{3+}$ in aqueous solution, so this explanation

is not wholly convincing.

The existence of two types of site on platinum surfaces at rest potential in aqueous solution has been suggested (97), to account for the observation that $Tl^+$ and $Tl^{3+}$ are additively, not competitively, adsorbed on platinum. $Tl^{3+}$ appears to adsorb specifically on oxidised $Pt(OH)_2$ sites, $Tl^+$ on vacant Pt sites. By analogy, $Cr^{3+}$ could adsorb on the "hard" oxidised sites, $SCN^-$ on the "softer" metal sites.

However, why platinum and mercury, but not the similar noble metals gold, silver and palladium, should be catalysts, is not clear. The difference may not be as absolute as suggested by these experiments, which, as discussed in the next section, were not carried out under optimum conditions.

IV.4.2:  Discussion of the magnitude of the catalytic effects.

The heterogeneous catalysts found for the reaction of $Cr^{3+}$ with $SCN^-$ all had rather small effects. At the time at which the work was done, it was not realised how the experiments might have been modified to observe greater effects, and consequently, no quantitative investigation of the catalysts was carried out. Subsequent experiments on the catalysis of the $[Co(NH_3)_5X]^{2+}$

aquation reaction, however, threw light on the importance of factors disregarded at the time, and these will now be discussed.

The rate-determining step of the reaction between $Cr^{3+}$ and $SCN^-$ on the catalysts is clearly a surface step. In a vigorously stirred solution, diffusion-controlled catalysis would be a much faster process.

The most simple and most probable rate law for the surface-controlled catalytic reaction between $Cr^{3+}$ and $SCN^-$ is

$$v_{het} = A \, k_{het} [Cr^{3+}]_{ads} [SCN^-]_{ads} , \qquad (4.6)$$

where $v_{het}$ = no. of moles $[Cr(NCS)]^{2+}$ produced per unit time,

$\qquad A$ = area of catalyst surface,

$[Cr^{3+}]_{ads}, [SCN^-]_{ads}$ = no. of moles of $Cr^{3+}$, $SCN^-$ respectively adsorbed on unit area of catalyst surface.

This rate law is similar in form to the homogeneous rate law (4.2a) which may be expressed:

$$v_{hom} = V \, k_2 [Cr^{3+}]_{bulk} [SCN^-]_{bulk} \qquad (4.7)$$

where V litres is the volume of solution.

Although the validity of equation (4.6) has been in no way tested, it is proposed because it is exactly analogous to the rate law found for the heterogeneous catalysis of the aquation of $[Co(NH_3)_5X]^{2+}$ (see Part III), and also to the rate law for the heterogeneously catalysed

$Tl^+/Tl^{3+}$ electron exchange on platinum (97). These
are discussed in detail in Part III. The important
point is that the concentration of adsorbed reactants
should be well described by Langmuir or Freundlich
adsorption isotherms. In other words, the reactants
quickly reach adsorptive equilibrium on the catalyst
surface, and then react, the rate constant $k_{het}$ varying
only slightly with large changes in the bulk reactant
concentrations.

A typical Langmuir adsorption isotherm for a species
i is shown in Figure IV:

FIGURE IV : THE LANGMUIR ADSORPTION ISOTHERM.
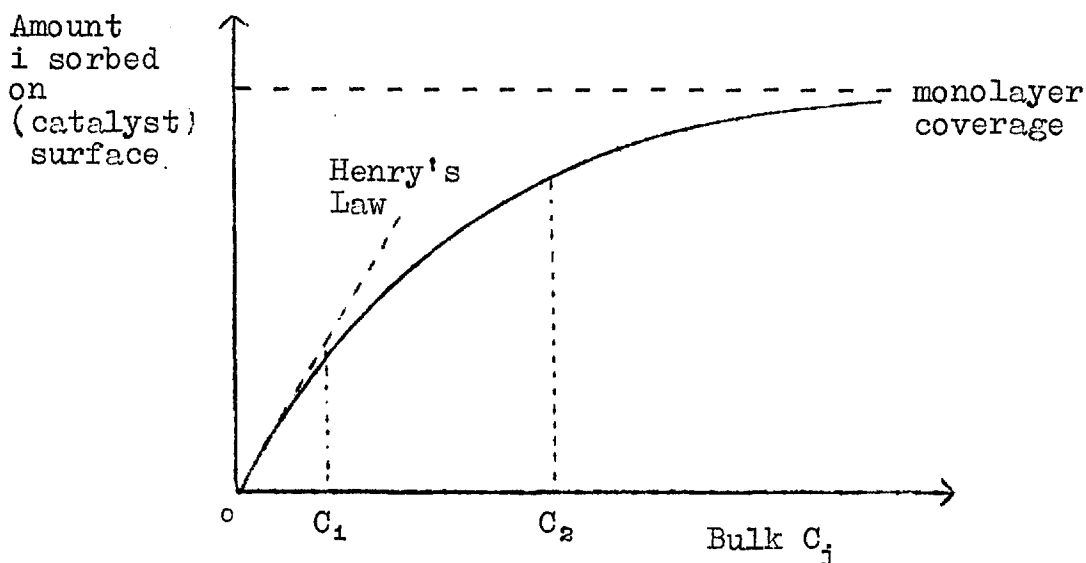


In the concentration range 0 to $C_1$, Henry's Law is
obeyed, i.e. $[C_i]_{ads}$ is proportional to $[C_i]_{bulk}$.

Assuming $[Cr^{3+}]_{ads}$ and $[SCN^-]_{ads}$ in equation (4.6) to be governed by Langmuir isotherms, then the ratio $v_{het}/v_{hom}$ in this concentration range is a constant. Equations (4.6) and (4.7) show that this ratio will then depend on the ratio $k_{het}/k_2$, (i.e. $k_{het}/k_{hom}$).

In the concentration range $C_1$ to $C_2$, $[C_i]_{ads}$ increases less rapidly with $[C_i]_{bulk}$ than indicated by Henry's Law. The ratio $v_{het}/v_{hom}$ therefore drops continually.

Above the concentration $C_2$, monolayer coverage of the surface is achieved. $v_{het}$ therefore remains substantially constant, but $v_{hom}$ will increase as some function of $C_i$. The ratio $v_{het}/v_{hom}$ may therefore become very small.

The concentration range in which a search for heterogeneous catalytic effects is made is therefore most important. If $k_{het}$ is very small, or zero, then the ratio $v_{het}/v_{hom}$ will be negligibly small even at very low concentrations. However, even if $k_{het}$ is quite large, the overall catalytic effect will appear small if experiments are confined to the concentration region $C_i \gg C_2$.

Comparison of equations (4.6) and (4.7) shows that the overall rate of the heterogeneous reaction may be increased compared to the overall rate of the homogeneous reaction by the following means:

(i)  decreasing the bulk concentration of reactants, until $C_i$ is not greatly larger than $C_2$, as explained above. However, this may make the actual rates of reaction inconveniently slow, and analytical methods difficult to apply.

(ii)  increasing the surface area of the catalyst. If the catalyst is powdered, the maximum amount that can be used is limited by the amount that can be properly stirred.

(iii)  decreasing the volume of solution. However, the smaller the volume, the greater the sampling correction that may have to be applied to quantitative work.

(iv)  lowering the temperature. As explained in Chapter I, $\Delta H^{\ddagger}_{het}$ is always less than $\Delta H^{\ddagger}_{hom}$, so $k_{het}$ becomes larger compared with $k_{hom}$ as the temperature is lowered. Again, the overall rate may become inconveniently slow, unless the catalytic reaction is rather fast.

It is retrospectively apparent that the concentrations of $Cr^{3+}$ and $SCN^-$ used in these experiments did not fulfil the conditions set out in (i) above. Assuming, as a rough guide, that $Cr^{3+}$ and $SCN^-$ each occupy half the surface at monolayer coverage, and that each ion occupies 25 $\overset{o}{A}^2$, then $[Cr^{3+}]_{ads}$ and $[SCN^-]_{ads}$ are both roughly

$3\times10^{-10}$ moles cm$^{-2}$ at monolayer coverage. In 500ml.
of solution, there were altogether roughly $2\times10^{-2}$ moles
of each reactant. Even with a catalyst of surface
area $10^6$cm$^2$, the "homogeneous" concentration is still
at least $10^2$ times greater than the "heterogeneous"
concentration, so the ratio $v_{het}/v_{hom}$ is bound to be
slight unless the ratio $k_{het}/k_{hom}$ is rather large.

It is therefore not surprising that the hetero-
geneous catalytic effects observed were rather slight.
There was, regrettably, no time to carry out a modified
series of experiments, but the following suggestions are
made for possible future work on the Cr$^{3+}$ - SCN$^-$ reaction.

(i) The catalytic effect of platinum could be further
investigated, using heavily platinised platinum
surfaces, as did Jonasson and Stranks (97).
1cm$^2$ of smooth surface can be platinised to yield
a real surface area of over $10^3$cm$^2$, so high surface
areas are readily available.

(ii) The bulk concentrations of reactants should be
reduced by at least ten-fold. This would reduce
the rate of the homogeneous reaction by 100-fold,
so days rather than hours would be required for
each homogeneous run. The heterogeneous reaction,
however, should be considerably faster in proportion.

(iii) The heterogeneous rate should be investigated as a function of both $[Cr^{3+}]_{bulk}$ and $[SCN^-]_{bulk}$, and this related to the separately determined adsorption isotherms.

(iv) The activation energy of the heterogeneous reaction should be determined from experiments over a temperature range of 20-30°. It should be larger than for a diffusion controlled reaction, but smaller than for the homogeneous reaction.

(v) A Langmuir-Hinshelwood mechanism for the catalytic reaction, as expressed by equation (4.6) seems much more likely than an Eley-Rideal mechanism, in which only one of the two reactants is adsorbed on the catalyst surface. However, both possibilities should be borne in mind.

IV.5: The reaction $[Cr(H_2O)_6]^{3+} + Cl^- \rightarrow [Cr(H_2O)_5Cl]^{2+} + H_2O$

As thiocyanate is not particularly stable, and as it causes disproportionation of mercurous compounds, use of a halide as anating ligand might seem preferable. $[Cr(H_2O)_5Br]^{2+}$ and $[Cr(H_2O)_5I]^{2+}$ are too unstable thermodynamically for $Br^-$ or $I^-$ to be used (98,64), but use of $Cl^-$ is possible. Production of $[Cr(H_2O)_5Cl]^{2+}$ can be followed spectrophotometrically in the ultra-violet (64). The rate of anation of $Cr^{3+}$ by $Cl^-$ is not much slower than for $SCN^-$ but the position of equilibrium is less favourable (99). If $[Cr^{3+}]_{bulk}$ is to be kept low, this means rather high bulk concentrations of $Cl^-$ will have to be used.

The catalytic effect of $Hg^{2+}$, $HgCl^+$ and $HgCl_2$ (53) on the aquation of $[Cr(H_2O)_5Cl]^{2+}$ was mentioned in Table III, page 30. It may be added, however, that freshly precipitated AgCl did not catalyse the aquation of $[Cr(H_2O)_5Cl]^{2+}$ (52).

PART III


HETEROGENEOUS CATALYSIS OF Co(III) REACTIONS

# CHAPTER V : THE HOMOGENEOUS AQUATION OF $[Co(NH_3)_5Br]^{2+}$ AND $[Co(NH_3)_5Cl]^{2+}$.

The reactions

$$[Co(NH_3)_5Br]^{2+} + H_2O \underset{k_{-1}}{\overset{k_1}{\rightleftarrows}} [Co(NH_3)_5H_2O]^{3+} + Br^- \quad (5.1)$$

and $[Co(NH_3)_5Cl]^{2+} + H_2O \underset{k_{-1}}{\overset{k_1}{\rightleftarrows}} [Co(NH_3)_5H_2O]^{3+} + Cl^- \quad (5.2)$
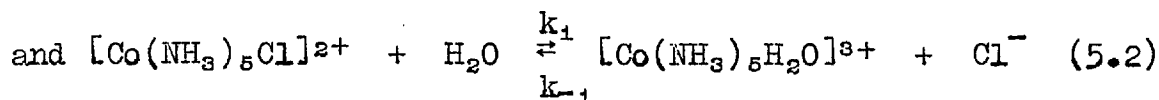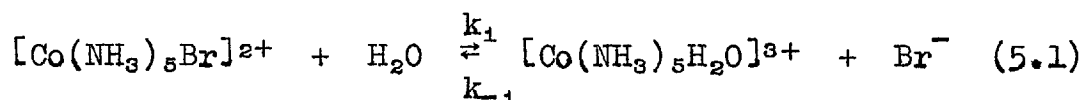
are suitable for the study of heterogeneous effects, for the general reasons given in Chapter III. The forward reactions proceed virtually to completion in dilute solution, and the reaction rates at 25°C are convenient and independent of pH in the range 1-4. The course of the reactions is easily followed spectrophotometrically.

Several literature examples of the homogeneous and heterogeneous catalysis of reactions (5.1) and (5.2) were. mentioned in Chapter II.

Preliminary work on the catalysis of reactions (5.1) and (5.2) was qualitative, and is described in Chapter VI. The best catalysts were then studied in more detail, and quantitative work with HgS, AgBr and Pt is reported in Chapters VIII, IX and X respectively. Chapter VII is a general introduction to the quantitative work. Chapter XI describes work carried out with a silver rotating disc on the redox reaction between silver and $[Co(NH_3)_5X]^{2+}$.

Aquation of the iodo-complex $[Co(NH_3)_5I]^{2+}$ was not studied because this complex also undergoes a slow autonomous redox reaction in solution, producing $Co(II)$ and iodine (100). Reference to $[Co(NH_3)_5X]^{2+}$ in this and subsequent chapters is a reference to $[Co(NH_3)_5Br]^{2+}$ and $[Co(NH_3)_5Cl]^{2+}$ only.

V.1 : Kinetics and mechanism of the homogeneous aquation of $[Co(NH_3)_5X]^{2+}$ in acid solution.

The aquation is a reversible process, as indicated in equations (5.1) and (5.2). The forward reaction is first order, the back reaction second order. Some data for reactions (5.1) and (5.2) are listed in Table XI.

Log-log plots show that $k_1$ correlates well with $K_{eq}$ and also with the basicity of $X^-$, where X = NCS, F, $H_2PO_4$, Cl, Br, I and $NO_3$ (109). From correlations such as these, the mechanism of the aquation reaction has been classified as "solvent assisted dissociation" (109). That is, the mechanism is predominantly bond-breaking, and the nature of the $X^-$ group in the transition state is the same as that in the product (110). The rate of aquation of a series of Co(III) complexes with chelating ligands shows that the incoming water ligand enters cis to the leaving group. The five-coordinate "intermediate" $[Co(NH_3)_5]^{3+}$ is probably square pyramidal in shape: this shape involves

TABLE XI : DATA FOR REACTION (5.3),

$$[Co(NH_3)_5X]^{2+} + H_2O \rightleftharpoons [Co(NH_3)_5H_2O]^{3+} + X^-,$$

at 25°C.

| | $[Co(NH_3)_5Br]^{2+}$ | $[Co(NH_3)_5Cl]^{2+}$ |
|---|---|---|
| Aquation rate constant, $k_1$ | $3.9 \times 10^{-4} \text{min}^{-1}$ (101) <br><br> $4.02 \times 10^{-4}\text{min}^{-1}(?)$ (70) <br><br> $(3.70 \pm 0.03) \times 10^{-4}\text{min}^{-1}$ <br><br> (present work) | $1.38 \times 10^{-4}\text{min}^{-1}$ (101) <br><br> $1.02 \times 10^{-4}\text{min}^{-1}$ (70) <br><br> $1.007 \times 10^{-4}\text{min}^{-1}$ (102) <br><br> $0.96 \times 10^{-4}\text{min}^{-1}$ (60) <br><br> $0.97 \times 10^{-4}\text{min}^{-1}$ (103) <br><br> $(1.01 \pm 0.01) \times 10^{-4}$ $\text{min}^{-1}$ (present work) |
| Anation rate constant, $k_{-1}$ | $(3.80 \pm 0.2) \times 10^{-4}\text{M}^{-1}\text{min}^{-1}$ <br> at I=0.01M (present <br> work) | $4.0 \times 10^{-4}\text{M}^{-1}\text{min}^{-1}$ <br> at I=0.05M (102) <br> $3.0 \times 10^{-4}\text{M}^{-1}\text{min}^{-1}$ <br> at I=0.12M (102) |
| $K_{eq} = \left[\dfrac{k_1}{k_{-1}}\right]$ | $0.98 \pm 0.07$M at I=0.01M <br> (present work) <br> 2.7M at I=0.5M (107) | 0.13M at I=0.0145M <br> (103) <br> 0.17M at I=0.0156M <br> (103) <br> 0.8M at I=0.5M <br> (104) |
| For aquation reaction <br> $\Delta H^{\ddagger}$ <br> $\Delta S^{\ddagger}$ | 24 kcal.mole$^{-1}$ (70) <br> -4 e.u. (70) | 23 kcal.mole$^{-1}$ (70) <br> -9 e.u. (70) |

## TABLE XI (contd.)

|  | $[Co(NH_3)_5Br]^{2+}$ | $[Co(NH_3)_5Cl]^{2+}$ |
|---|---|---|
| Base hydrolysis constant | $3.72 \times 10^2 M^{-1} min^{-1}$ at I=0    (105) | $89.4 M^{-1} min^{-1}$ at I=0   (105) |
| First acid dissociation constant | $< 10^{-14} M$   (106) | $< 10^{-14} M$   (106) |

loss of less crystal field stabilisation energy than
the alternative trigonal bipyramidal shape. In some
assisted aquations (47,111), a true $[Co(NH_3)_5]^{3+}$
intermediate is formed.

All Co(III) complexes are octahedral and all
(except $[CoF_6]^{3-}$) have a low-spin $t_{2g}^6$ configuration of
d electrons, giving rise to large crystal field stabili-
sation energy.

Base hydrolysis of $[Co(NH_3)_5X]^{2+}$ is a rapid second
order process (70,107), but the base-dependent path is
negligible in media of pH<5.

The product, $[Co(NH_3)_5H_2O]^{3+}$, is stable indefinitely
in acid solution, but tends to become colloidal in media
of pH≥4 (19). It is a weak acid (pKa≈6.2) (108), and
exchanges water slowly in solution ($k_{ex} = 3.533 \times 10^{-4} min^{-1}$)
(108) at 25°C.


V.2 : Preparation and analysis of reagents.


The salts $[Co(NH_3)_5Br]Br_2$ and $[Co(NH_3)_5Cl]Cl_2$ were
used for most experiments, as they are easy to prepare and
purify. Unlike the perchlorates, they contain no water
of crystallisation to exchange with the complexed halide.
In dilute solution, the free halide had a negligible
effect on the position of equilibrium (see Section (V.4)).

Doubly distilled water was used throughout the experiments, and A.R. perchloric acid solutions were standardised by titration against sodium carbonate.

$[Co(NH_3)_5Br]Br_2$ was prepared by oxidation of Co(II) in the presence of ammonia and bromide (112a): 46g.$CoBr_2$ (0.21 mole), 50g.$NH_4Br$(0.51 mole) and 250ml. concentrated ammonia (3.5 mole) were dissolved in water. 40ml. of 30% $H_2O_2$ (0.39 mole) were added slowly, with stirring. When vigorous effervescence ceased, the oxidation of Co(II) to the Co(III) complex $[Co(NH_3)_5H_2O]^{3+}$ was complete:

$$Co^{2+} + 5NH_3 + H_2O + \tfrac{1}{2} H_2O_2 \rightarrow [Co(NH_3)_5H_2O]^{3+} + OH^-$$

(5.5)
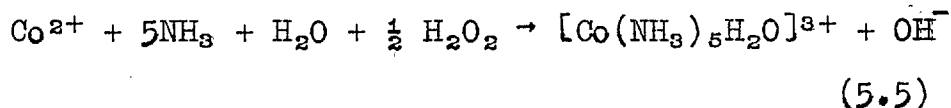
Excess $H_2O_2$ rapidly decomposed in the alkaline solution. Excess ammonia was removed by passing nitrogen through the solution for 3 hours. Concentrated HBr was then added until a precipitate of $[Co(NH_3)_5H_2O]Br_3$ persisted. Another 50ml. HBr was added, and the whole heated gently for 2 hours. Heat and the high bromide concentration caused quantitative conversion of $[Co(NH_3)_5H_2O]^{3+}$ to $[Co(NH_3)_5Br]^{2+}$, and $[Co(NH_3)_5Br]Br_2$ was precipitated. This was filtered off and purified by dissolving 25g. in 500ml. of 1M $NH_4OH$ at 90°C. $[Co(NH_3)_5H_2O]^{3+}$ was instantly re-formed, and again converted to $[Co(NH_3)_5Br]^{2+}$ by heating with 60ml. concen-

trated HBr. The precipitate of $[Co(NH_3)_5Br]Br_2$ was filtered off, washed in a little water and ether and dried at 110°C.

$\underline{[Co(NH_3)_5Cl]Cl_2}$ was prepared and purified by an exactly analogous method (112b).

$\underline{[Co(NH_3)_5Br](ClO_4)_2}$ was prepared by slow addition of cold concentrated perchloric acid to a saturated ($\sim 10^{-2}$M) solution of $[Co(NH_3)_5Br]Br_2$ in 3M $HClO_4$ at 10°C. The precipitate was filtered off, washed with cold water and methanol and dried at 110°C (113).

$\underline{[Co(NH_3)_5H_2O](ClO_4)_3}$ was prepared from $[Co(NH_3)_5CO_3](NO_3)$ (112c). The latter was prepared by dissolving 100g. $Co(NO_3)_2$ and 150g. $(NH_4)_2CO_3$ in 200ml. water and 250ml. concentrated $NH_4OH$, and passing air through the solution for 24 hours. Co(II) was oxidised to $[Co(NH_3)_5CO_3](NO_3)$, which was precipitated. The solution was cooled in an ice-salt bath overnight, and the deep red salt filtered off and washed with a little cold water. To convert to $[Co(NH_3)_5H_2O](ClO_4)_3$, a 0.5M solution of this salt in 2M $HClO_4$ was boiled (114). The product separated on cooling, and was recrystallised from dilute perchloric acid, and dried in a vacuum desiccator.

All salts were stored in the solid form in a desiccator.

The acidopentammine salts are moderately soluble in water (0.02-0.10M at 25. °C) and the aquopentammine salts are freely soluble (115). The $[Co(NH_3)_5H_2O]^{3+}$ ion is light red, the $[Co(NH_3)_5Br]^{2+}$ ion purple and the $[Co(NH_3)_5Cl]^{2+}$ ion is a somewhat reddish purple. These colours are not apparent in solutions more dilute than $5 \times 10^{-4}$M.

These salts were analysed by the following general method: a known weight of complex was destroyed by boiling in alkaline solution. The solution was then just acidified with nitric acid, and sulphur dioxide passed, to ensure Co(III) was completely reduced to Co(II). Excess sulphur dioxide was then boiled off, and the solution made up to a standard volume. The solution was analysed for halide by titration with silver nitrate, and for Co(II) by titration in a buffered alkaline solution with EDTA, using murexide as indicator (116). The results, expressed as percentages by weight, were:

| | | | |
|---|---|---|---|
| $[Co(NH_3)_5Br]Br_2$ | Co | 15.0 | (theor. 15.36) |
| | Br | 61.6 | (theor. 62.5) |
| $[Co(NH_3)_5Cl]Cl_2$ | Co | 23.2 | (theor. 23.53) |
| | Cl | 42.1 | (theor. 42.5) |
| $[Co(NH_3)_5H_2O](ClO_4)_3$ | Co | 12.6 | (theor. 12.7) |
| $[Co(NH_3)_5Br](ClO_4)_3 \cdot xH_2O$ | | Co:Br = 1:1.01 | |

V.3:  Spectrophotometric data.

The experimentally determined ultra-violet and
visible spectra of the ions $[Co(NH_3)_5Br]^{2+}$, $[Co(NH_3)_5Cl]^{2+}$
and $[Co(NH_3)_5H_2O]^{3+}$ are given in Figure V.  They are in
quite good agreement with literature data, as shown in
Table XII on page 83.

The $[Co(NH_3)_5X]^{2+}$ ions have an intense charge-transfer
band in the ultra-violet, which is absent in $[Co(NH_3)_5H_2O]^{3+}$.
All three have weaker d-d bands in the visible region.
Linhard and Weigel (117) showed that Beer's Law was obeyed
throughout the range 200-700mμ by all three ions.

The aquation reactions were followed by measurements
of the optical density, D, at a wavelength at which, in
general, both reactant and product absorbed.

The wavelengths used in kinetic runs are shown in
Table XIII on page 84.

82



FIGURE V: SPECTRA OF THE IONS $[Co(NH_3)_5Br]^{2+}$, $[Co(NH_3)_5Cl]^{2+}$ AND $[Co(NH_3)_5H_2O]^{3+}$ IN $10^{-2}M$ $HClO_4$. *
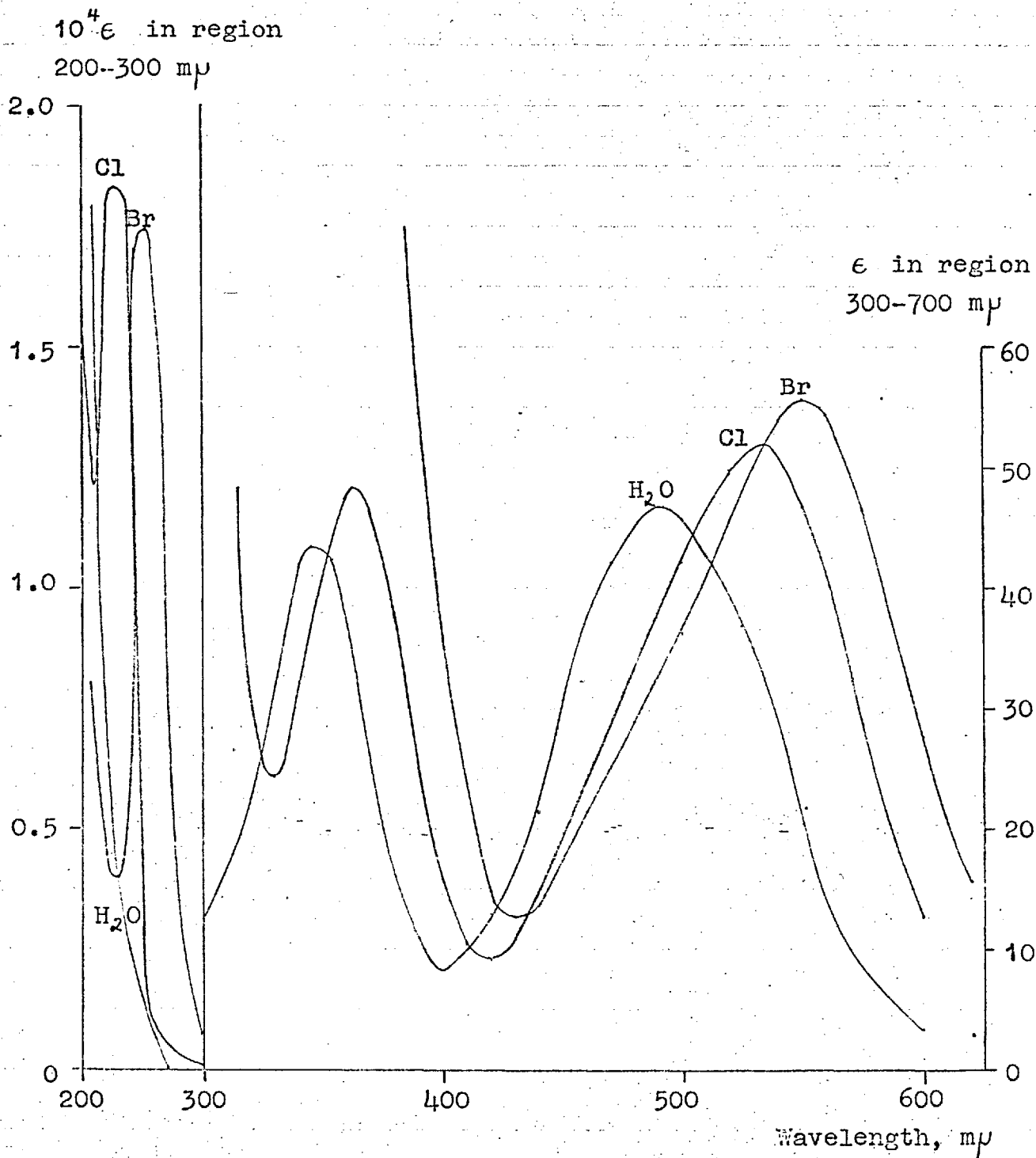
*Reference liquid doubly distilled water.

TABLE XII :  SPECTROPHOTOMETRIC DATA FOR $[Co(NH_3)_5Br]^{2+}$

$[Co(NH_3)_5Cl]^{2+}$ and $[Co(NH_3)_5H_2O]^{3+}$ IN ACID SOLUTION.

| Ion | Absorbance peak | $\epsilon$ | Reference |
|---|---|---|---|
| $[Co(NH_3)_5Br]^{2+}$ | 253mμ | $1.744 \times 10^4$ | Present work |
| | 253mμ | $\sim 1.7 \times 10^4$ | (121) |
| | 253.5mμ | $1.862 \times 10^4$ | (117) |
| | 300mμ* | $9.865 \times 10^2$ | Present work |
| | 550mμ | 55.56 | " " |
| | 549mμ | 58.9 | (117) |
| $[Co(NH_3)_5Cl]^{2+}$ | 228mμ | $1.835 \times 10^4$ | Present work |
| | 227.5mμ | $2.04 \times 10^4$ | (117) |
| | 363mμ | 48.36 | Present work |
| | 363.6mμ | 52.5 | (117) |
| | 360mμ | 45.0 | (118) |
| | 363mμ | 48.3 | (120) |
| | 534mμ | 51.9 | Present work |
| | 532mμ | 50.8 | (119) |
| | 550mμ* | 46.86 | Present work |

TABLE XII (contd.)

| Ion | Absorbance peak | $\epsilon$ | Reference |
|---|---|---|---|
| $[Co(NH_3)_5H_2O]^{3+}$ | $228m\mu$* | $3.696 \times 10^3$ | Present work |
| | $253m\mu$* | $86.26$ | " " |
| | $300m\mu$* | $6.72$ | " " |
| | $346m\mu$ | $43.44$ | " " |
| | $345m\mu$ | $44.8$ | (120) |
| | $492m\mu$ | $46.8$ | Present work |
| | $491m\mu$ | $47.6$ | (119) |
| | $550m\mu$* | $20.44$ | Present work |
| | $550m\mu$* | $20.3$ | (122) |

* Not peaks.

TABLE XIII : WAVELENGTHS AT WHICH AQUATION OF $[Co(NH_3)_5X]^{2+}$

WAS FOLLOWED.

| Aquation of | $\lambda$ | $\epsilon_{pr}/\epsilon_1$* | Concentration range** |
|---|---|---|---|
| $[Co(NH_3)_5Br]^{2+}$ | $253m\mu$ | $4.946 \times 10^{-3}$ | $c_0 < 1.5 \times 10^{-4}M$ |
| | | ($D^\infty$ taken as 0) | |
| | $300m\mu$ | $6.812 \times 10^{-3}$ | $1.5 \times 10^{-4} - 2 \times 10^{-3}M$ |
| | $550m\mu$ | $0.3679$ | $c_0 < 2 \times 10^{-3}M$ |
| $[Co(NH_3)_5Cl]^{2+}$ | $228m\mu$ | $0.2014$ | $c_0 < 1.5 \times 10^{-4}M$ |
| | $550m\mu$ | $0.4362$ | $c_0 < 2 \times 10^{-3}M$ |

* pr = product, r = reactant     ** $c_0 = [Co(NH_3)_5X]^{2+}_{t=0}$

Most experiments were carried out in the concentration region $1 \times 10^{-5} < c_0 < 1.5 \times 10^{-4} M$, the concentration of $[Co(NH_3)_5X]^{2+}$ being followed at the ultra-violet charge transfer peak. To observe the production of $[Co(NH_3)_5H_2O]^{3+}$, spectra of reacting solutions in the region $350-700m\mu$ were recorded graphically on a Perkin Elmer 350 spectrophotometer. Use of a X20 or X50 scale expansion accessory and 5cm. cells was necessary, as extinction coefficients in the visible region are rather small.

The concentration of $[Co(NH_3)_5H_2O]^{3+}$ was deduced from the decrease in D at $550m\mu$. Provided that the sum $([Co(NH_3)_5X]^{2+} + [Co(NH_3)_5H_2O]^{3+})$ was equal to $c_0$, as it was for all homogeneous and truly catalytic heterogeneous runs, it was assumed that no reaction other than aquation was occurring. If the sum was less the $c_0$, another process (usually reduction of the Co(III) complexes: see Section (V.6) ) was also occurring.

V.4:   Rate of the back reaction and position of equilibrium in the $[Co(NH_3)_5Br]^{2+}$ / $[Co(NH_3)_5H_2O]^{3+}$ system.

The equilibrium constant, $K_{eq}$, of reaction (5.3),

$$[Co(NH_3)_5X]^{2+} + H_2O \underset{k_{-1}}{\overset{k_1}{\rightleftharpoons}} [Co(NH_3)_5H_2O]^{3+} + X^-, \qquad (5.3)$$

is well established for X=Cl (see Table XI, pages 75 and 76) but not for X=Br. The rate of reaction of $[Co(NH_3)_5H_2O]^{3+}$ with $Br^-$ was therefore measured, to determine $k_{-1}$ and

and hence $K_{eq}$, at 25°C.

Suitable volumes of $[Co(NH_3)_5H_2O](ClO_4)_3$ solution and KBr solution of known concentration were separately equilibrated at 25°C. At time $t_0$ they were mixed together. The pH of the resulting solution was always 2. The production of $[Co(NH_3)_5Br]^{2+}$ was followed at 253mμ for 4 days, after which time less than 2% of the $[Co(NH_3)_5H_2O]^{3+}$ was converted. The initial slope of a graph of $D_{253}$ versus time therefore sufficed to give $k_{-1}$ with reasonable accuracy from the relationship.

$$k_{-1} = \frac{\text{Slope}}{\varepsilon r.[Co(NH_3)_5H_2O]^{3+}_{t=0}.[Br^-]_{t=0}} \qquad (5.4)$$

Seven runs were carried out: the details are given in Table XIV below.

TABLE XIV : ANATION OF $[Co(NH_3)_5H_2O]^{3+}$ BY BROMIDE.

| Run | $[Co(NH_3)_5H_2O]^{3+}$ at $t_0$ | $[Br^-]$ at $t_0$ | Ionic strength at $t_0$ | $k_{-1}$ |
|---|---|---|---|---|
| 1 | $2 \times 10^{-4}$M | $0.987 \times 10^{-2}$M | $2.107 \times 10^{-2}$M | $3.38 \times 10^{-4}$ $M^{-1}min^{-1}$ |
| 2 | " | 1.007 " | 2.137 " | 3.29 " " |
| 3 | " | 1.974 " | 3.094 " | 3.00 " " |
| 4 | " | 2.014 " | 3.144 " | 2.72 " " |
| 5 | " | 3.012 " | 4.140 " | 2.74 " " |
| 6 | " | 3.021 " | 4.151 " | 2.72 " " |
| 7 | $4 \times 10^{-4}$M | 4.028 " | 5.288 " | 2.39 " " |

Each $k_{-1}$ value is subject to an error of $\pm$ 5%, as the increase in $D_{253}$ was too slight to be measured with great accuracy. Runs 1, 3 and 6 of Table XIV are illustrated in Figure VI, and a Brönsted plot of $\log k_{-1}$ versus $I^{\frac{1}{2}}(1+I^{\frac{1}{2}})^{-1}$ is given in Figure VII. Extrapolation to $I=10^{-2}M$ gives $k_{-1}=(3.8\pm0.2)\times10^{-4}$ $M^{-1}min^{-1}$, and hence $K_{eq}=0.98\pm0.07M$.

Knowledge of $K_{eq}$ at the appropriate ionic strength enables the position of equilibrium in each run to be calculated by standard algebraic methods. Four typical runs are given in the table below.

| Initial concentration of $[Co(NH_3)_5X]X_2$ in $10^{-2}M$ $HClO_4$ | Percentage of $[Co(NH_3)_5X]^{2+}$ at equilibrium at 25°C. | |
|---|---|---|
| | X=Br | X=Cl |
| $1\times10^{-4}M$ | 0.03 | 0.3 |
| $2\times10^{-3}M$ | 0.5 | 5 |
| $1\times10^{-2}M$ | 1 | 10 |
| $1\times10^{-4}M$, in presence of $10^{-3}M$ added $Br^-$ or $[Co(NH_3)_5H_2O]^{3+}$ | 0.1-0.4 | 1-4 |

Nearly all the runs carried out in these experiments were for $c_0 \leq 10^{-4}M$, for which aquation proceeds almost to completion.

FIGURE VI: THE ANATION OF $[Co(NH_3)_5H_2O]^{3+}$ BY BROMIDE.

PLOTS OF $D_{292}$ vs. TIME, FOR RUNS 1,3 and 6

(See Table XIV).

FIGURE VII: BRÖNSTED PLOT OF $k_{-1}$ vs. $I^{\frac{1}{2}}/(1+I^{\frac{1}{2}})$
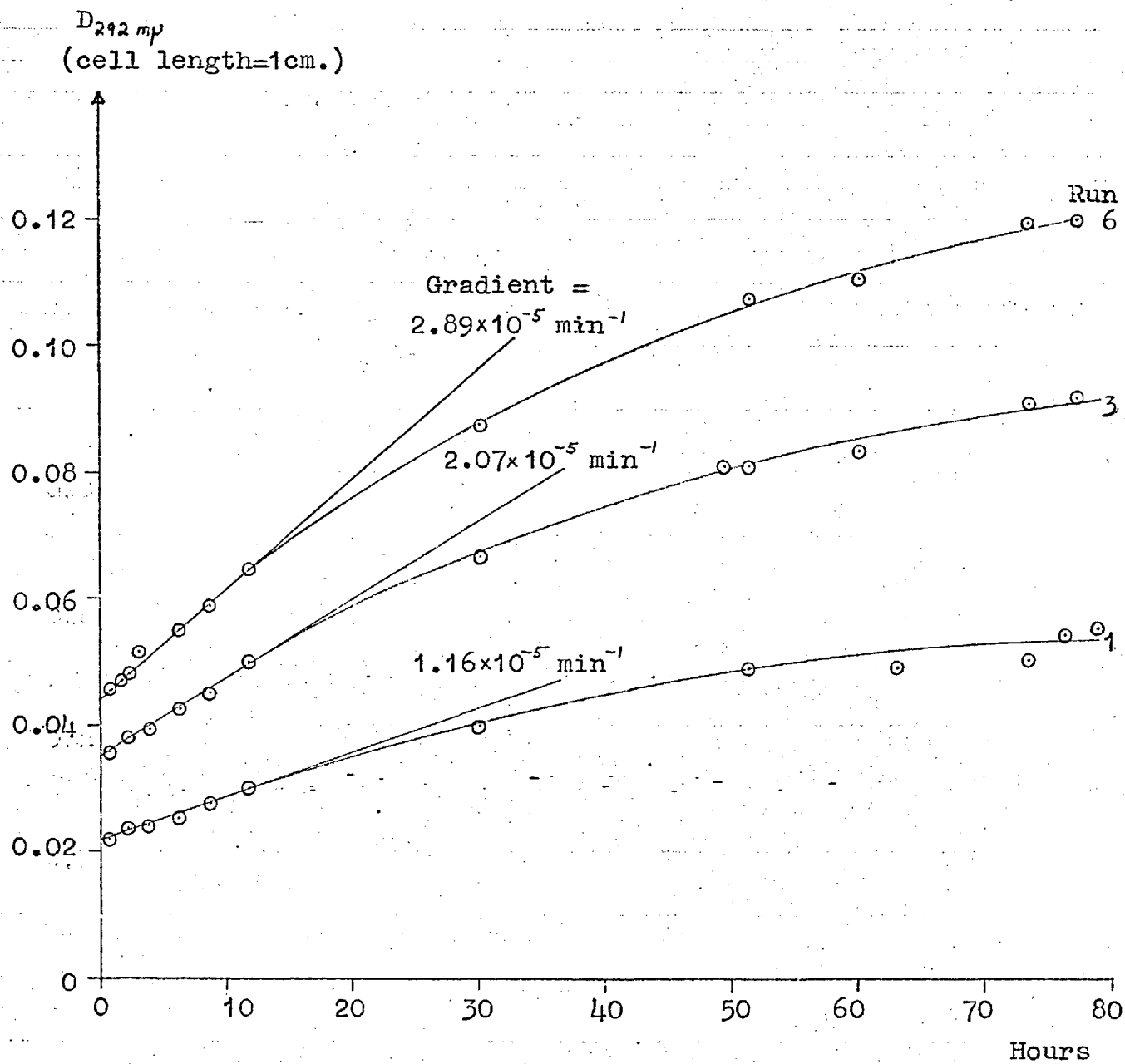
FOR THE ANATION REACTION.
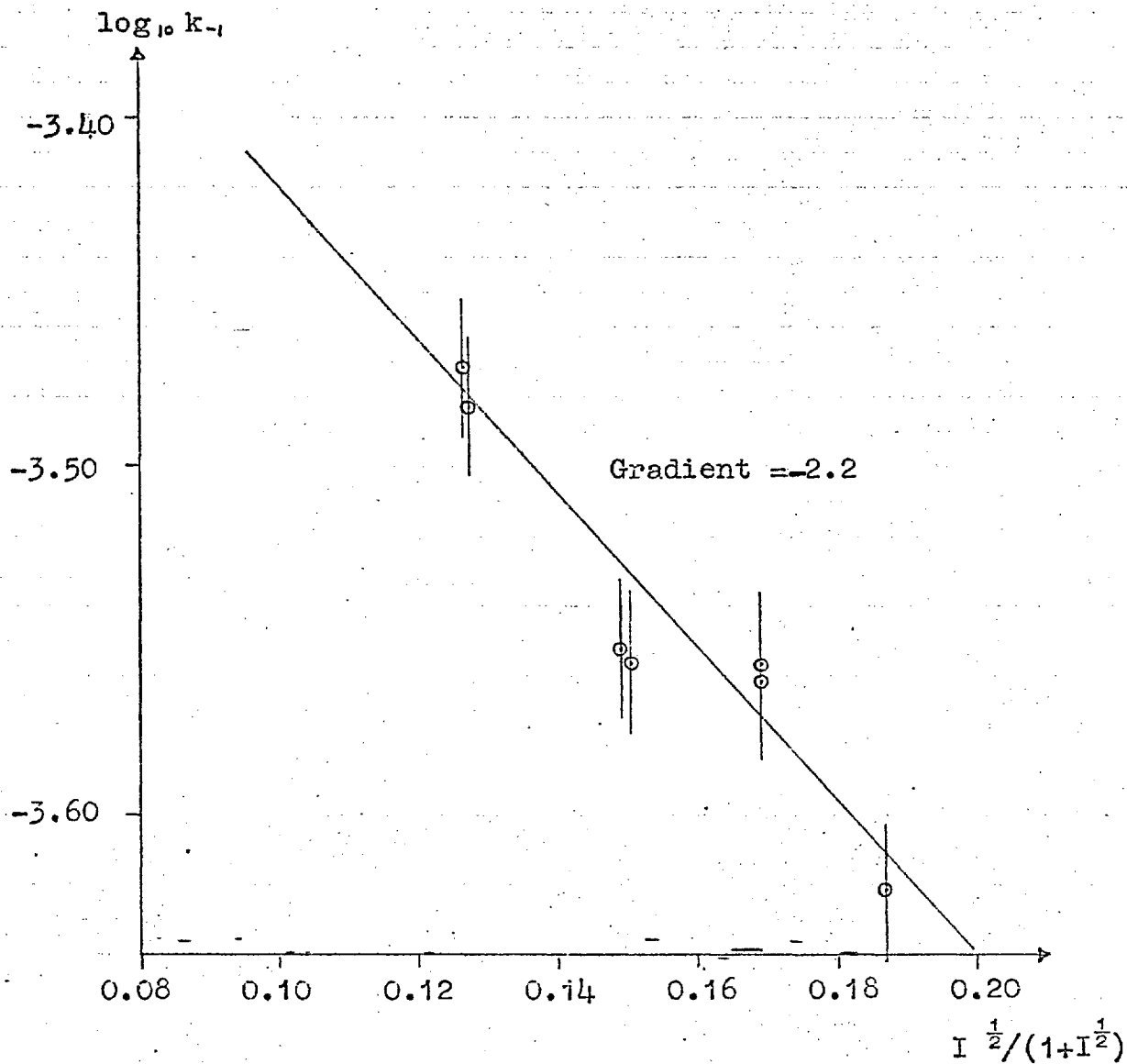
$I$ = ionic strength

$$\Delta D = k_2 \, \epsilon \left[ C_r(H_2O)_6 \right]_0 \left[ sen^- \right]_0 = k_2 \, \epsilon \, A_0 \, B_0$$
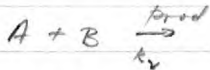
$$A + B \xrightarrow[k_2]{prod} \qquad\qquad A = \epsilon \, D$$

$$Rate = \frac{-dA}{dt} = k_2 \, A B$$

$$Init \; rate = -\left( \frac{dA}{dt} \right)_0 = k_2 \, A_0 \, B_0$$

$$K = \frac{k_1}{k_{-1}} \qquad \log K = \log k_1 - \log k_{-1}$$

V.5: The calculation of $k_1$.

The rate equation for the opposing first and second order reactions

$$[Co(NH_3)_5X]^{2+} + H_2O \underset{k_{-1}}{\overset{k_1}{\rightleftharpoons}} [Co(NH_3)_5H_2O]^{3+} + X^- \quad (5.3)$$
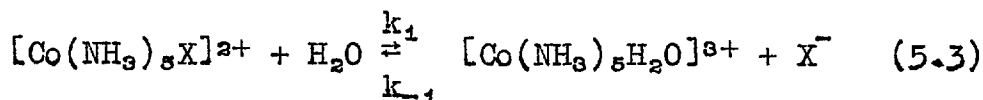
is $\quad \dfrac{dc}{dt} = -k_1 c + k_{-1} (c_0-c) [X^-] \quad (5.5)$

where $c$ is the concentration of $[Co(NH_3)_5X]^{2+}$ at time $t$.

The position of equilibrium in these experiments lay well to the right hand side of (5.3), and the second term of the rate law was always small, and usually negligible, compared with the first. The approximation $[X^-] = [X^-]_0$ was therefore made.

Integrating equation (5.5),

$$\ln \frac{c_0 - c_\infty}{c - c_\infty} = k_{obs} t \quad (5.6)$$

where $k_{obs} = k_1 + k_{-1} [X^-]_0$, and where $c_\infty$ is the concentration of $[Co(NH_3)_5X]^{2+}$ at equilibrium.

For spectrophotometric measurements at a given wavelength, therefore, since $D_0 = \epsilon_r c_0$

$$D = \epsilon_r c + \epsilon_{pr} (c_0-c)$$
$$D_\infty = \epsilon_r c_\infty + \epsilon_{pr} (c_0-c_\infty),$$

$$2.303 \log \frac{D_0-D_\infty}{D -D_\infty} = k_{obs} t \quad (5.7)$$

Plots of log $(D-D_\infty)$ versus time for all homogeneous runs were linear.

$D_\infty$ was calculated on the assumption that aquation proceeded to completion, except for a few runs with $[Co(NH_3)_5Cl]^{2+}$ at high $c_0$. $k_{obs}$ was assumed to be equal to $k_1$, except in these few runs. The errors introduced by these two assumptions were partly self-compensating, and did not affect the values of $k_1$ obtained.

Data for a typical run with $[Co(NH_3)_5Br]^{2+}$ and a run with $[Co(NH_3)_5Cl]^{2+}$ at exceptionally high $c_0$ are tabulated in Table XV and plotted in Figure VIII.

$k_1$ values were found to be independent of $c_0$, of pH in the range 1-4 and also of the nature of the anion (either $X^-$ or $ClO_4^-$) also present. The presence or absence of laboratory fluorescent lighting had no effect.

The experimental procedure was very simple. 500ml. $10^{-2}M$ perchloric acid were equilibrated at 25°C in the thermostat. At time $t_0$, a weighed amount of complex was added, and the flask shaken. The solid quickly dissolved. Readings of $D_\lambda$ were taken at suitable time intervals by removal of small aliquots (<3ml.). $c_0$ was calculated from $D_0$, obtained either directly or by extrapolation, as the mass of solid used was too small to be weighed accurately.

TABLE XV : DATA FOR AQUATION OF

1)  $[Co(NH_3)_5Br]^{2+}$, followed at 253m$\mu$

2)  $[Co(NH_3)_5Cl]^{2+}$, followed at 550m$\mu$


In both experiments, temperature = 25°C

$[HClO_4]$ = 10⁻²M

cell length = 1cm.

$[Co(NH_3)_5X]X_2$ used.

## TABLE XV (contd.)

| RUN 1 | | | RUN 2 | | | |
|---|---|---|---|---|---|---|
| $c_0=3.38\times10^{-5}M$ (from $D_0$) $D_\infty$ taken as 0 | | | $c_0=9.72\times10^{-3}M$ (from $D_0$) $c_{eq} \approx 1\times10^{-3}M$ (from $K_{eq}$) $D_\infty=\epsilon_r c_\infty+\epsilon_{pr}(c_0-c_\infty)$ $=0.2243$ $k_{-1}[X^-]_0 \approx 8\times10^{-6}min^{-1}$ | | | |
| Time (min) | $D_{253}$ | log D | Time (hr) | $D_{550}$ | $D-D_\infty$ | $\log(D-D_\infty)$ |
| 0 | 0.589 | $\bar{1}.7701$ | 0 | 0.4555 | 0.2312 | $\bar{1}.3640$ |
| 9 | 0.5855 | $\bar{1}.7676$ | 1.93 | 0.454 | 0.2297 | $\bar{1}.3611$ |
| 78 | 0.571 | $\bar{1}.7566$ | 14.00 | 0.4344 | 0.2101 | $\bar{1}.3224$ |
| 104 | 0.568 | $\bar{1}.7543$ | 19.25 | 0.427 | 0.2027 | $\bar{1}.3069$ |
| 134 | 0.5595 | $\bar{1}.7478$ | 21.55 | 0.4215 | 0.1972 | $\bar{1}.2949$ |
| 171 | 0.553 | $\bar{1}.7427$ | 24.17 | 0.4215 | 0.1972 | $\bar{1}.2949$ |
| 231 | 0.541 | $\bar{1}.7332$ | 26.62 | 0.4195 | 0.1952 | $\bar{1}.2905$ |
| 269 | 0.532 | $\bar{1}.7259$ | 30.95 | 0.4125 | 0.1882 | $\bar{1}.2746$ |
| 293 | 0.527 | $\bar{1}.7218$ | 42.73 | 0.3975 | 0.1732 | $\bar{1}.2386$ |
| 328 | 0.522 | $\bar{1}.7177$ | | | | |
| 359 | 0.516 | $\bar{1}.7126$ | | | | |
| 393 | 0.5105 | $\bar{1}.7080$ | | | | |

Slope of graph log $(D_0-D_\infty)$vs. t
$= 4.78\times10^{-5}$ min$^{-1}$
i.e. $k_{obs} = 1.10\times10^{-4}$ min$^{-1}$
i.e. $k_1 = 1.02\times10^{-4}$ min$^{-1}$

Slope of graph log D vs. t
$= 1.63\times10^{-4}$ min$^{-1}$
i.e. $k_1 = 3.75\times10^{-4}$ min$^{-1}$

FIGURE VIII: FIRST ORDER PLOTS FOR AQUATION OF
(1) $[Co(NH_3)_5Br]^{2+}$, (2) $[Co(NH_3)_5Cl]^{2+}$
(Data from Table XIV).
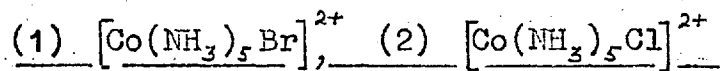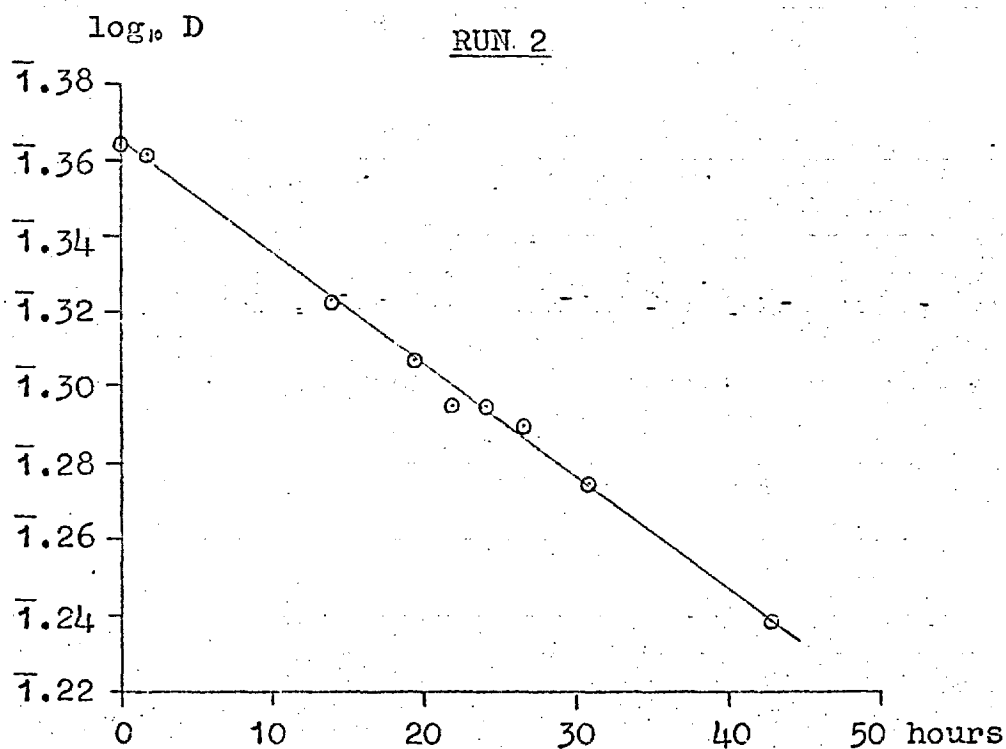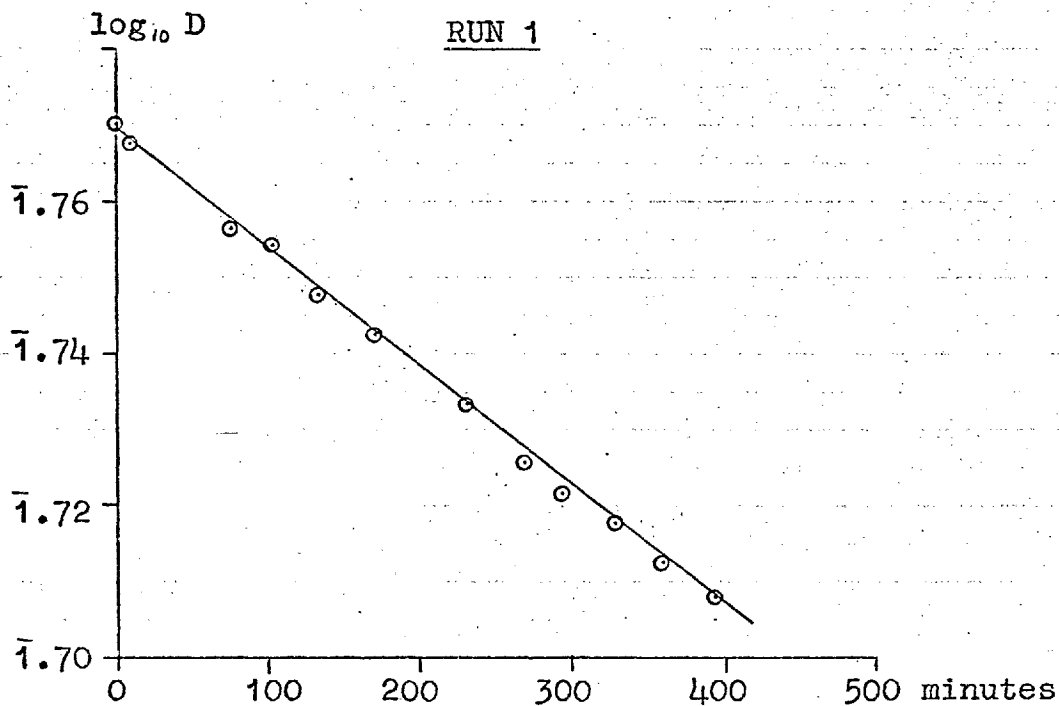
V.6:   Reduction of $[Co(NH_3)_5X]^{2+}$

Although cobaltammines are much more stable than
the simple cobaltic ion, they are readily reduced by,
for example, $Cr^{2+}$, $Fe^{2+}$, $V^{2+}$ and $Eu^{2+}$ (124).  In the
course of the present work, silver and charcoal were
also found to be reducing agents and these redox reactions
were investigated.

Co(II) was estimated spectrophotometrically after
complexation with chloride, forming complexes of the type
$[CoCl_n]^{(2-n)+}$, n=1-4.  The ratio of total chloride to
total Co(II) was at least $10^4$, so that the concentration
of free chloride was negligibly affected by complex
formation.  The degree of formation of the complexes was
therefore unaffected by [Co(II)], and Beer's Law applied,
provided the total chloride concentration was always the
same.

Experimentally, small aliquots (2-5ml.) of Co(II)
solution were mixed with concentrated AR hydrochloric
acid (~11.6M) in the proportion 1:4 by volume.  The spectra
of these solutions were observed using HCl solution of
the same concentration as reference liquid.  The highly
characteristic spectrum in the region 600-700m$\mu$ is shown
in Figure IX, on page 96, with the spectrum of aqueous
$Co^{2+}$ for comparison.

# FIGURE IX: SPECTRUM OF Co(II) IN ca. 10M HCl AND IN 10⁻²M HClO₄, AT ROOM TEMPERATURE.



FIGURE IX: SPECTRUM OF Co(II) IN ca. 10M HCl AND IN $10^{-2}$M $HClO_4$, AT ROOM TEMPERATURE.

in ca. 10M HCl

in $10^{-2}$M $HClO_4$
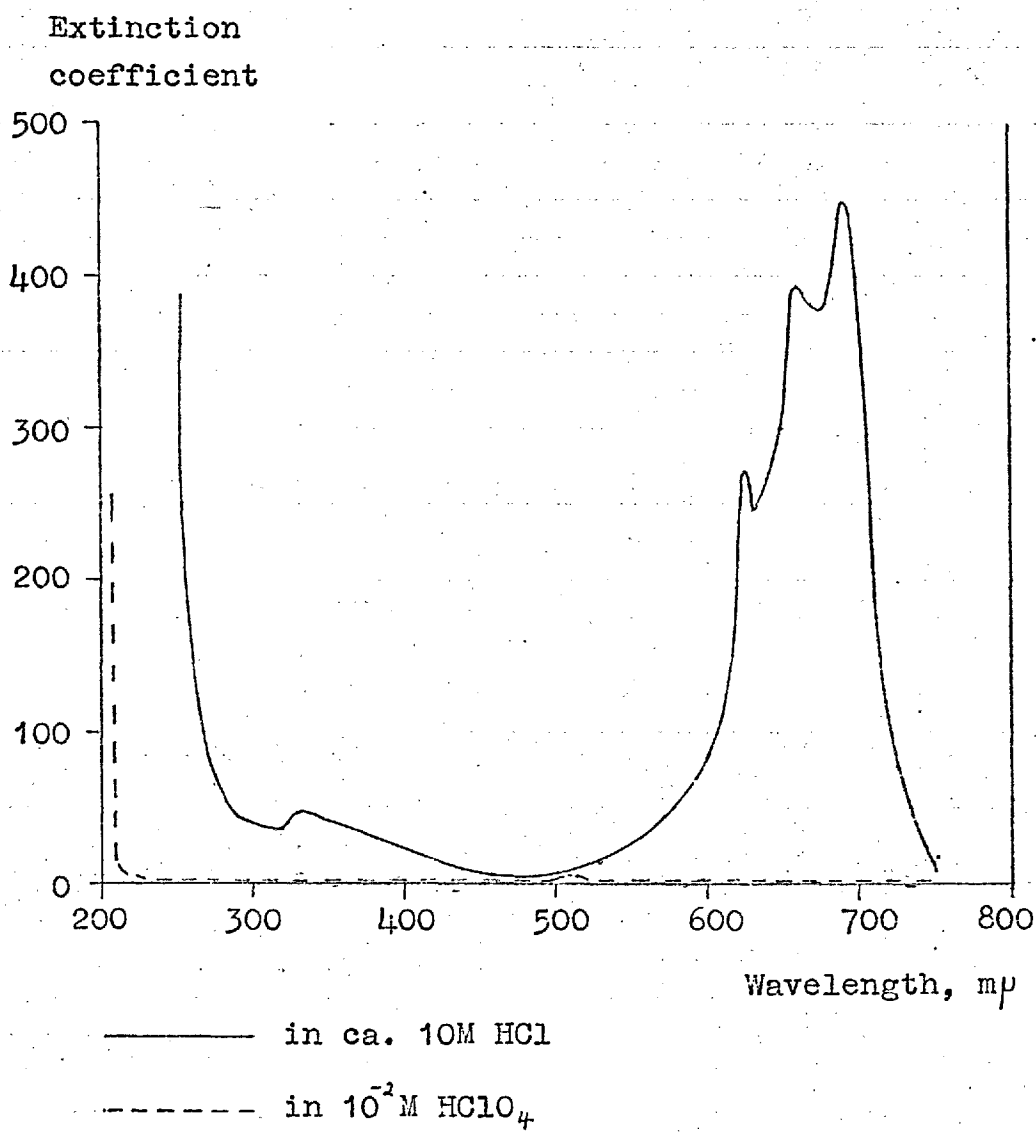
Co(II) in the HCl solution was estimated at
690mμ, at which $\epsilon=449.7$ up to the highest Co(II)
concentration tested, $10^{-3}$M. Using a spectrophoto-
meter with a scale expansion accessory, the limit of
detection of Co(II) in the chloride solution was about
$2\times10^{-6}$M.

Attempts to determine the paramagnetic $Co^{2+}$, both
as the aquo- and as the chloro-complex, by ESR spectro-
scopy at $-196^{\circ}$C, failed, as the signal heights were
not sufficiently reproducible.

The redox potential of the $[Co(NH_3)_5X]^{2+}$ ions was
calculated from literature data as follows:

For the redox couple

$$[Co(NH_3)_5H_2O]^{3+} + e^- \rightleftharpoons [Co(NH_3)_5H_2O]^{2+}, \quad (5.8)$$

Yalman (125) found $E^\circ=0.35\pm0.02$V. at $25^{\circ}$C, I=1M. From
this value, and using data from Table XI for $K_{eq}$ at
I=0.5M, it is found:

$$E^\circ \quad [Co(NH_3)_5Br]^{2+} / Co(II) \quad = \quad 0.38\pm0.02V.$$

$$E^\circ \quad [Co(NH_3)_5Cl]^{2+} / Co(II) \quad = \quad 0.34\pm0.02V.$$

## CHAPTER VI : SEMI-QUALITATIVE WORK ON THE HETEROGENEOUS CATALYSIS OF THE AQUATION OF $[Co(NH_3)_5X]^{2+}$

Preliminary work on the catalysis of the aquation of $[Co(NH_3)_5X]^{2+}$ by various solids is reported in this chapter. The results are designated semi-qualitative, because the specific surface areas of the catalysts investigated were not determined: quantitative comparison of the catalytic efficiency of different solids was therefore not possible. Quantitative work is reported in Chapters VII - X.

### VI.1. Choice of solid.

Since heterogeneous catalysts were sought, work was restricted to insoluble compounds which did not dissolve in perchloric acid. This excluded investigation of the mercuric halides and several metals. Anion exchange on the solid surface was also to be avoided. If, for example, solid AgCl is added to a dilute solution of $[Co(NH_3)_5Br]Br_2$, some AgBr will precipitate onto the solid surface, as AgBr is less soluble than AgCl. It is then uncertain whether the effective catalyst surface is AgBr or AgCl.

Commercially obtained solids were used without further purification in the preliminary work. Powders, if much coagulated, were lightly crushed with a pestle, and

batches of each solid were shaken and stirred to obtain powders of uniform appearance. The effect of solids homogenised in this way was reproducible to $\pm 5\%$.

VI.2.   Experimental procedure.

A weighed amount of solid was placed in a 500ml. conical flask with a magnetic stirrer, and the empty flask placed in a holder and immersed to its neck in a water thermostat at 25°C.   500ml. of $10^{-2}$M perchloric acid were separately equilibrated in the thermostat. At time $t_0$, a weighed amount of $[Co(NH_3)_5Br]Br_2$ or $[Co(NH_3)_5Cl]Cl_2$ was dissolved in the acid, and the solution quickly poured into the conical flask, which was then stoppered.   This operation took less than a minute.   The magnetic stirrer was started at such a speed that all the solid, which was usually in the powdered form, was agitated in the solution.

The aquation reactions were followed spectrophoto-metrically for 5-8 hours, in the case of $[Co(NH_3)_5Br]^{2+}$ and 2-3 days, in the case of $[Co(NH_3)_5Cl]^{2+}$, by removing 1 ml. aliquots from the reaction vessels at suitable time intervals.   Sometimes the magnetic stirrer was switched off for a minute before removal of each aliquot, to allow the solid to settle, and sometimes the stirrer was left on throughout the run, and aliquots were

centrifuged to remove solid before measurement of optical density. Reduction in volume, due to removal of aliquots, did not amount to more than 5%, and no sampling corrections were made. The time required for each optical measurement was 30-90 seconds.

A Unicam SP 500 spectrophotometer and 1cm. matched silica microcells were used for all optical measurements. The reference liquid was doubly distilled water. Spectro-photometric data are given in Chapter V, Section V.3. Nearly all runs were carried out in low concentration ($3-7 \times 10^{-5}$M) by following the optical absorbance of the reactant.

If a catalytic effect was observed, the solid was separated from the solution by rapid filtration before the end of the run, and the remainder of the reaction studied at 25°C. In all cases, the rate returned to the homogeneous, uncatalysed value, to within $\pm 5\%$. The rate enhancement was therefore concluded to be due to a heterogeneous effect, and not to catalyst dissolved in solution. However, this check did not exclude the possibility of a heterogeneous redox reaction between $[Co(NH_3)_5 X]^{2+}$ and the solid, and this was tested for separately.

VI.3.    Experimental results.


Data from catalytic runs were plotted according to a first order law.  These runs during which only 15-30% of the complete aquation reaction was followed, gave good first order plots, as exemplified by line 1, Figure X, page 105.  The first order rate constant for the catalytic reaction, $k_{het}$, was calculated from the overall rate constant, $k_{obs}$, by the relationship.


$$k_{het} = k_{obs} - k_1 \qquad\qquad (6.1)$$

Incidentally, any other treatment of the kinetic data, such as a zero order plot, would require a more complicated correction for the homogeneous contribution.

The effects of miscellaneous solids on the aquation of $[Co(NH_3)_5X]^{2+}$ are tabulated in Tables XVI - XIX, and three typical plots of kinetic data are illustrated in Figure X.

First order plots for catalytic aquation reactions followed to completion sometimes showed downward curvature (e.g. line 2, Figure X).  It is also clear from Tables XVI and XVII that $k_{het}$ decreases as $c_0$ increases.  This variation is discussed in the next chapter.

## TABLE XVI : SOLIDS WITH CATALYTIC EFFECT ON THE AQUATION OF $[Co(NH_3)_5Cl]^{2+}$ DATA FOR 25°C.

| Solid, source | $m_{cat}$ in 500ml. | $10^5 c_0$ | $10^4 k_{het}$ $min^{-1}$ | $\dfrac{10^4 k_{het}}{m_{cat}}$ | Comments |
|---|---|---|---|---|---|
| AgCl,BDH | 1.04g. | 5.6 | 0.06 | 0.06 | Subject to photochemical effect. In dark $k_{het} \approx 0$ |
| | 2.08g. | " | 0.12 | 0.06 | |
| | 1.2g. | 1000 | 0 | | |
| | 3.2g. | " | 0 | | |
| AgCl,freshly ppted.(1) | 1.73g. | 5.6 | 0.31 | 0.18 | |
| | 3.0g. | " | 0.53 | 0.17 | |
| (2) | 1.0g. | " | 0.43 | 0.43 | |
| AgBr,BDH | 3.0g. | 2.8 | 4.41 | 1.47 | |
| | " | 5.6 | 1.71 | 0.56 | |
| AgI,BDH | 3.0g. | 5.6 | 3.66 | 1.17 | Subject to photochemical effect. In dark $k_{het} \approx 0.85 \times 10^{-4} min^{-1}$ |
| | " | " | 3.43 | | |
| HgS,BDH | 2.0g. | 3.0 | 2.38 | 1.19 | |
| $Hg_2Cl_2$,BDH | 2.9g. | 5.5 | 0.58 | 0.2 | |
| Pt powder, Johnson Matthey. | 3.5g. | 2.25 | 3.36 | 0.95 | |

TABLE XVII : SOLIDS WITH CATALYTIC EFFECT ON THE AQUATION OF $[Co(NH_3)_5Br]^{2+}$. DATA FOR 25°C.

| Solid, source | $m_{cat}$ in 500ml. | $10^5 c_0$ | $10^4 k_{het}$ min$^{-1}$ | $\dfrac{10^4 k_{het}}{m_{cat}}$ | Comments |
|---|---|---|---|---|---|
| AgCl, BDH | 2.0g. | 3.0 | 1.59 | 0.795 | Cl-Br exchange on surface? |
| " | | 5.6 | 0.92 | 0.46 | |
| AgBr, BDH | 3.0g. | 3.1 | 30.84 | 10.28 | Catalysis subject to photochemical effect and repression by Br⁻. See also Chapter IX. |
| | 2.0g. | 3.34 | 22.14 | 11.07 | |
| | 3.0g. | 5.8 | 10.17 | 3.39 | |
| AgI, BDH | 1.54g. | 3.0 | 27.4 | 17.79 | Catalysis subject to photochemical effect and repression by I⁻. |
| | 2.0g. | 3.16 | 38.0 | 19.00 | |
| | " | 3.63 | 32.75 | 16.38 | |
| | 3.0g. | 5.6 | 31.25 | 10.42 | |
| HgS, BDH | 1.0g. | 2.9 | 8.73 | 8.73 | Catalysis subject to slight photochemical effect and repression by Br⁻. See also Chapter VIII. |
| | " | 7.4 | 6.23 | 6.23 | |
| Hg$_2$Br$_2$, BDH | 2.9g. | 3.5 | 25.9 | 8.93 | |
| | 2.2g. | 5.8 | 8.27 | 3.76 | |
| | 4.4g. | " | 18.7 | 4.25 | |
| | 3.3g. | 100 | 0.26 | 0.08 | |
| Pd powder | 1.1g. | 3.5 | 11.8 | 10.7 | |
| Au " | 0.4g. | 2.74 | 0.6 | 1.2 | |
| Pt " | 0.65g. | 3.6 | 1.1 | 1.7 | Catalysis investigated quantitatively with Pt rotating disc. See Chapter X. |
| (Johnson Matthey). | | | | | |

**TABLE XVIII : SOLIDS WITHOUT CATALYTIC EFFECT ON THE**

**AQUATION OF $[Co(NH_3)_5Br]^{2+}$**

| Solid | Source | Mass used in 500ml. solution | $c_o$ |
|---|---|---|---|
| PbS | BDH | 1.3g. | $3.5 \times 10^{-5}M$ |
| BaSO$_4$ | Freshly ppted. | 2.0g. | " |
| BN | BDH | 1.0g. | " |
| Crushed Pyrex glass. | | 10.0g. | " |
| Stainless steel turnings. | | Surface area $\approx 50 cm^2$ | " |

For these substances, $k_{obs} = (3.7 \pm 0.2) \times 10^{-4}min^{-1}$.

**TABLE XIX : SOLIDS WHICH REDUCE $[Co(NH_3)_5Br]^{2+}$ to $Co(II)$**

| Solid | Source | Mass used in 500ml. solution. | $c_o$ | First order rate constant for disappearance of $[Co(NH_3)_5Br]^{2+}$ |
|---|---|---|---|---|
| Hg | Re-distilled | 4.5g. | $3.5 \times 10^{-5}M$ | $10.6 \times 10^{-4}min^{-1}$ |
| Activated decolourising charcoal. | Hopkin and Williams | 0.5g. | $3.5 \times 10^{-5}M$ | $\sim 65 \times 10^{-4}min^{-1}$ |
| | | 0.7g. | $5.6 \times 10^{-5}M$ | $88.5 \times 10^{-4}min^{-1}$ |
| Ag powder | Johnson Matthey. | 0.85g. | $3.5 \times 10^{-5}M$ | $\sim 125 \times 10^{-4}min^{-1}$ |
| | | | | See Chapter XI. |

FIGURE X: FIRST ORDER PLOTS FOR

(i) Catalysis of the aquation of $[Co(NH_3)_5Br]^{2+}$ at 25°C by

⊙ (1) 1.0g. HgS      $c_o = 2.9 \times 10^{-5} M$

△ (2) 1.54g. AgI      $c_o = 3.0 \times 10^{-5} M$

(ii) Reduction of $[Co(NH_3)_5Br]^{2+}$ at 25°C by

⊡ (3) 39 cm² Ag foil      $c_o = 3.1 \times 10^{-5} M$

$\log_{10} D_{253\,m\mu}$
(cell length = 1cm.)
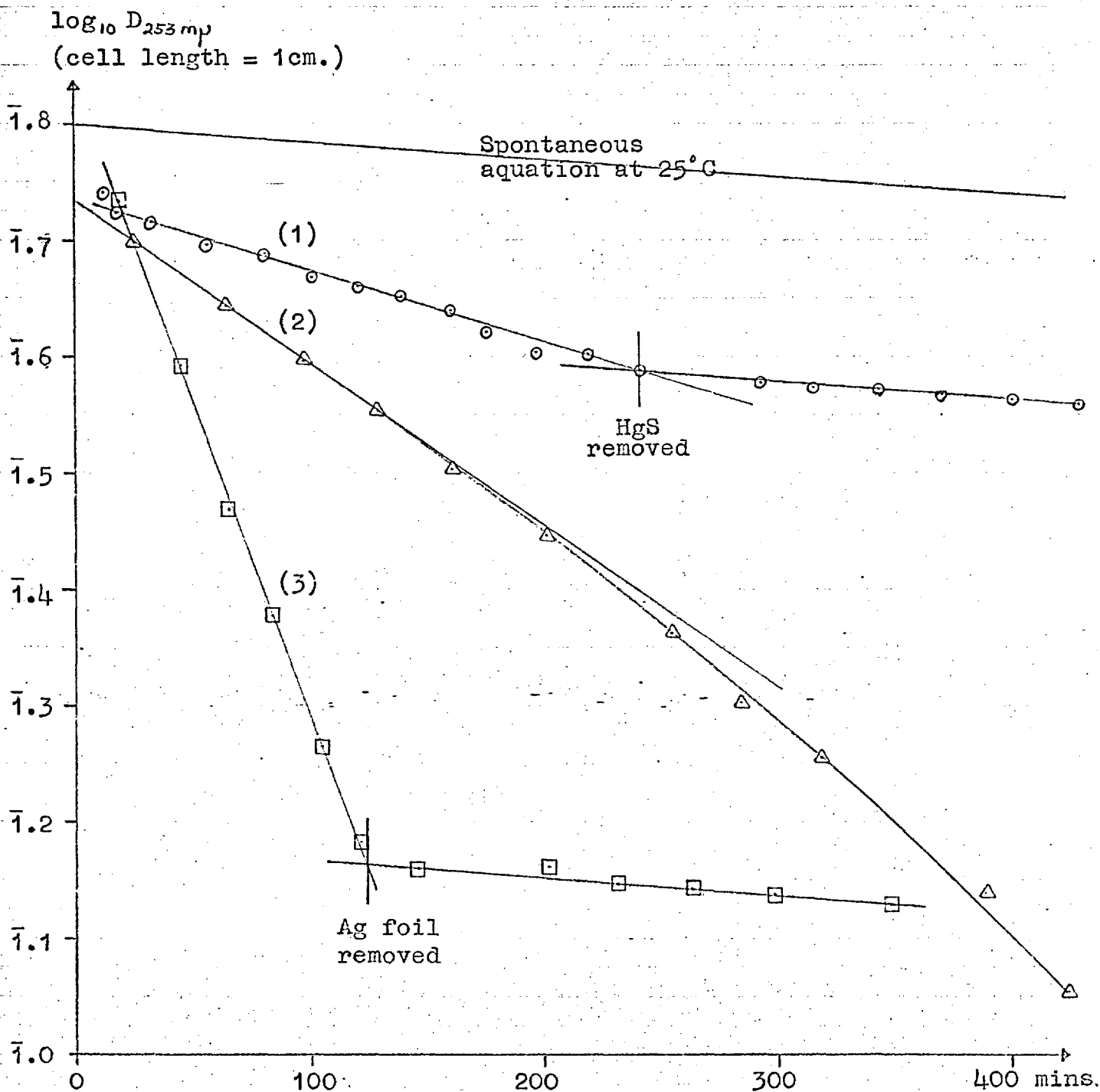
VI.3.1:  Heterogeneous catalysis.


All results given in Tables XVI - XIX were for the
first 15-25% of aquation in normal laboratory lighting.
Catalysis by the silver halides was found to be subject
to a considerable photochemical effect, which is further
discussed in Chapter IX.

Inspection of Tables XVI and XVII shows that for a
given system (catalyst, complex, $c_0$), $k_{het}$ is proportional
to $m_{cat}$, as would be expected.  For example, $k_{het}$ for the
catalysis of $[Co(NH_3)_5Br]^{2+}$ aquation by $Hg_2Br_2$ at $c_0 =$
$5.8 \times 10^{-5}M$ is $8.27 \times 10^{-4} min^{-1}$ for 2.2g., and $18.7 \times 10^{-4} min^{-1}$
for 4.4g. of catalyst.  This relationship was more string-
ently verified for the catalysis of $[Co(NH_3)_5Br]^{2+}$ aquation
by AgBr (see Chapter IX).

The proportionality of $k_{het}$ to $m_{cat}$ is good for a given
batch of one solid, but as shown for the $AgCl/[Co(NH_3)_5Cl]^{2+}$
system, the difference between differently prepared batches
of the same solid can be striking.  A freshly precipitated
batch of AgCl had roughly three times the catalytic effect
of the BDH substance, while a very carefully prepared
second batch had seven times the effect.  Unfortunately,
some AgCl became colloidal and ruined spectrophotometric
measurements during most runs with these freshly prepared
batches.

The greater effect of the freshly prepared batches of AgCl was thought to be due to their greater specific surface area. This was verified for the AgBr / $[Co(NH_3)_5 Br]^{2+}$ system, from experiments with different AgBr batches of known specific surface area, and the intrinsic heterogeneous rate was found to be independent of the particle size of the catalyst (See Chapter IX.)

There is little point in quantitative comparison of the catalytic effects of different solids, since these probably had widely differing surface areas. Indeed, even had these been known, direct comparison of $k_{het}$ would still not be meaningful, as the sticking probability of $[Co(NH_3)_5X]^{2+}$ on the different solids is also different.

It is interesting to compare the effects of the same catalyst on the aquation of the two complexes. Comparison must obviously be carried out at the same value of $c_0$, and the relevant data are reproduced from Tables XVI and XVII below.

| | $10^5 c_0$ | $k_{het}/m_{cat}$ for $[Co(NH_3)_5Br]^{2+}$ | $k_{het}/m_{cat}$ for $[Co(NH_3)_5Cl]^{2+}$ |
|---|---|---|---|
| AgCl(BDH) | 5.6 | 0.46 | 0.06 |
| AgBr( " ) | 5.6 | 3.39 | 0.56 |
| | ~3.0 | 10.28 | 1.47 |
| AgI(BDH) | 5.6 | 10.42 | 1.17 |
| HgS( " ) | ~3.0 | 8.73 | 1.19 |

All catalysts have roughly eight times the effect on $[Co(NH_3)_5Br]^{2+}$ that they have on $[Co(NH_3)_5Cl]^{2+}$. There is possibly, therefore, a correlation between the rates of spontaneous and catalysed aquation reaction. Bifano and Linck (123) found an excellent correlation of this type for the spontaneous and homogeneously Hg(II)-catalysed aquation of various cobalt(III) chloroammines.

VI.3.2: Repression of catalysis by halide ions.

Any ions which adsorb on the catalytic sites will repress catalysis, the more strongly sorbed ions having a greater effect. Bromide ions had, for example, a greater repressive effect on catalysis by AgBr than did $[Co(NH_3)_5 H_2O]^{3+}$ ions (see Chapter IX).

Figures XI and XII illustrate the repressive effects of $Br^-$ and $I^-$ on the catalysis of $[Co(NH_3)_5Br]^{2+}$ aquation by AgBr and AgI respectively. The effect of iodide above $10^{-3}M$ was not investigated, as reduction of $[Co(NH_3)_5Br]^{2+}$ interfered. Below $10^{-3}M$, starch tests for iodine carried out at the end of each run were negative.

It is seen that halide exerts a considerable repressive effect upon $k_{het}$, and also a slight accelerating effect upon $k_1$. The latter is due to ion-pair formation (61). $k_{het}$ at each halide concentration was therefore calculated by subtracting from $k_{obs}$ the $k_1$ value appropriate to that halide concentration.

FIGURE XI: REPRESSIVE EFFECT OF BROMIDE ON THE AgBr-
CATALYSED AQUATION OF [Co(NH₃)₅Br]²⁺ AT 25°C
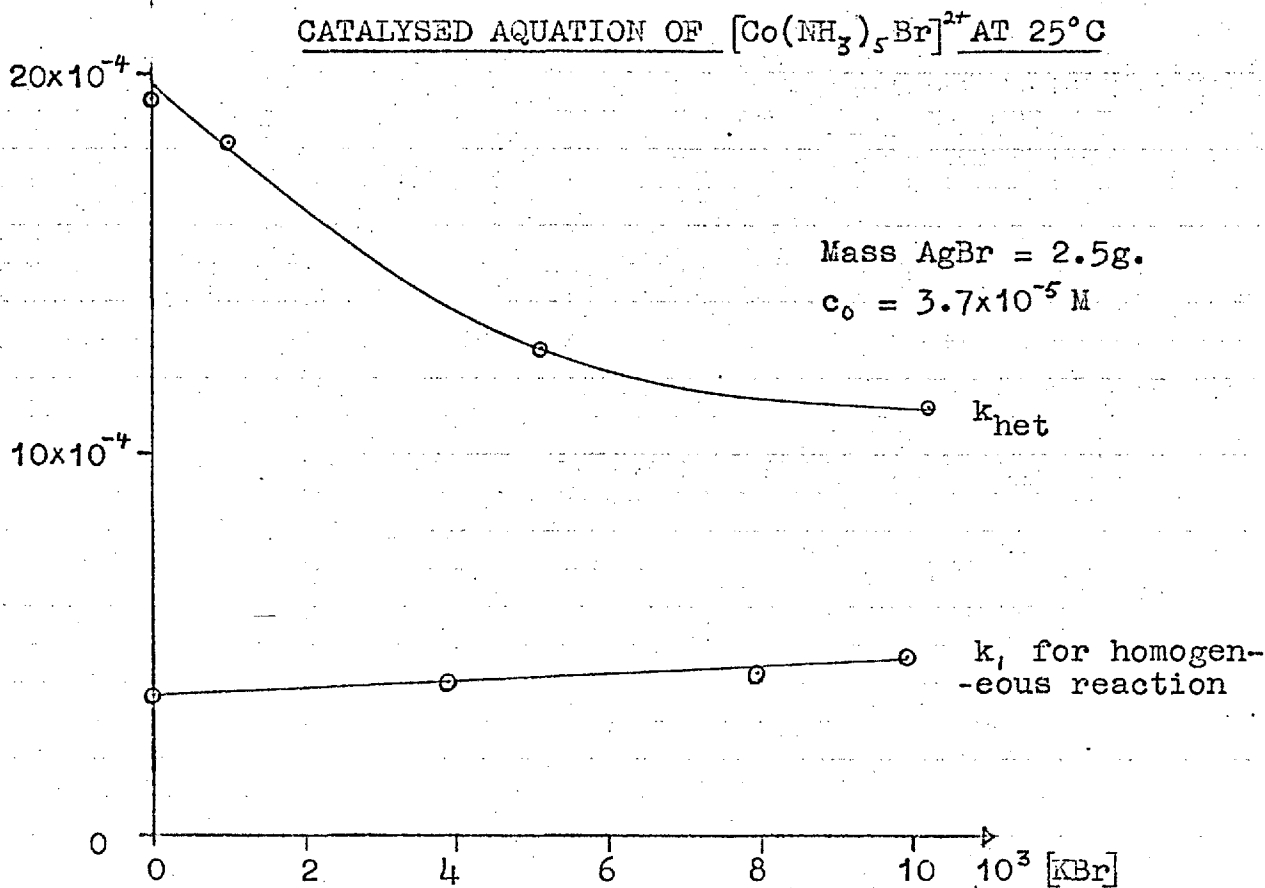
FIGURE XII: REPRESSIVE EFFECT OF IODIDE ON THE AgI-
CATALYSED AQUATION OF [Co(NH₃)₅Br]²⁺ AT 25°C
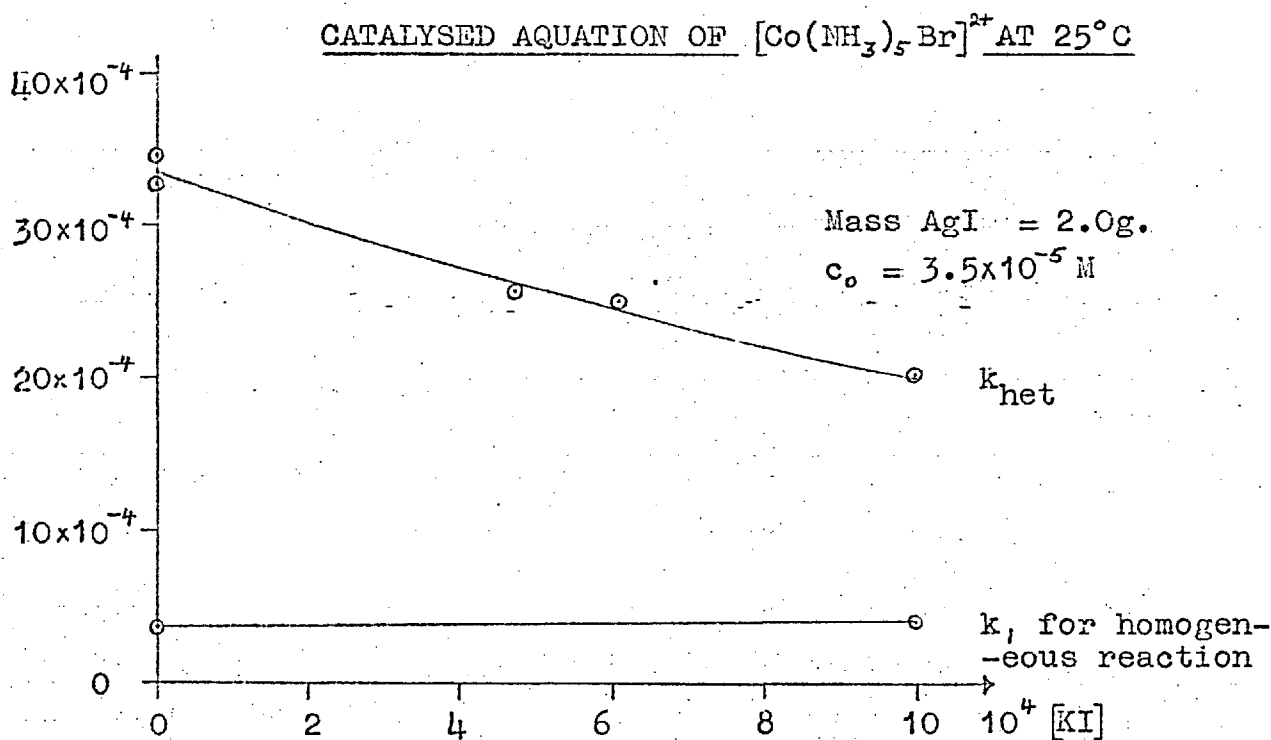
Figure XI indicates that the repressive effect of extra bromide produced by the aquation of $[Co(NH_3)_5Br]Br_2$ at $c_0 \leq 10^{-4}M$ is negligibly small.

## VI.3.3: Heterogeneous reduction of $[Co(NH_3)_5X]^{2+}$.

It was discovered by application of the routine test for Co(II), that $[Co(NH_3)_5Br]^{2+}$ was reduced by mercury, charcoal and silver. The overall rates of disappearance of $[Co(NH_3)_5Br]^{2+}$, measured at 253mμ, were all rather fast, as shown by the final column of Table XIX, page 104.

The mercury surface became covered with a fine powder, which was assumed to be $Hg_2Br_2$ ($E^0$ $Hg_2Br_2/Hg,Br^- = 0.14V$. at 25°C). The stoichiometry of the redox reaction was not, however, investigated.

The stoichiometry of the reaction of 0.7g. of purified activated charcoal, obtained from Messrs. Hopkin and Williams, with $[Co(NH_3)_5Br]^{2+}$ at $c_0 = 5.6 \times 10^{-5}M$ was investigated. The production of Co(II) and the disappearance of $[Co(NH_3)_5Br]^{2+}$ were followed spectrophotometrically for 5 hours, after which time 95% of the $[Co(NH_3)_5Br]^{2+}$ had reacted to form Co(II). Reduction was stoichiometric, and the rate constant for the disappearance of the complex was $88.5 \times 10^{-4} min^{-1}$. Very little Co(II) was "lost" by permanent adsorption on the charcoal. The small amount of $[Co(NH_3)_5H_2O]^{3+}$ that might have been formed by sponta-

neous aquation was not detected: it was probably also reduced by the charcoal.

The nature of the oxidising reaction undergone by charcoal (or possibly some sorbed impurity) was not investigated. As mentioned in Chapter II, charcoal is an excellent catalyst for interconversion of Co(III) complexes at much higher concentration, and it may be that the stoichiometric redox reaction observed at $c_0 = 5.6 \times 10^{-5} M$ is no more than a negligible side reaction at higher $c_0$.

$[Co(NH_3)_5X]^{2+}$ is reduced by Ag, $Co^{2+}$ and AgX being formed. ($E^0$ AgCl/Ag, $Cl^- = 0.22V.$, $E^0$ AgBr/Ag, $Br^- = 0.07V.$). This redox reaction was investigated in detail by use of a rotating disc (see Chapter XI). The rate of reaction was found to be diffusion-controlled. This explains why line 3 of Figure X, page 105, which shows the first order plot for the disappearance of $[Co(NH_3)_5Br]^{2+}$ in the presence of $39cm^2$ of silver foil, is linear and not down-ward curving as for a surface-controlled reaction.

VI.3.4: The use of Ag/AgX electrodes to follow the aquation of $[Co(NH_3)_5X]^{2+}$.

The course of ionic reactions is often followed potentiometrically or conductimetrically. Unforeseen interaction with the electrodes may, however, affect results. Silver-silver halide electrodes, for example, may both reduce $[Co(NH_3)_5X]^{2+}$ and catalyse aquation in

the vicinity of the electrode, increasing the rate of production of $X^-$.

The production of $Br^-$ by aquation of $[Co(NH_3)_5Br]^{2+}$ was followed potentiometrically with a small wire form $Ag/AgBr$ electrode in two experiments at $c_0 = 10^{-3}M$. In stirred solution, the correct homogeneous rate constant was obtained, but in unstirred solution, although spectrophotometric measurement of the rate still gave the homogeneous value, $[Br^-]$ in the region of the electrode was higher than in the bulk solution, and potentiometric determination of $k_1$ therefore gave a high value.

The cell used was

$$- \; Ag,AgBr \; | \; 5 \times 10^{-3}M \; KBr \; | \; 0.2M \; KNO_3 \; | \; [Co(NH_3)_5Br]Br_2 \; | \; Ag,AgBr+$$

$$\text{solution} \qquad \text{salt bridge} \qquad \text{solution in}$$
$$\text{(reference)} \qquad\qquad\qquad 10^{-3}M \; HClO_4,$$
$$c_0 = 10^{-3}M.$$
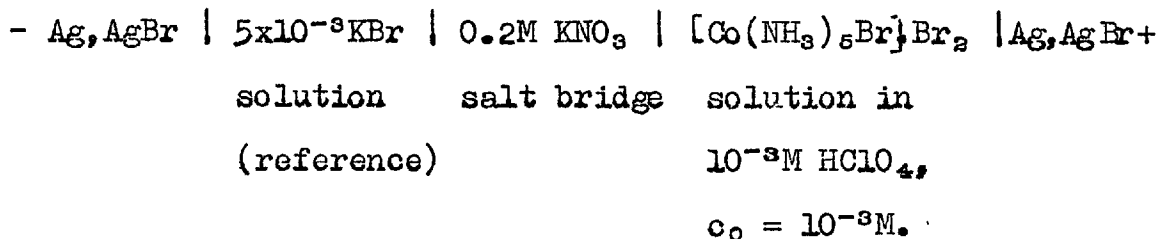
Ignoring the liquid junction potential, the cell e.m.f. is given by

$$E_t = \frac{RT}{F} \ln \frac{\{Br^-\}_{ref}}{\{Br^-\}_t}$$

where $\{Br^-\}_t$ is the activity of bromide ions in the right hand side at time t.

$$\therefore \; \{Br^-\}_t = \{Br^-\}_{ref} \; e^{-FE_t/RT}$$

As $\{Br^-\}_{ref}$ is constant, and the variation in activity coefficients in the right hand half cell will be small,

$$[Br^-]_t = Ae^{-FE_t/RT}$$

where A is a constant.

Guggenheim's method was used to determine the reaction rate constant from a knowledge of $[Br^-]_t$ :

At time t, $\quad \ln \dfrac{c_0}{3c_0-[Br^-]_t} \quad = \quad k_{obs} \, t.$

At time (t+τ), $\quad \ln \dfrac{c_0}{3c_0-[Br^-]_{t+\tau}} \quad = \quad k_{obs} \, (t+\tau)$

$\therefore \ln \left[ [Br^-]_{t+\tau} - [Br^-]_t \right] = \ln A \left[ e^{-FE_{t+\tau}/RT} - e^{-FE_t/RT} \right]$

$$= -k_{obs} \, t + \ln c_0 \, (1-e^{-k_{obs}\tau})$$

A graph of $\log \left[ e^{-FE_{t+\tau}/RT} - e^{-FE_t/RT} \right]$ versus time should therefore be linear, with gradient $k_{obs}/2.303$. Figure XIII, page 114, shows a graph of this function for a run carried out in unstirred solution. τ was taken as 2 hours. As seen, $k_{obs}$ is ten times greater than the homogeneous aquation rate constant, which dramatically illustrates the unreliability of the potentiometric method in this and similar cases.

FIGURE XIII: THE USE OF AN Ag/AgBr ELECTRODE TO FOLLOW THE
AQUATION OF $[Co(NH_3)_5Br]^{2+}$ at $25°C$
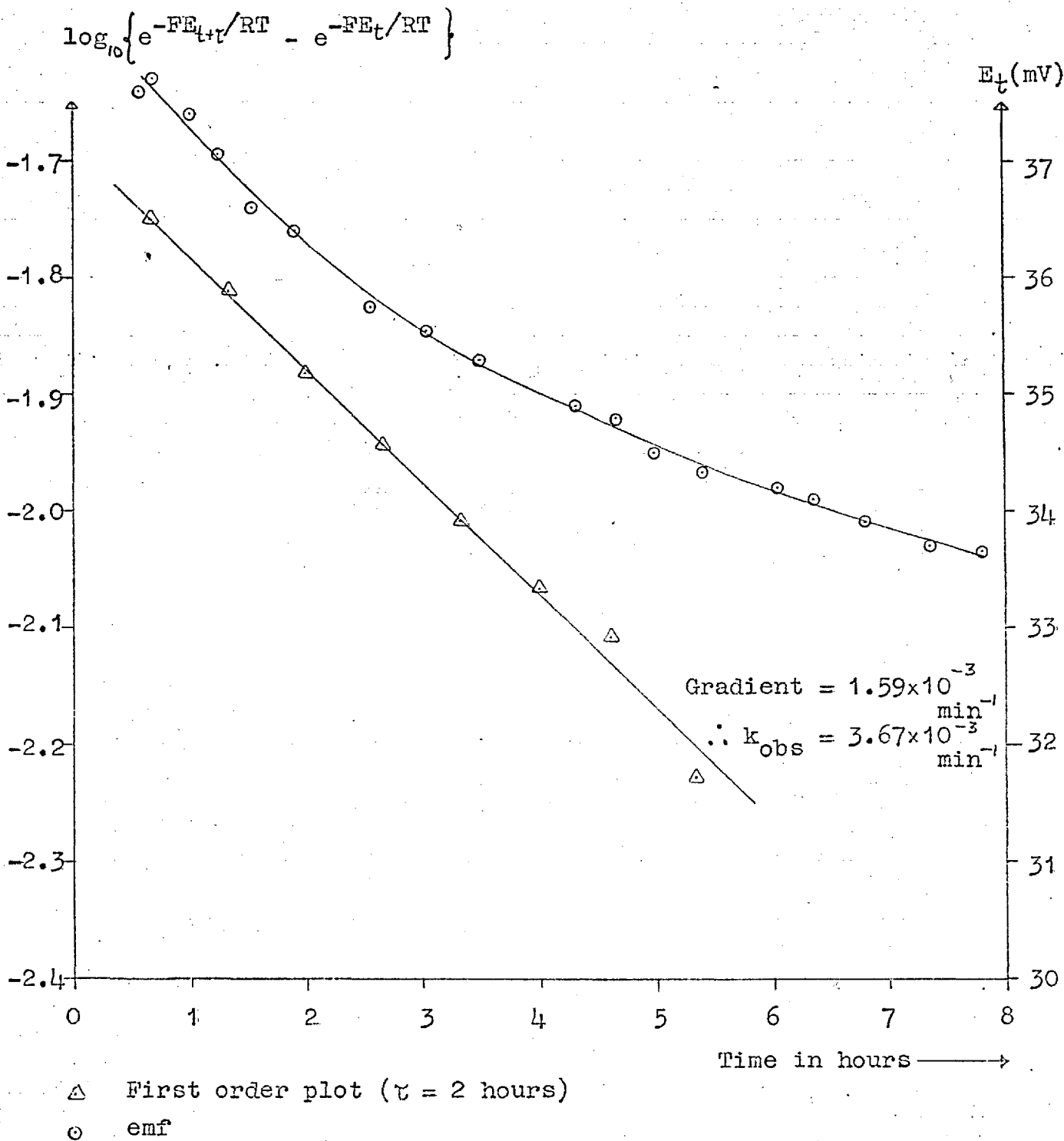
## VI.3.5: Effect of ion exchange resins upon $[Co(NH_3)_5X]^{2+}$.

It was thought that absorption of $[Co(NH_3)_5X]^{2+}$ by a cation exchange resin might weaken the complex ion and catalyse the aquation reaction. There was, however, no evidence from four experiments with the strongly acid sulphonate resin Zeo-Karb 225 in the H form that this was so. $[Co(NH_3)_5Br]^{2+}$ and $[Co(NH_3)_5Cl]^{2+}$ were rapidly absorbed from solution, but no $[Co(NH_3)_5H_2O]^{3+}$ appeared in the solution. In fact, the aquation reaction seemed to be hindered by absorption of $[Co(NH_3)_5X]^{2+}$, since the distinct colours of the occupied resin remained the same over a period of weeks, instead of changing within a few days to the quite distinct colour of $[Co(NH_3)_5H_2O]^{3+}$. The sorbed $[Co(NH_3)_5X]^{2+}$ ions were, strangely, not eluted by 3M $La(NO_3)_3$ or by saturated $[Co(NH_3)_6]Cl_3$.

## VI.4. Discussion.

The dependence of $k_{het}$ on the bulk concentration of reactant is discussed in the next Chapter.

## VI.4.1: The mechanism of the catalytic and redox reactions.

Homogeneous "catalysis" of the aquation of $[Co(NH_3)_5X]^{2+}$ by a metal ion $M^{n+}$ produces $MX^{(n-1)+}$:

as the latter is either insoluble or labile, this does not prove that a halide-bridging mechanism operates. However, the repression of the heterogeneous catalytic effects of the insoluble silver and mercuric salts by halide strongly suggests that $[Co(NH_3)_5X]^{2+}$ is adsorbed on metal ion sites on the catalyst surface through the halide. Free $X^-$ in solution can also adsorb on these sites, and therefore specifically repress catalysis. The $Co(III)-X^-$ bond in $[Co(NH_3)_5X]^{2+}$ is weakened by adsorption, so that production and desorption of $[Co(NH_3)_5H_2O]^{3+}$ and $X^-$ follow rather rapidly. The essential mechanism is thus the same in homogeneous and heterogeneous catalysis. However, localised adsorption of $[Co(NH_3)_5X]^{2+}$ on a heterogeneous catalyst could precede a mobile transition state. Catalysts normally have particularly active sites at crystal imperfections, and thus adsorption and catalytic reaction of $[Co(NH_3)_5X]^{2+}$ at low coverage may not be representative of the entire surface.

The oxidation of solid silver by $[Co(NH_3)_5X]^{2+}$ produced a coherent layer of AgX on the silver surface (see Chapter XI). Similarly, the redox reaction between $[Co(NH_3)_5X]^{2+}$ and $Cr^{2+}$ in homogeneous solution produced inert $CrX^{2+}$ complexes (126). The Co(II) produced in both cases forms labile complexes with $X^-$. The mechanism of the redox reaction is therefore concluded to be halide-bridged, an electron passing through the bridge and $X^-$

transferring from $Co^{2+}$ to form a stable complex with $Ag^+$ or $Cr^{3+}$.

There is therefore a formal similarity between the mechanisms of these catalytic and redox reactions, as illustrated in Figure XIV, page 118. However, although there is correlation between the rates of the spontaneous and catalysed aquations, there is no such correlation between the rate of aquation and of reduction (123).

It is not known whether the incoming water ligand in the heterogeneously catalysed aquation reaction is sorbed on the catalyst surface or not. It seems likely that bond breaking between $Co^{III}$ and $X^-$ is the important transition step, attack of water following rapidly. Although, by analogy with the spontaneous reaction, this has been depicted as cis attack, it could in fact be a trans attack, or a mixture of both.

# FIGURE XIV : MECHANISMS OF SPONTANEOUS AND CATALYSED AQUATION AND OF INNER-SPHERE REDUCTION OF $[Co(NH_3)_5X]^{2+}$.

1 = spontaneous aquation. (See Chapter V, Section V.1).

2 = aquation induced by homogeneous $M^{n+}$ (eg. $Ag^+$, $Hg^{2+}$).

3 = catalytic aquation on surface of insoluble $M^{n+}$ salt.

4 = redox reaction between $[Co(NH_3)_5X]^{2+}$ and $M^{n+}$ (eg. $Ag^0$, $Cr^{2+}$)

1. $[Co(NH_3)_5X]^{2+} + H_2O \rightleftharpoons \left[Co^{III}(NH_3)_5\right]^{2+} \rightarrow [Co(NH_3)_5H_2O]^{3+} + X^-$

2. $[Co(NH_3)_5X]^{2+} + H_2O + M^{n+} \rightleftharpoons$

$\left[Co^{III}(NH_3)_5\right]^{2+} \rightarrow [Co(NH_3)_5H_2O]^{3+} + MX^{(n-1)+}$

3. $[Co(NH_3)_5X]^{2+} + H_2O + catalyst \rightleftharpoons$

$\left[Co^{III}(NH_3)_5\right]^{2+} \rightarrow [Co(NH_3)_5H_2O]^{3+} + X^- + catalyst.$

catalyst surface $\underline{\qquad M^{n+} \qquad}$

4. $[Co(NH_3)_5X]^{2+} + M^{n+} \rightleftharpoons \left[Co^{III}(NH_3)_5\right]^{2+} \rightarrow \left[Co^{II}(NH_3)_5\right]^+$

$\rightarrow Co^{2+} + 5NH_3 + MX^{n+}$
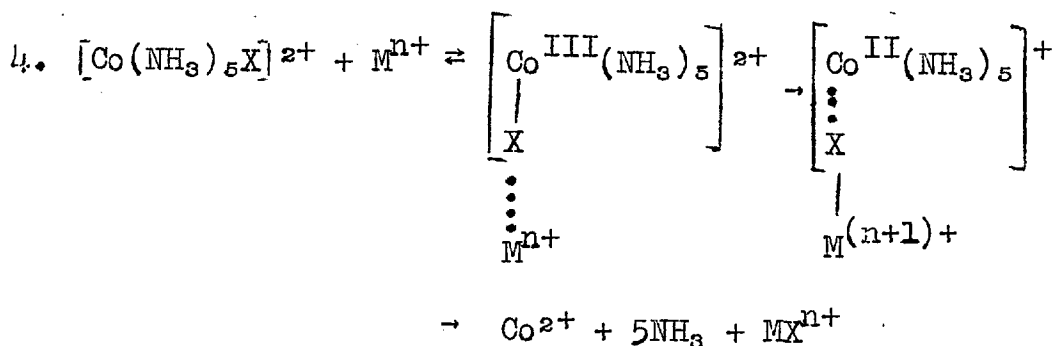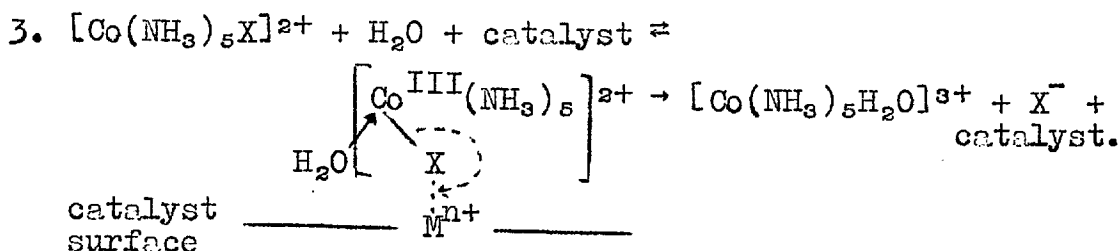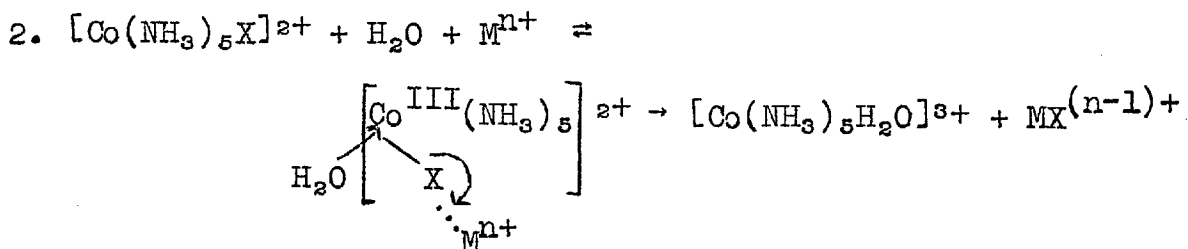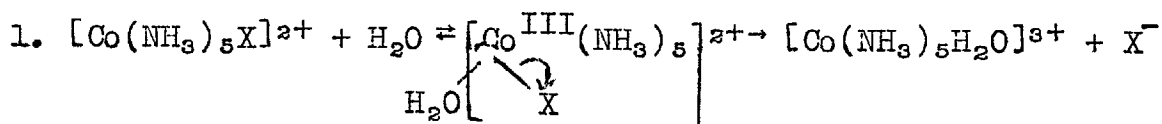
VI.4.2:  The nature of the heterogeneous catalysts.

It was shown on page 28 that the catalytic effect
of a metal ion in solution was related to the stability
of the complexes formed with halide released in the
aquation reaction.  The same broad conclusion applies to
the heterogeneous catalysts.  The nature of the catalyst
anion is considered irrelevant, and the catalyst cation
attracts halide from $[Co(NH_3)_5X]^{2+}$.  After reaction,
however, most of this halide must be released, as other-
wise a macroscopic charge would build up in solution and
on the solid.

$Hg^{2+}$ and $Ag^+$, which form stable halide complexes, are
thus a part of heterogeneous catalysts.  However, PbS
(see Table XVIII) was not a catalyst and $Hg_2X_2$ was,
although $Pb^{2+}$ complexes with halide more than $Hg_2^{2+}$ (see
page 28).  The crystal structure of a solid may, however,
modify the catalytic effect of the cation.

The noble metals Pt, Au and Pd were also catalysts.
Interaction with $[Co(NH_3)_5X]^{2+}$ and $X^-$ cannot in this case
be so specific, but halide ions are capillary active, and
are therefore probably adsorbed to some extent on these
metal surfaces.

# CHAPTER VII : INTRODUCTION TO QUANTITATIVE WORK ON THE CATALYTIC AQUATION OF $[Co(NH_3)_5X]^{2+}$.

## VII.1: Surface control of catalytic aquation reactions.

The decrease in $k_{het}$ with $c_{bulk}$ is evidence that the rates of the catalytic reactions are surface-controlled. As shown below, not only would $k_{het}$ for a diffusion-controlled process be independent of $c_{bulk}$, but its magnitude would be much greater than is actually observed.

The rate of a diffusion-controlled heterogeneous reaction (either catalytic or redox) is, by definition, equal to the rate of diffusion of the slowest moving reactant to the surface. For a single species i, this is given by Fick's first law, which may be stated in the general form

$$\frac{-dN_i}{dt} = 10^{-3}D_i \, A \, \frac{dc_i}{dx} \qquad (7.1)$$

where $-dN_i$ is the flux (in mole ⧸⧸⧸⧸) of species i, due to a concentration gradient $\frac{dc_i}{dx}$, across a plane of area A. $c_i$ is expressed in mole litre$^{-1}$ and $D_i$ is the diffusion coefficient of species i. If the system is well-stirred, then

$$\frac{dc_i}{dx} = \frac{c_{bulk} - c_s}{\delta} \qquad (7.2)$$

where $\delta$ is the thickness of the Nernst diffusion layer, and $c_s$ is the concentration of i at the surface. For a diffusion-controlled process, $c_s = 0$, and equation (7.1) becomes

$$\frac{-dN_i}{dt} = \frac{10^{-3}D_i \; A \; c_{bulk}}{\delta} \qquad (7.3)$$

If species i undergoes a pseudo first order hetero-geneous reaction, then

$$\frac{-dN_i}{dt} = k_{het} \; N_i \qquad (7.4)$$

Therefore $\quad k_{het} = \dfrac{10^{-3}D_i \; A}{V \; \delta} \qquad (7.5)$

where V litres is the volume of solution.

$k_{het}$ is therefore independent of $c_{bulk}$ for a first order diffusion-controlled reaction. Moreover, the magnitude of $k_{het}$ given by equation (7.5) is much greater than the value obtained from any of the present work on catalysis of the aquation of $[Co(NH_3)_5X]^{2+}$. For example 1g. of silver bromide of specific surface area $4.5 \times 10^3 \, cm^2 g^{-1}$ acting on 500ml. of stirred $[Co(NH_3)_5Br]^{2+}$ solution ($c_0 = 2.0 \times 10^{-5}M$) gave $k_{het} = 11.48 \times 10^{-4} min^{-1}$ (data from Chapter IX).

For this catalytic reaction, therefore

$$k_{het} = 2.55 \times 10^{-7} \ min^{-1} \ cm^{-2} \ surface \qquad (7.6)$$

Taking $\delta$, for a well-stirred solution, as $2 \times 10^{-3} cm$. and D for $[Co(NH_3)_5Br]^{2+}$ as $6.85 \times 10^{-6} \ cm^2 \ sec^{-1}$ (see Chapter XI), equation (7.5) gives for a diffusion-controlled reaction

$$k_{het} = 4.11 \times 10^{-4} \ min^{-1} \ cm^{-2} \ surface \qquad (7.7)$$

Comparing equations (7.6) and (7.7), it is clear that the rate of heterogeneous catalysis is governed by some process much slower than the rate of diffusion of the reactant, $[Co(NH_3)_5Br]^{2+}$ to the surface. The rate of diffusion of the other reactant, water, is certainly not the rate-determining factor, as water is the bulk medium. Moreover, since the mobilities of $[Co(NH_3)_5X]^{2+}$ and $[Co(NH_3)_5H_2O]^{2+}$ cannot be greatly different, the rate of diffusion of the product away from the catalyst surface cannot be the rate-controlling step. The slowest step must therefore be the adsorption of reactant, the desorption of product, or the rate of reaction of the reactant once adsorbed. Evidence will be presented that the latter is the slowest step in the heterogeneous catalysis of $[Co(NH_3)_5Br]^{2+}$ aquation.

The importance of stirring in systems containing catalysts is clear from equation (7.5). In unstirred solution, $\delta$ may have quite a large value, so that observed catalytic rates for relatively fast surface-controlled processes may be partially dependent on the rate of diffusion, and results are irreproducible.

## VII.2. Preliminary consideration of the variation of $k_{het}$ with $c_{bulk}$.

Experiments, reported in Chapters VIII-X, with HgS, AgBr and Pt catalysts of known surface area acting on $[Co(NH_3)_5Br]^{2+}$ solutions of concentration $c_{bulk}$, all gave the same general result: first order rate constants for the catalytic reaction decreased as $c_{bulk}$ increased according to the law

$$\frac{1}{k_{het}} = p\, c_{bulk} + q \qquad (7.8)$$
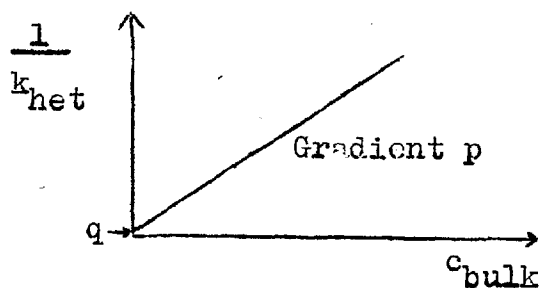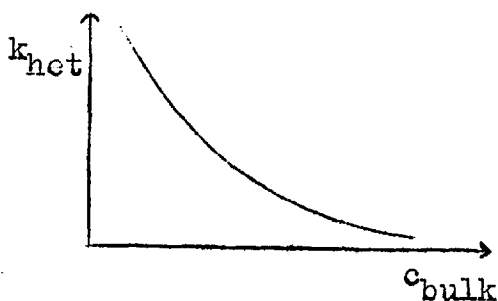
This form of variation of $k_{het}$ with $c_{bulk}$, illustrated on page 123, was immediately reminiscent of a Langmuir adsorption isotherm, and suggested that the adsorption of reactant on the catalyst surface was in accordance with an equilibrium isotherm of this type.

It was concluded that the aquation of adsorbed $[Co(NH_3)_5X]^{2+}$ was the rate determining step of the catalytic reaction:

$$[Co(NH_3)_5X]^{2+} + Catalyst \overset{fast}{\rightleftharpoons} [Co(NH_3)_5X]^{2+}_{ads}$$

$$\overset{+H_2O}{\underset{slow}{\rightarrow}} [Co(NH_3)_5H_2O]^{3+} + X^- + Catalyst \quad (7.9)$$
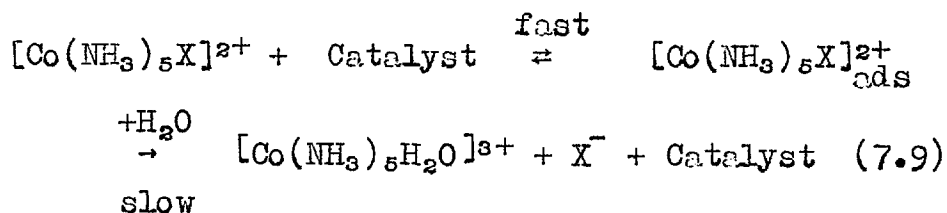
$[Co(NH_3)_5X]^{2+}_{ads}$ is thus equivalent to the activated complex of the theory of absolute reaction rates.

A similar reaction scheme was proposed (123) for the homogeneous reaction between $Hg^{2+}$ and several cobalt(III) chlorammines:

$$Hg^{2+} + [Co(en)_2XCl]^{n+} \rightleftharpoons [Co(en)_2XClHg]^{(n+2)+}$$

$$\overset{+H_2O}{\rightarrow} [Co(en)_2XH_2O]^{(n+1)+} + [HgCl]^+,$$

$$(7.10)$$
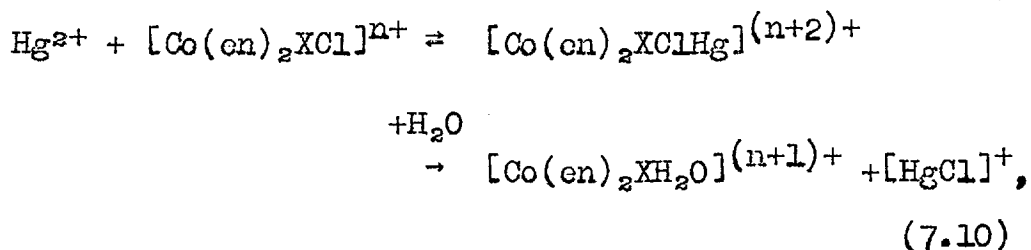
and also for the rate of Tl(I)/Tl(III) exchange on platinum (97).

The form of equation (7.9) prompts two questions: whether it is reasonable to assume that the rate of

adsorption of $[Co(NH_3)_5X]^{2+}$ is faster than its rate of reaction once adsorbed, and what the correct form of adsorption isotherm is. Once these are answered, then the observed kinetics can be related to the mechanism of catalysis by equation (7.9).

VII.3. Adsorption of $[Co(NH_3)_5X]^{2+}$ on catalyst surfaces.

VII.3.1: Rate of attainment of adsorptive equilibrium.

The rate of chemisorption is generally quite slow at moderate temperatures, because the heat of activation required for formation of a chemical bond is considerable. Halide-bridged bonds are thought to be responsible for the adsorption of $[Co(NH_3)_5X]^{2+}$ on catalysts: since permanent bond formation between $X^-$ and the catalyst does not result, this has the character of physical adsorption, which is a rapid process involving a low activation energy. For example, adsorption equilibrium of $Tl^+$ and $Tl^{3+}$ on platinised platinum was reached in less than 15 seconds (97). Moreover, in many polarographic experiments, equilibrium uptake of capillary-active species is assumed within the fall-time (3-6 seconds) of the mercury drop. Parsons (127) concluded from a mathematical analysis that physical adsorption equilibrium was reached in about 5 seconds in conditions of forced convection.

In comparison, the first order rate constant, $k_s$, for the aquation at 25°C of $[Co(NH_3)_5Br]^{2+}$ sorbed on HgS, was ~$5 \times 10^{-3}$ min$^{-1}$ (Chapter VIII) so the half-life of adsorbed $[Co(NH_3)_5Br]^{2+}$ was ~140 minutes (in homogeneous solution $t_{\frac{1}{2}} \approx 31$ hours). The ion $[Co(NH_3)_5Br]^{2+}$ must therefore adsorb and desorb many times on the catalyst surface before reacting, and adsorptive equilibrium is established at a fast rate compared to the catalytic aquation rate.

Moreover, as experiments on the repression of catalysis by addition of the products, Br$^-$ and $[Co(NH_3)_5H_2O]^{3+}$, showed that these ions were not strongly adsorbed on any of the catalyst surfaces, it was assumed that the rate of desorption of the products from the catalyst surface was not the rate-determining step either.

VII.3.2:  Adsorption isotherm of $[Co(NH_3)_5X]^{2+}$ on catalyst
surfaces.

Multilayer uptake of a relatively small ion such as $[Co(NH_3)_5X]^{2+}$ is very unlikely. The adsorption isotherm probably has a plateau region corresponding to monolayer coverage, as is the case for several ionic or polar species adsorbed on polar solids (eg. $[Co(NH_3)_5H_2O]^{3+}$ on HgS (Chapter VIII), dicarboxylic acids (128) and resorcinol (129) on Al$_2$O$_3$, stearic acid on Al$_2$O$_3$, TiO$_2$ and SiO$_2$ (130) ).

The experimental variation of $k_{het}$ with $c_{bulk}$ conformed to the Langmuir and Freundlich isotherms almost equally well. The assumptions implicit in the Langmuir isotherm, which is for monolayer uptake only, are that the adsorbent surface is energetically uniform, and that adsorbed species do not interact with each other. The Freundlich isotherm corresponds to a system in which the heat of adsorption decreases logarithmically with the degree of coverage of the surface (2).

VII.4. Derivation of the relationship between $k_{het}$ and $c_{bulk}$.

Consider the ion $[Co(NH_3)_5X]^{2+}$ undergoing a catalytic aquation reaction.

Let $c_{bulk}$ = bulk concentration of $[Co(NH_3)_5X]^{2+}$.

$c_{ads}$ = no. of moles $[Co(NH_3)_5X]^{2+}$ adsorbed per square cm. catalyst surface.

$c_{mono}$ = $c_{ads}$ at monolayer coverage

$\theta$ = $c_{ads}/c_{mono}$

= fraction of catalyst surface covered with reactant.

$A$ = specific surface area of catalyst ($cm^2 g^{-1}$)

$m_{cat}$ = mass of catalyst used.

$V$ = volume of solution in litres.

$k_{het}$ = observed first order rate constant for
catalytic reaction

$k_s$ = first order rate constant for reaction of
adsorbed $[Co(NH_3)_5X]^{2+}$ ions (assumed
independent of $\theta$).

The rate of the catalytic reaction may be expressed
in two ways:

$$\frac{-d}{dt} c_{bulk} = k_{het} c_{bulk} \qquad (7.11)$$

$$\frac{-d}{dt} c_{bulk} = k_s c_{ads}. \frac{Am_{cat}}{V} \qquad (7.12)$$

$c_{ads}$ in equation (7.12) can be replaced by some
function of $c_{bulk}$ by use of a suitable adsorption isotherm,
and expressions (7.11) and (7.12) equated. It is assumed
in equation (7.12) that $[Co(NH_3)_5X]^{2+}$ is the only
adsorbing species.

(i) The Langmuir model.

The Langmuir adsorption isotherm is

$$\theta/(1-\theta) = \sigma c_{bulk} \qquad (7.13)$$

where $\sigma$ is a constant proportional to the sticking

probability of $[Co(NH_3)_5X]^{2+}$ on the catalyst surface.

From (7.13), $\theta = \dfrac{c_{ads}}{c_{mono}} = \dfrac{\sigma \, c_{bulk}}{1 + \sigma \, c_{bulk}}$ (7.14)

Substituting for $c_{ads}$ in equation (7.12),

$$- \frac{d \, c_{bulk}}{dt} = k_s \, c_{mono} \cdot \frac{Am_{cat}}{V} \cdot \frac{\sigma \, c_{bulk}}{1 + \sigma \, c_{bulk}} \quad (7.15)$$

Equating (7.15) and (7.11),

$$k_{het} = k_s \, c_{mono} \cdot \frac{Am_{cat}}{V} \cdot \frac{\sigma}{1 + \sigma \, c_{bulk}} \quad (7.16)$$

$$\therefore \quad \frac{1}{k_{het}} = \frac{c_{bulk}}{k_s \, c_{mono}} \cdot \frac{V}{Am_{cat}} + \frac{V}{\sigma k_s \, c_{mono} \, Am_{cat}} \quad (7.17)$$

(7.17) is of the same form as equation (7.8), which, as stated, fits the experimental data quite well. The slope and intercept of linear plots of $1/k_{het}$ against $c_{bulk}$ yield the values of $\sigma$ and $k_s$, provided that $c_{mono}$ is known.

(ii) The Freundlich model.

The Freundlich isotherm is $c_{ads} = \sigma_F \, c_{bulk}^{\,\alpha}$ (7.18)

where $\alpha$ is a constant greater than 0 and less than 1.

Substituting for $c_{ads}$ in equation (7.12),

$$-\frac{d}{dt} c_{bulk} = k_s \cdot \frac{Am_{cat}}{V} \cdot \sigma_F \, c_{bulk}^{(\alpha-1)} \quad (7.20)$$

$$\therefore \quad \log k_{het} = (a-1) \log c_{bulk} + \log (k_s A m_{cat} \sigma_F / V)$$

$$(7.21)$$

Plots of $\log k_{het}$ vs. $\log c_{bulk}$ should therefore be linear with negative fractional slopes: it is, however, not possible to deduce the value of $k_s$ from the intercept, as $\sigma_F$ cannot be determined separately. For this reason, the Freundlich plot, although it fits experimental data quite reasonably, is not very useful, and applicability of the Langmuir isotherm is assumed in further theoretical considerations.

## VII.5. Catalytic aquation in the presence of added electrolytes.

The product of the aquation reaction, $X^-$ and $[Co(NH_3)_5H_2O]^{3+}$, added in concentrations of $10^{-3}M$, exerted a repressive effect on most catalytic reactions. It is assumed that this is because they competed, although not very effectively, with $[Co(NH_3)_5X]^{2+}$ for adsorption sites. The Langmuir treatment is readily extended to this situation, the adsorption isotherms becoming

$$\frac{\theta}{1 - \theta - \theta_y} = \sigma c_{bulk} \qquad (7.22)$$

$$\frac{\theta_y}{1 - \theta - \theta_y} = \sigma_y c_y \qquad (7.23)$$

where $\theta$, $\sigma$ and $c_{bulk}$ have their former meanings, and the subscript y refers to the added electrolyte.

From (7.22) and (7.23),

$$\theta = \frac{\sigma c_{bulk}}{1 + \sigma c_{bulk} + \sigma_y c_y} \qquad (7.24)$$

and substitution into equations (7.11) and (7.12) gives the relationships

$$k_{het} = k_s c_{mono} \cdot \frac{Am_{cat}}{V} \cdot \frac{\sigma}{1 + \sigma c_{bulk} + \sigma_y c_y} \qquad (7.25)$$

and
$$\frac{1}{k_{het}} = \frac{c_{bulk}}{k_s c_{mono}} \cdot \frac{V}{Am_{cat}} + \frac{c_y}{k_s c_{mono}} \cdot \frac{\sigma_y}{\sigma} \cdot \frac{V}{Am_{cat}}$$

$$+ \frac{V}{\sigma k_s c_{mono} Am_{cat}} \qquad (7.26)$$

Equations (7.25) and (7.26) should be compared with equations (7.16) and (7.17) respectively. In the presence of a constant concentration of repressive ions, the gradient of a plot of $1/k_{het}$ versus $c_{bulk}$, which should still be linear, will be unchanged. The intercept will be greater by addition of the term

$$\frac{c_y}{k_s c_{mono}} \cdot \frac{\sigma_y}{\sigma} \cdot \frac{V}{Am_{cat}} \cdot$$

These conclusions are borne out only moderately well by the experimental results for HgS and AgBr, as shown in Chapters VIII and IX.

VII.6:  Derivation of a function of $c_{bulk}$ linear with
time over a wide range of $c_{bulk}$.

As previously mentioned, first order plots of data
from catalytic runs are linear over rather short ranges
in $c_{bulk}$ (<20%) but tend to show downward curvature if
a large part of the aquation reaction is followed.  By
use of equation (7.8), a function of $c_{bulk}$ which should
be accurately linear with respect to time can be deduced.
This function is given in equation (7.30) below.  When
it is applied to data which give curved first order plots,
a linear plot is obtained, as shown on page 156 for HgS
acting on $[Co(NH_3)_5Br]^{2+}$.  Data which give linear first
order plots also give linear plots of the derived function,
but this is not so sensitive a test.

At any particular bulk concentration of $[Co(NH_3)_5X]^{2+}$,
the rate of reaction is given by the expression

$$-\frac{d\,c_{bulk}}{dt} = (k_1 + k_{het})\,c_{bulk} \qquad (7.27)$$

Substituting for $k_{het}$ the Langmuir expression (7.8),

$$-\frac{d\,c_{bulk}}{dt} = \left(k_1 + \frac{1}{pc_{bulk} + q}\right) c_{bulk} \qquad (7.28)$$

Rearrangement of (7.28) gives expression (7.29), in which
the subscript has been dropped.

$$p \int \frac{dc}{1 + k_1 q + k_1 pc} + q \int \frac{dc}{c} = -(1 + k_1 q) \, dt \qquad (7.29)$$

Integration gives the relationship

$$\frac{1}{k_1 q} \log \frac{(1 + k_1 q + k_1 pc_0)}{(1 + k_1 q + k_1 pc)} + \log \frac{c_0}{c} = \frac{(1 + k_1 q)}{2.303 q} \cdot t \qquad (7.30)$$

The function on the left-hand side is linear with respect to time. The gradient of the plot should be $(1 + k_1 q)/2.303q$. The values of q and p are obtained from a graph of $1/k_{het}$ against c.

## Vll.7. Use of rotating discs to investigate catalytic phenomena.

The hydrodynamic equations for fluid flow and mass transport to the surface of a horizontal disc rotating in a fluid have been solved by Levich (131) and reviewed by Riddiford (132): the rate of mass transport to the disc surface is controlled by the speed of rotation of the disc.

Rotating disc electrodes are now widely used to determine diffusion coefficients and the mechanisms of electrochemical and fast homogeneous reactions. Large discs, of several centimetres diameter, not used as electrodes, can be used to study relatively slow heterogeneous processes undergone by species in solution. In the present work, a platinum disc of surface area 25.16 cm² was used to study the catalytic aquation of $[Co(NH_3)_5Br]^{2+}$ (Chapter X), and a silver disc of area 12.57 cm² to study the heterogeneous reduction of $[Co(NH_3)_5Cl]^{2+}$ and $[Co(NH_3)_5Br]^{2+}$ (Chapter XI).

## VII.7.1: Theory of the rotating disc.

The main points will be briefly outlined.

Mass transport to the rotating disc surface occurs convectively up to the so-called "transport boundary layer", of thickness $\delta$, through which diffusive flow to the actual

surface occurs. The magnitude of δ is the same at all points on the disc, and its value for a species i is given by the Levich expression

$$\delta = 1.613 D_i^{\frac{1}{3}} v_s^{\frac{1}{6}} \omega^{-\frac{1}{2}} \left[ 1 + 0.354 (D_i/v_s)^{0.36} \right], \quad (7.31)$$

where $D_i$ = diffusion coefficient of species i ($cm^2 \ sec^{-1}$)

$v_s$ = kinematic viscosity (=viscosity/density) of the bulk medium (poise $ml.g^{-1}$).

$\omega$ = angular speed of rotation of disc (radians $sec^{-1}$).

The term in brackets is a correction, which affects δ by less than 3%. It is seen that in a given system, δ is inversely proportional to the square root of the speed of rotation.

The rate of mass transport to a rotating disc surface of area A, from equations (7.1) and (7.2), is

$$\frac{-dN_i}{dt} = \frac{10^{-3} D_i A (c_{bulk} - c_s)}{\delta} \quad (7.32)$$

The maximum flux occurs when $c_s = 0$.

The flux to a rotating disc surface can therefore be calculated by combining equations (7.31) and (7.32).

Equation (7.31) was deduced for an infinite horizontal lamina rotating with constant angular velocity in a fluid of infinite extent. In real systems, edge effects can

interfere. In the present work, the discs on inert trumpet-shaped formers were immersed 2-4cm. below the surface of 500ml. solution contained in a cylindrical vessel of diameter 10cm. Johnston's extensive investigation of edge effects (133) shows that they are quite negligible under these circumstances.

Equation (7.31) is valid only for streamlined flow. Turbulence set in at the periphery of the discs used in the present work above 1000 rpm. Experiments were confined to the range 100-1000 rpm: at very low rotation speeds, behaviour is, not surprisingly, erratic (133).

The surface of the discs must be smooth for equation (7.31) to apply. Abrasion with finest grade emery paper produces a surface with irregularities of the order of $10^{-4}$cm. This is only about $^1/20$th of the value of $\delta$ at 1000 rpm, and can be ignored (133).

VII.7.2: Rotating disc apparatus.

The characteristics of the platinum and silver discs are described in the relevant chapters. The discs were mounted on the assembly shown in Figure XV. The electrical connection to the disc surface from the top of the rotating shaft was used with the platinum disc, but not with the silver disc.

The discs were detachably mounted onto the lower

FIGURE XV: ROTATING DISC
ASSEMBLY

Electrical
connection
to Servomex
motor
controller

Stroboscopic
disc

Teflon cup
for mercury

platinum
contact

hollow
steel shaft

insulated
rod screws
into disc

insulated
rod screws
into disc

hollow
steel shaft

3 nylon
retaining
screws

insulating
sleeve
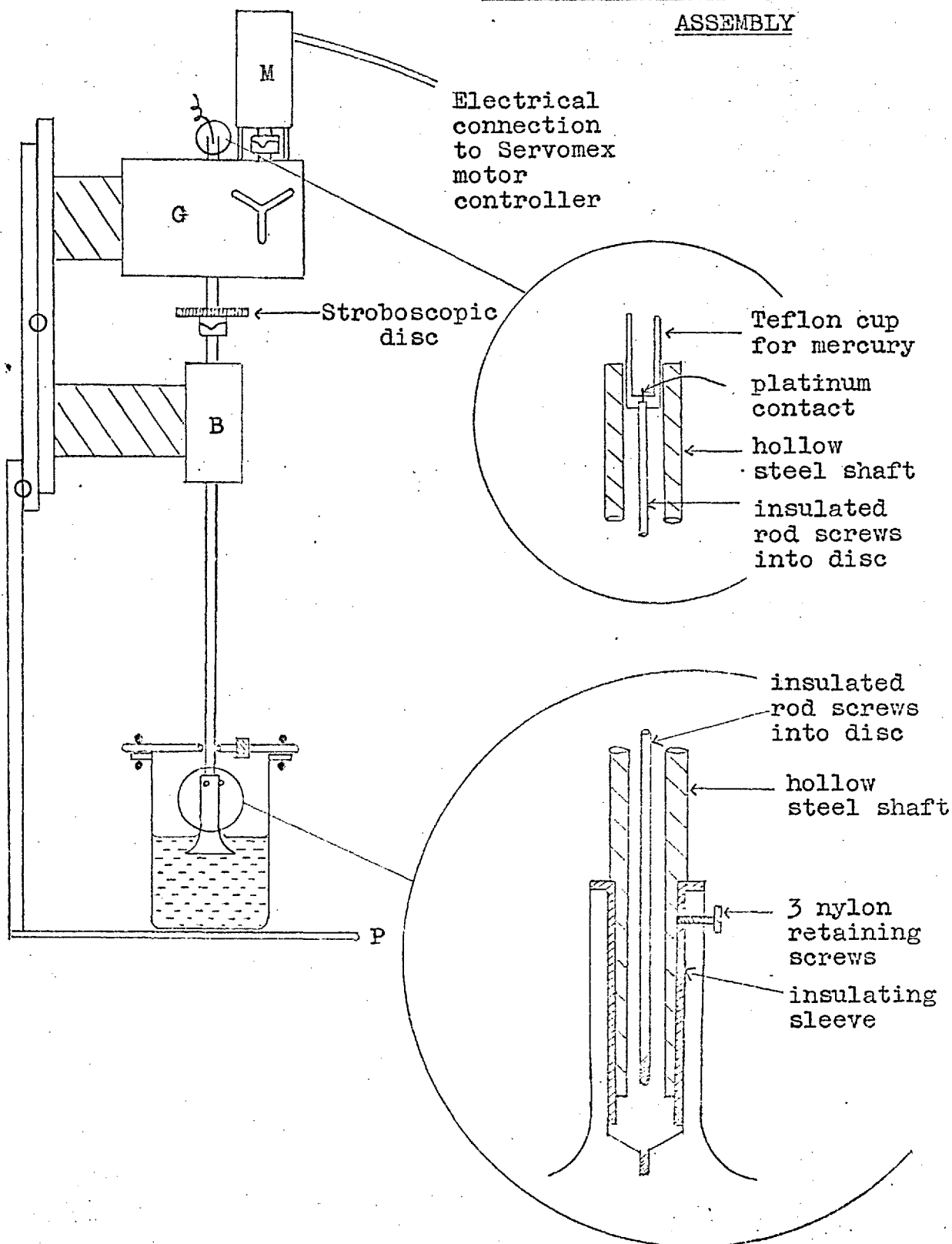
end of a vertical steel shaft connected through cone
roller bearings, B, and a three speed gearbox, G, to
a d.c. motor, M, coupled to a Servomex M.C.43 controller.
The motor speed could be read directly from the Servomex
dial, but frequent calibration with a stroboscopic disc
was necessary, and it was simpler to set the controller
unit by reference to the stroboscope than to the dial.

The rotation of the shaft, and the discs, which
were both carefully balanced, was true to the eye.

The assembly described above was mounted on a metal
frame, upon which was also mounted a platform, P, to
support the reaction vessel, into which the disc was
lowered.  The height of the platform and the shaft were
separately adjustable, so that the apparatus could be
readily assembled, and the reaction vessel partially
immersed in a thermostatted water bath.

# CHAPTER VIII : CATALYSIS BY MERCURIC SULPHIDE OF THE AQUATION OF $[Co(NH_3)_5Br]^{2+}$.

All experiments were carried out at 25°C, using samples of the same batch of HgS. The variation of $k_{het}$ with the concentration of reactant, $[Co(NH_3)_5Br]^{2+}$, was investigated, and also the repressive effect of the product, $[Co(NH_3)_5H_2O]^{3+}$. The latter was complemented by determination of the adsorption isotherm of $[Co(NH_3)_5H_2O]^{3+}$ on HgS. The equations derived in Chapter VII were tested, and found to fit experimental data quite well, and the efficiency of $Hg^{2+}$ in the homogeneous and heterogeneous states as an aquation catalyst was compared.

## VIII.1. Mercuric sulphide

Red mercuric sulphide (cinnabar) has a helical chain structure, in which each Hg atom has two neighbours at 2.36Å, two more at 3.10Å and two more at 3.3Å (134). (The Goldschmidt radii of $Hg^{2+}$ and $S^{2-}$ are 1.1Å and 1.84Å respectively). The surface area occupied per HgS molecule is therefore in the region 22 - 44Å².

The solubility product at 25°C is $2.915 \times 10^{-15}$M, so a saturated solution contains a negligible concentration ($\sim 6 \times 10^{-8}$M) of $Hg^{2+}$ ions.

A uniform batch of mercuric sulphide was prepared

by vigorously stirring 50g. of the product supplied by
BDH with 1 M nitric acid for 1 hour. This broke up lumps
into a fine powder, and, it was hoped, removed any
oxidisable impurities. The solid was filtered and washed
with much water and dried under vacuum. The specific
surface area of this batch of HgS was determined by B.E.T.
uptake of nitrogen, and found to be $(2.5 \pm 0.5)m^2 \ g^{-1}$. Mr.
J.D.W. Hudson kindly undertook this measurement. The
powder had a uniformly fine appearance, and formed a
suspension in water even on gentle stirring.

VIII.2.   Experimental procedure.

The procedure was as described in Section (VI.2.).
Aliquots were removed without stopping the stirrer, and
therefore no sampling correction was applied to the results,
since the amount of HgS per unit volume remained unchanged.

The production of $[Co(NH_3)_5H_2O]^{3+}$ was followed in
several experiments. Conversion of $[Co(NH_3)_5Br]^{2+}$ to
$[Co(NH_3)_5H_2O]^{3+}$ was always quantitative for at least the
first twelve hours, the maximum time required for hetero-
geneous runs. Thereafter, a slow secondary reaction
producing Co(II) occurred, such that ~5% of the total
cobalt was present as Co(II) after 4 days. Solutions
after this time gave a slight positive test for sulphate,
and it was concluded that a slow redox reaction between

the Co(III) complexes and $S^{2-}$ was responsible. This does not interfere significantly with the much faster catalytic aquation reaction.

The rate of the catalytic aquation was found to be subject to a slight photochemical effect. The rate in the dark was roughly 70% of the rate in normal laboratory lighting. A much more pronounced effect was found for silver bromide (see the next chapter) and it was concluded that light enhanced the reaction rate, rather than the adsorption of $[Co(NH_3)_5Br]^{2+}$ on AgBr. The same phenomenon could be operating for HgS. However, it has been reported that red mercuric sulphide adsorbs six times as much phenolphthalein in the light as in the dark (135). All the experiments with HgS were carried out in the light.

# RESULTS

VIII.3.  The first order dependence of $k_{het}$ on $m_{cat}$.

Equation (7.16) predicts that $k_{het}$ should be proportional to $m_{cat}$, other factors being equal.  This proportionality was verified by the three experiments shown in Figure XVI below.

FIGURE XVI :  PLOT OF $k_{het}$ vs. $m_{cat}$ AT 25°C.
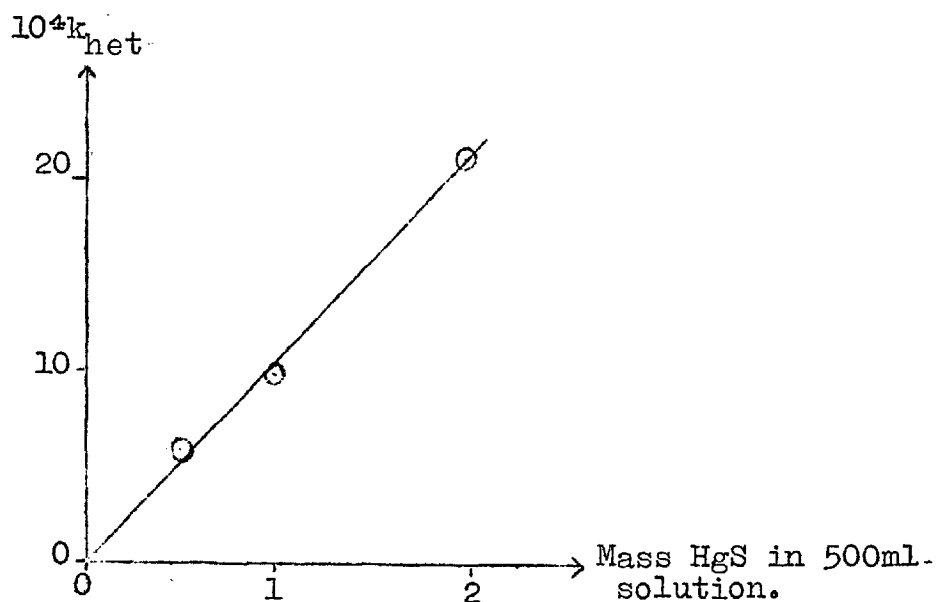


| $10^5 c_0$ | Mass HgS in 500ml. | $10^4 k_{het}$, min$^{-1}$ |
|---|---|---|
| 2.9 | 0.5005g. | 5.65 |
| 2.9 | 1.000g. | 9.65 |
| 2.9 | 2.001g. | 21.12 |

VIII.4.  The dependence of $k_{het}$ on $c_{bulk}$.

As the concentration of $[Co(NH_3)_5Br]^{2+}$ decreases
during each pseudo first order run, each value of $k_{het}$
obtained is appropriate to a range of concentration,
rather than to a single value.  However, it is necessary
to choose a single value in order to present the results
graphically.  The mean concentration, $\bar{c}$, was therefore
calculated for each run from the optical densities at
the beginning and end of the run.  The range of $c_{bulk}$ in
each run is then $\bar{c} \pm (c_0 - \bar{c})$.  The quantity $\bar{c}$ is clearly
somewhat arbitrary, as it depends on the extent to which
the catalytic reaction was followed.  However, this series
of runs was carried out over such a large overall range,
that the uncertainty in $\bar{c}$ was unimportant.  The term $\bar{c}$
is taken to be synonymous with the term $c_{bulk}$ used in
Chapter VII.

This series of experiments was carried out in the
range $\bar{c} = 6 \times 10^{-6} - 2.4 \times 10^{-3} M$.  The values of $k_{het}$ in this
range are tabulated in Table XX and plotted in Figure XVII.
Figures XVIII and XIX are "Langmuir plots" of $1/k_{het}$
versus $\bar{c}$, and Figure XX is a "Freundlich plot" of log $k_{het}$
versus log $\bar{c}$.  The equations leading to the Langmuir and
Freundlich plots were derived in Chapter VII.  The
experimental uncertainty in $k_{het}$, and the concentration
range in each run, are shown for representative points

TABLE XX :   THE PSEUDO FIRST ORDER RATE CONSTANT $k_{het}$

AS A FUNCTION OF THE CONCENTRATION OF $[Co(NH_3)_5Br]^{2+}$.

$c_0$ = initial concentration in each run.

$\bar{c}$ = mean concentration in each run.

$k_{het} = k_{obs} - k_1 = k_{obs} - 3.7 \times 10^{-4}$.

All results for 1.000g. HgS in 500ml. solution at 25°C.

| $10^5 c_0$, M. | $10^5 \bar{c}$, M. | $10^4 k_{het}$, min$^{-1}$. |
|---|---|---|
| 0.903 | 0.60 | 21.6 ± 0.5 |
| 1.26 | 0.97 | 18.0 ± 0.5 |
| 1.54 | 1.23 | 11.5 ± 0.3 |
| 2.87 | 2.36 | 8.73 ± 0.3 |
| 3.87 | 3.00 | 8.60 ± 0.3 |
| 7.37 | 6.08 | 6.23 ± 0.2 |
| 11.15 | 9.15 | 5.13 ± 0.2 |
| 30.96 | 28.0 | 2.31 ± 0.15 |
| 58.89 | 53.6 | 0.71 ± 0.11 |
| 100.0 | 93.0 | 0.60 ± 0.11 |
| 134.7 | 127 | 0.71 ± 0.11 |
| 200.0 | 187 | 0.31 ± 0.11 |
| 254.6 | 222 | 0.34 ± 0.11 |
| 254.6 | 237 | 0.28 ± 0.11 |

FIGURE XVII: PLOT OF $k_{het}$ vs. $\bar{c}$

(All data for 25°C)

$10^4$ $k_{het}$

$\theta$ = degree of coverage of surface by reactant (see Section VIII.4.2)

Adsorption isotherm

$10^5 \bar{c}$
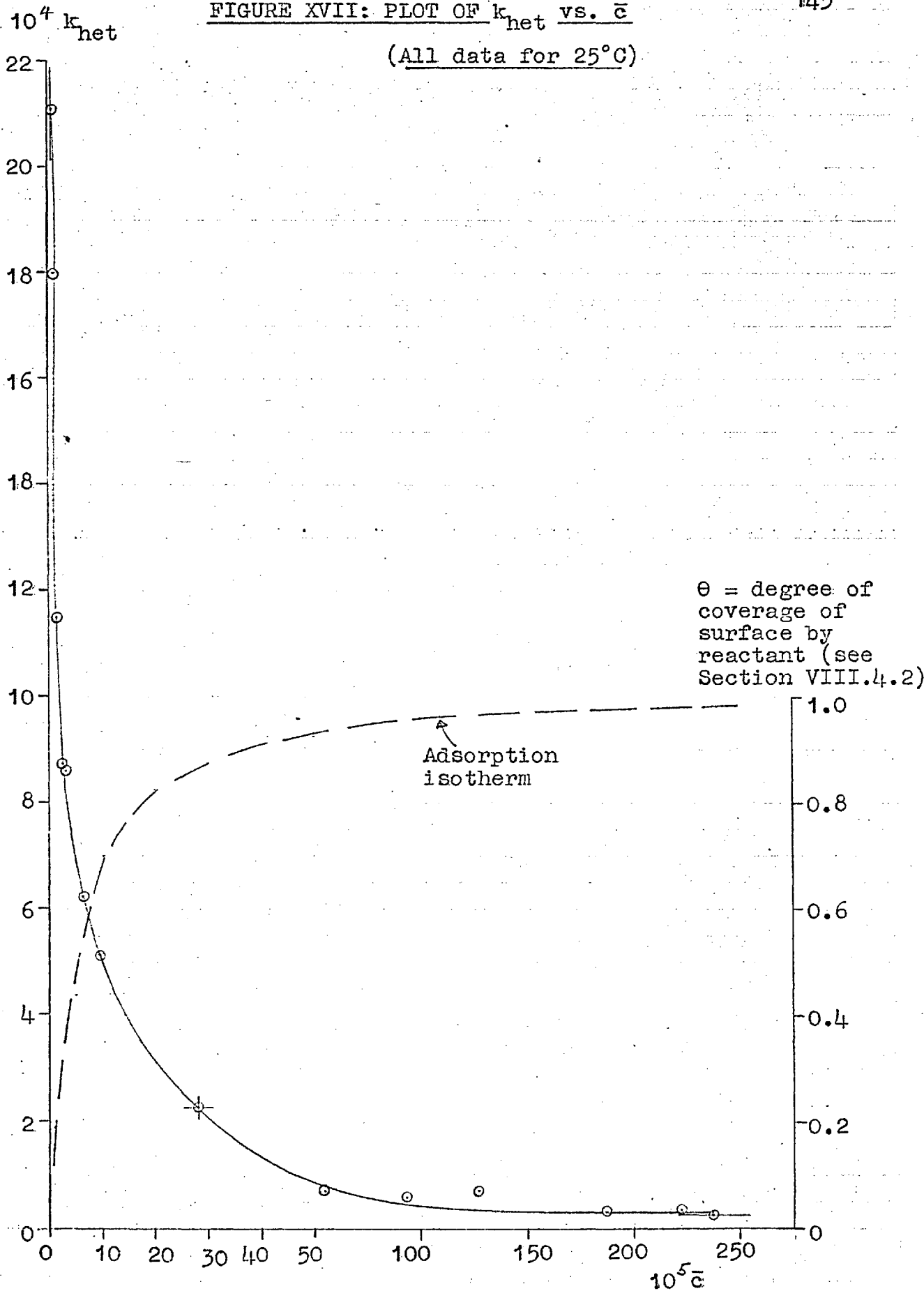
FIGURE XVIII: LANGMUIR PLOT IN RANGE $\bar{c} = 0 - 2.5 \times 10^{-3}$ M



$10^{-3}/k_{het}$

Gradient = $1.56 \times 10^7$ M$^{-1}$ min$^{+1}$

$10^4\,\bar{c}$
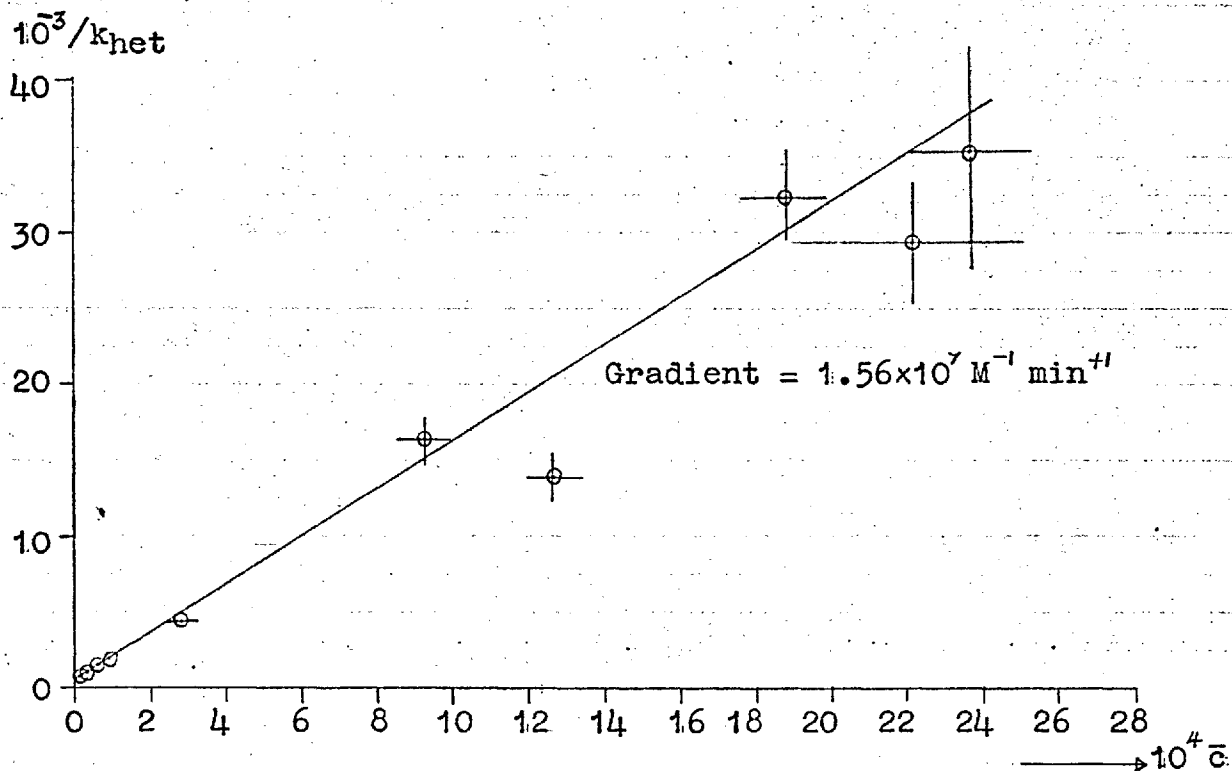
FIGURE XIX: LANGMUIR PLOT IN RANGE $c = 0 - 10^{-4}$ M



$10^{-3}/k_{het}$

Gradient = $(1.56 \pm 0.15) \times 10^7$ M$^{-1}$ min$^{+1}$
Intercept = $(6.7 \pm 0.3) \times 10^3$ min$^{+1}$

$10^5\,\bar{c}$
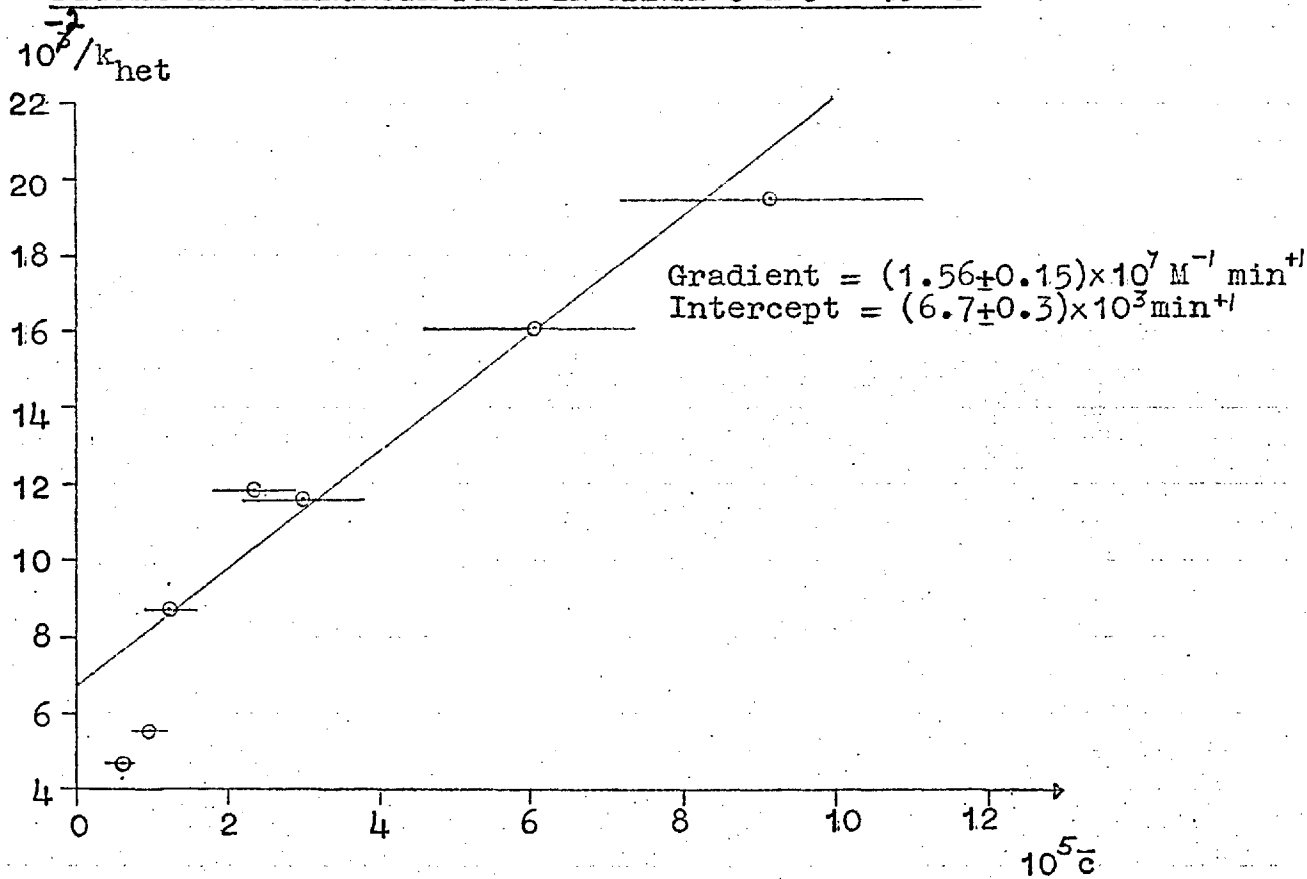
# FIGURE XX: FREUNDLICH PLOT



Gradient = -0.7 i.e. $\alpha = 0.3$
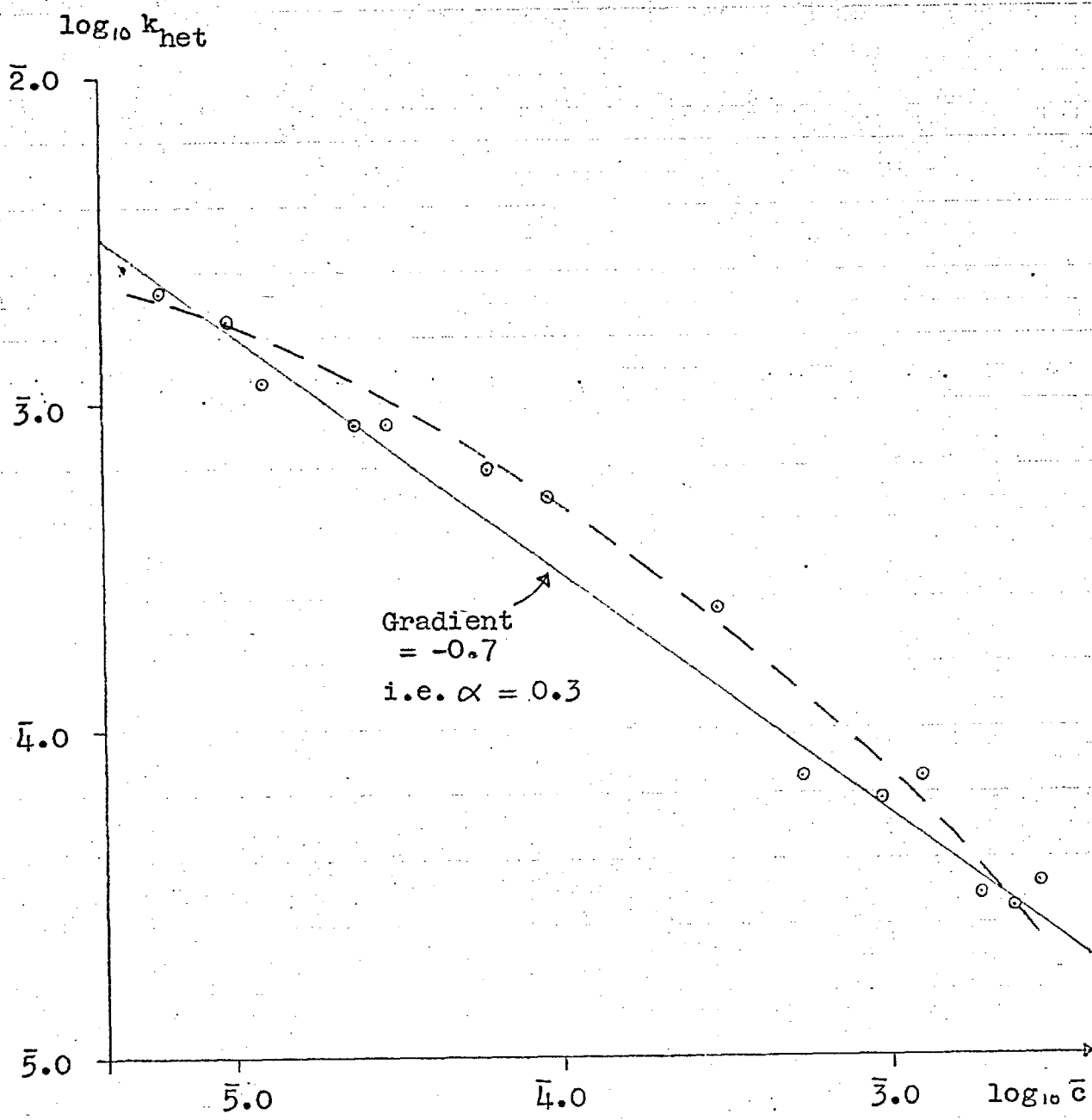
on each graph.

$k_{het}$ is calculated as $(k_{obs} - k_1)$. The error in $k_{obs}$ is $\pm 2\%$ for all values of $\bar{c}$, but the error in $k_{het}$ increases as $k_{obs}$ decreases, from $\pm 2.5\%$ at $\bar{c} = 6\times 10^{-5}M$ to $\pm 40\%$ at $\bar{c} = 2.5\times 10^{-3}M$.

VIII.4.1: Validity of first order plots of kinetic data.

The curvature of the graph of $k_{het}$ vs. $\bar{c}$ (Figure XVII) is so pronounced that it seems suprising that the value of $k_{het}$ does not increase in each individual run, causing first order plots to be curved. On reflection, however, the reason for this is clear.

Figures XVIII and XIX show that the data are fitted by the expression

$$\frac{1}{k_{het}} = 6.7\times 10^2 + 1.56\times 10^7 c.$$

Combining this with the equation

$$k_{obs} = k_{het} + k_1 = k_{het} + 3.7\times 10^{-4}\ min^{-1},$$

the percentage change in $k_{obs}$ due to a given percentage change in c at any value of $\bar{c}$ can be evaluated:

| $\bar{c}$ | Percentage decrease in c in run. | Percentage change in $k_{het}$ | Percentage change in $k_{obs}$ |
|---|---|---|---|
| $10^{-5}M$ | 50 | 10 | 7 |
| | 25 | 4 | 3 |
| $10^{-4}M$ | 50 | 42 | 21 |
| | 25 | 18 | 10 |
| $10^{-3}M$ | 50 | 63 | 7 |
| | 25 | 26 | 2 |

The change in $k_{het}$ increases with increasing $\bar{c}$, for
a given percentage change in c. However, the overall
magnitude of $k_{het}$ decreases, so the observed change in
$k_{obs}$ passes through a maximum in the region of $10^{-4}M$
(the region of greatest curvature in Figure XVII). A
change in $k_{obs}$ of less than 10% is not apparent on a
first order plot if the data are at all scattered, but
the curvature of a first order plot will be clear if the
change in $k_{obs}$ during the run is much greater than 10%.
Thus, runs followed for ~25% of their total course are
always pseudo first order, but runs followed to completion,
especially in the range $c_0 = 2 \times 10^{-4} - 5 \times 10^{-5}M$, deviate
somewhat from a first order law: the appropriate linear
function, equation (7.30), in such cases is tested in
Section (VIII.4.4:).

VIII.4.2:   The Langmuir plot.

There is considerable scatter both in the Langmuir plot and in the less sensitive Freundlich plot. There is, however, no systematic deviation from linearity in the Langmuir plot, which fits the data over a wide range of $\bar{\theta}$ quite well, except for the points for the two lowest concentrations. These fall significantly off the straight line, $k_{het}$ being greater than predicted. This is possibly due to a small proportion of especially active sites on the catalyst. These two points are not considered representative, and the line drawn is the best fit for all the other data.

The slope of the Langmuir plot is $(1.56\pm0.15)\times10^7 M^{-1} min$, and the intercept at $\bar{c} = 0$ is $(6.7\pm0.3)\times10^2 min^{+1}$. Therefore, from equation (7.17),

$$V/k_s\ c_{mono}\ Am_{cat} = (1.56\pm0.5)\times10^7\ M^{-1}\ min^{+1} \quad (8.1)$$

$$V/{}^\sigma k_s\ c_{mono}\ Am_{cat} = (6.7\pm0.3)\times10^2\ min^{+1} \quad (8.2)$$

In these experiments, $V = 0.5$ litre, $m_{cat} = 1.000$ g., $A = (2.5\pm0.5)\ m^2\ g^{-1}$.

The value of $c_{mono}$ is required to calculate $k_s$. Summation of ionic radii shows that the radius of $[Co(NH_3)_5Br]^{2+}$ is $\sim3.0\overset{o}{A}$. Close packing of spheres of this radius gives the value $c_{mono} = 2.8\times10^{14}$ ions $cm^{-2}$.

The adsorption isotherm of $[Co(NH_3)_5H_2O]^{3+}$ on HgS gave the value $c_{mono} = 2.2 \times 10^{14}$ ions $cm^{-2}$ (see Section VIII.5.1:). The value of $c_{mono}$ for $[Co(NH_3)_5Br]^{2+}$ on HgS was therefore taken as $(2.5 \pm 0.3) \times 10^{14}$ ions $cm^{-2}$, which is $(4.2 \pm 0.5) \times 10^{-10}$ moles $cm^{-2}$. (By comparison, the number of $Hg^{2+}$ sites on the HgS surface is $(5.7 \pm 1.8) \times 10^{-10}$ moles $cm^{-2}$).

Substituting in equations (8.1) and (8.2),

$$\sigma = (2.33 \pm 0.35) \times 10^4 \ M^{-1}$$
$$k_S = (3.0 \pm 1.2) \times 10^{-3} \ min^{-1}$$

Substituting this value of $\sigma$ in equation (7.14),

$$\theta = \sigma c_{bulk} / (1 + \sigma c_{bulk}), \qquad (7.14)$$

the approximate shape of the adsorption isotherm for $[Co(NH_3)_5Br]^{2+}$ on HgS can be calculated, and it is plotted as a dashed line in Figure XVII.

The amount of reactant that is adsorbed at each concentration can be calculated from the isotherm by the relationship

$$\text{No. of moles sorbed} = c_{ads} \ Am_{cat}$$
$$= \theta c_{mono} \ Am_{cat}$$

where $\theta$ is the degree of coverage at any given bulk concentration. For 1g. of HgS in 500ml., this formula

shows that quite appreciable fractions of the total
amount of $[Co(NH_3)_5Br]^{2+}$ in the system are sorbed in
the lower range of $\bar{c}$:

| $\bar{c}$ | $10^{-5}$ | $5 \times 10^{-5}$ | $10^{-4}$ | $10^{-3}$ |
|---|---|---|---|---|
| Percentage total reactant sorbed at equilibrium. | 27 | 18 | 13 | 1.7 |

Several experiments were undertaken to detect
adsorptive uptake of $[Co(NH_3)_5Br]^{2+}$ by HgS. Adsorption
is not sufficiently rapid to produce a discontinuity in
the concentration-time plots at the time of addition of
the solid, but the rate of disappearance of $[Co(NH_3)_5Br]^{2+}$
from solution during the first few minutes of runs at low
concentration was up to twice the rate for the rest of
the run. Since in normal runs, the first reading was not
taken for about 30 minutes, this initial uptake was not
usually observed. However, when measuring the rate of a
heterogeneous reaction by the rate of disappearance of the
reactant, it is clearly necessary to check the rate of
appearance of the product, to show that adsorption of the
reactant is not responsible for the apparently fast rate
of reaction.

VIII.4.3: The value of $k_s$ : comparison of $Hg^{2+}$ as a homogeneous and heterogeneous catalyst.

The value of $k_s$ is about eight times the value of $k_1$, so a $[Co(NH_3)_5Br]^{2+}$ ion sorbed on HgS has only one eighth of the life expectancy of an ion in homogeneous solution. However, mercuric ions are much more efficient homogeneous than heterogeneous catalysts for the aquation of $[Co(NH_3)_5Br]^{2+}$, as shown by the following calculation.

The heterogeneous catalytic reaction may be considered as a second order process between $[Co(NH_3)_5Br]^{2+}$ and $Hg^{2+}$, which occurs within the diffusion layer of the solid. The effective "concentration" of $Hg^{2+}$ in this layer is

No. of $Hg^{2+}$ sites per sq.cm./$N_0$ $\delta$ moles $ml^{-1}$

$\approx 5.7 \times 10^{-7}/\delta$ M  for HgS.

The second order rate constant, $(k_2)_{het}$, is given by

$$(k_2)_{het} = k_s / [Hg^{2+}]$$

$$= k_s \delta / 5.7 \times 10^{-7} \text{ M}^{-1} \text{ min}^{-1}$$

If $\delta$ is given the reasonable range of values $(1-5) \times 10^{-3}$ cm, then

$$(k_2)_{het} \approx 5 - 25 \text{ M}^{-1} \text{ min}^{-1} \text{ at } 25^\circ C.$$

By comparison,

$$(k_2)_{hom} = 2.6 \times 10^2 \ M^{-1} \ min^{-1} \ at \ 25°C, \ I = 10^{-2}M$$

$$(19,121).$$

The homogeneous reaction is at least ten times faster than the heterogeneous reaction, possibly because the attraction of the $Hg^{2+}$ ions for bromide is decreased more by the adjacent $S^{2-}$ ligands in the solid than by $H_2O$ in homogeneous solution.

However, it should be added that a case may be made for using the double layer thickness, rather than the diffusion layer thickness, as the value for $\delta$, which would increase $(k_2)_{het}$ by a factor of $\sim 10^5$.

VIII.4.4: Test of function of $c_{bulk}$ linear with
respect to time.

As shown in Section VII.6, a function of $c_{bulk}$,
which should be linear in time even if a first order
plot of the data is curved, can be derived, assuming
the validity of the Langmuir treatment. The general
function is given in equation (7.30): for the HgS
system, $p = 1.56 \times 10^7$ and $q = 6.7 \times 10^2$, so the function
becomes

$$4.034 \log \left[ \frac{1.248 + 5.77 \times 10^3 c_0}{1.248 + 5.77 \times 10^3 c} \right] + \log \frac{c_0}{c} = 8.09 \times 10^{-4} t \quad (8.3)$$

A plot of $\left[ 4.034 \log[1.248 + 5.77 \times 10^3 c] + \log c \right]$
versus time should therefore be linear, with gradient
$-8.09 \times 10^{-4} \text{min}^{-1}$. A plot of this function, together with
a normal first order plot, is shown in Figure XXI, for a
run in which $c_0$ was $1.115 \times 10^{-4} M$, and the aquation was
followed over 3 days to 95% completion. 1.000g. HgS was
used and the volume of solution was 500ml. The result
shown is typical: although the "linear function"
substantially corrects the curvature of the first order
plot, the latter is not so great as would be expected from
Figure XVII, so the gradient of the linear function is
somewhat less than its theoretical value. This effect
could be due to the formation of $[Co(NH_3)_5H_2O]^{3+}$ or to
a gradual loss in activity of HgS.

FIGURE XXI: TEST OF LINEAR FUNCTION (7.30)

$4.034 \log_{10}\left[1.248 + 5.77\times10^{3}c\right] + \log_{10} c$

Gradient $= -7.0\times10^{-4}\,\text{min}^{-1}$

First order plot ($\log_{10} c$)

Gradient $= -3.83\times10^{-4}\,\text{min}^{-1}$
i.e. $k_{obs} = 8.83\times10^{-4}\,\text{min}^{-1}$

Hours $\longrightarrow$
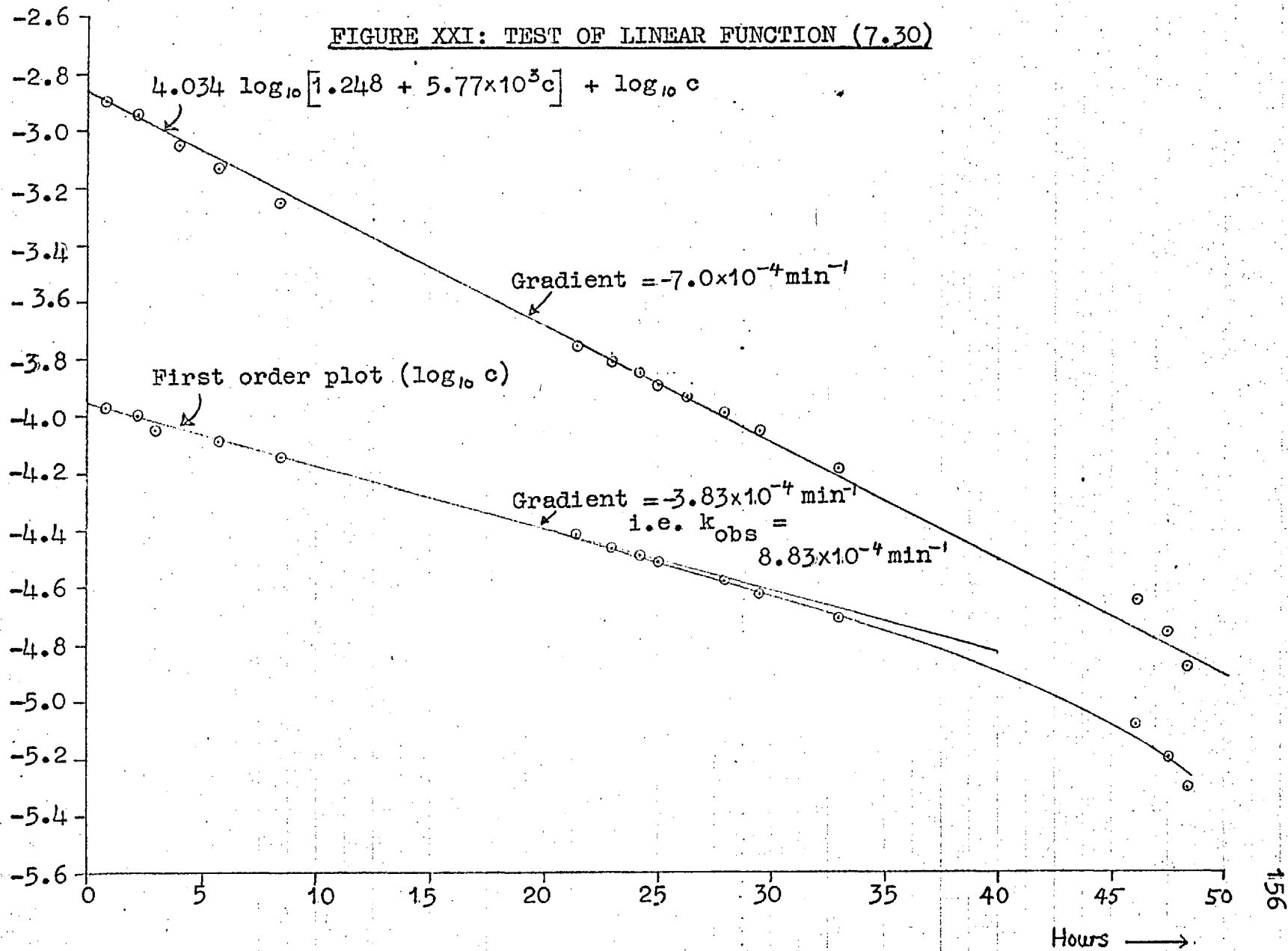
VIII.5.  The adsorption of $[Co(NH_3)_5H_2O]^{3+}$ on HgS.


Adsorption experiments showed that the product of
the aquation reaction, $[Co(NH_3)_5H_2O]^{3+}$, was adsorbed by
HgS, although not nearly so strongly as $[Co(NH_3)_5Br]^{2+}$.
The $[Co(NH_3)_5H_2O]^{3+}$ ion can, in principle, adsorb either
on $S^{2-}$ or $Hg^{2+}$ sites.  If it adsorbs on sulphide sites,
then it is not in direct competition with $[Co(NH_3)_5Br]^{2+}$,
which it is if it sorbs on $Hg^{2+}$ sites.  As $Hg^{2+}$ forms
more stable complexes with $Br^-$ than with $NH_3$ or $H_2O$ (48),
the triply charged $[Co(NH_3)_5H_2O]^{3+}$ ion should not be
nearly so strongly sorbed on $Hg^{2+}$ as the doubly charged
$[Co(NH_3)_5Br]^{2+}$ ion.


VIII.5.1:  Determination of the adsorption isotherm.


25ml. aliquots of $[Co(NH_3)_5H_2O](ClO_4)_3$ solution
in $10^{-2}M$ $HClO_4$ were shaken in stoppered bottles with
known weights of HgS for one day.  5ml. aliquots were
then withdrawn and centrifuged thoroughly before analysis.
The optical density at the $[Co(NH_3)_5H_2O]^{3+}$ peak of
492mµ was measured for the equilibrated and original
solutions.  The difference gives the amount sorbed.  As
the extinction coefficient at 492mµ is rather low (46.8),
the accuracy of measurement is rather poor.  The
adsorption isotherm determined in this way is shown
in Figure XXII, on page 158.

# FIGURE XXII: THE ADSORPTION ISOTHERM OF

## $[Co(NH_3)_5H_2O]^{3+}$ ON HgS
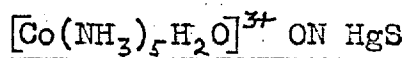
### (Temperature = 20±1°C, pH = 2)



Moles sorbed per gm. × $10^6$

10³× Equilibrium concentration in solution
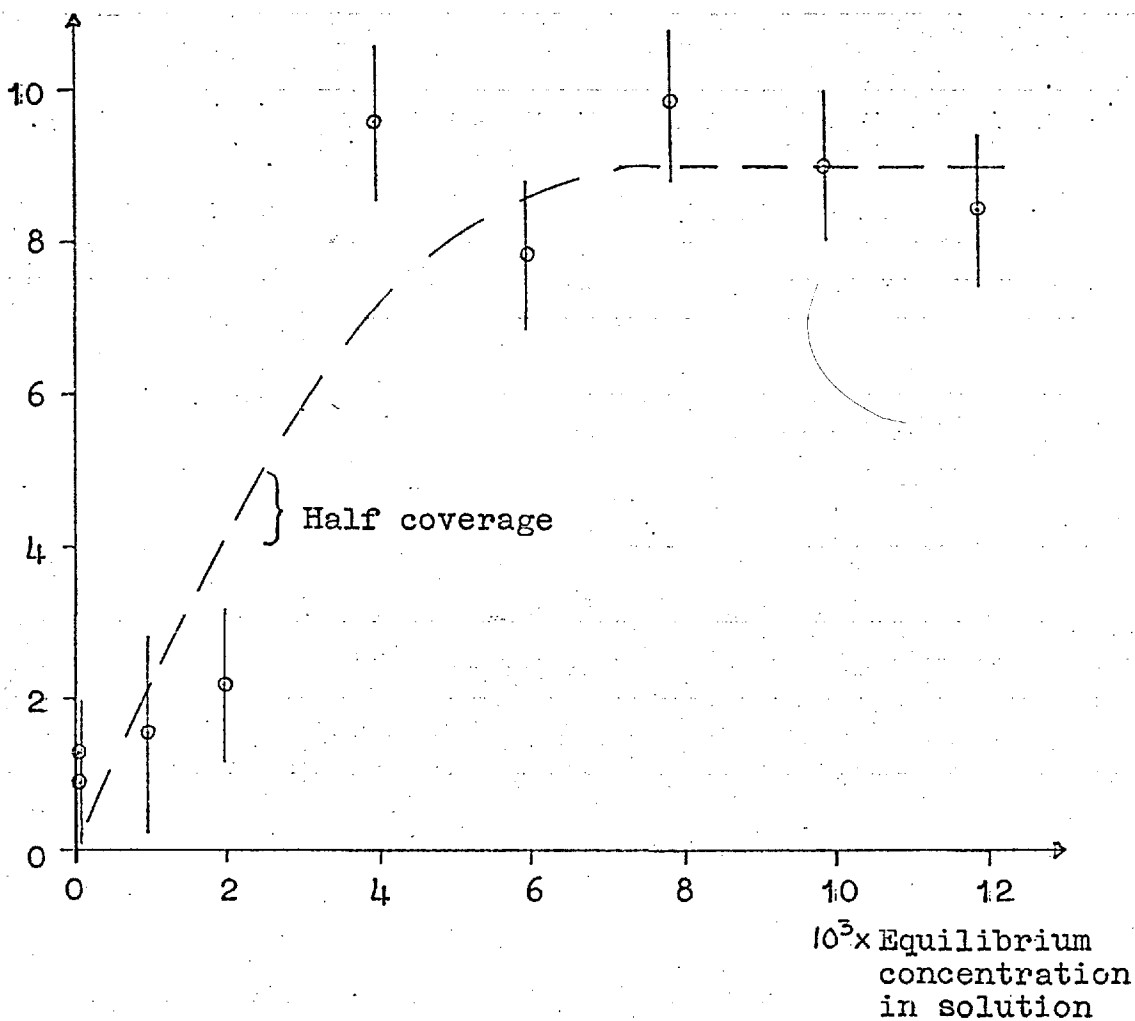
The plateau region, $(9\pm1)\times10^{-6}$ moles $[Co(NH_3)_5H_2O]^{3+}$ sorbed per gm. HgS, is assumed to correspond to monolayer coverage. Since the specific surface area of the HgS is $(2.5\pm0.5)m^2\ g^{-1}$, this means monolayer coverage is $(2.2\pm0.8)\times10^{14}$ ions $cm^{-2}$, and each ion occupies an area of $(46\pm13)\overset{o}{A}{}^2$:

To compare the sticking probabilities of $[Co(NH_3)_5H_2O]^{3+}$ and $[Co(NH_3)_5Br]^{2+}$, Figure XXII is assumed to conform to a Langmuir equation,

$$\theta/(1-\theta)\ =\ {}^\sigma c_{bulk} \qquad\qquad (7.13)$$

The reciprocal of $c_{bulk}$ at half coverage therefore gives the value of $\sigma$, which is then $(4.5\pm0.5)\times10^2\ M^{-1}$. By comparison, the value of $\sigma$ for $[Co(NH_3)_5Br]^{2+}$ on HgS was $(2.33\pm0.35)\times10^4\ M^{-1}$ (see Section VIII.4.2:), so this ion has a much higher sticking probability.

VIII.5.2:  Repression of the catalytic aquation reaction by $[Co(NH_3)_5H_2O]^{3+}$.

A series of experiments was carried out on the repressive effect of $[Co(NH_3)_5H_2O]^{3+}$ on the catalytic effect of HgS. The experimental procedure was the same as before, except that the runs were carried out in

$[Co(NH_3)_5H_2O](ClO_4)_3$ solution in $10^{-2}M$ $HClO_4$. The amount of $[Co(NH_3)_5H_2O]^{3+}$ produced during the runs was ignored. The results are presented in Table XXI and Figure XXIII.

Figure XXIII is plotted as $1/k_{het}$ vs. $\bar{c}$. The form of this graph was deduced in Section (VII .5), assuming that the added ion and $[Co(NH_3)_5Br]^{2+}$ competed for adsorption sites. The equation connecting $1/k_{het}$ and $\bar{c}$ is (7.26). This equation, in which the various constants are replaced by their determined values, becomes

$$\frac{1}{k_{het}} = 1.56\times10^7 \cdot c_{bulk} + 6.7\times10^2 \left[ 1 + 4.5\times10^2[Co(NH_3)_5H_2O]^{3+} \right] \tag{8.4}$$

The slopes and intercepts calculated from this expression do not agree well with the observed values, as shown by the table below

| $[Co(NH_3)_5H_2O]^{3+}$ | Intercept | | Slope | |
| --- | --- | --- | --- | --- |
| | obs. | calc. | obs. | calc. |
| 0 | $6.7\times10^2$ | $6.7\times10^2$ | $1.56\times10^7$ | $1.56\times10^7$ |
| $5\times10^{-4}M$ | 9.0 " | 8.2 " | 1.67 " | " |
| $1\times10^{-3}M$ | 12.5 " | 9.7 " | 2.45 " | " |
| $2\times10^{-3}M$ ) | 14.6 " | 12.7 " | 2.93 " | " |
| $5\times10^{-3}M$ ) | | 21.8 " | | |

## TABLE XXI : CATALYSIS BY HgS OF $[Co(NH_3)_5Br]^{2+}$ AQUATION

## IN PRESENCE OF $[Co(NH_3)_5H_2O](ClO_4)_3$.

All results for 1.000g. HgS in 500ml. solution at 25°C.

| $[Co(NH_3)_5H_2O]^{3+}$ | $10^5 c_0$ | $10^5\bar{c}$ | $10^4 k_{het},min^{-1}$ |
|---|---|---|---|
| 0 | | | See Table XX. |
| $5\times10^{-4}$M | 4.21 | 3.60 | 6.02 |
| " | 7.29 | 6.41 | 5.06 |
| " | 10.3 | 9.21 | 4.16 |
| $1\times10^{-3}$M | 1.98 | 1.71 | 6.47 |
| " | 3.96 | 3.52 | 4.62 |
| " | 10.0 | 9.10 | 2.89 |
| $2\times10^{-3}$M | 4.06 | 3.56 | 4.11 |
| " | 6.93 | 6.13 | 2.97 |
| | 9.95 | 8.90 | 2.47 |
| $5\times10^{-3}$M | 2.29 | 1.99 | 4.93 |
| " | 5.17 | 5.27 | 3.08 |
| " | 10.0 | 9.11 | 2.56 |

FIGURE XXIII: PLOT OF $1/k_{het}$ vs. $\bar{c}$ IN PRESENCE OF $[Co(NH_3)_5H_2O](ClO_4)_3$
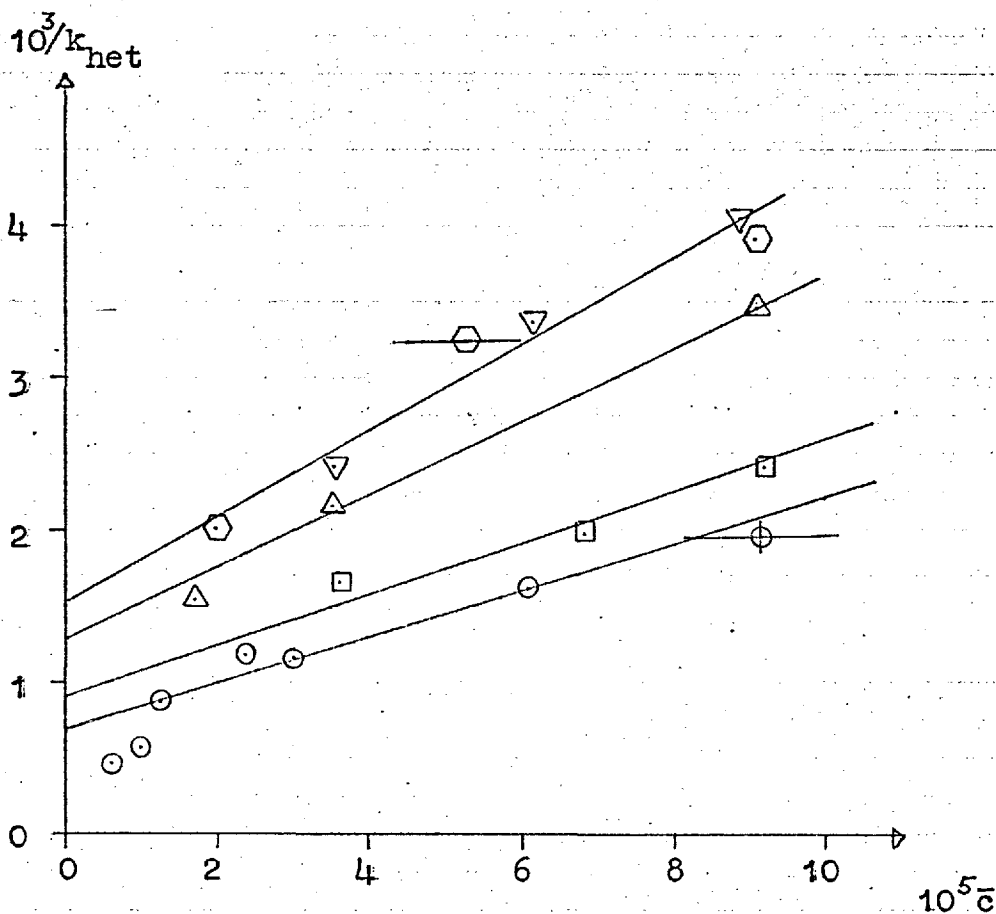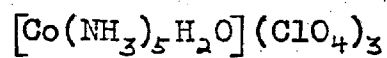
The repressive effect of $[Co(NH_3)_3H_2O]^{3+}$ is greater than calculated from its sticking probability, and the results for $2 \times 10^{-3}M$ and $5 \times 10^{-3}M$ are practically the same. There is probably competitive, not additive, adsorption of $[Co(NH_3)_5Br]^{2+}$ and $[Co(NH_3)_5H_2O]^{3+}$, and it is quite possible that the term $k_s$, considered to be a constant in equation (8.2), actually decreases with increasing $[Co(NH_3)_5H_2O]^{3+}$ concentration.

## CHAPTER IX : CATALYSIS BY SILVER BROMIDE OF THE AQUATION
### OF $[Co(NH_3)_5Br]^{2+}$.

Experiments were carried out at 25°C with several batches of silver bromide. The variation of $k_{het}$ with $\bar{c}$ was investigated, and also the repressive effects of $[Co(NH_3)_5H_2O]^{3+}$ and $Br^-$. The equations derived in Chapter VII were tested. The rate of reaction of $[Co(NH_3)_5Br]^{2+}$ with $Ag^+$ in homogeneous solution was measured, and compared with the rate of heterogeneous catalysis.

Heterogeneous catalysis was found to be subject to a considerable photochemical effect.

IX.1. Silver bromide.

Silver bromide has a sodium chloride crystal structure. The crystal radii of $Ag^+$ and $Br^-$ are 1.2Å and 1.95Å respectively. According to Johnston, the cross sectional area per molecule in the solid is 13.3Å² (136), so the concentration of surface $Ag^+$ sites is $1.25 \times 10^{-9}$ moles cm⁻². The solubility product of AgBr at 25°C is $5.3 \times 10^{-13} M^2$.

The following batches of silver bromide were used in these experiments:

0    BDH product, lightly ground.

1    BDH product, stirred for 3 days in $10^{-3}$M $HClO_4$, filtered, washed and dried at 110°C.

2    BDH product, stirred for 30 minutes in 0.1M $HNO_3$, filtered, washed, dried at 110°C and sieved through a sieve of <76 μ mesh.

3    BDH product, ground and sieved (<76 μ mesh), stirred for 30 minutes in 0.1M $HNO_3$, filtered, washed and dried at room temperature under vacuum.

4    As 3, except 0.01M $HNO_3$ used.


The specific surface areas of batches 1, 2 and 4 were determined by adsorption experiments with p-nitrophenol which was recommended by Giles et al. (137). This adsorbate is highly polar, which ensures strong attachment to the whole surface of polar solids. From aqueous solution, one molecule of p-nitrophenol is adsorbed with one molecule of water, and the effective cross-sectional area per phenol molecule is 25$\overset{o}{A}{}^2$.

GPR p-nitrophenol was re-crystallised from 2% HCl according to the procedure of Vogel (138). All experiments were carried out in $10^{-2}$M $HClO_4$, as the phenol tends to resinify in alkaline solution.

A series of solutions in the concentration range $5 \times 10^{-5} - 1 \times 10^{-2}$M was made up by weight and by dilution in $10^{-2}$M $HClO_4$. The concentration was estimated spectrophotometrically at an intense peak at 316m$\mu$, at which $\epsilon$ was found to be $9.72 \times 10^3$.

25ml. or 50ml. aliquots of these solutions were shaken at room temperature in stoppered bottles with known weights of solid. Experiment showed that adsorption equilibrium was reached well within 12 hours. 5ml. aliquots were then withdrawn and centrifuged thoroughly before analysis.

The optical density at 316m$\mu$ of the equilibrated and original p-nitrophenol solutions were measured against water. Volumetric dilution of samples of concentration greater than $2 \times 10^{-4}$M was necessary.

Figures XXIV and XXV, on pages 167 and 168, show the adsorption isotherms at room temperature ($21 \pm 1^{\circ}$C) and the Langmuir plots of the reciprocal of the amount of p-nitrophenol sorbed vs. the reciprocal of the bulk concentration.

Both plots are very scattered, because the concentration difference between the original and equilibrated solutions was very small. From intercepts on the Langmuir plot the amount of p-nitrophenol adsorbed at monolayer coverage is taken to be:

$$\text{Batch 1} \quad : \quad 2 \times 10^{-6} \text{ mole g}^{-1}$$

$$\text{" } \quad 2 \quad : \quad 3.3 \times 10^{-7} \quad \text{"}$$

$$\text{" } \quad 4 \quad : \quad 5 \times 10^{-7} \quad \text{"}$$

FIGURE XXIV: ADSORPTION OF p-NITROPHENOL ON BATCHES 1,2 and 4 AgBr AT ROOM TEMPERATURE

$c_{AgBr}$ = moles p-nitrophenol adsorbed per gm. AgBr

$c_{eq}$ = concentration of p-nitrophenol in solu--tion at equilibrium

⊙ Batch 1 (in light)

△ Batch 2 (in light)
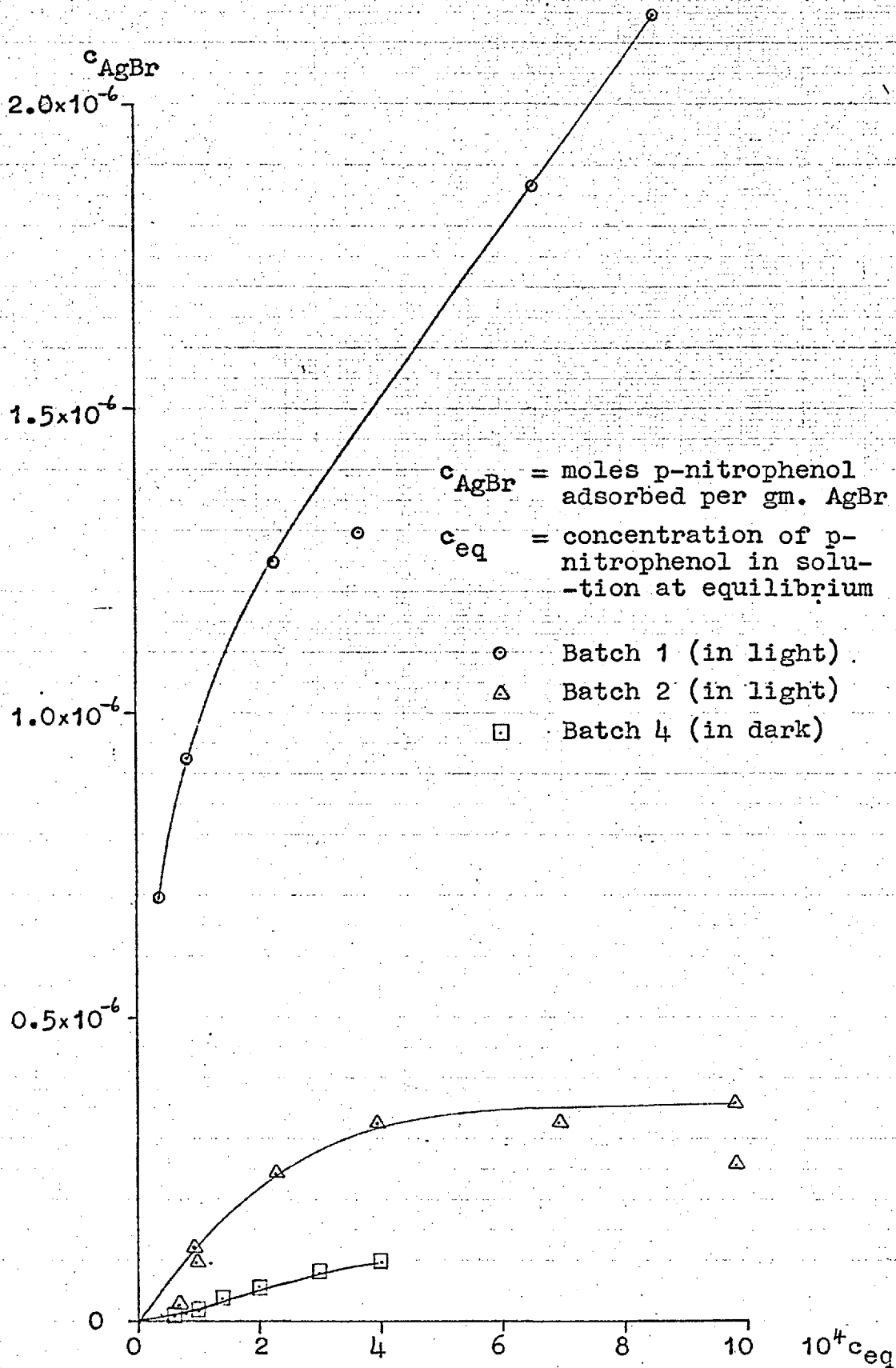
□ Batch 4 (in dark)

FIGURE XXV: LANGMUIR PLOTS OF p-NITROPHENOL ADSORPTION DATA
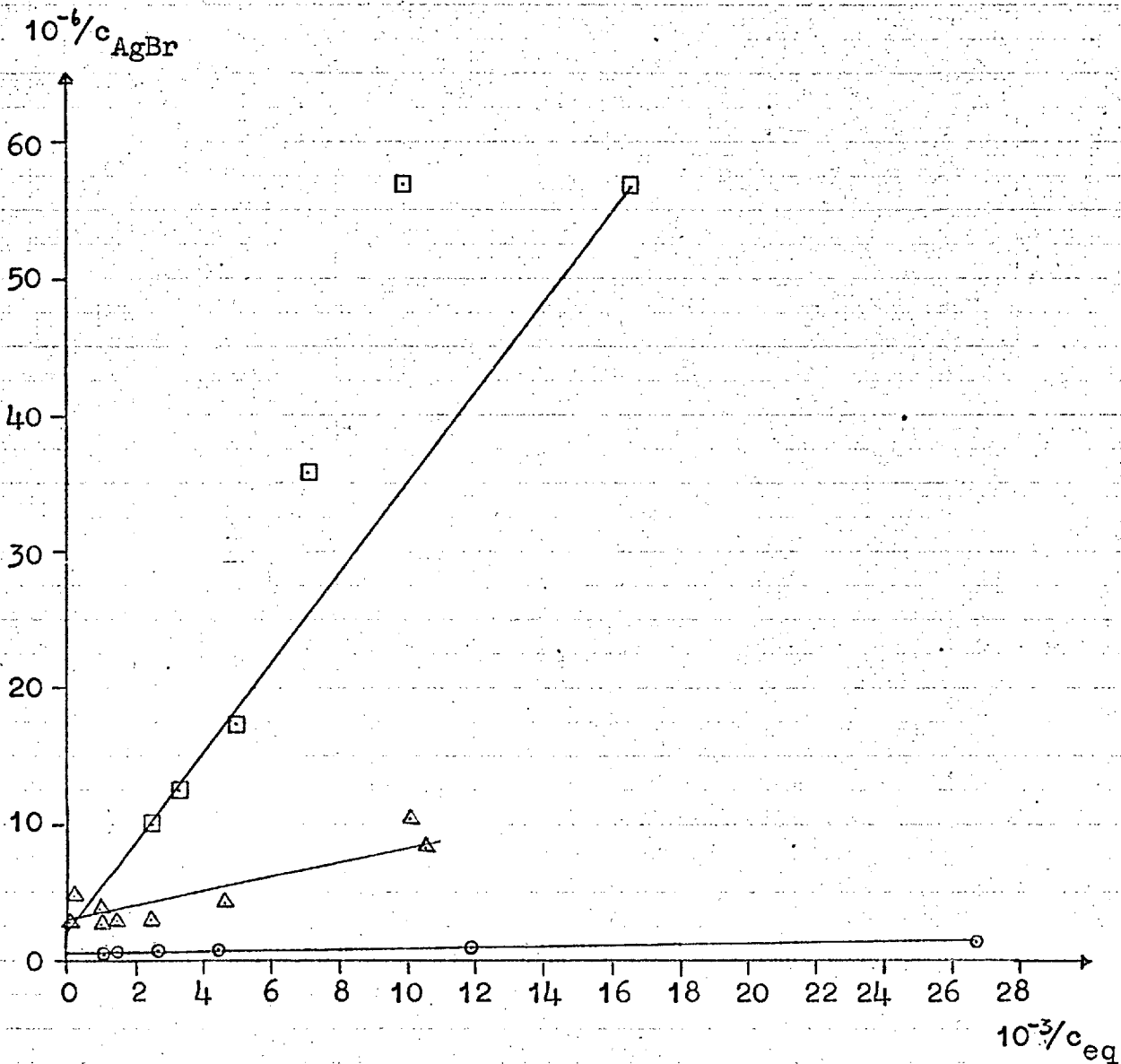


$c_{AgBr}$ = no. of moles of p-nitrophenol adsorbed per gm. AgBr

$c_{eq}$ = concentration of p-nitrophenol in solution at equil-
-ibrium

⊙      Batch 1 (in light)

△      Batch 2 (in light)

⊡      Batch 4 (in dark)

As each p-nitrophenol molecule occupies an area of 25Å$^2$ (133), the specific surface areas are:

<div>

Batch 1 : 3x10$^3$ cm$^2$g$^{-1}$

" 2 : 5x10$^2$ "

" 4 : 7.5x10$^2$ "

</div>

The absolute accuracy of these figures is no better than $\pm$20%, but the relative accuracy should be considerably better.

The adsorption on batch 4 is anomalous, in that less p-nitrophenol is adsorbed on it than on batch 2 at the same concentration, although it has a larger surface area (and greater catalytic activity under comparable conditions). The adsorption experiments on batch 4 were carried out in the dark, while those on batches 1 and 2 were carried out in normal laboratory lighting. It is concluded that more p-nitrophenol adsorbs on silver bromide in the presence of light than in its absence; this result is considered significant because the catalytic effect of silver bromide on [Co(NH$_3$)$_5$Br]$^{2+}$ was found to be about ten times as great in the presence of light as in its absence.

IX.2.  Experimental procedure.

The procedure was as described in Section (VI.2).
Aliquots were removed without stopping the stirrer, and
no sampling corrections were applied.

The catalytic reaction was subject to a photochemical
effect.  Experiments in the dark were carried out in
reaction vessels completely masked in black Neoprene
rubber.  Experiments in the light were carried out in
glass vessels exposed to laboratory fluorescent lighting
and daylight, which entered the thermostat tank through
the open top and through two windows in the side.

All the silver bromide batches had low specific surface
areas, so experiments were confined to very dilute solutions
of $[Co(NH_3)_5Br]^{2+}$, which made spectrophotometric estimation
of the products very difficult.  Conversion to $[Co(NH_3)_5H_2O]^{3+}$
seemed always to be quantitative in the dark.  In the light,
some Co(II) is also formed in some runs, but it could not
be estimated quantitatively.

## RESULTS

IX.3.   The dependence of $k_{het}$ on $\bar{c}$ (in the dark).

A series of runs was carried out at 25°C to determine the first order catalytic rate constant, $k_{het}$, for $c_0$ values in the range $(1-7) \times 10^{-5}M$. The repressive effects of $[Co(NH_3)_5H_2O](ClO_4)_3$ and KBr were also investigated in this concentration range. All runs were followed for less than 20% of their course, and the reaction rates were pseudo first order. The results are summarised in Table XXII, on page 172, and Figures XXVI - XXVIII.

As for the other catalysts, $k_{het}$ decreased as $\bar{c}$ increased. $10^{-3}M$ $[Co(NH_3)_5H_2O]^{3+}$ had a slight repressive effect, and $10^{-3}M$ $Br^-$ a greater effect. By comparison, $2 \times 10^{-3}M$ $Br^-$ had a disproportionately large effect.

Figure XXVII is a plot of $1/k_{het}$ vs. $\bar{c}$. All four lines are distinctly curved, indicating that the hypothesis of Langmuir adsorption of the reactant prior to reaction does not fit the facts so well for AgBr as for HgS (or Pt). Figure XXVIII, the Freundlich plot, shows less curvature, but the slope of the dotted line gives a negative value, -0.3, for $a$ (see equation (7.18) ), which could indicate increasing heat of adsorption with increasing degree of coverage of the surface.

TABLE XXII : THE PSEUDO FIRST ORDER RATE CONSTANT $k_{het}$ AS A FUNCTION OF THE CONCENTRATION OF $[Co(NH_3)_5Br]^{2+}$, IN THE DARK.

$c_0$ = initial concentration in each run.

$\bar{c}$ = mean        "        "   "   "

All results for 2.000g. batch 4 AgBr in 500ml. solution in the dark, at 25°C.

| Background electrolyte | $10^5 c_0$ | $10^5 \bar{c}$ | $10^4 k_{het}$, min$^{-1}$ |
|---|---|---|---|
| $10^{-2}$M HClO$_4$ | 0.906 | 0.813 | 3.58 |
| | 1.58 | 1.48 | 3.15 |
| | 2.05 | 1.95 | 1.15 |
| | 3.10 | 2.96 | 1.06 |
| | 4.11 | 3.88 | 0.67 |
| | 5.10 | 4.89 | 0.48 |
| | 7.07 | 6.7 | 0.32 |
| $10^{-2}$M HClO$_4$, | 0.929 | 0.856 | 2.66 |
| $10^{-3}$M$[Co(NH_3)_5H_2O](ClO_4)_3$ | 3.99 | 3.78 | 0.61 |
| | 7.09 | 6.79 | 0.30 |
| $10^{-2}$M HClO$_4$, | 0.800 | 0.745 | 1:96 |
| 1.01x10$^{-3}$M KBr | 3.92 | 3.72 | 0.55 |
| | 7.17 | 6.90 | 0.27 |
| $10^{-2}$M HClO$_4$, | 1.06 | 1.00 | 1.57 |
| 2.02x10$^{-3}$M KBr | 1.87 | 1.76 | 0.62 |
| | 3.13 | 2.96 | 0.23 |
| | 4.05 | 3.87 | 0.22 |
| | 7.00 | 6.69 | 0.07 |

# FIGURE XXVI: PLOT OF $k_{het}$ vs. $\bar{c}$

## (All data for 25°C and batch 4 AgBr in dark)
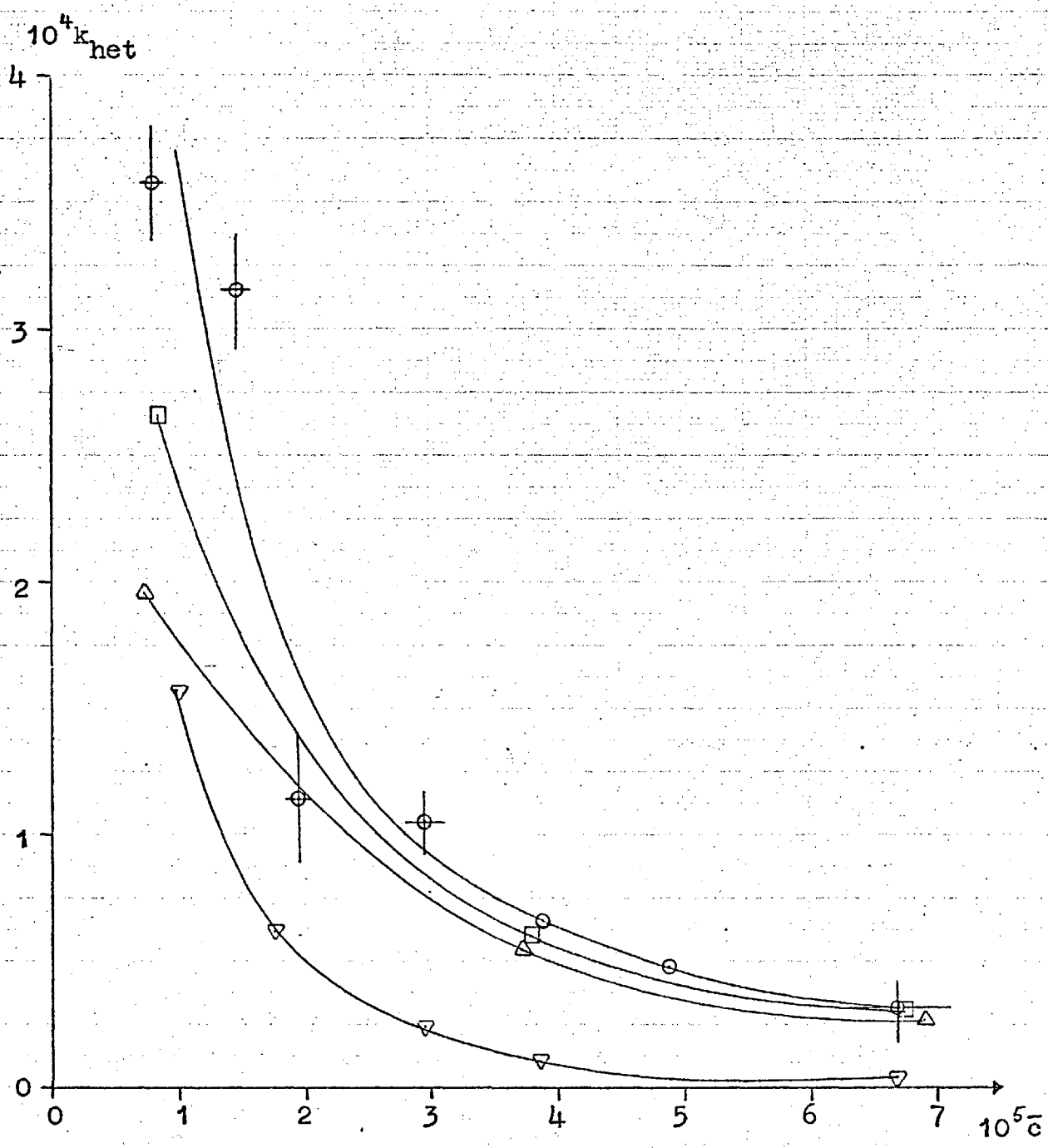


BACKGROUND ELECTROLYTE

⊙  $10^{-2}$ M $HClO_4$

☐  $10^{-2}$ M $HClO_4$ plus $10^{-3}$M $\left[Co(NH_3)_5H_2O\right]$ $(ClO_4)_3$

△  $10^{-2}$ M $HClO_4$ plus $1.01 \times 10^{-3}$ M KBr

▽  $10^{-2}$ M $HClO_4$ plus $2.02 \times 10^{-3}$ M KBr

# FIGURE XXVII: LANGMUIR PLOT

## (All data for 25°C and batch 4 AgBr in dark)
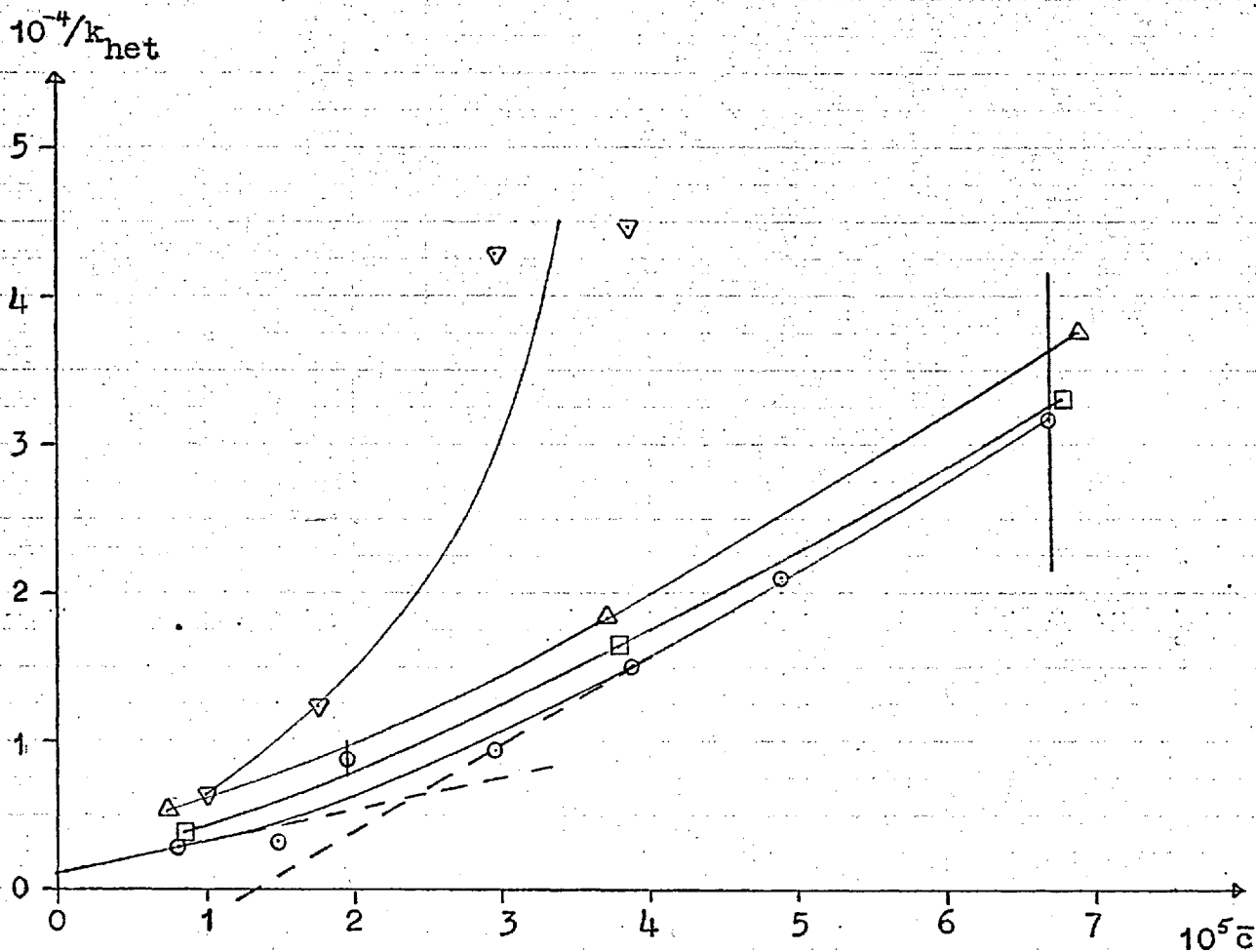


## BACKGROUND ELECTROLYTE

⊙  $10^{-2}$ M $HClO_4$

□  $10^{-2}$ M $HClO_4$ plus $10^{-3}$ M $[Co(NH_3)_5H_2O](ClO_4)_3$

△  $10^{-2}$ M $HClO_4$ plus $1.01 \times 10^{-3}$ M KBr

▽  $10^{-2}$ M $HClO_4$ plus $2.02 \times 10^{-3}$ M KBr

FIGURE XXVIII: FREUNDLICH PLOT.

(All data for 25°C and batch 4 AgBr in dark)
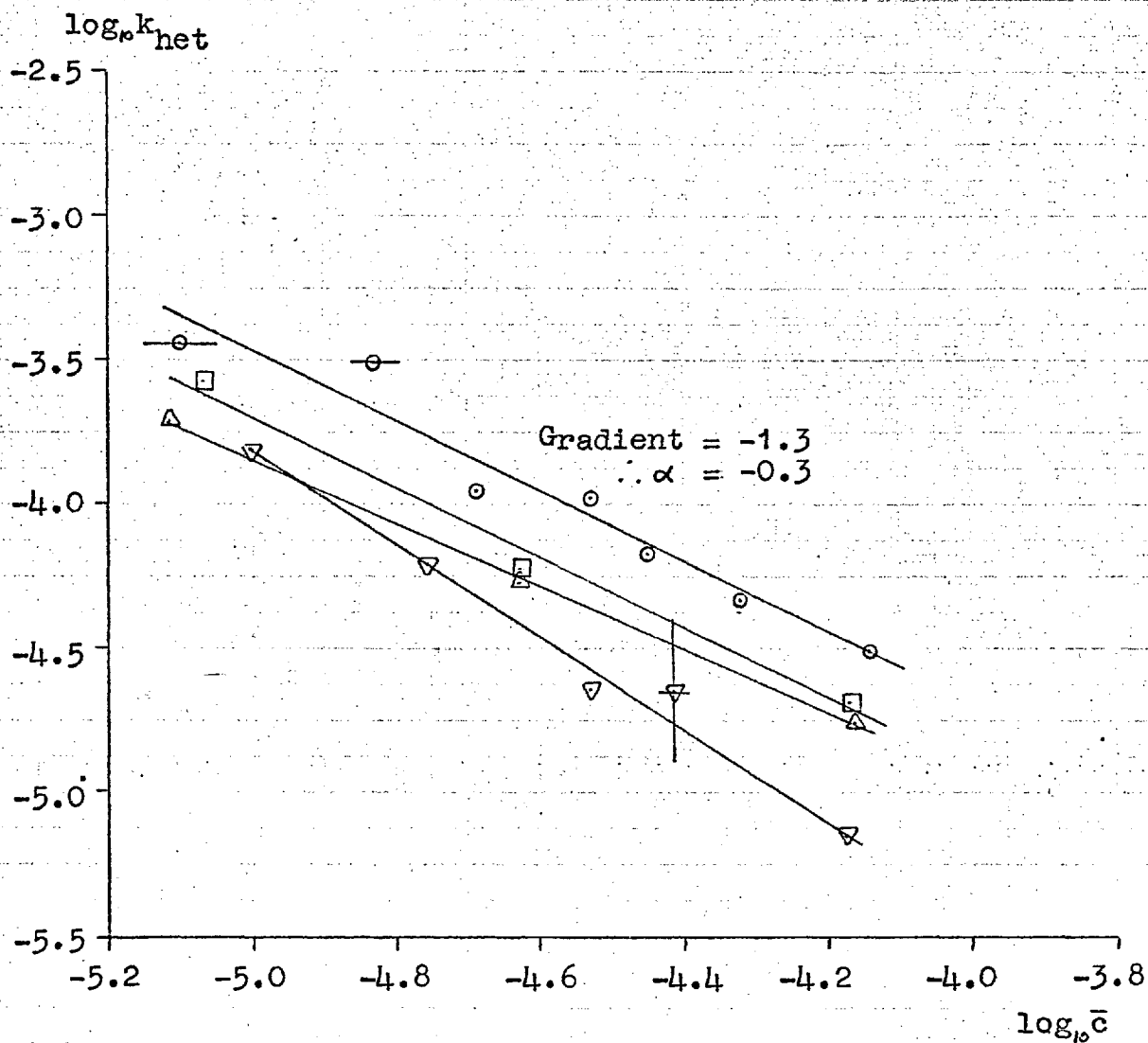
$\log_{10} k_{het}$

Gradient = -1.3

$\therefore \alpha = -0.3$

$\log_{10} \bar{c}$

Background electrolyte

⊙ $10^{-2}$ M $HClO_4$

□ $10^{-2}$ M $HClO_4$ plus $10^{-3}$ M $[Co(NH_3)_5 H_2O](ClO_4)_3$

△ $10^{-2}$ M $HClO_4$ plus $1.01 \times 10^{-3}$ M KBr

▽ $10^{-2}$ M $HClO_4$ plus $2.02 \times 10^{-3}$ M KBr

To determine the value of $k_s$, the slope and intercept of the Langmuir plot is required. Negative intercepts are obtained by extrapolating the curves in the region $\bar{c} = (3-7) \times 10^{-5}M$; these are meaningless in terms of the theory set out in Section (VII.4(i) ), so extrapolation is made in the region $\bar{c} = (1-3) \times 10^{-5}M$. In the absence of repressive electrolytes, the slope and intercept for the low concentration region are $2.1 \times 10^8 \text{min.M}^{-1}$ and $1.2 \times 10^3 \text{min.}$ respectively. Substituting $V = 0.5$ litres, $m_{cat} = 2.000g.$, $A = 7.5 \times 10^2 \text{cm}^2\text{g}^{-1}$ and $c_{mono} = 4.2 \times 10^{-10}$ moles $\text{cm}^{-2}$ in equation (7.17), the values of $k_s$ and $\sigma$ for the $[Co(NH_3)_5Br]^{2+}/AgBr$ system at low concentration in the dark are calculated to be:

$$\sigma = 1.7 \times 10^5 M^{-1}$$

$$k_s = 3.8 \times 10^{-3} \text{min}^{-1}$$

The ion $[Co(NH_3)_5H_2O]^{3+}$ had only a slight repressive effect on AgBr, compared with HgS (cf. Figures XX and XXV).

IX.4. The dependence of $k_{het}$ on $\bar{c}$ (in the light).

Several series of runs were carried out in normal light (fluorescent lighting and daylight) before the photochemical effect was discovered. The results of these series can be combined, as the specific surface areas of the different batches are known. Preliminary experiments showed that $k_{het}$ was roughly ten times as great in the presence as in the absence of light and that the results conformed quite well to the Langmuir equation (7.17). This equation may be re-written

$$\frac{A \, m_{cat}}{V k_{het}} = \frac{c_{bulk}}{k_s \, c_{mono}} + \frac{1}{\sigma \, k_s \, c_{mono}} \qquad (9.1)$$

A plot of the left-hand side against $\bar{c}$ for all the runs should therefore be a single line. This is illustrated for runs carried out in the presence of light with batches 1, 2 and 4 AgBr in Figure XXIX, on page 179, and the results are tabulated in Table XXIII, on page 178.

Figure XXIX shows that the scatter between runs with the same batch of AgBr was as great as that between runs with different batches. In other words, once the difference in specific surface areas had been taken into account, there is no significant difference between the activity of the three batches. The scatter in the plot was

# TABLE XXIII : THE PSEUDO FIRST ORDER RATE CONSTANT $k_{het}$ AS A FUNCTION OF THE CONCENTRATION OF $[Co(NH_3)_5Br]^{2+}$, IN THE LIGHT.

All results for 500ml. solution in ordinary light, at 25°C.
Background electrolyte = $10^{-2}M$ $HClO_4$.

| Batch No. | $m_{cat}$ | $10^5 c_0, M$ | $10^5 \bar{c}, M$ | $10^4 k_{het}, min^{-1}$ |
|---|---|---|---|---|
| 1 | 3.000g. | 2.01 | 1.65 | 34.4 |
| | 3.000 | 3.10 | 2.47 | 30.8 |
| | 2.500 | 3.75 | 2.97 | 19.3 |
| | 4.650 | 4.15 | 3.36 | 23.3 |
| | 3.000 | 4.65 | 3.96 | 11.8 |
| | 3.000 | 5.79 | 4.90 | 10.2 |
| 2 | 3.000g. | 4.01 | 3.60 | 2.05 |
| | 3.000 | 5.89 | 5.35 | 1.47 |
| 4 | 2.000g. | 0.900 | 0.685 | 21.6 |
| | " | 1.57 | 1.38 | 12.8 |
| | " | 2.72 | 1.57 | 11.6 |
| | " | 3.98 | 3,67 | 3.11 |
| | " | 4.46 | 3.95 | 3.85 |
| | " | 5.03 | 4.59 | 5.73 |
| | " | 6.41 | 5.61 | 4.58 |

# FIGURE XXIX: LANGMUIR PLOT

### (Results at 25°C for batches 1,2 and 4 AgBr in light)



$10^{-6} Am_{cat} / Vk_{het}$

Batch 4 AgBr in dark (for comparison)

$10^5 \bar{c}$
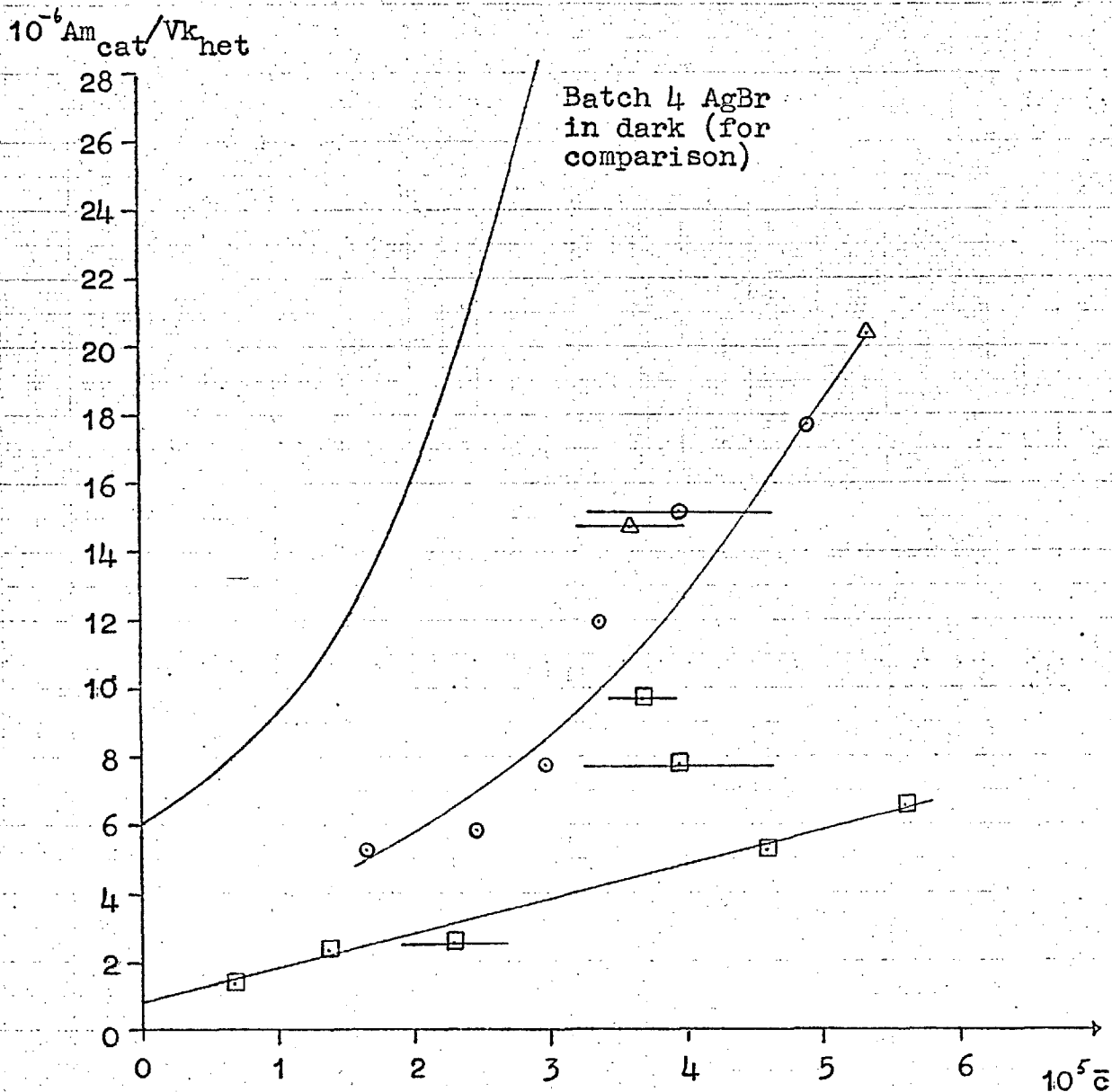
$\odot$     Batch 1: $A = 3.0 \times 10^3 \, cm^2 \, g^{-1}$

$\triangle$     Batch 2: $A = 5.0 \times 10^2$ " "

$\boxdot$     Batch 4: $A = 7.5 \times 10^2$ " "

ascribed to random fluctuations in light intensity, since experiments with batch 4 AgBr showed that merely altering the position of the reaction vessel in the thermostat could change $k_{het}$ by 40% (for $\bar{c} = 3.5 \times 10^{-5}$M) and 20% (for $\bar{c} = 5.0 \times 10^{-5}$M).

The lowest line in Figure XXIX corresponds to the highest catalytic rate. The slope and intercept of this line give the values $k_s = 2.3 \times 10^{-2}$min$^{-1}$, $\sigma = 1.5 \times 10^5$M$^{-1}$. By comparison, the values for the same batch of AgBr (batch 4) in the dark were $k_s = 3.8 \times 10^{-3}$min$^{-1}$, $\sigma = 1.7 \times 10^5$M$^{-1}$, at low concentrations. The sticking probability of $[Co(NH_3)_5Br]^{2+}$ on AgBr is therefore much the same in the light and the dark (although that of p-nitrophenol seemed to be greatly affected). The rate of reaction of adsorbed $[Co(NH_3)_5Br]^{2+}$ is therefore greater in the light than in the dark.

Adamson (139) investigated the photochemistry of $[Co(NH_3)_5Br]^{2+}$ in homogeneous solution in the wavelength range 370-600m$\mu$. He concluded that the primary process at all wavelengths was homolytic fission, producing Co(II) and ·Br. At low wavelengths, a photoredox reaction ensues (quantum yield 0.12 at 370m$\mu$, 0.03 at 450m$\mu$) and at longer wavelengths, some photoaquation occurs (quantum yield ~1.5 × 10$^{-3}$ in range 520-600m$\mu$).

In ordinary light, these photochemical reactions are negligible in homogeneous solution, but evidently are not

for $[Co(NH_3)_5Br]^{2+}$ sorbed on AgBr. It may be that the photochemical quantum yields are substantially higher for the sorbed complex, so that an increased rate of aquation is observed, and a little Co(II) is also produced.

IX.5. The dependence of $k_{het}$ on $m_{cat}$.

A series of runs was carried out with batch O AgBr to verify the first order dependence of $k_{het}$ on $m_{cat}$. At the time of the experiments, it was not realised that $k_{het}$ changed with bulk concentration, and therefore $c_0$ was not constant throughout this series. The variation was slight, however, and was corrected for by plotting $k_{het}$ $(1+\sigma\bar{c})$ against $m_{cat}$. As shown by equation (7.16), this plot should be a straight line passing through the origin.

The results are tabulated and plotted in Table XXIV and Figure XXX respectively. First order dependence is maintained up to ~3g. solid in 500ml. If more solid than this is present, then efficient stirring of the whole is impossible and the catalytic rate is irreproducible.

TABLE XXIV : THE DEPENDENCE OF $k_{het}$ ON $m_{cat}$.

All results for 500ml. solution (background $10^{-2}M$ $HClO_4$) and batch O AgBr in the light, at 25°C.

$$\sigma = 1.5 \times 10^5 M^{-1}$$

| $10^5 c_0$ | $10^5 \bar{c}$ | $m_{cat}$ | $10^4 k_{het}, min^{-1}$ |
|---|---|---|---|
| 3.59 | 2.89 | 0.917g. | 10.6 |
| 3.83 | 3.16 | 1.443 | 12.3 |
| 3.34 | 2.50 | 1.994 | 18.4 |
| 3.54 | 2.56 | 3.049 | 30.4 |
| 3.88 | 3.32 | 4.407 | 23.7 |
| 4.08 | 3.08 | 6.953 | 42.7 |



FIGURE XXX.
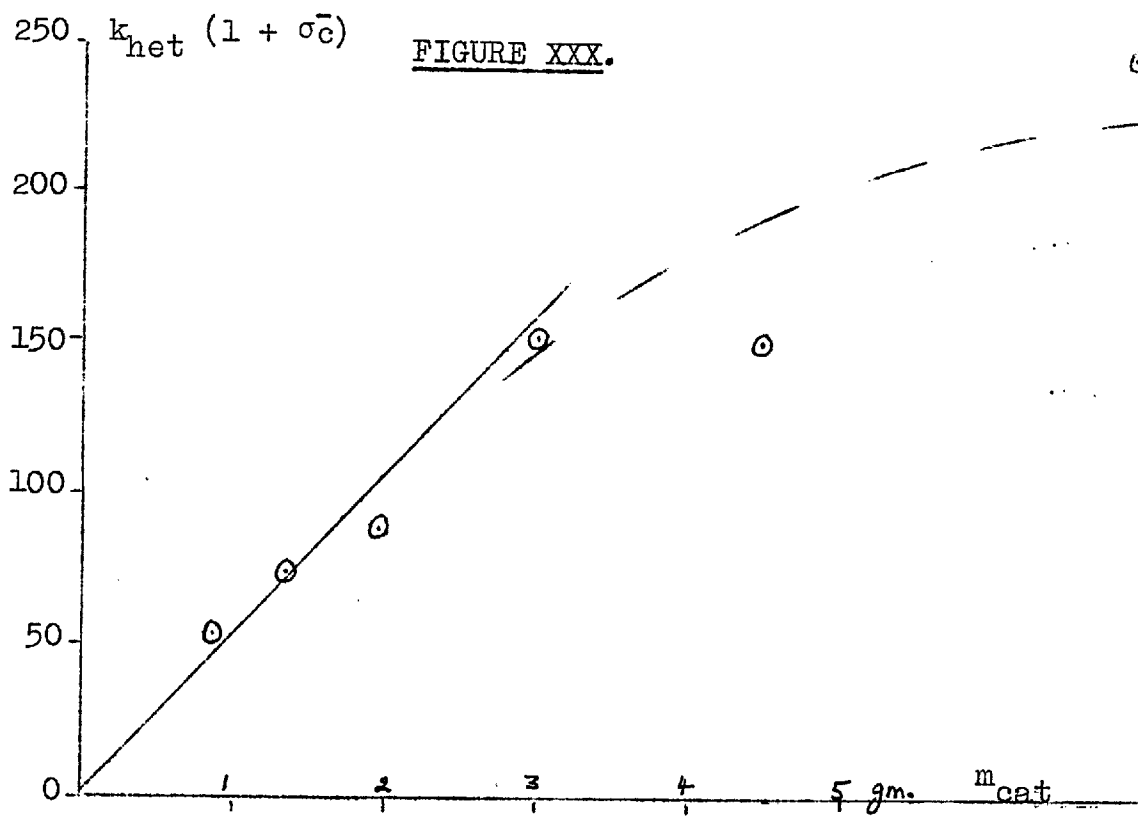
IX.6.  Comparison of $Ag^+$ as a homogeneous and heterogeneous
       catalyst.

Although $Ag^+$ in homogeneous solution is known to
accelerate the aquation of $[Co(NH_3)_5Br]^{2+}$ (47), no kinetic
data have been reported.  The rate of the homogeneous
reaction was therefore measured, so that comparison might
be made with the catalytic effect of AgBr.

IX.6.1:  The rate of the homogeneous reaction between
         $Ag^+$ and $[Co(NH_3)_5Br]^{2+}$.

The reaction is

$$Ag^+ + [Co(NH_3)_5Br]^{2+} + H_2O \rightarrow [Co(NH_3)_5H_2O]^{3+} + AgBr$$

$$(9.2)$$
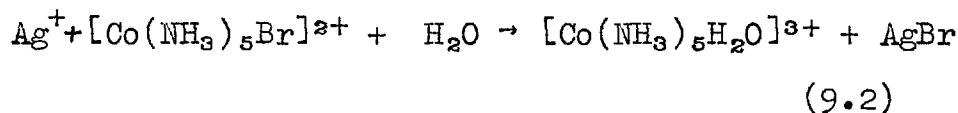
Low concentrations of $[Co(NH_3)_5Br]^{2+}$ ($3\times10^{-5} - 4\times10^{-5}M$)
were used, so that the small amount of AgBr produced had
a negligible autocatalytic effect.

All experiments were carried out at $25^\circ C$, in the light.
500ml. AgNO_3 or AgClO_4 solution, which also contained $10^{-2}M$
$HClO_4$, were equilibrated in the thermostat, and at time $t_o$,
a small quantity of $[Co(NH_3)_5Br](ClO_4)_2$ was added, and a
stirrer started.  The solid dissolved rapidly, and the
disappearance of $[Co(NH_3)_5Br]^{2+}$ was followed spectro-
photometrically at $253m\mu$, using the appropriate AgNO_3 or

$AgClO_4$ solution as reference. Aliquots were centrifuged to remove any AgBr before each measurement. As $Ag^+$ ions were present in large excess, the reactions were pseudo first order, and the second order rate constant, $k_2$, was calculated from first order plots by the relationship

$$k_{obs} = k_1 + k_2 [Ag^+] \qquad (9.3)$$

The experiments carried out are summarised in Table XXV, (see below). First order plots of data from runs 1, 4 and 6 are shown in Figure XXXI, and Figure XXXII is a Brönsted plot of log $k_2$ against $I^{\frac{1}{2}}/(1+I^{\frac{1}{2}})$. It is seen from the latter plot that $AgNO_3$ and $AgClO_4$ have rather specific effects.

TABLE XXV : DATA FOR REACTION (9.2) AT 25°C.

| Run | $[Co(NH_3)_5Br]^{2+}_{t=0}$ | $[Ag^+]$ | $k_2,$ $M^{-1}$ $min^{-1}$ | Ionic strength. |
|---|---|---|---|---|
| 1 | $3.83\times10^{-5}M$ | $5.00\times10^{-3}M$ | 0.160 | $1.52\times10^{-2}M$ |
| 2 | 3.75 " | $9.99\times10^{-3}$ | 0.183 | 2.01 " |
| 3 | 3.69 " | $2.00\times10^{-2}$ | 0.249 | 3.01 " |
| 4 | 3.66 " | $4.00\times10^{-2}$ | 0.353 | 5.12 " |
| 5 | 3.68 " | $3.64\times10^{-3}$ | 0.171 | 1.36 " |
| 6 | 3.34 " | $7.27\times10^{-3}$ | 0.178 | 1.73 " |
| 7 | 3.04 " | $9.09\times10^{-3}$ | 0.178 | 1.91 " |

Runs 1 - 4 with $AgNO_3$

Runs 5 - 7 with $AgClO_4$

# FIGURE XXXI: PSEUDO FIRST ORDER PLOTS FOR REACTION

## (9.2) at 25°C

## (Data from runs 1,4 and 6, Table XXV)



$\log_{10}\left[Co(NH_3)_5 Br\right]^{2+}$

Homogeneous aquation

Reaction 90% complete
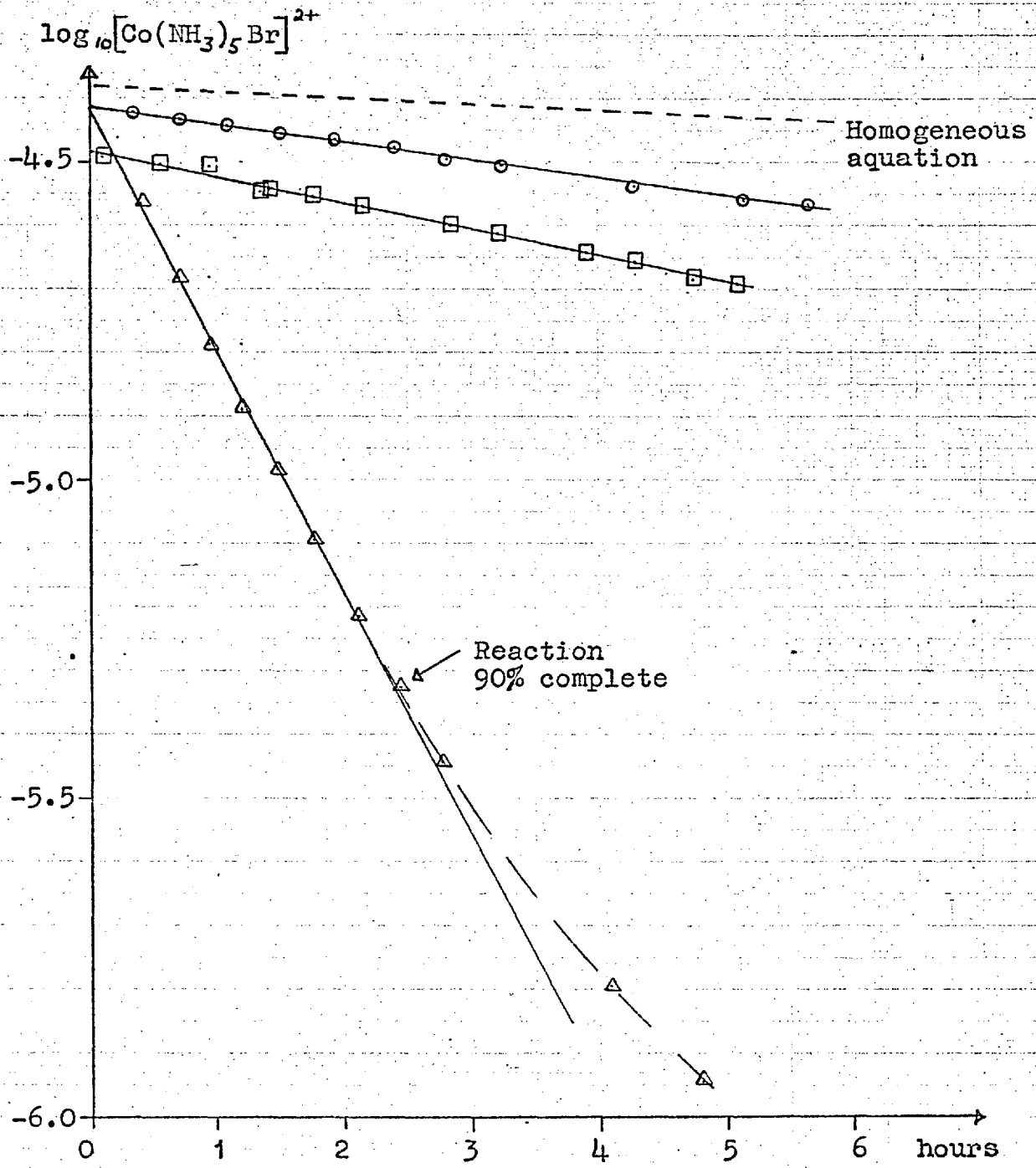
⊙ Run 1

△ Run 4

▫ Run 6

FIGURE XXXII: BRÖNSTED PLOT OF RESULTS OF TABLE XXV



Gradient = 4.7

Gradient = 1.2

$I^{\frac{1}{2}}/(1+I^{\frac{1}{2}})$
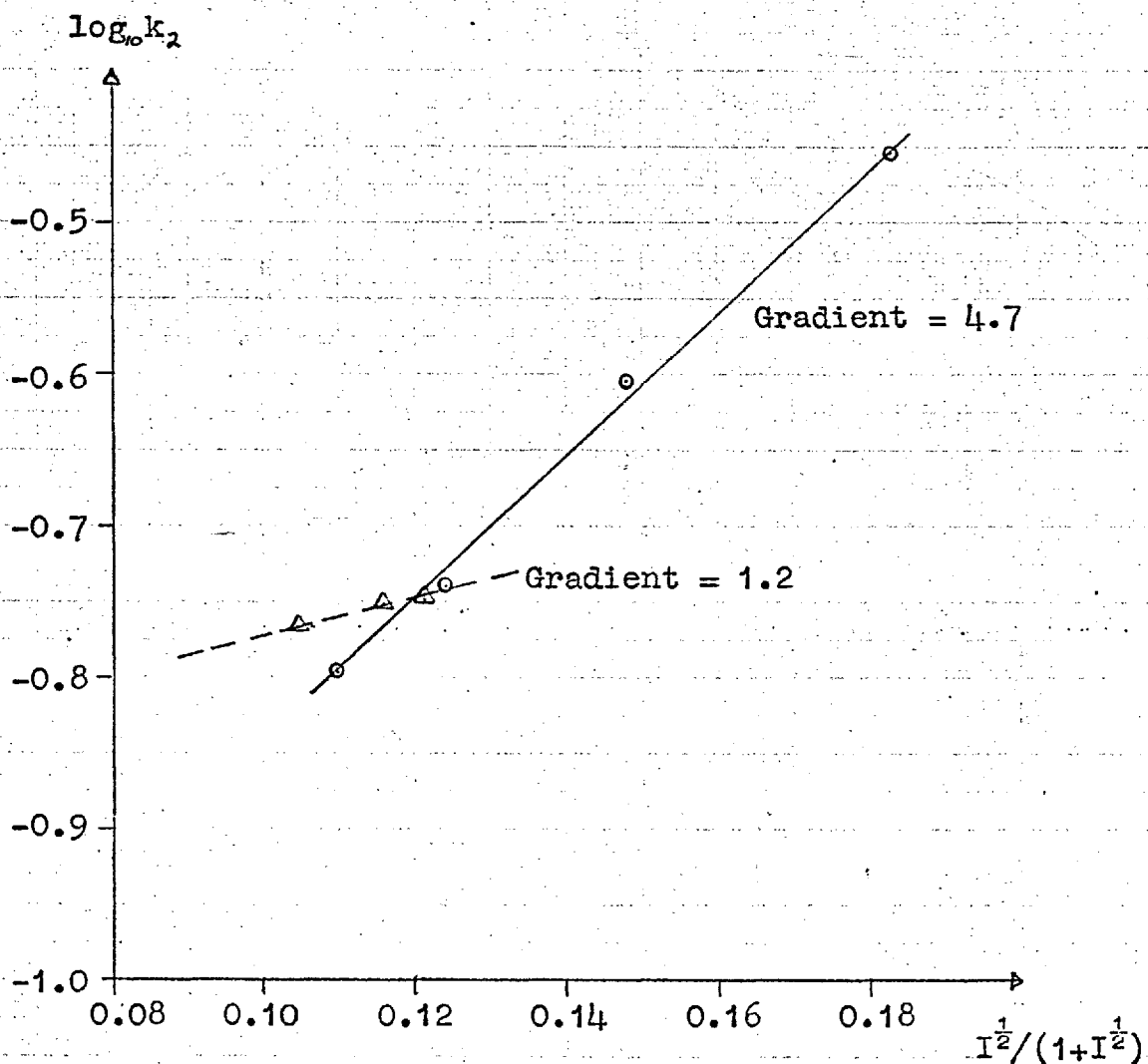
⊙ Runs with $AgNO_3$

△ Runs with $AgClO_4$

According to the Brönsted theory of primary salt effects, the gradient of a plot of log $k_2$ against $I^{\frac{1}{2}}/(1+I^{\frac{1}{2}})$ should be 2.04 for this reaction, whereas for $AgNO_3$ it is actually 4.7 and for $AgClO_4$ 1.2. Ion pair formation between $[Co(NH_3)_5Br]^{2+}$ and $NO_3^{-}$ could possibly enhance the rate of reaction with $Ag^+$. (0.1M $NaNO_3$ raised the aquation rate of $[Co(NH_3)_5Cl]^{2+}$ by 3.4% (60) ).

The value of $k_2$ at I = $10^{-2}$M was taken to be $(0.15\pm0.02)$ $M^{-1}$ $min^{-1}$.

IX.6.2: The value of $k_s$.

The value of $k_s$ for AgBr was $3.8\times10^{-3}min^{-1}$ in the dark and $2.3\times10^{-2}min^{-1}$ in the light. Treating these values as for HgS (see Section (VIII.4.3:) ),

$(k_2)_{het}$ in the dark $\quad = \quad 3 - 17 \quad M^{-1}$ $min^{-1}$

$(k_2)_{het}$ in the light $= 18 - 90 \quad$ " $\quad$ "

$(k_2)_{hom} \quad\quad\quad\quad = (0.15\pm0.02)$ $M^{-1}$ $min^{-1}$

All values are for I = $10^{-2}$M. The diffusion layer was taken to be $(1-5)\times10^{-3}$cm., and Johnston's value of $1.25\times10^{-9}$ moles $cm^{-2}$ (136) for the surface concentration of $Ag^+$ on AgBr was used.

It appears that the heterogeneous reaction is considerably faster than the homogeneous reaction, even in the dark. The opposite was true for HgS.

IX.6.3: The effect of AgBr on the reaction between
$[Co(NH_3)_5Br]^{2+}$ and $Ag^+$.

Silver ions are adsorbed by AgBr, presumably on bromide sites ($\sigma \approx 2.3 \times 10^2$ (27) ). Since $[Co(NH_3)_5Br]^{2+}$ is also sorbed, it was thought possible that AgBr would catalyse the bimolecular reaction between $Ag^+$ and $[Co(NH_3)_5Br]^{2+}$. However, no significant catalysis (or inhibition) was observed in three series of runs with batches 3 and 4 AgBr, with $[Ag^+]$ in the range $(3-10) \times 10^{-3}M$ and $[Co(NH_3)_5Br]^{2+}_{t=0}$ in the range $(3-4) \times 10^{-5}M$. It would seem, therefore, that $Ag^+$ and $[Co(NH_3)_5Br]^{2+}$ ions are adsorbed additively rather than competitively, and that sorption does not enhance the bimolecular reaction rate, possibly because juxtaposition is not sterically favourable. In contrast, silver iodide efficiently catalysed the reaction between ethyl iodide and silver ions (27).

IX.7. Use of silver halide rotating discs.

Attempts were made to study catalysis by the silver halides by use of rotating discs of these materials.

A circular lamina of fused silver chloride, obtained from Johnson Matthey, was glued onto a former to make a rotating disc of active surface area $28.27cm^2$. Experiments with 500ml. $5.6 \times 10^{-5}M$ $[Co(NH_3)_5Cl]Cl_2$ showed that

the catalytic effect of this disc, even at high rotation speeds, on the aquation of $[Co(NH_3)_5Cl]^{2+}$ was negligible. The catalysis of $[Co(NH_3)_5Br]^{2+}$ aquation was not followed for fear of contaminating the disc surface with AgBr.

It was originally thought that AgBr and AgI could be studied in disc form by depositing a thin layer of silver on a platinum disc electrolytically, and then bromidising or iodinising this layer anodically. Unfortunately, experiments at controlled potential (140) showed that before conversion of Ag to AgX was complete, the potential invariably rose and bromine or iodine was formed at the anode. Discs formed in this way are therefore not only probably contaminated by halogen, but also contain unchanged silver. Therefore, although an AgI disc of surface area 30cm² had a considerable effect upon $[Co(NH_3)_5Br]^{2+}$, its use was discontinued.

# CHAPTER X : CATALYSIS BY PLATINUM OF THE AQUATION OF
## $[Co(NH_3)_5Br]^{2+}$.
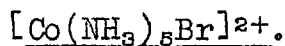
A platinum rotating disc of active surface area
25.16cm$^2$ was used in a series of experiments at 25°C with
$[Co(NH_3)_5Br]^{2+}$. The catalytic aquation reaction was found
to be surface-controlled. The effect of electrochemical
pre treatment on the activity of the disc was investigated.
The addition of Br$^-$ and $[Co(NH_3)_5H_2O]^{3+}$ was found to
enhance the rate of the catalytic reaction. It appeared
from this and other observations that the surface potential
of the disc played an important part in determining its
catalytic activity.

## X.1. The platinum rotating disc.

The shape of the rotating disc is illustrated in
Figure XXXIII, on page 194. The disc was prepared by
soldering a circular lamina of pure platinum (Engelhard
Industries, Ltd.) onto a trumpet-shaped stainless steel
former. The thickness of the platinum lamina was 1mm.
and the area of the plane face was 25.16cm$^2$. The sides
of the lamina and the steel former were protected by two
coats of Araldite clear lacquer AR 1501 (Ault and Wiborg
Paints, Ltd.). Each coat was applied by carefully
immersing the disc in the lacquer to just below the screw

holes, draining for 30 minutes, and then curing the coating at 180°C for 30 minutes.

Before the lacquer covering the platinum surface was removed, a test run was carried out at 500 r.p.m. The disc had no effect on the aquation rate of $[Co(NH_3)_5Br]^{2+}$, and it was concluded that the Araldite coating was satisfactorily inert.  It was also non-conducting.

The coating was then removed from the platinum face of the disc by brushing on Stripalene 713 (Sunbeam Anti-Corrosives, Ltd.).  The disc surface was then gently abraded with finest grade emery paper, which produced a surface almost smooth to the eye.  During the series of runs carried out with this disc, no further mechanical treatment was applied to the platinum surface.

Microscopic imperfections are bound to render the actual surface area of the platinum greater than its geometric area.  The roughness factor (real/geometric area) for smooth platinum has been estimated from 1.5 to 3.0, with a value of 2.0 often being used (141, 142, 143). However, Laitinen and Enke (144) deduced the lower value of (1.12±0.10) from gas adsorption experiments.

X.2. Apparatus and experimental procedure.


Before each run, the disc surface was cleaned by
anodising and cathodising it at controlled potential, in
the apparatus shown in Figure XXXIII, on page 194. A
controlled current, measured by the d.c. microammeter (A),
was passed through the right hand circuit by means of a
9V. grid bias battery (B) and a Beckman $10^4$ ohm precision
helipot (H). The disc potential with respect to a
Radiometer type K401 saturated calomel electrode (C) was
measured on a Radiometer pH meter 4, used as a potentio-
meter (P). The potential was maintained at a constant
value by suitable adjustment of the helipot.

To reverse the polarity of the disc, the helipot
connections were reversed. The salt bridge connecting
the reference electrode with the disc contained 0.1M
$NaClO_4$ in agar gel. Both ends of the bridge tapered into
fine, upturned capillaries, to minimise diffusive contamin-
ation. The disc was rotated at 100 r.p.m. throughout the
pre-treatment.

After cleaning, the disc was disconnected from the
current-carrying circuit and withdrawn from solution,
rinsed with distilled water and spun rapidly to fling off
excess water. It was then lowered into the reaction vessel,
containing 500ml. $10^{-3}M$ $HClO_4$ or other background electro-
lyte. The whole was lowered into the thermostat as shown

# FIGURE XXXIII: ROTATING DISC APPARATUS

## PRETREATMENT OF THE PLATINUM DISC

(For diagram of complete rig and details
of electrical connections to disc,
see Figure XV , p.137)



Reaction
vessel lid
present,
but not
shown in
this diagram

Level of
thermostat
liquid

Platform

0.1M
NaClO₄

10⁻² M
HClO₄

Pt
surface

sintered
glass disc

1 cm²
Pt foil
(current
carrying
electrode)

salt bridge
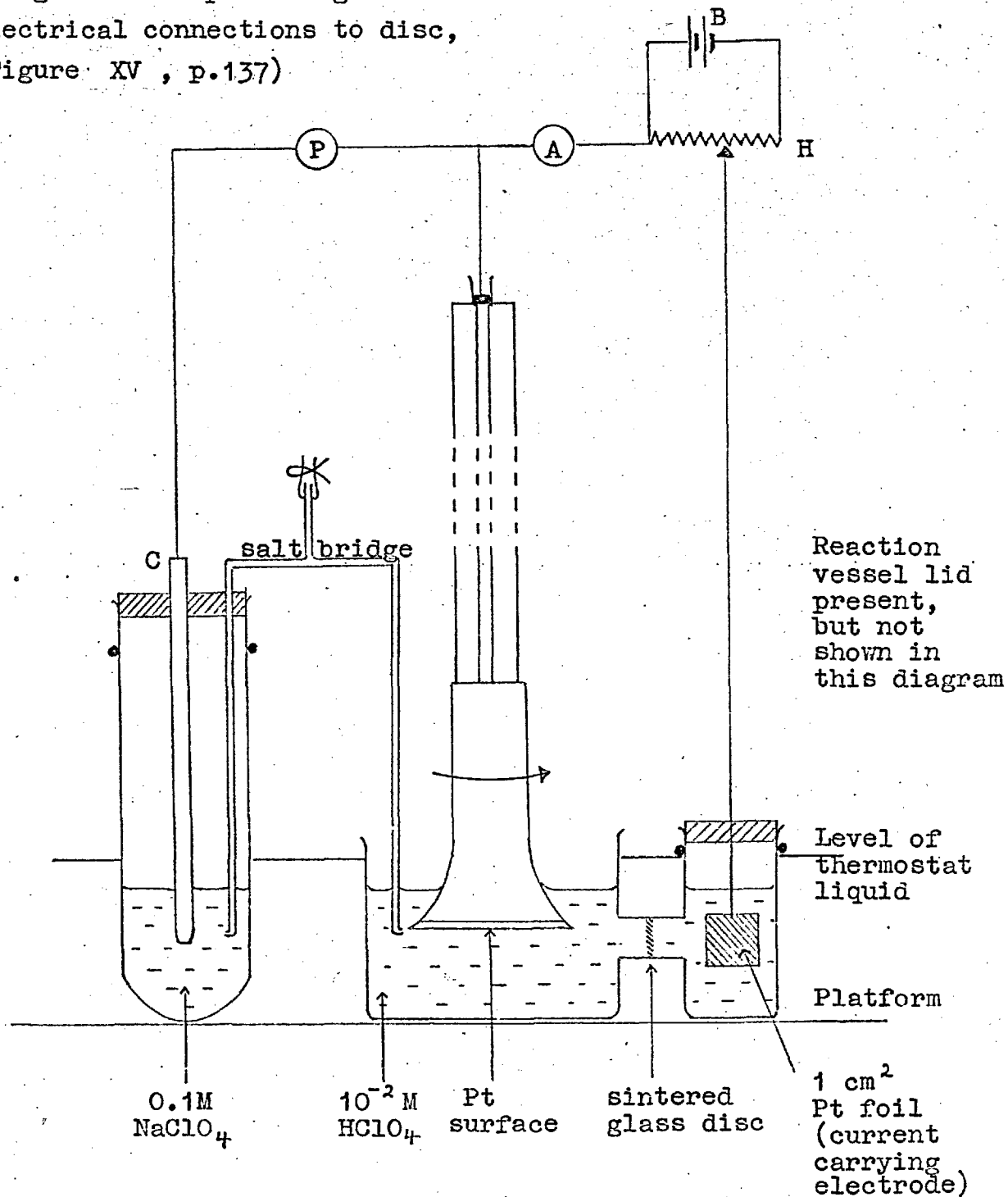
FIGURE XXXIV: ROTATING DISC APPARATUS

MEASUREMENT OF DISC POTENTIAL

DURING RUNS
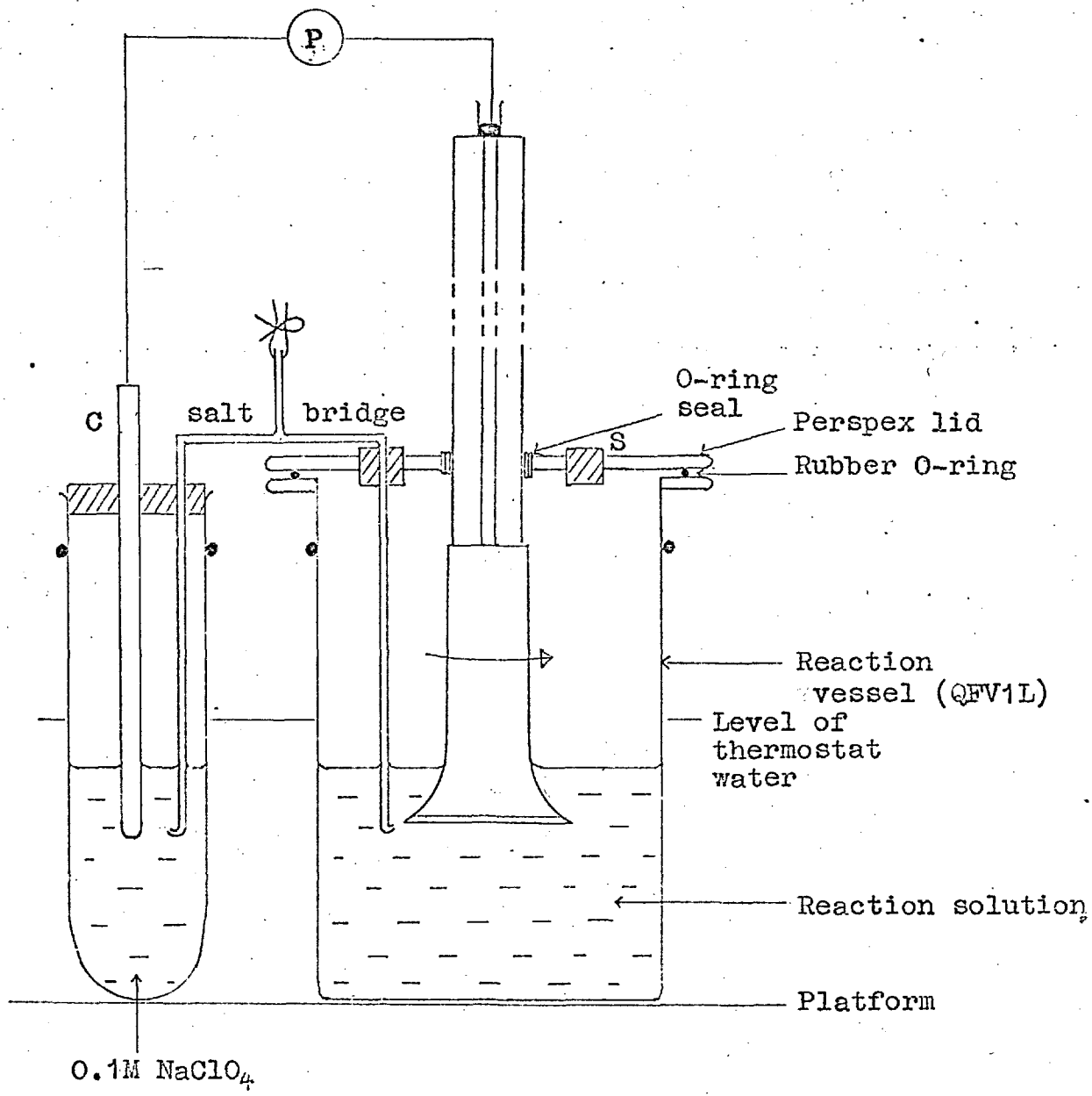
in Figure XXXIV, on page 195. The disc was rotated at constant speed, and at time $t_0$ to a small quantity of solid $[Co(NH_3)_5Br]Br_2$ was added through S. The reaction was followed spectrophotometrically by removing aliquots for analysis through S. The reaction vessel was closed to the air except when removing samples. The potential of the platinum disc was monitored before and during each run by means of the potentiometer (P), which drew only very small currents ($\sim 10^{-9}$ amp.).

## X.3. Electrochemical pretreatment of platinum disc.

There is extensive literature on the electrochemical activation of platinum electrodes and catalysts (145). Anodisation (A) produces oxidised surfaces and causes most surface impurities to desorb (146). Cathodisation (C) produces reduced surfaces, in which hydrogen may be occluded. The state of maximum activity of the surface depends upon the nature of the heterogeneous process. James (146), for example, found electrodes pre-anodised at 2.0V (nhe) had maximum activity for the Fe(III)/Fe(II) electron exchange reaction. On the other hand, Baker and MacNevin (147) found cathodised surfaces were roughly ten times as active as anodised ones for the electrolytic oxidation of arsenic and iron.

The thermodynamics of surface phenomena on platinum as a function of potential and pH have been summarised

by Pourbaix (148). Table XXVI, on page 198, gives a summary of this, and other information, for pH 2 (used in the present series of experiments).

In a series of preliminary experiments, the catalytic activity of the platinum disc for the aquation of $[Co(NH_3)_5Br]^{2+}$ was examined. The results are summarised in Table XXVII, on page 199. All pre-treatment was carried out on the disc while stationary, and the disc was left for 30 minutes before starting each run.

Pre-cathodisation produced the most active surface. However, the disc activity seemed to be rapidly lost, as first order plots showed up to 50% decrease in $k_{het}$ in one hour: the values in Table XXVII are for the initial rate of the reaction. For this reason, and also because it was feared that hydrogen occluded during pre-cathodisation might reduce $[Co(NH_3)_5Br]^{2+}$, (A+C) treatment was discontinued.

(C+A) treatment did not produce a very active surface, but kinetics were accurately first order and the catalytic rates were reproducible. This method was therefore developed. During pre-treatment experiments at fixed potentials, it was discovered that both anodic and cathodic currents increased if the disc was rotated: this is to be expected if the disc processes are at least partly diffusion-controlled. Further increase was negligible above 100 r.p.m. The finally adopted pre-treatment

TABLE XXVI : SURFACE STATE OF SOLID PLATINUM AT

pH 2 and 25°C.

| Potential (versus normal hydrogen electrode). | Surface State. | Reference |
|---|---|---|
| <-0.2V. | Hydrogen evolved on smooth Pt. | |
| -0.12V. | Reversible $H_2$ evolution potential. | |
| < 0.84V. | Pt is stable surface phase. | (148) |
| 0.84-0.92V. | $Pt(OH)_2$ is stable surface phase. | (148) |
| 0.88V. | Formation of electronically conducting chemisorbed layer of oxygen. | (144), (149)-(151) |
| 1.11V. | Reversible $O_2$ evolution potential: several monolayers taken up. | (144), (152) |
| 0.92-1.87V. | $PtO_2.xH_2O$ is stable surface phase. | (148) |
| <~1.6V. | Oxygen evolved on smooth Pt. | (149) |
| < 1.87V. | $PtO_3.xH_2O$ is stable surface phase. | (148) |

TABLE XXVII : CATALYTIC ACTIVITY OF PLATINUM DISC AFTER

ELECTROCHEMICAL PRETREATMENT.

| Run No. | Disc pretreatment[*] | $10^5 c_0$ (Disc speed = 400 r.p.m.) | $10^4 k_{het}$, min$^{-1}$ at 25°C. |
|---|---|---|---|
| 1 | No pretreatment. | 4.8 | 1.61 |
| 2 | C 5 mins. at 0.28V., A 5 mins. at 2.0V. | 4.8 | 1.26 |
| 3 | C 5 mins. at 0.28V., A 10 mins. at 1.1V. | 4.8 | 2.37 |
| 4 | A 2 mins. at 2.0V., C 10 mins. at 0.28V. | 4.8 | 4.80 |
| 5 | A 10 mins. at 1.1V., C 20 mins. at 0.08V. | 1.20 | 12.79 at $t_0$. |
| 6 | "          " | 2.35 | 8.13 at $t_0$. |
| 7 | "          " | 4.8 | 7.28 at $t_0$. |
| 8 | "          " | 9.51 | 6.16 at $t_0$. |

[*]All potentials on normal hydrogen scale.

A = anodisation.

C = cathodisation.

procedure was:

With disc rotating at 100 r.p.m., in $10^{-2}M$ HClO$_4$ at 25°C,

(i) C 15 mins. at 0.4V. (i.e. low enough to reduce surface completely to Pt, but not to cause hydrogen evolution).

(ii) A 10 mins. at 1.11V. (the reversible oxygen evolution potential).

The current passing during this procedure fell with time, as shown in Figure XXXV, on page 201. Cathodisation carried out immediately after a run with [Co(NH$_3$)$_5$Br]$^{2+}$ always required larger currents than when the disc was left to soak in $10^{-2}M$ HClO$_4$ before-hand, presumably because the disc surface is "dirtier" in the former case. The anodisation current curve, on the other hand, was always the same, and it was therefore assumed that the final state of the disc was reproducible.

After pretreatment, the disc was rinsed and left to soak overnight in the reaction vessel in 500ml. of the background electrolyte to be used in the following run. At least 1-2 hours were required for the disc to attain rest potential. No loss in activity was observed after time lags of 3-48 hours between pre-treatment and the catalytic run.

The runs with the pre-treated disc were purposely carried out in random order, so that any systematic

FIGURE XXXV: CURRENT-TIME CURVES FOR DISC PRETREATMENT

      (1) CATHODISATION AT 0.4V., 100 r.p.m.

      (2) ANODISATION AT 1.11V., 100 r.p.m.
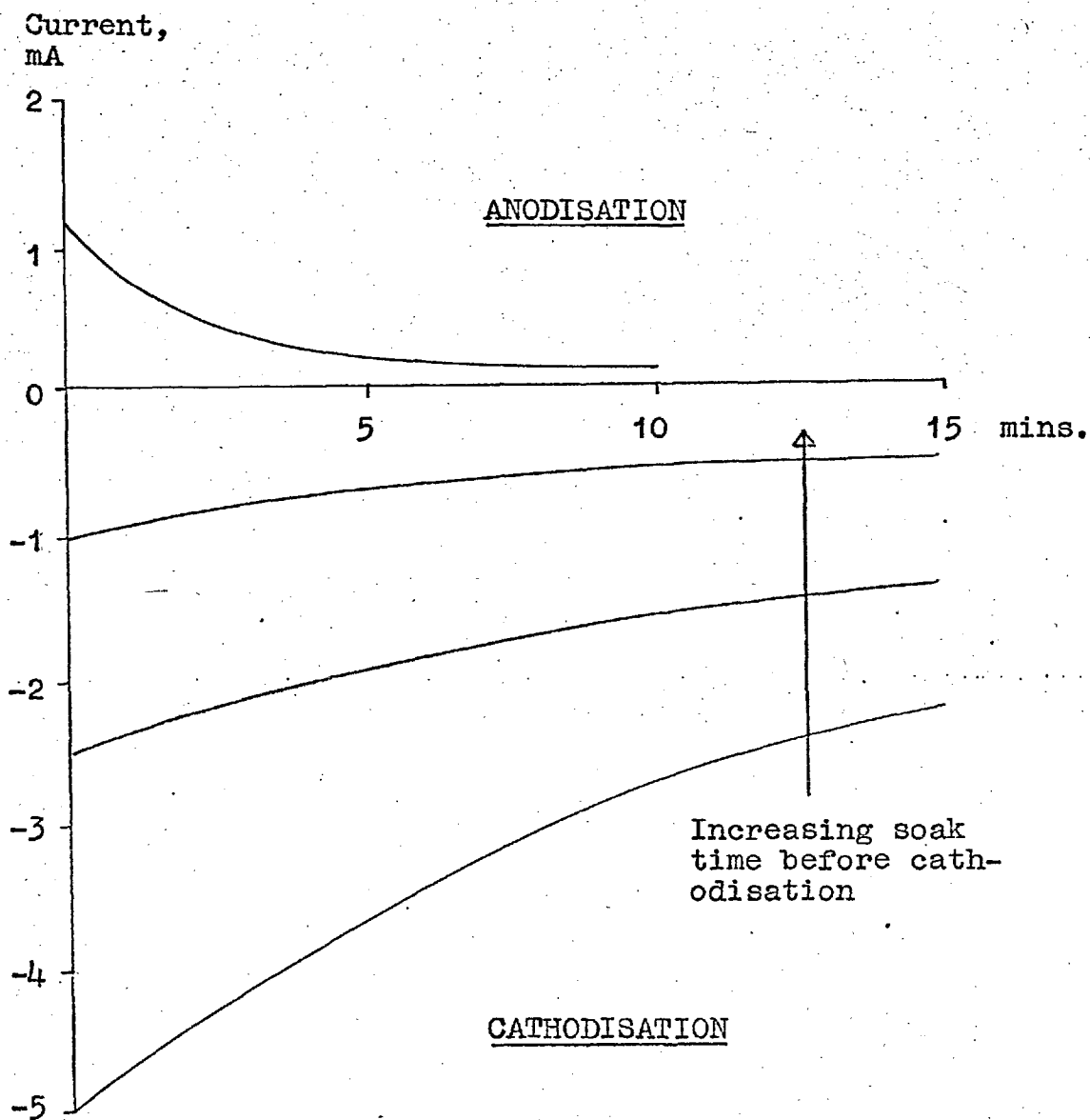
change in the activity might not be masked by a systematic change in the reaction conditions.


X.4.   Sampling corrections.


During each run, 9-12 samples of *ca.* 3ml. and occasionally *ca.* 5ml. each were removed from the reaction vessel for spectrophotometric analysis.   The ratio of the surface area of the platinum catalyst to the volume of solution therefore increased by up to 7% during runs.   The spontaneous aquation rate, expressed in M min$^{-1}$, is unaffected by this, but the heterogeneous rate, thus expressed, increases, so the value of $k_{obs}$ obtained could be greater than if no samples had been taken.   A method of correcting experimental data for this sampling effect is derived below.


Let the initial volume of solution be V litres and let $\Delta V$ litres be removed per aliquot.   The concentration of the reactant, $[Co(NH_3)_5Br]^{2+}$, is $c_n$ at time $t_n$.   The times $t_1$, $t_2$ .... are the times of taking samples 1, 2 .... The following table may be constructed:


| Time interval | No. of moles reacted in this interval $(=\Delta N)$ | Mean reaction rate in this interval $(=dN/dt)$ |
|---|---|---|
| $t_0$ to $t_1$ | $-V(c_1-c_0)$ | $\Delta N_{0,1}/(t_1-t_0) = v_{0,1}$ |
| $t_1$ to $t_2$ | $-(V-\Delta V)(c_2-c_1)$ | $\Delta N_{1,2}/(t_2-t_1) = v_{1,2}$ |
| $t_n$ to $t_{n+1}$ | $-(V-n\Delta V)(c_{n+1}-c_n)$ | $\Delta N_{n,n+1}/(t_{n+1}-t_n)$ $= v_{n,n+1}.$ |

The "mean reaction rate" refers to the mean concentrations during the sampling intervals, i.e. $(c_0 + c_1)/2$, $(c_1 + c_2)/2$ etc., and must be corrected for the homogeneous contribution (i.e. the spontaneous aquation of $[Co(NH_3)_5Br]^{2+}$) to obtain the mean heterogeneous rate in each time interval:

$$V_{n,n+1}^{het} = V_{n,n+1} - V_{n,n+1}^{hom}$$

$$V_{n,n+1}^{hom} = k_1(V-n\Delta V)(c_n + c_{n+1})/2$$

Now for a first order process, $dN/dt = -kN$. A plot of $V_{n,n+1}^{het}$ versus the mean number of moles of reactant $(\bar{N})$ present in the time interval $t_n$ to $t_{n+1}$ should therefore be a straight line of gradient $k_{het}$, where the value of $k_{het}$ is corrected for sampling effects. This plot is illustrated for two runs, one in which $k_{het}$ was large and one in which it was small, in Figure XXXVI. Details of the runs are given below and in Table XXVIII.

Run 1:

Initial volume $= 500ml.$

Aliquots $= 5ml.$

$c_0 = 1.091 \times 10^{-5}M$ (in $2.024 \times 10^{-3}M$ KBr)

$k_{het} = 19.0 \times 10^{-4}min^{-1}$ (from 1st.order plot).

$k_{het} = 19.4 \times 10^{-4}min^{-1}$ (from Figure XXXVI).

Run 2:

Initial volume = 500ml.

Aliquots = 3ml.

$c_0$ = 15.08x10$^{-5}$M (in 2.024x10$^{-3}$M KBr)

$k_{het}$ = 2.21x10$^{-4}$min$^{-1}$ (from 1st.order plots).

$k_{het}$ = 2.2$_1$x10$^{-4}$min$^{-1}$ (from Figure XXXVI).

The data from Run 2 were smoothed in order to plot Figure XXXVI, as the change in c during each interval was so small. No smoothing was applied to the much faster Run 1. In both cases, rather scattered plots are obtained. However, in either case, as the $k_{het}$ values above show, the "corrected" value of $k_{het}$ is only slightly different from the value obtained from a normal first order plot of experimental data. It is concluded that the effect of sampling is largely self-compensating: removal of an aliquot increases the heterogeneous reaction rate, so that at the end of the next time interval, there is less reactant left than if no sample had been taken, and the overall rate of the first order reaction is less. No sampling corrections have therefore been applied to the data reported in this chapter.

## TABLE XXVIII : SAMPLING CORRECTION FOR RUNS 1 AND 2.

| Reading number. | Time, min. | $10^5 c, M.$ | In time interval. | $-10^9 \nu_{het}$ | $10^6 \bar{N}$ |
|---|---|---|---|---|---|
| RUN 1. | (unsmoothed data) | | | | |
| 0 | 0 | 1.091 | | | |
| 1 | 5 | 1.089 | 0-1 | $-\nu_e$ | 5.45 |
| 2 | 20 | 1.044 | 1-2 | 12.9 | 5.28 |
| 3 | 34 | 1.010 | 2-3 | 10.0 | 5.03 |
| 4 | 46 | 0.983 | 3-4 | 9.13 | 4.84 |
| 5 | 55 | 0.965 | 4-5 | 7.76 | 4.68 |
| 6 | 67 | 0.935 | 5-6 | 10.4 | 4.51 |
| 7 | 80 | 0.908 | 6-7 | 8.12 | 4.33 |
| 8 | 93 | 0.882 | 7-8 | 7.69 | 4.16 |
| 9 | 105 | 0.863 | 8-9 | 5.75 | 4.02 |
| RUN 2. | (smoothed data) | | | | |
| 0 | 0 | 15.08 | | | |
| 1 | 10 | 14.98 | 0-1 | 22.2 | 75.1 |
| 2 | 29 | 14.83 | 1-2 | 11.9 | 74.1 |
| 3 | 70 | 14.48 | 2-3 | 13.4 | 72.1 |
| 4 | 90 | 14.30 | 3-4 | 18.0 | 70.7 |
| 5 | 110 | 14.14 | 4-5 | 13.4 | 69.4 |
| 6 | 129 | 13.98 | 5-6 | 15.6 | 68.2 |
| 7 | 149 | 13.81 | 6-7 | 16.2 | 66.9 |
| 8 | 169 | 13.65 | 7-8 | 14.0 | 65.8 |
| 9 | 189 | 13.49 | 8-9 | 14.2 | 64.6 |
| 10 | 214 | 13.29 | 9-10 | 14.4 | 63.3 |
| 11 | 235 | 13.13 | 10-11 | 12.8 | 62.1 |
| 12 | 249 | 12.94 | 11-12 | 14.5 | 60.9 |

RUN 1

Gradient $= 19.4 \times 10^{-4}\,min^{-1}$

RUN 2

Gradient $= 2.21 \times 10^{-4}\,min^{-1}$
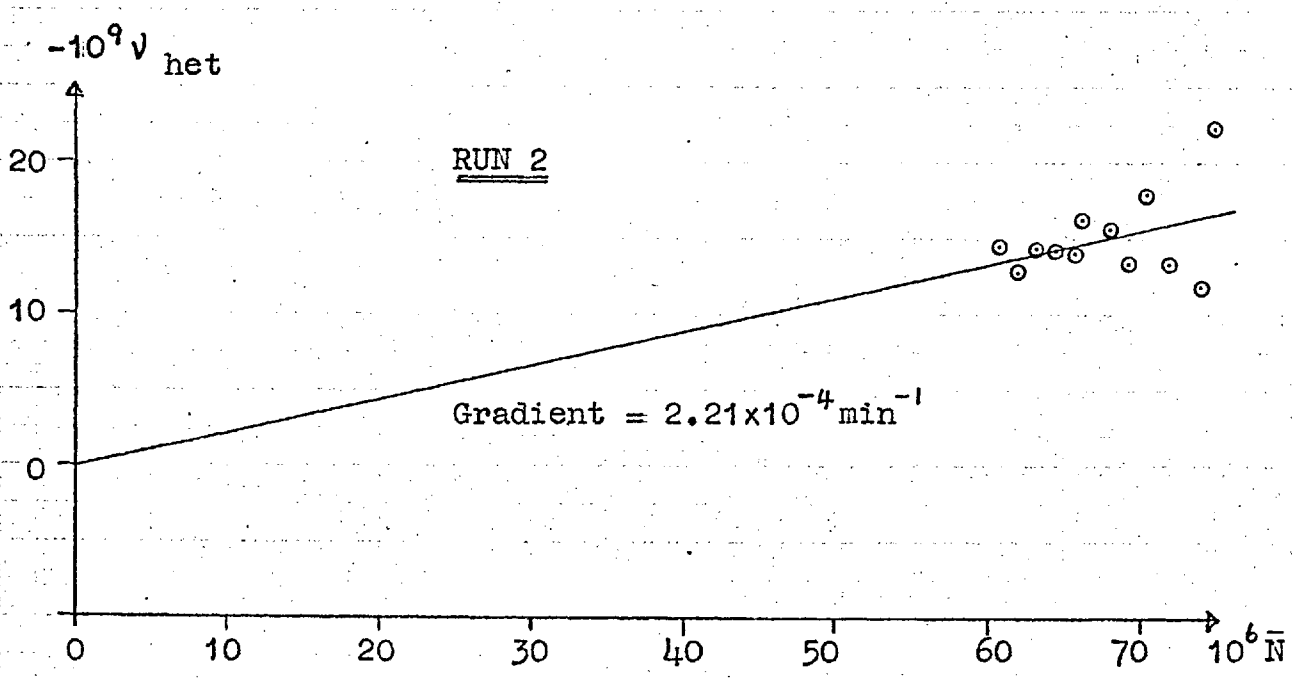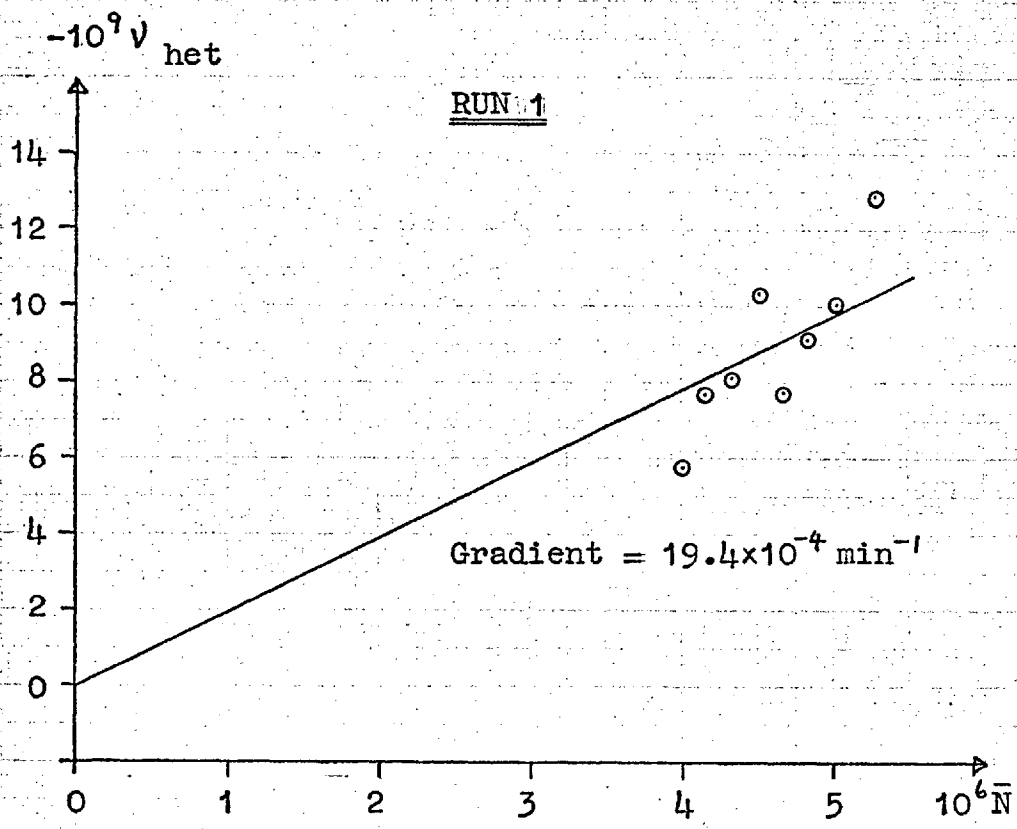
# RESULTS.

X.5.  Surface control of catalytic aquation.

The rate of a diffusion-controlled reaction at the platinum disc can be calculated from equations (7.31) and (7.32).  Substituting in these equations the values $D_i = 6.85 \times 10^{-6} cm^2 sec^{-1}$ (see Chapter XI) and $A = 25.16 cm^2$, the limiting rate of flux of $[Co(NH_3)_5Br]^{2+}$ to the disc rotating at $\omega$ radians $sec^{-1}$ is $1.205 \times 10^{-2} \omega^{\frac{1}{2}} c_{bulk}$ moles $sec^{-1}$.  Therefore $k_{het}$ for a system of 500ml. would be $2.41 \times 10^{-5} \omega^{\frac{1}{2}} sec^{-1}$.  This is $46.8 \times 10^{-4} min^{-1}$ at 100 r.p.m. and $93.6 \times 10^{-4} min^{-1}$ at 400 r.p.m.

The highest observed value of $k_{het}$ was only $25.7 \times 10^{-4} min^{-1}$, considerably lower than the diffusion-controlled value.  In runs 4 and 7 (Table XXVII) and 11 (Table XXIX) there was no dependence of $k_{het}$ on rotation speed in the range tested, 100-1,000 r.p.m.  However, $k_{het}$ increased by 15% in run 23 (Table XXIX) on reducing the rotation speed from 400 to 100 r.p.m.  This change is in the wrong direction to be due to partial diffusion control, and was attributed to a discontinuous fall of 20mV. in the disc potential that occurred when the rotation speed  was decreased.  All experiments were therefore carried out at 400 r.p.m.  This preliminary observation, however, isolates one of the several factors that control the disc potential.

X.6.  The dependence of $k_{het}$ on $\bar{c}$.

A series of runs was carried out at 25°C to determine the pseudo first order rate constant, $k_{het}$, for $c_0$ values in the range $(1-15) \times 10^{-5}M$. The effects of $[Co(NH_3)_5H_2O](ClO_4)_3$ and KBr were also investigated in this concentration range. The results are summarised in Table XXIX on page 209, and Figures XXXVII and XXXVIII on pages 210 and 211 respectively.

As for the other catalysts, $k_{het}$ decreased as $\bar{c}$ increased. However, the ions $[Co(NH_3)_5H_2O]^{3+}$ and $Br^-$ increased $k_{het}$, instead of decreasing it as for AgBr and HgS. Figure XXXVIII is a Langmuir plot of $1/k_{het}$ vs. $\bar{c}$. It is seen that all four systems gave good linear plots. However, according to the theory set out in Section (VII.5), the effect of the ions $[Co(NH_3)_5H_2O]^{3+}$ and $Br^-$ means that these ions have negative sticking probabilities on platinum. This is meaningless, and it is shown in Section (X.7.1:) that the effect of these ions is probably connected with their effect on the potential of the platinum surface.

The slope and intercept of the Langmuir plot in the presence of $10^{-2}M$ $HClO_4$ (system A) are $4.5 \times 10^7$ min.$M^{-1}$ and $7.8 \times 10^2$ min. respectively. From equation (7.17), the values of $k_s$ and $\sigma$ can be calculated, substituting the disc area, $25.16cm^2$, for $Am_{cat}$, $V = 0.5$ litre and

## TABLE XXIX : THE PSEUDO FIRST ORDER RATE CONSTANT $k_{het}$ AS A FUNCTION OF THE CONCENTRATION OF $[Co(NH_3)_5Br]^{2+}$

$c_0$ = initial concentration in each run.

$\bar{c}$ = mean " " " "

All results for Pt disc (area = 25.16cm²) at 400 r.p.m. in 500ml. solution at 25°C.

| Background electrolyte. | Run No. | $10^5 c_0$, M | $10^5 \bar{c}$, M | $10^4 k_{het}$, min$^{-1}$ |
|---|---|---|---|---|
| $10^{-2}$M HClO$_4$ | 9 | 0.895 | 0.732 | 20.7 |
| (A) | 10 | 2.35 | 2.11 | 5.70 |
| | 11 | 4.82 | 4.31 | 3.63 |
| | 12 | 6.89 | 6.21 | 2.66 |
| | 13 | 9.77 | 9.10 | 2.15 |
| | 14 | 14.4 | 13.7 | 1.42 |
| $10^{-2}$M HClO$_4$ plus | 15 | 2.32 | 1.99 | 8.40 |
| $1.00 \times 10^{-3}$M | 16 | 5.05 | 4.74 | 3.76 |
| $[Co(NH_3)_5H_2O](ClO_4)_3$ | 17 | 9.98 | 9.33 | 2.78 |
| (B) | 18 | 10.1 | 9.58 | 2.15 |
| | 19 | 15.1 | 14.2 | 1.43 |
| $10^{-2}$M HClO$_4$ plus | 20 | 1.01 | 0.765 | 25.7 |
| $1.012 \times 10^{-3}$M KBr | 21 | 5.80 | 5.38 | 4.17 |
| (C) | 22 | 14.6 | 13.7 | 1.71 |
| $10^{-2}$M HClO$_4$ plus | 23 | 1.09 | 0.995 | 19.0 |
| $2.024 \times 10^{-3}$M KBr | 24 | 4.79 | 4.34 | 7.48 |
| (D) | 25 | 9.83 | 9.20 | 3.27 |
| | 26 | 14.8 | 13.8 | 2.21 |

FIGURE XXXVII: PLOT OF $k_{het}$ vs. $\bar{c}$

(Data from Table XXIX)

Background electrolyte

⊙ A  $10^{-2}$ M HClO$_4$

⊡ B  $10^{-2}$ M HClO$_4$ plus $1.00\times10^{-3}$ M $[Co(NH_3)_5\text{-}H_2O]\,(ClO_4)_3$

△ C  $10^{-2}$ M HClO$_4$ plus $1.012\times10^{-3}$ M KBr

▽ D  $10^{-2}$ M HClO$_4$ plus $2.024\times10^{-3}$ M KBr

– – – – Adsorption isotherm of $[Co(NH_3)_5Br]^{2+}$ on Pt (see text)

211



FIGURE XXXVIII: LANGMUIR PLOT

(Data from Table XXIX)
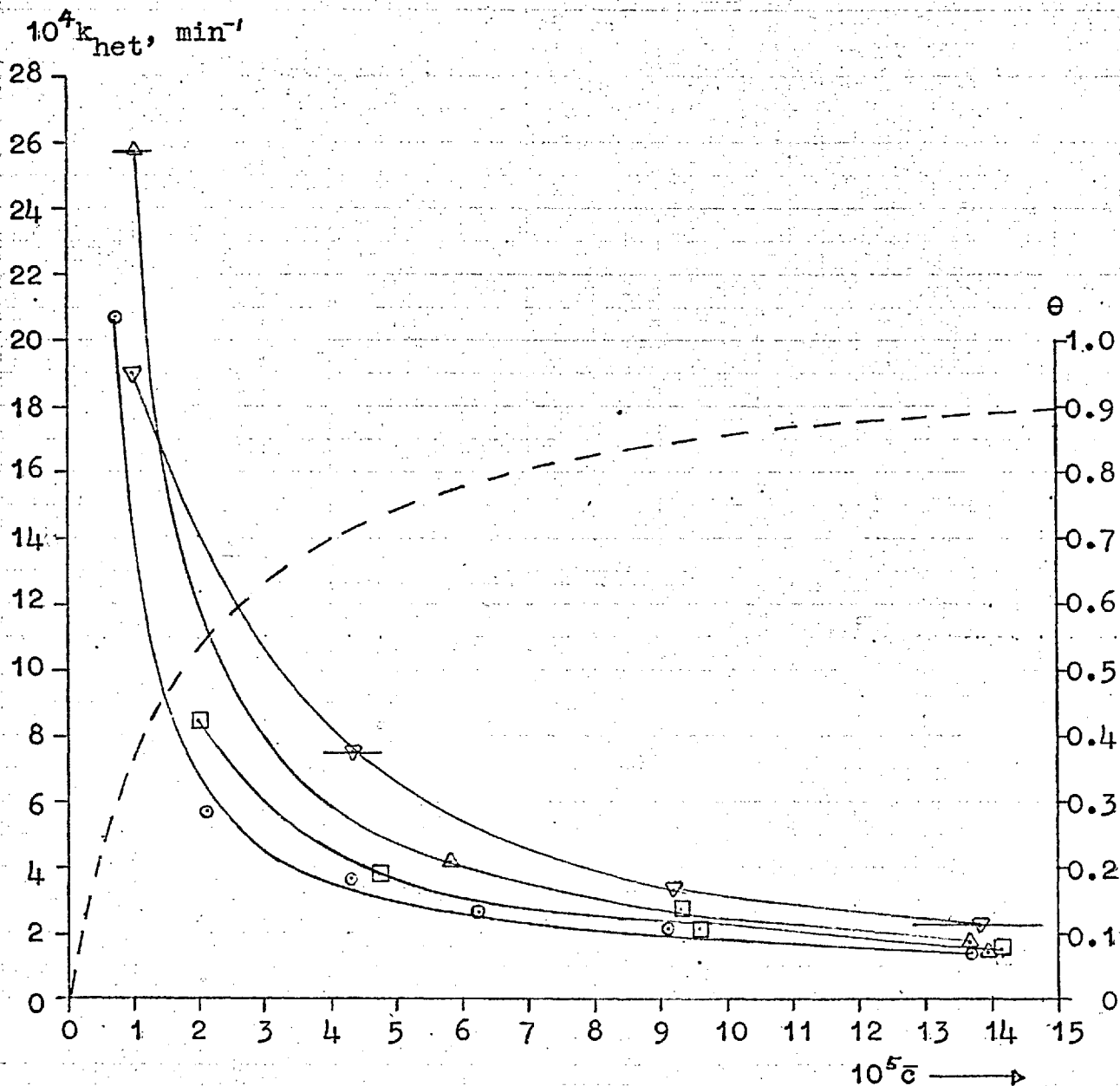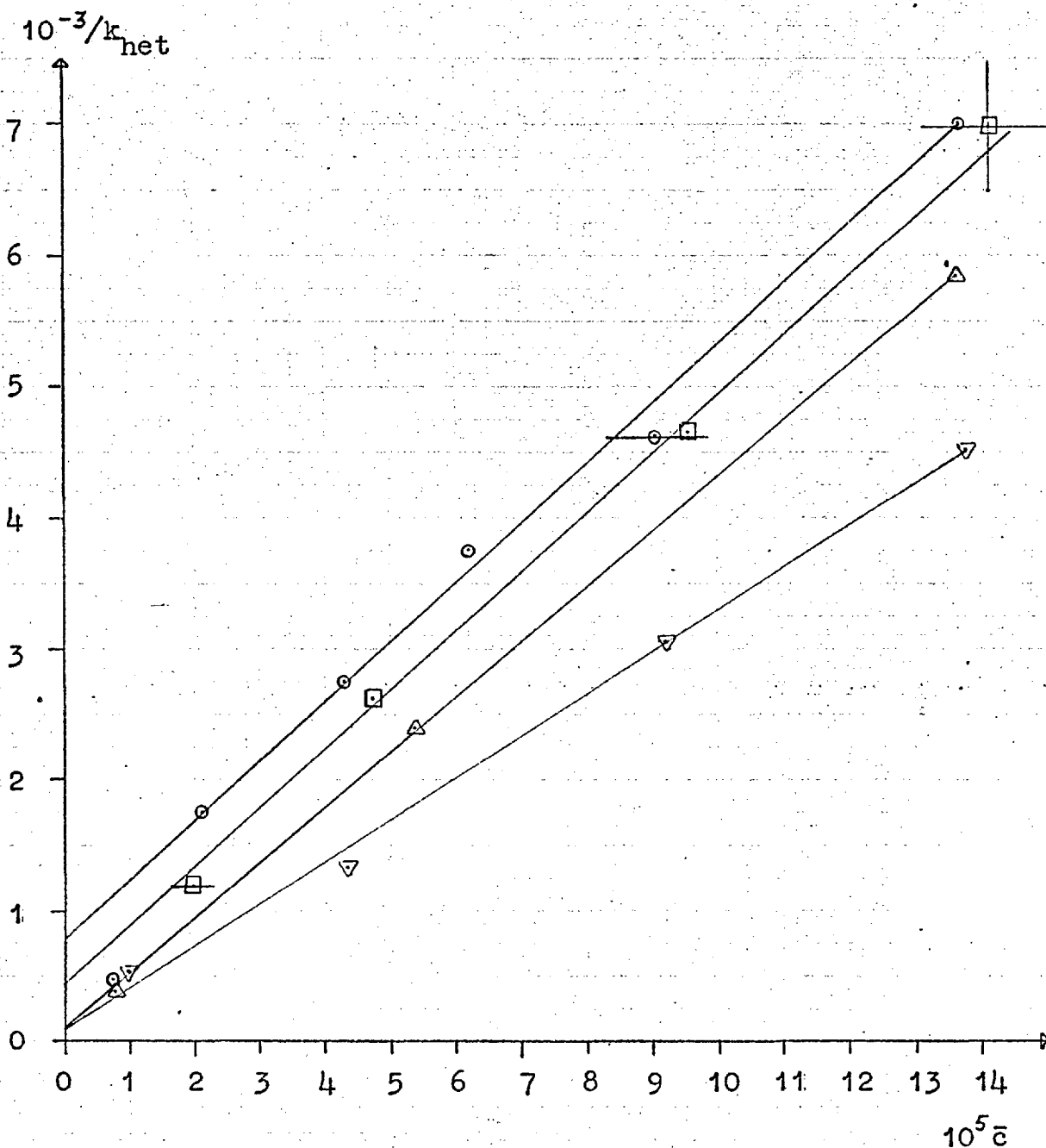
Background electrolyte

⊙ A  $10^{-2}$ M $HClO_4$
▣ B  $10^{-2}$ M $HClO_4$ plus $1.00\times10^{-3}$ M $[Co(NH_3)_5H_2O](ClO_4)_3$
△ C  $10^{-2}$ M $HClO_4$ plus $1.012\times10^{-3}$ M KBr
▽ D  $10^{-2}$ M $HClO_4$ plus $2.024\times10^{-3}$ M KBr

$c_{mono} = 4.2 \times 10^{-10}$ moles $cm^{-2}$ (as for HgS and AgBr).
The values are $\sigma = 5.8 \times 10^4$ $M^{-1}$, $k_s = 1.05$ $min^{-1}$. (If
the roughness factor of the platinum disc were 2, this
value of $k_s$ would be halved). The significance of
these figures is discussed in Section (X.8).

Substituting the above value of $\sigma$ in the Langmuir
adsorption isotherm

$$\theta = \sigma c_{bulk} / (1 + \sigma c_{bulk}), \qquad (7.14)$$

the isotherm for the adsorption of $[Co(NH_3)_5Br]^{2+}$ on Pt
can be calculated, and it is plotted as a dashed line in
Figure XXXVII, on page 210.

X.7.   The surface potential of the platinum catalyst.

X.7.1:   The disc potential during runs.


The disc potential during all the runs in Table XXIX
was measured as described in Section (X.2).   The pre-
treated disc was left soaking in background electrolyte
for several hours, and shortly before the start of the
run, it was rotated at 400 r.p.m., the speed at which the
runs were carried out.   The potential was steady during
this time.   At time $t_0$, a small amount of $[Co(NH_3)_5Br]Br_2$
was added.   This caused a rapid rise in potential of
20-250mV, followed by a much slower fall, as shown for
two typical runs in Figure XXXIX, on page 214.   Despite
this slow fall, first order plots of the reaction rate are
accurately linear, as also shown in Figure XXXIX.   All
potentials are expressed with respect to the saturated
calomel electrode;   values on the normal hydrogen scale
are obtained by adding 0.2415V.   The potential data are
summarised in Table XXX, on page 215.   The term $E_1$ is the
potential of the rotating disc before addition of
$[Co(NH_3)_5Br]Br_2$, $E_2$ is the highest potential reached after
the addition, and $-dE/dt$ is the potential drop thereafter.
$(E_2-E_1)$ is the rise in potential on addition of the reactant.
$E_1$ and $E_2$ are expressed with respect to the saturated
calomel electrode.

214

# FIGURE XXXIX: DISC POTENTIAL DURING CATALYTIC RUNS AT $25°C$
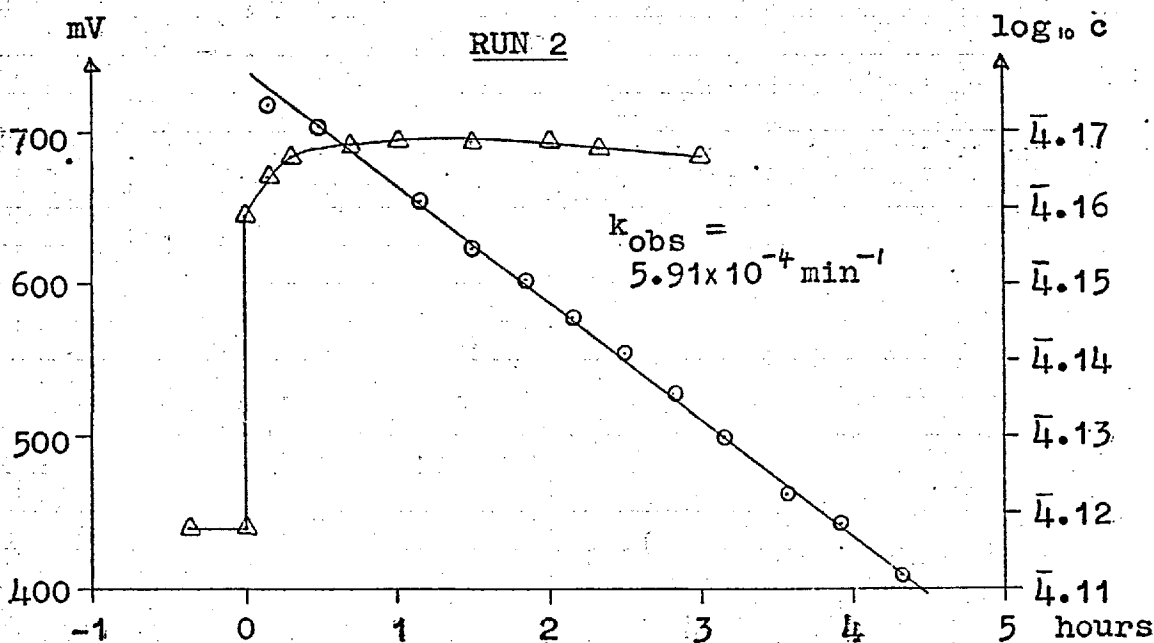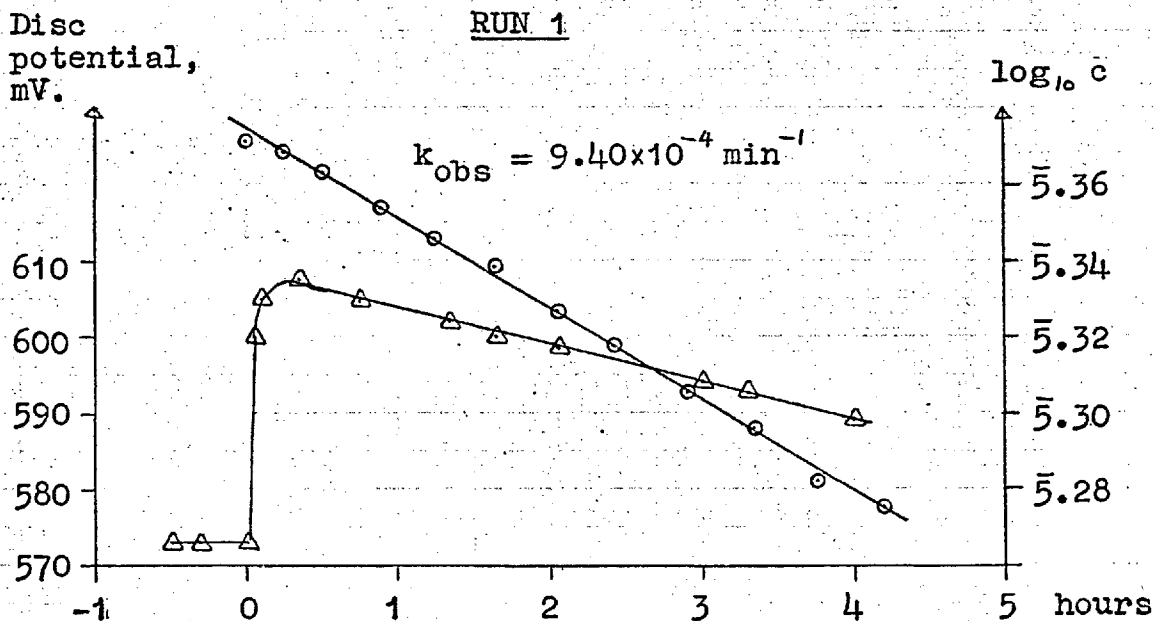


Disc speed = 400 r.p.m.

⊙  $\log_{10} \bar{c}$ (first order plot)

△  Disc potential with respect to the saturated calomel electrode

Run 1:  $c_0 = 2.35 \times 10^{-5}$ M

Background electrolyte = $10^{-2}$ M $HClO_4$

Run 2:  $c_0 = 14.8 \times 10^{-5}$ M

Background electrolyte = $10^{-2}$ M $HClO_4$ plus $2.024 \times 10^{-3}$ M KBr

TABLE XXX : DISC POTENTIAL DURING CATALYTIC RUNS AT 25°C.

Disc rotating at 400 r.p.m. throughout in 500ml. solution.
Potentials expressed with respect to the saturated calomel
electrode.

| Background electrolyte | $10^5 c_0$, M | $E_1$, mV | $E_2$, mV | $E_1-E_2$, mV | $-dE/dt$, mV hr$^{-1}$ |
|---|---|---|---|---|---|
| A | 0.895 | 563.0 | 590.8 | 27.8 | 15.7 |
| $10^{-2}$M HClO$_4$ | 2.35 | 573.5 | 609.2 | 35.6 | 4.8 |
| | 3.22 | 550.0 | 608.3 | 58.3 | 14.4 |
| | 4.82 | 609.8 | 664.2 | 54.4 | 3.5 |
| | 6.89 | 581.2 | 677.7 | 96.6 | 2.0 |
| | 9.77 | 574.0 | 687.6 | 113.5 | 3.4 |
| | 14.4 | 590.0 | 676.6 | 86.6 | 4.4 |
| | 14.5 | 568.0 | 678.4 | 110.5 | 1.7 |
| B | 5.05 | 563.3 | 581.3 | 18.0 | 2.7 |
| $10^{-2}$M HClO$_4$ | 9.98 | 562.2 | 597.6 | 35.5 | 3.3 |
| plus $10^{-3}$M | 10.1 | 572.0 | 619.5 | 47.5 | 5.0 |
| [Co(NH$_3$)$_5$H$_2$O](ClO$_4$)$_3$ | 15.1 | 563.3 | 624.0 | 57.7 | ~0 |
| C | 1.01 | 404.2 | 525.0 | 125.8 | 22.1 |
| $10^{-2}$M HClO$_4$ | 5.80 | 484.0 | 701.8 | 217.8 | 3.4 |
| plus | 14.6 | 449.0 | 704.2 | 255.1 | ~0 |
| 1.012x$10^{-3}$M KBr | 14.8 | 434.5 | 672.2 | 236.6 | 1.3 |
| D | 1.09 | 440.0 | 645.6 | 205.5 | 3.7 |
| $10^{-2}$M HClO$_4$ | 4.79 | 438.0 | 681.2 | 243.3 | ? |
| plus | 9.83 | 442.8 | 688.1 | 253.2 | 3.0 |
| 2.024x$10^{-3}$M KBr | 14.8 | 438.5 | 700.0 | 261.5 | 5.5 |

FIGURE XL: $(E_2-E_1)$ = POTENTIAL RISE ON ADDITION OF
REACTANT

$E_2$ = HIGHEST POTENTIAL REACHED ON

ADDITION OF REACTANT

(Data from Table XXX)
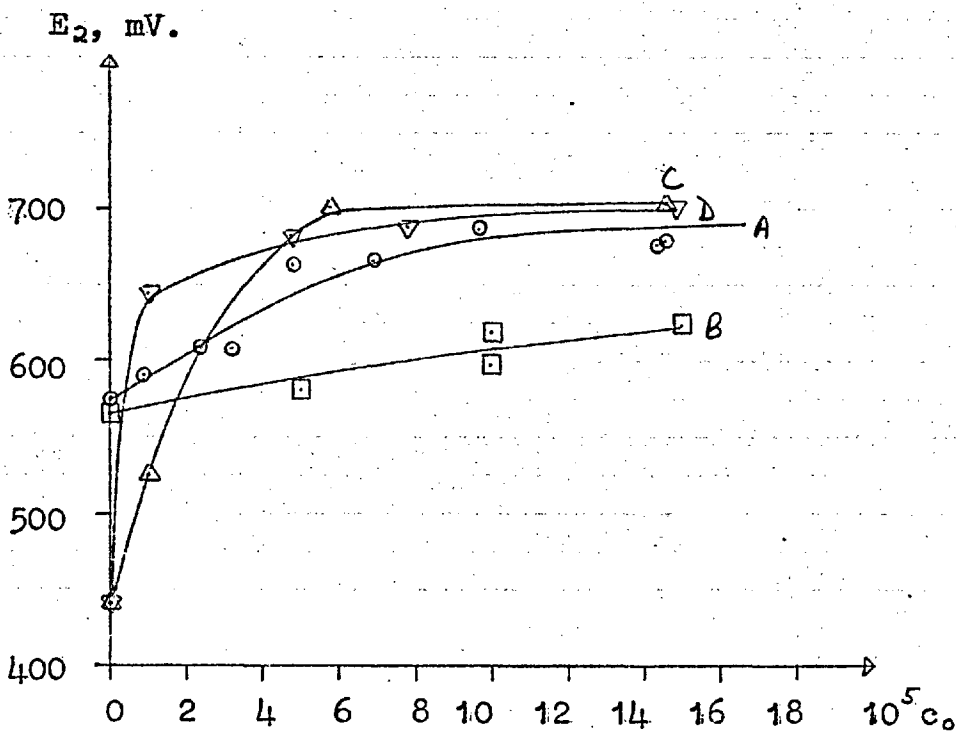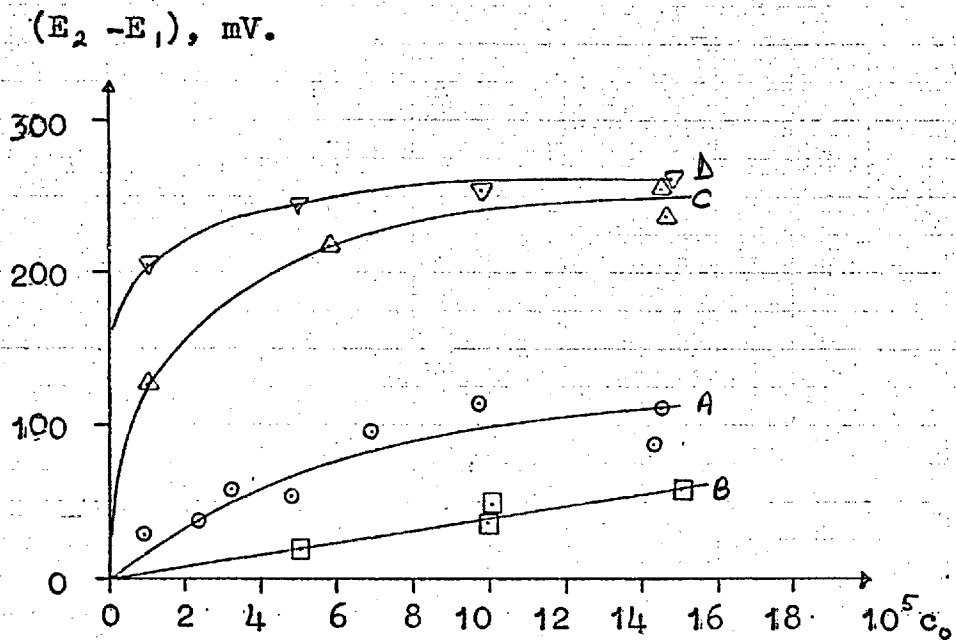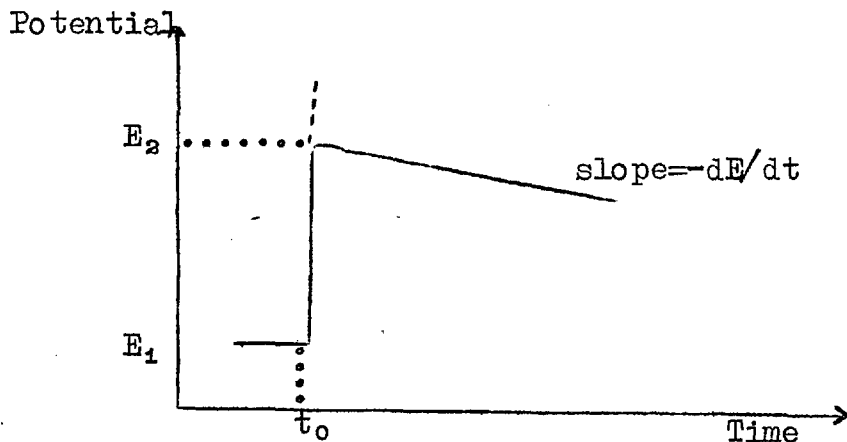
$(E_1-E_2)$ and $E_2$ are plotted as functions of $c_0$ (in this case, $c_0$ is more appropriate than $\bar{c}$) in Figure XL, on page 216.

Several points may be made from Table XXX and Figure XL:

i) Before addition of the reactant, the mean disc potential in the presence of various background electrolytes was

| | | |
|---|---|---|
| A | $575 \pm 25$mV | (vs. SCE) |
| B | $565 \pm 7$mV | " |
| C | $440 \pm 40$mV | " |
| D | $440 \pm 2$mV | " |

The potential is bound to be susceptible to stray impurities, etc. as there were no couples in these solutions to exert a poising effect. Potassium bromide caused quite a marked fall in potential, no doubt because bromide ions are electrocapillary-

active. $10^{-3}$M $[Co(NH_3)_5H_2O](ClO_4)_3$ also caused
a slight, but significant, drop in potential.

ii) The rates of potential drop during each run were
scattered, not surprisingly, as they were small, and
the potential profile was by no means always so
regular in outline as shown on page 217. The trend,
for system A at least, was for the potential drop to
be smaller, the greater the value of $c_0$. Inspection
of lines B, C and D, Figure XL (2), shows that the
small concentration of product ions produced in each
run was unlikely to be the whole cause of the potential
drop: the curvature of line A of this Figure suggests
that the decrease in the concentration of $[Co(NH_3)_5Br]^{2+}$
during the run was the major factor.

iii) $10^{-3}$M $[Co(NH_3)_5H_2O]$ $(ClO_4)_3$ lowered both the initial
potential, $E_1$, of the disc, and the potential rise,
$(E_2-E_1)$, so that $E_2$ was significantly less for system
B than for A, C or D. Why a tripositive ion should
have this effect is not known, but it was concluded
from the experiment described in the next section that
this lowering of the disc potential was the cause of
the increase in $k_{het}$ in system B.

iv) Although $1 \times 10^{-3}$ and $2 \times 10^{-3}$M KBr caused $E_1$ to be
lowered, the value of $E_2$ was much the same whether
bromide was there or not, above $c_0 = 4 \times 10^{-5}$M. Below
this value of $c_0$, $E_2$ was lower in the presence than

in the absence of bromide, and the effect of bromide
on $k_{het}$ (see Figure XXXVII) was more pronounced.

Two extreme cases may be postulated: either
$[Co(NH_3)_5Br]^{2+}$ on addition displaced $Br^-$ from the surface,
or it displaced none, being present on different sites
or maybe in the outer Helmholtz layer. Determination
of $k_s$ and $\sigma$ for $[Co(NH_3)_5Br]^{2+}$ as a function of added
bromide should in principle distinguish between these
two models, but in the latter case, it is difficult to
see why $E_2$ at higher $c_0$ values should be the same in
the absence or presence of bromide. It is concluded that,
at higher $c_0$, $[Co(NH_3)_5Br]^{2+}$ displaced essentially all
of the bromide initially adsorbed on the disc, but, at
lower $c_0$, only part of the bromide was displaced. The
disc potential was lower because of this, and $k_{het}$ was
greater.

X.7.2:  Catalytic experiment at controlled disc potential.

This run was carried out to test the hypothesis of
Section (X.7.1:), that lowering the disc potential caused
$k_{het}$ to increase. The disc was maintained at a potential
higher or lower than its equilibrium potential by passing
a small anodic or cathodic current during the run.
Preliminary experiments showed that the current (of the
order of $10^{-5}A$) required to maintain the disc at a poten-

tial displaced by a given amount from its equilibrium potential was the same in the presence and absence of $[Co(NH_3)_5Br]Br_2$. It was concluded that $[Co(NH_3)_5Br]^{2+}$ was not involved in the electrode process at the disc.

The apparatus used in this run is illustrated in Figure XLI. The disc was pretreated as described in Section (X.2) and the run was started normally (i.e. no current was passed). Once the rate at the equilibrium potential was established, the current-carrying circuit was closed and the potential maintained first above, and then below, the open circuit potential. The disappearance of $[Co(NH_3)_5Br]^{2+}$ was followed as usual. The result is shown graphically in Figure XLII. The rate of the heterogeneous reaction was clearly retarded by anodic polarisation of the disc, and accelerated by cathodic polarisation, as concluded from catalysis in the presence of $Br^-$ and $[Co(NH_3)_5H_2O]^{3+}$.

X.7.3: Significance of the surface potential.

The catalytic aquation of $[Co(NH_3)_5Br]^{2+}$ is accelerated by lowering the potential of the platinum catalyst. This may be due both to an increase in the adsorption of the cation (146,153) and to an increase in $k_s$, i.e. to a decrease in the free energy of adsorption and reaction. The platinum potential is affected by sorbed ions, so

# FIGURE XLI: ROTATING DISC APPARATUS

## EXPERIMENT AT CONTROLLED DISC POTENTIAL

(See also Fig. XV , p.137)
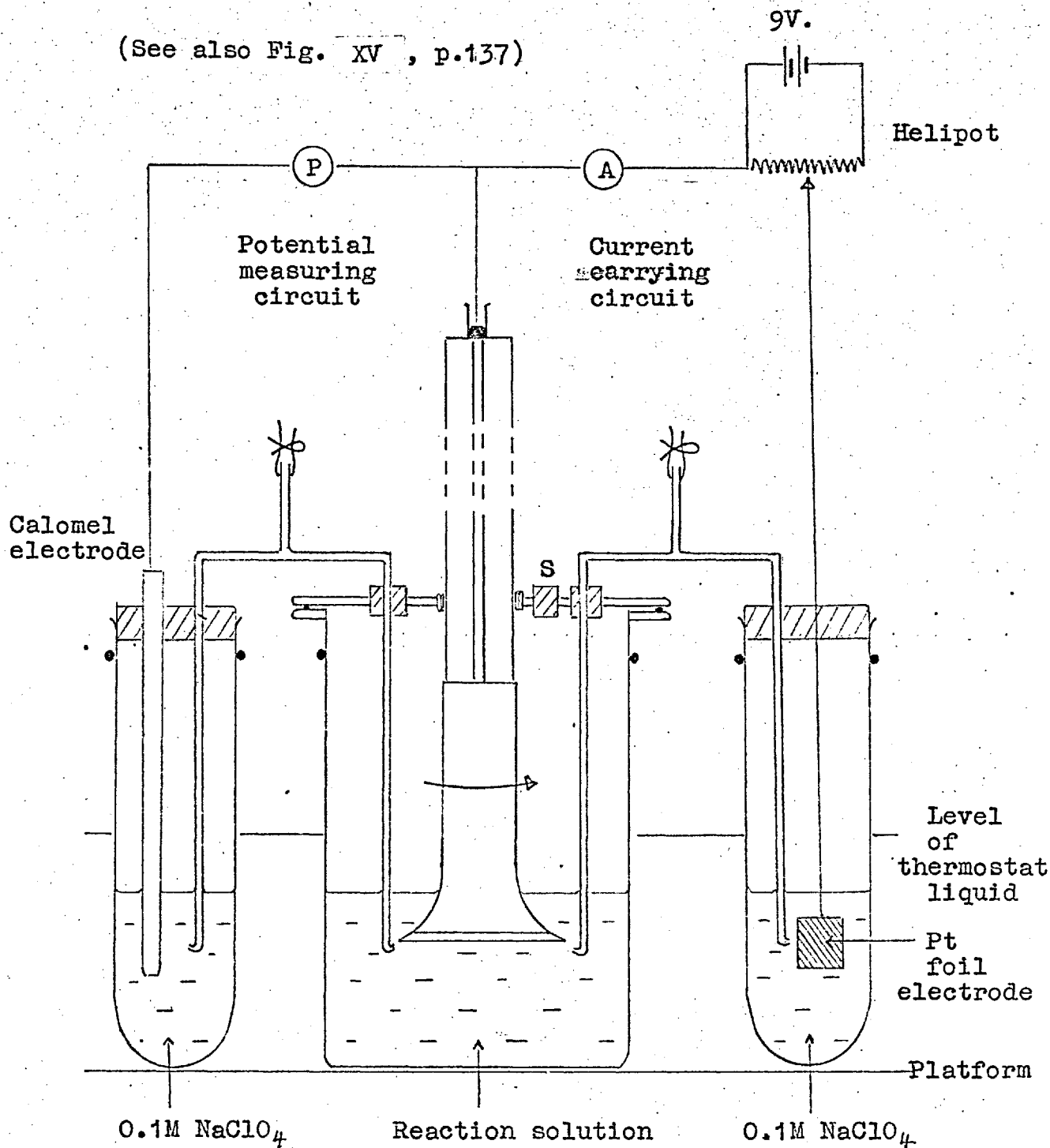


Both salt bridges contain 0.1M NaClO$_4$ in agar gel

# FIGURE XLII: CATALYTIC RUN AT CONTROLLED DISC POTENTIAL
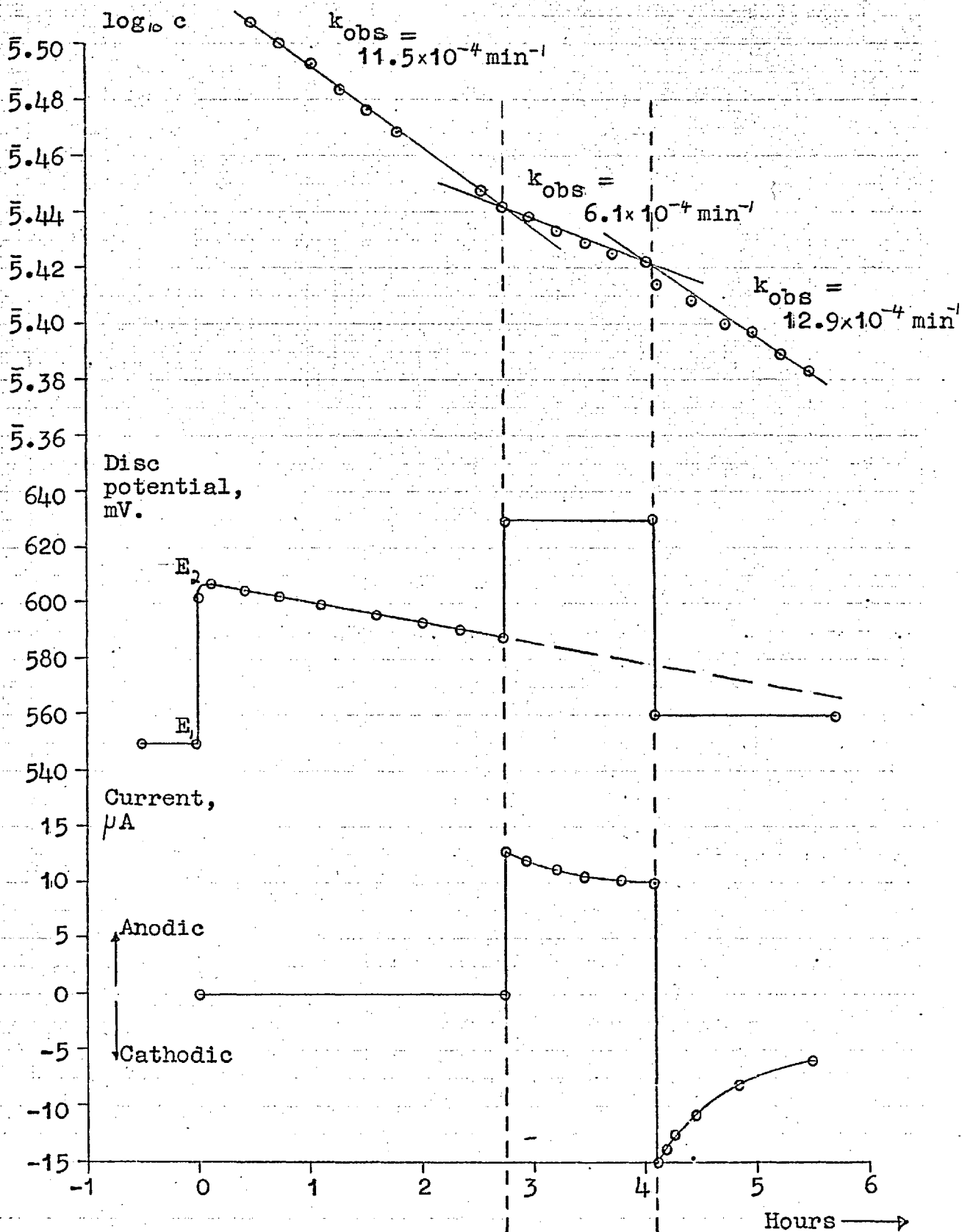
the structure of the ionic double layer, the catalyst potential, $k_s$ and $\sigma$ are all interdependent, and dependent on the bulk ion concentrations. It was not possible to separate these effects with the platinum disc. However, if a platinum catalyst of larger surface area were used, the dependence of $\sigma$ on potential for stable divalent ions similar to $[Co(NH_3)_5Br]^{2+}$ could be determined.

The surface potential of the non-conducting catalysts HgS and AgBr must be very restricted in range by the lack of mobile electrons in the solid, so sorbed ions simply reduce the effective surface area of the catalyst without greatly affecting the free energy of the catalytic process. Consequently the behaviour of conducting and non-conducting catalysts is rather different.

X.8.  Comparison of catalysis by HgS, AgBr and Pt of
the aquation of $[Co(NH_3)_5Br]^{2+}$.

The values of $\sigma$ and $k_s$ for these three catalysts
at 25°C are:

| | $\sigma, M^{-1}$ | $k_s, min^{-1}$ |
|---|---|---|
| HgS | $2.3 \times 10^4$ | $3.0 \times 10^{-3}$ |
| AgBr in dark | $1.7 \times 10^5$ | $3.8 \times 10^{-3}$ |
| "    " light | $1.5 \times 10^5$ | $2.3 \times 10^{-2}$ |
| Pt | $5.8 \times 10^4$ | $1.05$ |

The high value of $k_s$, and the important role of
the surface potential, differentiate platinum from the
other catalysts.  The catalytic mechanism in this case
is possibly temporary electron transfer from metal to
complexed bromide, which assists heterolytic fission.
Such temporary transfer also occurs in many other compounds,
and is responsible for charge-transfer spectra.  Movement
of charge across oxidised platinum surfaces is hindered
and hence platinum when anodically polarised is a less
active catalyst than when cathodically polarised.

X.9.   Future work with a platinum catalyst.


As the catalytic aquation is surface, not diffusion,
controlled, there is small advantage in using a platinum
disc.  Use of a platinised platinum catalyst which is
fixed in the reaction vessel while stirring is effected
by some other means would be advantageous.  The specific
surface area of platinised platinum is a factor of
$10^2$-$10^4$ greater than that of smooth platinum (154).
The catalytic aquation could therefore be followed at
much higher concentrations, with consequent easier
identification of products.  It might be advisable to
conduct future experiments in the dark.  The effect of
the catalyst pretreatment and potential on the catalytic
reaction merits further attention, and the heat of
activation of the heterogeneous reaction should be
determined.  A comparative study of $[Co(NH_3)_5Cl]^{2+}$ under
similar conditions might be rewarding.

# CHAPTER XI : THE REDUCTION OF $[Co(NH_3)_5Br]^{2+}$ AND $[Co(NH_3)_5Cl]^{2+}$ BY SILVER.

The discovery that solid silver reduced $[Co(NH_3)_5X]^{2+}$ to $Co^{2+}$:

$$[Co(NH_3)_5X]^{2+} + Ag^0 \rightarrow Co^{2+} + 5NH_3 + AgX \qquad (11.1)$$
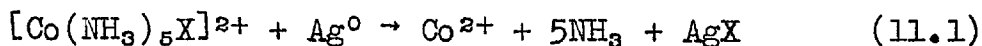
was mentioned in Chapter VI. As two silver rotating discs were available, it was decided that this redox reaction should be investigated.

Experiments were carried out at 25°C and 0°C. Reaction with a clean silver surface was diffusion-controlled, but the rate decreased as the thickness of the silver halide deposit on the disc increased. The heat of activation of the redox reaction was small, as expected for a diffusion-controlled process.

## XI.1. The silver rotating discs.

The silver discs used in these experiments are illustrated in Figure XLIII, on page 227. The silver used in both discs was chemically pure (99.98% +, obtained from Johnson Matthey).

Disc 1 consisted of a thick silver lamina soldered onto a brass former. The sides of the silver disc and the former were protected by two coats of Araldite clear

# FIGURE XLIII: THE SILVER ROTATING DISCS



DISC 1

(For diagram
of complete
rig, see
Fig. XV,
p.137)

— rotating shaft

— nylon retaining
   screws

— insulating sleeve

— brass former

— screw-in electrical
  connection to disc
  surface

— silver

←4cm→

DISC 2

— electrical
  connection

— stainless
  steel
  former

— Teflon

— silver

←3.9cm→
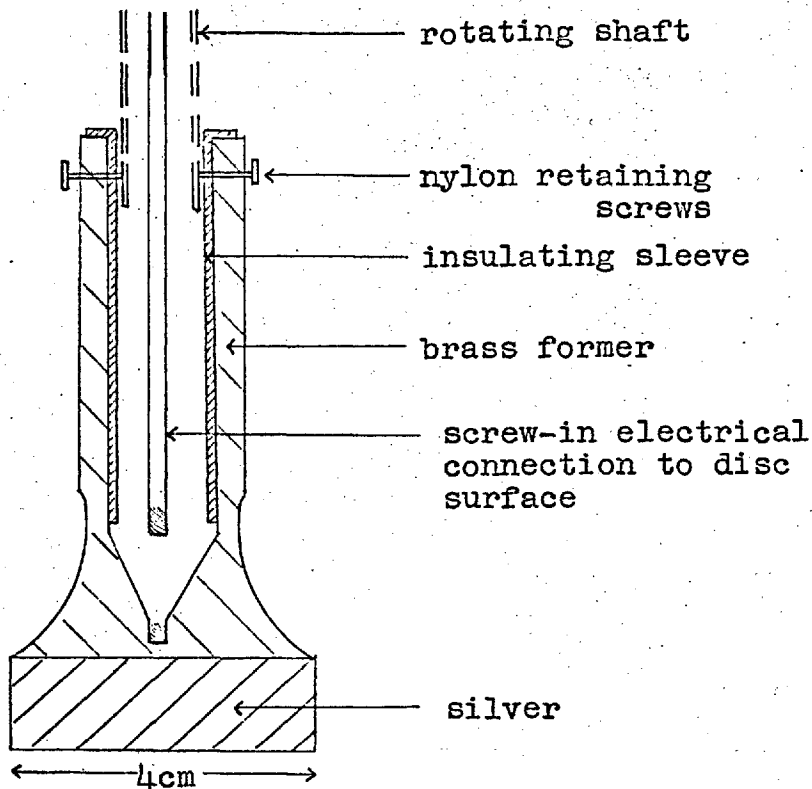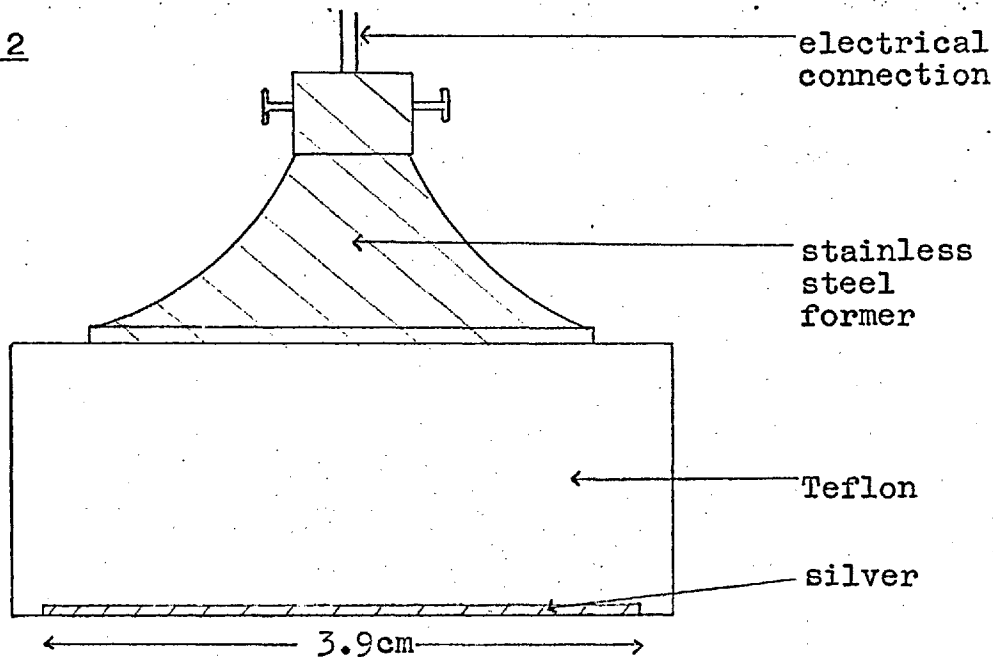
lacquer AR 1501. The active surface area of this disc was 12.57cm².

The former of disc 2 was made of Teflon, into which a thin silver lamina was forced by heating. The active surface area was 47.8cm².

Experiments with disc 1 were carried out in a Quickfit FV1L reaction vessel, of diameter 10.5cm. Those with disc 2 were carried out either in an FV2L vessel (d = 12.5cm.) or a round-bottomed vessel (Quickfit Q-FR 2LF, d = 15.0cm.).

The complete rotating disc rig is illustrated in Figure XV, on page 137.

Silver atoms in the solid metal are closely packed in a face-centred cubic crystal structure. The inter-atomic distance is 2.88$\overset{o}{A}$ (155). Each surface atom therefore occupies an area of 7.74$\overset{o}{A}$², so there are 2.16x10⁻⁹ moles of silver per sq.cm. of surface.

Silver is stable in non-oxidising, non-complexing aqueous solutions at all pH values (148).


XI.2. Experimental procedure.


The silver discs, when not in use, were allowed to stand in 10⁻²M HClO₄. Before each run, the disc to be used was rinsed in distilled water and attached to the rotating shaft, the reaction vessel and lid were clamped

into place, and the empty apparatus was lowered into
the thermostat. At time $t_0$, a small weighed quantity
of $[Co(NH_3)_5X]X_2$ was dissolved in a known volume of
background electrolyte previously equilibrated in the
thermostat. The solution was poured quickly into the
reaction vessel, and the disc started.

The disappearance of $[Co(NH_3)_5X]^{2+}$ was followed
spectrophotometrically by periodic removal of aliquots
of ca. 3ml. The reactions were followed for 2-3 hours
to 70-80% completion. In some runs, the appearance of
$Co^{2+}$ was similarly followed by diluting 2ml. aliquots
with 8ml. concentrated HCl and measuring D at 690m$\mu$
(see Section V.6). Because of sampling the ratio of the
surface area of silver to the volume of solution
increased during all runs, and sampling corrections, as
explained in Section (X.4), were applied to results where
indicated.

During runs, the silver surface became coated with
a layer of silver halide, producing a slight and uneven
discoloration at low $c_0$ and a uniform dark grey completely
coherent deposit at higher $c_0$. During one series of runs,
this deposit was allowed to build up, to test its
inhibiting effect on the redox reaction, but otherwise
the discs were cleaned before every run by abrasion with
finest grade emery paper and washing in ether, alcohol
and water.

Nearly all the deposit could be removed from the discs electrolytically by passing a cathodic current of ca.1 mA for a few hours ($AgX + e^- \rightarrow Ag + X^-$). $10^{-2}M$ $HClO_4$ was used as electrolyte, and the anode was a platinum wire. The halide in solution was then readily estimated volumetrically or gravimetrically with $Ag^+$. However, even after prolonged electrolysis, the discs always appeared faintly discoloured, some AgX seeming "trapped" under the silver surface. Abrasion was therefore necessary to produce a completely clean surface.

The redox reaction was found to be accurately first order in $[Co(NH_3)_5X]^{2+}$. The aquation product, $[Co(NH_3)_5H_2O]^{3+}$, was found to be unaffected by silver, and $k_{het}$, the first order rate constant for the reduction of $[Co(NH_3)_5X]^{2+}$, was therefore calculated from the observed first order rate constant, $k_{obs}$, by subtracting $k_1$, which was always small compared with $k_{obs}$. (Co(II) concentrations of $5 \times 10^{-4}M$ and $1 \times 10^{-3}M$ were found to have no effect on $k_1$). On removing the disc from a reacting solution, $k_{obs}$ immediately fell to the value of $k_1$.

XI.3. Calculation of the rate of a diffusion-controlled reaction at the silver discs at 25°C.

This calculation requires knowledge of the diffusion coefficients of the reactant ions. These do not appear to have been directly measured, but they are readily

calculated from the Nernst equation for tracer diffusion,

$$D_i = RT\lambda_i / |z|F^2 \tag{11.2}$$

The equivalent conductivities at 25°C are $51.5 cm^2 ohm^{-1}$ for $[Co(NH_3)_5Br]^{2+}$ and $54.4 cm^2 ohm^{-1}$ for $[Co(NH_3)_5Cl]^{2+}$ (101), and the diffusion coefficients at 25°C are calculated to be $6.85 \times 10^{-6} cm^2 sec^{-1}$ for $[Co(NH_3)_5Br]^{2+}$ and $7.24 \times 10^{-6} cm^2 sec^{-1}$ for $[Co(NH_3)_5Cl]^{2+}$.

The theory of the rotating disc was outlined in Section (VII.7). The maximum flux of species i to the disc surface is given by

$$-\frac{dN_i}{dt} = -V \frac{dc_i}{dt} = 10^{-3} D_i A c_i / \delta \tag{7.32}$$

The first order rate constant for the heterogeneous reaction is therefore given by

$$k_{het} = 10^{-3} D_i A / V\delta \tag{11.3}$$

The value of $\delta$ can be calculated from equation (7.31), taking the kinematic viscosity of water at 25°C as $8.929 \times 10^{-3}$ poise ml. $g^{-1}$, to be

$$\delta = 1.43 \times 10^{-2} \omega^{-\frac{1}{2}} cm. \text{ for } [Co(NH_3)_5Br]^{2+}$$

$$\delta = 1.46 \times 10^{-2} \omega^{-\frac{1}{2}} cm. \text{ for } [Co(NH_3)_5Cl]^{2+},$$

where $\omega$ radians $sec^{-1}$ is the speed of rotation of the disc.

Substituting for $\delta$ in equation (11.3),

$$k_{het} = 4.79 \times 10^{-7} \, A \, \omega^{\frac{1}{2}}/V \, sec^{-1} \quad \text{for } [Co(NH_3)_5Br]^{2+} \quad (11.4)$$

$$k_{het} = 4.96 \times 10^{-7} \, A \, \omega^{\frac{1}{2}}/V \, sec^{-1} \quad \text{for } [Co(NH_3)_5Cl]^{2+} \quad (11.5),$$

both equations referring to a temperature of 25°C.

# RESULTS

XI.4. Stoichiometry of the redox reaction.

The stoichiometry of the redox reaction was verified by a run at 25°C with disc 2. Both the disappearance of $[Co(NH_3)_5Cl]^{2+}$ and the appearance of $Co^{2+}$ were followed spectrophotometrically, and the silver chloride deposited on the disc was estimated at the end of the run. The particulars of the run and the results are given in Figure XLIV, on page 234. The reaction was first order in $[Co(NH_3)_5Cl]^{2+}$, and the amount of $Co^{2+}$ produced was within experimental error, equal to the amount of $[Co(NH_3)_5Cl]^{2+}$ consumed, as shown in Table XXXI.

At time 5 hrs. 48 mins. a final reading of c, the concentration of $[Co(NH_3)_5Cl]^{2+}$ was taken, and the disc removed from solution. To remove the silver chloride deposit, a cathodic current of 0.65mA was passed for 18 hours while the disc was rotated slowly in 50ml. $10^{-2}$M $HClO_4$. At the end of this time the disc was rinsed and the solution and rinsings made up to 100ml. Aliquots of this solution were neutralised with $CaCO_3$ and titrated against $10^{-2}$M $AgNO_3$, using dichloro-fluorescein as indicator. There were $2.804 \times 10^{-4}$ moles of chloride in the solution, which came from the disc.

# FIGURE XLIV: STOICHIOMETRY OF THE REACTION

$$[Co\,(NH_3)_5Cl]^{2+} + Ag \longrightarrow AgCl + Co^{2+} + 5NH_3 \text{ at } 25°C$$



Concentration × $10^4$          $\log_{10} c$

$k_{obs} = 163.0 \times 10^{-4} \text{ min}^{-1}$

Time in hours from $t_o \longrightarrow$
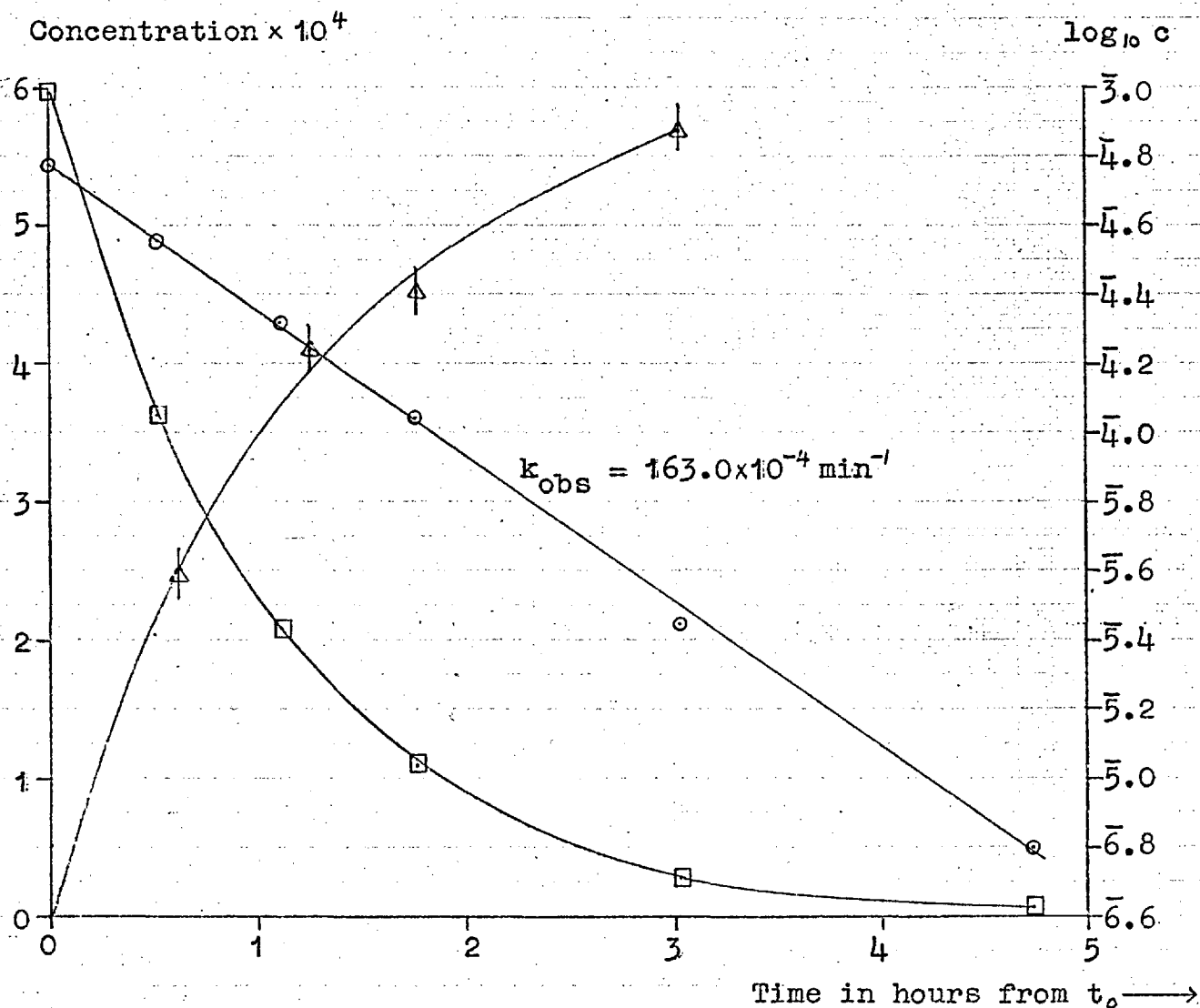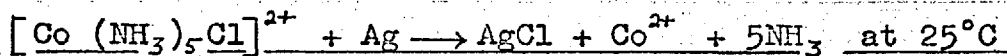
☐   Concentration of $[Co(NH_3)_5Cl]^{2+}$ ( = c)

△   Concentration of $Co^{2+}$

⊙   $\log_{10} c$

Disc speed = 400 r.p.m.   (Disc 2 used)

V = 0.5 litre

Background electrolyte = $10^{-2}$ M $HClO_4$

TABLE XXXI : STOICHIOMETRY OF THE REDOX REACTION.

| Time (mins) | Conc. of $[Co(NH_3)_5Cl]^{2+}$ x$10^4$ | Conc. of $Co^{2+}$ x$10^4$ | $10^4\Sigma c$ |
|---|---|---|---|
| 0 | 5.97 | 0 | 5.97 |
| 35 | 3.40 | 2.42±0.2 | 5.82±0.2 |
| 70 | 1.99 | 3.80±0.2 | 5.79±0.2 |
| 106 | 1.10 | 4.53±0.2 | 5.63±0.2 |
| 182 | 0.28 | 5.70±0.2 | 5.90±0.2 |

At the end of the run, c was found to be $0.179 \times 10^{-5}$M. At the start of the run, $c_0$ was $59.65 \times 10^{-5}$M.

If $[Co(NH_3)_5Cl]^{2+}$ is converted to $Co^{2+}$ and $[Co(NH_3)_5H_2O]^{3+}$ in the ratio $k_{het}/k_1$ (=162:1), then at the end of the run, $[Co^{2+}]$ should be $5.91 \times 10^{-4}$M and $[Co(NH_3)_5H_2O]^{3+}$ should be $0.04 \times 10^{-4}$M. The amount of chloride deposited on the disc should be equal to the amount of $Co^{2+}$ produced. The solution volume at the start of the run was 500ml. and at the end, due to the removal of samples, it was ca. 460ml. It was calculated that $(2.90 \pm 0.05) \times 10^{-4}$ moles of silver chloride should be formed on the disc. In fact, $2.80_4 \times 10^{-4}$ moles were formed, so the stoichiometry of reaction (11.1) was considered to be verified.

XI.5.   Reduction on a clean silver surface at 25°C.


A series of runs at 400 r.p.m. with disc 1, which
was cleaned before each run, is summarised in Table
XXXII.   The uncertainty in each value of $k_{het}$ is only
±0.5%.   It is seen that the scatter between runs is
appreciably greater than this, possibly because the
effective surface area of the disc varied slightly from
run to run.   The "uncorrected" values of $k_{het}$ were
calculated simply as $(k_{obs} - k_1)$, the "corrected" values,
which take account of the solution removed in sampling,
were calculated as explained in Section (X.4).   As for
the platinum disc, the correction plots were scattered,
and correction sometimes increased the value of $k_{het}$,
and sometimes decreased it.   Further discussion will
therefore be confined to the "uncorrected" values.

Within the limits of experimental error, $k_{het}$ for
the reduction of $[Co(NH_3)_5Cl]^{2+}$ was independent of pH
in the range 1-4 and of added chloride up to $10^{-2}M$:
the mean value of $k_{het}$ for $V = 0.5$ l. and disc speed =
400 r.p.m. was $(48.5 \pm 2) \times 10^{-4}$ min$^{-1}$.   The value calculated
from equation (11.5), substituting $A = 12.57$cm$^2$ and
$\omega = 45.48$ radians sec$^{-1}$, is $48.4 \times 10^{-4}$ min$^{-1}$, so the
actual rate is in excellent agreement with the diffusion-
controlled value, calculated from the Levich theory.

# TABLE XXXII : REDUCTION OF $[Co(NH_3)_5X]^{2+}$ BY DISC 1

## AT 25°C.

$c_0 = (5.5 \pm 0.1) \times 10^{-5}M$ in all these runs.

| Reactant | Disc speed (r.p.m.) | Volume V(litres) | Background electrolyte | $10^4 k_{het}$ uncorr. | $min^{-1}$ corr. |
|---|---|---|---|---|---|
| $[Co(NH_3)_5Cl]Cl_2$ | 400 | 0.500 | $10^{-1}M$ $HClO_4$ | 48.2 | |
| | " | " | $10^{-2}M$ " | 49.9 | 49.8 |
| | " | " | $10^{-3}M$ " | 46.0 | 44.5 |
| | " | " | $10^{-4}M$ " | 47.6 | |
| | 400 | 0.500 | $10^{-2}M$ $HClO_4$+ $10^{-3}M$ KCl | 50.7 | 48.8 |
| | " | " | $10^{-2}M$ $HClO_4$+ $10^{-2}M$ KCl | 48.3 | |
| | 400 | 1.000 | $10^{-2}M$ $HClO_4$ | 22.2 | |
| | " | 0.250 | " | 102.2 | 105.0 |
| $[Co(NH_3)_5Br]Br_2$ | 400 | 0.500 | $10^{-2}M$ $HClO_4$ | 48.6 | 51.0 |
| | 200 | " | " | 37.0 | 39.8 |

The agreement for $[Co(NH_3)_5Br]^{2+}$ is not quite so good. The values of $k_{het}$ calculated from equation (11.4) at 400 and 200 r.p.m. are $46.8 \times 10^{-4}$ $min^{-1}$, and $33.3 \times 10^{-4}$ $min^{-1}$ respectively, whereas the experimental values were $48.6 \times 10^{-4}$ $min^{-1}$ and $37.0 \times 10^{-4}$ $min^{-1}$.

As required by equation (11.4), the value of $k_{het}$ was inversely proportional to V, other factors being equal.

A few runs, summarised in Table XXXIII, were carried out at $25°C$ with $[Co(NH_3)_5X]X_2$ and silver disc 2, of surface area $47.8 cm^2$. It is seen that the values of $k_{het}$ calculated from equations (11.4) and (11.5) are in some cases appreciably different from the experimental values, calculated as $(k_{obs} - k_1)$. This is thought to be due to the difficulty of producing a uniformly smooth, clean surface on such a large disc. No systematic study of the dependence of $k_{het}$ on $c_0$ was undertaken: it was assumed that $k_{het}$ would be independent of $c_0$ until the AgX deposited on the disc during the run was sufficient to impair the progress of the reaction; this is evidently somewhere between $c_0 = 5 \times 10^{-5}$ and $60 \times 10^{-5} M$ for $[Co(NH_3)_5Cl]^{2+}$.

TABLE XXXIII : REDUCTION OF $[Co(NH_3)_5X]^{2+}$ BY DISC 2

AT $25^{\circ}C$.

Background electrolyte = $10^{-2}M$ $HClO_4$ in all these runs.

| Reactant | Disc speed (r.p.m.) | Volume V(litres) | $10^5c_0$,M | $10^4k_{het}$,min$^{-1}$ | |
|---|---|---|---|---|---|
| | | | | exp. | calc |
| $[Co(NH_3)_5Br]Br_2$ | 100 | 1.000 | 6.98 | 34.2 | 41.2 |
| | 200 | " | 3.38 | 45.4 | 62.7 |
| | 400 | " | 4.82 | 79.6 | 82.3 |
| $[Co(NH_3)_5Cl]Cl_2$ | 400 | 0.500 | 59.65 | 162.0 | 184.0 |
| | " | " | 5.54 | 189.8 | 184.0 |

XI.6. Reduction on a clean silver surface at $0^{\circ}C$.

Two runs with disc 1, freshly cleaned before each run, were carried out at $0^{\circ}C$, to determine the heat of activation of the redox reactions. The runs were, as at $25^{\circ}C$, first order in $[Co(NH_3)_5X]^{2+}$, and the results are summarised in Table XXXIV on page 240.

The experimental values of $k_{het}$ at $0^{\circ}C$ were calculated as $(k_{obs}-k_1)$: $k_1$ values at $0^{\circ}C$ were calculated to be $9.6 \times 10^{-6}$ min$^{-1}$ for $[Co(NH_3)_5Br]^{2+}$ and $2.6 \times 10^{-6}$ min$^{-1}$ for $[Co(NH_3)_5Cl]^{2+}$, from the values at $25^{\circ}C$ and the heat of

TABLE XXXIV : All rate constants refer to reduction by
silver disc 1, V = 0.5 l., background
electrolyte = $10^{-2}M$ $HClO_4$, disc speed =
400 r.p.m.

|  | $[Co(NH_3)_5Cl]^{2+}$ | $[Co(NH_3)_5Br]^{2+}$ |
|---|---|---|
| $k_{obs}$ at 0°C | $27.9 \times 10^{-4} min^{-1}$ | $28.4 \times 10^{-4} min^{-1}$ |
| $k_{het}$ at 0°C | 27.9  "  " | 28.3  "  " |
| $k_{het}$ at 25°C (from Table XXXII:mean values) | 48.6  "  " | 48.5  "  " |
| $\Delta H_a$ | 3.59 kcal. mole$^{-1}$. | 3.48 kcal. mole$^{-1}$. |
| Theoretical estimate of $k_{het}$ at 0°C. | $25.8 \times 10^{-4} min^{-1}$ | $24.9 \times 10^{-4} min^{-1}$ |

activation of the aquation reactions (see Table XI, page 75).
The heat of activation, $\Delta H_a$, of the redox reaction was
calculated from $k_{het}$ at 25°C and 0°C by the Arrhenius
equation. For both complexes, the value is low (~3.5 kcal.
mole$^{-1}$), which is characteristic of a diffusion-controlled
reaction.

The final entry in Table XXXIV is a rough estimate
from the Levich theory of $k_{het}$ at 0°C. The value of
$k_{het}$ is equal to $(10^{-3}D_i A/V\delta)$, from equation (11.3). The

terms $D_i$ and $\delta$ are temperature-dependent, and their values at 0°C were calculated by assuming Walden's Rule, which states $\lambda_i \eta_0$ = constant, where $\eta_0$ = solvent viscosity. The equivalent conductivities of $[Co(NH_3)_5Cl]^{2+}$ and $[Co(NH_3)_5Br]^{2+}$ at 0°C in water are calculated from Walden's Rule to be 27.1 and 25.7 cm² ohm⁻¹ respectively, so the diffusion coefficients are $3.31 \times 10^{-6}$ and $3.13 \times 10^{-6}$ cm² sec⁻¹ respectively, from equation (11.2). Substituting these values into equations (7.31) and (11.3), and taking the kinematic viscosity of water at 0°C to be $1.789 \times 10^{-2}$ poise ml. g⁻¹, the values of $k_{het}$ given in Table XXXIII were calculated. In view of the approximations involved in the calculation, the agreement with the experimental values is good.

XI.7. Reduction on a silver-silver halide surface at 25°C.

A series of runs, summarised in Table XXXV, on page 242, was carried out at 25°C with $[Co(NH_3)_5Cl]Cl_2$ and disc 1, to investigate the inhibiting effect of a deposit of silver chloride on the redox reaction. The silver disc was cleaned before run 1, but thereafter, the ever-thickening layer of AgCl was untouched. The disc was allowed to stand in $10^{-2}M$ $HClO_4$ between runs. The AgCl on the disc was assumed to have a negligible catalytic effect on the aquation reaction.

TABLE XXXV : REDUCTION OF $[Co(NH_3)_5Cl]^{2+}$ AT SILVER DISC 1,

ALLOWING AgCl DEPOSIT TO BUILD UP ON DISC.

In all these runs,     $V = 0.5$ litre

background electrolyte   $= 10^{-2}M$ $HClO_4$

temperature   $= 25^{\circ}C$.

$k_{het}$ values are calculated from equation (11.5), and determined experimentally as $(k_{obs} - k_1)$, from 1st order plots.

| Run No. | Disc speed (r.p.m.) | $10^5 c_0, M$ | $10^4 k_{het}, min^{-1}$ experimental | calc. | Moles AgCl formed x$10^5$ | Comments. |
|---|---|---|---|---|---|---|
| 1 | 200 | 5.85 | 32.9 | 34.3 | 1.49 | )Reaction )diffusion- )controlled, )within )experimental )error. |
| 2 | 200 | 5.73 | 35.1 | 34.3 | 1.75 | |
| 3 | 400 | 5.76 | 47.7 | 48.4 | 1.37 | |
| 4 | 200 | 2.42 | 34.2 | 34.3 | 0.27 | |
| 5 | 400 | 5.22 | 51.6 | 48.4 | 2.56 | |
| 6 | 400 | 15.35 | 44.5-23.2 | 48.4 | 6.50 | )First order )plots show )upward )curvature, )i.e. $k_{het}$ )decreasing )continuously. |
| 7 | " | 10.16 | 19.0-12.4 | " | 2.12 | |
| 8 | " | 5.68 | 14.8-10.4 | " | 0.76 | |
| 9 | " | 5.85 | 10.3, decr. slightly. | " | 0.41 | |

As seen from Table XXXV, the rate of the redox reaction was equal to the calculated diffusion-controlled rate, to the end of run 5, but the rate thereafter decreased steadily. After run 9, the AgCl deposit was electrolysed off the disc as completely as possible. By volumetric estimation of the chloride solution so produced, it was estimated that $1.18 \times 10^{-4}$ moles of AgCl were formed on the disc during runs 1 - 9. The amount of AgCl that should be formed in each run was calculated from knowledge of $k_{het}$, $k_1$ and the initial and final concentrations of $[Co(NH_3)_5Cl]^{2+}$, as explained in Section (XI.4). Summation of these values, shown in Table XXXIV, gives $7.44 \times 10^{-5}$ moles (runs 1 - 5 incl.) and $1.72 \times 10^{-4}$ moles (runs 1 - 9 incl.). The discrepancy between the experimental and calculated values for the total AgCl deposit possibly indicates that the AgCl deposit did have a significant catalytic effect on the aquation reaction: unfortunately, the formation of $Co^{2+}$ and $[Co(NH_3)_5H_2O]^{3+}$ was not followed during this series of runs. However, it appears that the redox reaction occurs with unimpaired efficiency through a layer of ca. $7.44 \times 10^{-5}$ moles AgCl on disc 1.

The cross sectional surface area of AgCl in the solid is $12\overset{o}{A}{}^2$ per molecule (136). Monolayer coverage of disc 1, of area $12.57 cm^2$, therefore requires ca. $1.75 \times 10^{-8}$ moles, so a diffusion-controlled redox reaction can occur through ca. $4.25 \times 10^3$ monolayers of AgCl. This probably mainly

because AgCl deposited on Ag is rather porous (156).
(In the latter stages of electrolytic deposition of
AgCl on Ag, the electrode reaction occurs beneath a
layer of porous AgCl (157). ).  Moreover, because of
the great number of Schottky (lattice vacancy) defects
at AgCl/Ag interfaces, the conductivity of AgCl is much
enhanced (156):  the redox reaction could therefore be
occurring by electron transfer through a thin layer of
AgCl.


XI.8.  Rate of reduction of $[Co(NH_3)_5X]^{2+}$ by silver,
compared with homogeneous reducing agents.


The present work on silver as a reductant and some
literature data on homogeneous reductants in aqueous
solution, are summarised in Table XXXVI, on page 245.
This Table provides an illustration of the general rule
that the activation energy (or enthalpy) of a reaction,
and not the overall energy change, governs the reaction
rate.  Silver is, thermodynamically, a less powerful
reductant than $Cr^{2+}$, $Eu^{2+}$ or $V^{2+}$.  However, the low
energy of the halide bridged ("inner sphere") activated
complex (see Section (VI.4.1:) ) in the reaction between
$[Co(NH_3)_5X]^{2+}$ and $Cr^{2+}$ and Ag, means that these reactions
are very fast, while the outer sphere reaction with $V^{2+}$
is slow by comparison.  ($Eu^{2+}$ is thought to react by an

inner sphere mechanism, but the lability of $EuX^{2+}$
apparently prevents this reductant from acting as fast
as the thermodynamically similar $Cr^{2+}$).

TABLE XXXVI : REDUCTION OF $[Co(NH_3)_5X]^{2+}$ TO $Co(II)$: ALL VALUES FOR 25°C.

| Oxidant | Reductant | E° of reducing couple (48). | $k_2, M^{-1}sec^{-1}$ | Heat of activation, $k_{cal} \cdot mole^{-1}$ | Mechanism | Reference |
|---|---|---|---|---|---|---|
| $[Co(NH_3)_5Cl]^{2+}$ | $Cr^{2+}$ | $CrCl^{2+}/Cr^{2+}, -0.41V$ | $>2 \times 10^6$ | | Inner sphere. | (124) |
| E° = 0.34V. | $Eu^{2+}$ | $Eu^{3+}/Eu^{2+}, -0.43V.$ | $3.9 \times 10^2$ | 5.0 | " " | " |
| (See Section | Ag | $AgCl/Ag, \quad 0.22V.$ | Diffusion controlled. | 3.6 | " " | Present work. |
| V.6) ). | $V^{2+}$ | $V^{3+}/V^{2+}, \quad -0.25V.$ | ~ 5 | | Outer sphere | (124) |
| | $Fe^{2+}$ | $Fe^{3+}/Fe^{2+}, 0.75V.$ | $1.4 \times 10^{-3}$ | 12.5 | " " | " |
| $[Co(NH_3)_5Br]^{2+}$ | $Cr^{2+}$ | $CrBr^{2+}/Cr^{2+}, -0.40V$ | $>2 \times 10^6$ | | Inner sphere | (124) |
| E° = 0.38V. | $Eu^{2+}$ | | $2.5 \times 10^2$ | 4.7 | " " | " |
| | Ag | $AgBr/Ag, 0.07V.$ | Diffusion controlled. | 3.5 | " " | Present work. |
| | $V^{2+}$ | | ~25 | | Outer sphere. | (124) |
| | $Fe^{2+}$ | | $7.3 \times 10^{-4}$ | 13.3 | " " | " |

# REFERENCES.

1. J.T. Davies in "Advances in Catalysis", Vol. VI, Acad. Press Inc., N.Y., 1954.

2. J.M. Thomas and W.J. Thomas, "Introduction to the Principles of Heterogeneous Catalysis", Academic Press, 1967, Ch. 2.

3. M.T. Beck, (a) Record of Chem. Progress, 27(1), 37(1966). Also (briefer), (b) J. Inorg. Nucl. Chem., 15, 250 (1960).

4. A.B. Ravnö and M. Spiro, J. Chem. Soc.,    (1965).
    (a)  p.97.
    (b)  p.78.

5. G.J. Hoijtink in J.H. de Boer (ed.), "The Mechanism of Heterogeneous Catalysis". (Proc. of Symposium, Amsterdam, 1959), Elsevier, 1960.

6. H. Taube, Chem. Revs., 50, 69 (1952).

7. J. Bjerrum, "Metal Ammine Formation in Aqueous Solution", English edition, P. Haase and Son, Copenhagen, 1957.
    (a)  Ch.11.
    (b)  p.236.
    (c)  p.237.

8. J. Bjerrum and J.P. McReynolds in "Inorganic Syntheses", Vol. II, McGraw-Hill, 1946, Ch.8.

9. R. Schwartz and W. Krönig, Ber. deutsch. Chem. Ges., 56, 208 (1923).

## REFERENCES (contd.)

10. B.E. Douglas and H.E. Swift, Nature, 193, 1173 (1962).

11. W.C. Erdman and B.E. Douglas, J. Inorg. Nucl. Chem., 24, 1355 (1962).

12. J. Bjerrum and S.E. Rasmussen, Acta Chem. Scand., 6, 1265 (1952).

13. B.E. Douglas, J.A.C.S., 76, 1020 (1954).

14. D. Sen and W.C. Fernelius, J. Inorg. Nucl. Chem., 10, 269 (1959).

15. F.P. Dwyer and A.M. Sargeson, Nature, 187, 1022 (1960).

16. J.C. Bailar and J.B. Work, J.A.C.S., 67, 176 (1945).

17. G. Schwarzenbach, Helv. Chim. Acta, 32, 839 (1949).

18. A.B. Lamb and A.T. Larsen, J.A.C.S., 42, 2024 (1920).

19. J.N. Brönsted and R. Livingston, J.A.C.S., 49, 435 (1927).

20. A.V. Ablov and A. Ya. Sychev, Russ. J. Inorg. Chem., 4, 1143 (1959).

21. D.R. Stranks in J. Lewis and R.G. Wilkins, eds., "Modern Coordination Chemistry", Interscience, 1960, p.85.

22. A.A. Vlcek and J. Kuta, Nature, 185, 95 (1960). G.W. Watt and J.W. Vaughn, Nature, 186, 309 (1960).

23. S.M. Jörgensen, Z.pr. Chem., 19, 51 (1873).

24. G.M. Waind, Chem. and Ind., 1388 (1955).

25. I.I. Zhukov and C.P. Shipulina, Kolloid Z., 49, 126 (1929).

# REFERENCES (contd.)

26. R.L. Burwell et al., Inorg. Chem., 4, 1123 (1965).

27. P.S. Walton, Ph.D. thesis, University of London, 1967.

28. J.M. Austin and O.D.E.-S. EL-Khouly, unpublished work.

29. I.M. Kolthoff, Rec. Trav. Chim., 48, 298 (1929).

30. A. Indelli and P.L. Bonora, Annali di Chimica, 57, 616 (1967).

31. T.W. Swaddle and E.L. King, Inorg. Chem., 3, 234 (1964).

32. C.W. Davies and G.G. Thomas, J. Chem. Soc., 1607 (1952).

33. H. Morawetz and E.W. Westhead, J. Polymer Sci., 16, 273 (1955).

34. H. Morawetz and J.A. Schafer, J. Phys. Chem., 67, 1293 (1963).

35. W. Kern, W. Harold and B. Scherlag, Makromol. Chem., 17, 231 (1956).

36. T.J. Painter, J. Chem. Soc., 3932 (1962).

37. C.L. Arcus, T.L. Howard and D.S. South, Chem. Ind., (London) 1756 (1964).

38. I. Sakurada et al, Makromol. Chem., 91, 243 (1966).

39. C.L. Arcus and B.A. Jackson, Chem. Ind. (London), 2022 (1964).

40. B. Vogel and H. Morawetz, J.A.C.S., 90, 1368 (1968).

41. F. Sebba and J.H. Wiggill, J. Colloid Sci., 21, 115 (1966).

42. E.F.J. Duynstee and E. Grunwald, J.A.C.S., 81, 4540, 4542 (1959).

# REFERENCES (contd.)

43. R.P. Bell and J.E. Prue, Trans. Far. Soc., 46, 5 and 14 (1950).

44. P.W. Griffin, Ph.D. thesis, University of London, 1968.

45. D.B. Broughton and R.L. Wentworth, J.A.C.S., 69, 741 (1947).

46. B.A. Zabin and H. Taube, Inorg. Chem., 3, 963 (1964).

47. F.A. Posey and H. Taube, J.A.C.S., 79, 255 (1957).

48. Chemical Society (London) Special Publication No. 17, "Stability Constants", 1964.

49. D.A. Loeliger and H. Taube, Inorg. Chem., 5, 1376 (1966).

50. R.B. Jorden, A.M. Sargeson and H. Taube, Inorg. Chem., 5, 486 (1966).

51. J.H. Espenson and S.R. Hubbard, Inorg. Chem., 5, 686 (1966).

52. P.J. Elving and B. Zemel, J.A.C.S., 79, 5855 (1957).

53. J.H. Espenson and J.P. Birk, Inorg. Chem., 4, 527 (1965).

54. J.H. Espenson and J.P. Birk, Inorg. Chem., 7, 991 (1968).

55. W.C. Waggener et al, J.A.C.S., 81, 2958 (1959).

56. D.L. Gay and G.C. Lalor, J. Chem. Soc. (A), 1179 (1966).

57. D. Dodd and M.D. Johnson, J. Chem. Soc. (A), 34 (1968).

58. K.G. Poulsen, J. Bjerrum and I. Poulsen, Acta Chem. Scand., 8, 921 (1954).

## REFERENCES (contd.)

59. M.L. Bender in "Advances in Chemistry", Series 37, publ. Am. Chem. Soc., 1963, Ch. 2.

60. S.H. Laurie and C.B. Monk, J. Chem. Soc., 724 (1965).

61. F.J. Garrick, Trans. Far. Soc., 33, 1882 (1911): 34, 1088 (1938).

62. T.P. Jones, W.E. Harris and W.J. Wallace, Can. J. Chem., 39, 2371 (1961).

63. F. Monacelli, Ricerca Scientifica, 37, 777 (1967).

64. T.W. Swaddle and E.L. King, Inorg. Chem., 4, 532 (1965).

65. F.A. Guthrie and E.L. King, Inorg. Chem., 3, 916 (1964).

66. C. Postmus and E.L. King, J. Phys. Chem., 59, 1216 (1955).

67. M.A. Levine et al., J.A.C.S., 83, 2453 (1961).

68. J.B. Walter and C.B. Monk, J. Chem. Soc. (A), 1372 (1966).

69. R.G. Yalman, Inorg. Chem., 1, 16 (1962).

70. A.W. Adamson and F. Basolo, Acta Chem. Scand., 9, 1261 (1955).

71. S.C. Chan, J. Chem. Soc., 2375 (1964).

72. G.C. Lalor and E.A. Moelwyn-Hughes, J. Chem. Soc., 1560 (1963).

73. N. Bjerrum, Z. anorg. allgem. Chem., 119, 179 (1921).

74. C. Postmus and E.L. King, J. Phys. Chem., 59, (1955).
(a) p.1216.
(b) p.1208.

# REFERENCES (contd.)

75. J.P. Hunt and H. Taube, J. Chem. Phys., 19, 602 (1951).

76. A.B. Lamb and G.R. Fonda, J.A.C.S., 43, 1155 (1921).

77. A.L. Phipps and R.A. Plane, J.A.C.S., 79, 2458 (1957).

78. I. Lindqvist and B. Strandberg, Acta Cryst., 10, 173 (1957).

79. S. Ahrland, J. Chatt and N.R. Davies, Quart. Rev., 12, 265 (1958).

80. R.J.P. Williams and J.D. Hale, in "Structure and Bonding", Vol. I, ed. Jörgenson et al., Springer-Verlag, 1966.

81. Y. Saito, Y. Takeuchi and R. Pepinsky, Z. Krist., 106, 476 (1955).

82. Y. Takeuchi and R. Pepinsky, Z. Krist., 109, 29 (1957): 110, 474 (1958).

83. Y. Takeuchi and Y. Saito, Bull. Chem. Soc. Jap., 30, 319 (1957).

84. W.C. Waggener, J.A. Mattern and G.H. Cartledge, Abstracts of papers, 122nd. Nat. meeting, Am. Chem. Soc., Sept. 1952, p.19-P.

85. T.E. Sloan and A. Wojcicki, Inorg. Chem., 7, 1268 (1968).

86. J.A. Laswick and R.A. Plane, J.A.C.S., 81, 3564 (1959).

87. E.L. King and J.A. Neptune, J.A.C.S., 77, 3186 (1955).

88. P.J. Elving and B. Zemel, J.A.C.S., 79, 1281 (1957).

89. E.L. King and E.B. Dismukes, J.A.C.S., 74, 1674 (1952).

# REFERENCES (contd.)

90. R.P. Buck, S. Singhadeja and L.B. Rogers, Anal. Chem., 26, 1240 (1954).

91. H.S. Frank and R.L. Oswalt, J.A.C.S., 69, 1320 (1947).

92. F.C. Anson and D.A. Payne, J. Electroanal. Chem., 13, 35 (1967).

93. G.E. Markle and D.F. Boltz, Anal. Chem., 26, 447 (1954).

94. R.G. Pearson, J.A.C.S., 85, 3533 (1963).

95. St. Ahrland in "Structure and Bonding", Vol. I. (See ref. 80).

96. P.C.H. Mitchell and R.J.P. Williams, J. Chem. Soc., 1912 (1960).

97. I.R. Jonasson and D.R. Stranks, Electrochim. Acta, 13, 1147 (1968).

98. J.H. Espenson and E.L. King, J. Phys. Chem., 64, 380 (1960).

99. H.S. Gates and E.L. King, J.A.C.S., 80, 5011 (1958).

100. R.G. Yalman, J.A.C.S., 75, 1842 (1953).

101. A.B. Lamb and J.W. Marden, J.A.C.S., 33, 1873 (1911).

102. F.J. Garrick, Trans. Far. Soc., 33, 487 (1937).

103. B. Adell, Z. anorg. all. Chem., 246, 303 (1941).

104. A. Haim and H. Taube, Inorg. Chem., 2, 1199 (1963).

105. S.C. Chan et al., J. Chem. Soc., 3207 (1965).

106. F. Basolo and R.G. Pearson, J.A.C.S., 78, 4878 (1956).

107. G.W. Bushnell and G.C. Lalor, J. Inorg. Nucl. Chem., 30, 219 (1968).

## REFERENCES(contd.)

108. H.R. Hunt and H. Taube, J.A.C.S., 80, 2642 (1958).

109. F. Basolo and R.G. Pearson, "Mechanisms of Inorganic Reactions", 2nd. ed., Wiley and Sons, 1967, Ch. 3.

110. C.H. Langford, Inorg. Chem., 4, 265 (1965).

111. D.A. Buckingham, I.I. Olsen and A.M. Sargeson, Aus. J. Chem., 20, 597 (1967).

112. "Inorganic Syntheses", McGraw-Hill, New York

    (a) H. Diehl, H. Clark and H.H. Willard, Vol. I (1939), p.186.

    (b) H.H. Willard and D. Hall, Vol. IX (1966), p.190.

    (c) F. Basolo and R.K. Murmann, Vol. IV (1953), p.171.

113. M. Green and H. Taube, Inorg. Chem., 2, 948 (1963).

114. A.C. Rutenberg and H. Taube, J. Chem. Phys., 20, 825 (1952).

115. A. Seidell, "Solubilities of Inorganic and Metal Organic Compounds", van Nostrand, 1940.

116. F.J. Welcher, "The Analytical Uses of Ethylenediamine-tetraacetic Acid", van Nostrand, 1957, p.230.

117. M. Linhard and M. Weigel, Z. anorg. allgem. Chem., 266, 53 (1951).

118. A.W. Adamson and A.H. Sporer, J.A.C.S., 80, 3865 (1958).

# REFERENCES (contd.)

119. C.H. Langford and W.R. Muir, J. Phys. Chem., 71, 2602 (1967).

120. H. Taube, J.A.C.S., 82, 525 (1960).

121. A.R. Olson and T.R. Simonson, J. Chem. Phys., 17, 1167 (1949).

122. R.C. Splinter, S.J. Harris and R.S. Tobias, Inorg. Chem., 7, 897 (1968).

123. C. Bifano and R.G. Linck, Inorg. Chem., 7, 908, 1968.

124. J.P. Candlin, J. Halpern and D.L. Trimm, J.A.C.S., 86, 1019 (1964).

125. R.G. Yalman, Inorg. Chem., 1, 16 (1962).

126. H. Taube, Adv. Inorg. Chem. Radiochem., 1, 1 (1959).

127. R.G. Parsons in "Advances in Electrochemistry and ~~Electrical~~ Electrochemical Engineering", Vol. I, 1961.

128. E.H.M. Wright, J. Chem. Soc. (B), 361 (1966).

129. T. Cummings et al., J. Chem. Soc., 535 (1959).

130. J.J. Kipling and E.H.M. Wright, J. Chem. Soc., 3535 (1964).

131. V.G. Levich, "Physiochemical Hydrodynamics", Prentice-Hall, 1962.

132. A.C. Riddiford, "The rotating disc system", in "Advances in Electrochemistry and ~~Electrical~~ Electrochemical Engineering", Vol. 4, 1967.

133. R.R. Johnston, Ph.D. thesis, University of London, 1965.

## REFERENCES (contd.)

134. K. Aurivillus, Acta Chem. Scand., 4, 1413 (1950).

135. J.A. Hedvall and S. Nord, Arkiv. Kemi. Mineral. Geol., 17A, No. 11 (1943): also Chemical Abstracts, 39, 2694 (1945).

136. F.J. Johnston, J. Int. Appl. Rad. Isotopes, 18, 435 (1967).

137. C.H. Giles et al., J. Chem. Soc., 3973 (1960).

138. A.I. Vogel, "Elementary Practical Organic Chemistry", Longmans, 1957.

139. A.W. Adamson, Disc. Far. Soc., 29, 163 (1960).

140. O.D. E.-S. El Khouly, unpublished observations.

141. S.E.S. El Wakkad and S.H. Emara, J. Chem. Soc., 461 (1952).

142. J. Giner, Z. Elektrochem., 59, 681 (1955).

143. T. Biegler, J. Electrochem. Soc., 114, 1261 (1967).

144. H.A. Laitinen and C.G. Enke, J. Electrochem. Soc., 107, 773 (1960).

145. S. Gilman, in "Electroanalytical Chemistry", Vol. II, ed. A.J. Board, Edward Arnold (1967).

146. S.D. James, J. Electrochem. Soc., 114, 1113 (1967).

147. B.B. Baker and W.M. MacNevin, J.A.C.S., 75, 1476 (1953).

148. M. Pourbaix, "Atlas d'Equilibres Electrochimiques", Paris, Gauthier-Villars (1963).

149. J.P. Hoare, J. Electrochem. Soc., 109, 858 (1962).

## REFERENCES (contd.)

150. A.K.N. Reddy et al., J. Electroanal. Chem., 8, 406 (1964).

151. J. O'M. Bockris et al., Electrochim. Acta, 11, 376 (1966).

152. S. Schuldiner and T.B. Warner, J. Electrochem. Soc., 112, 212 (1965), Electrochim. Acta, 11, 307 (1966).

153. A.D. Obrucheva, Doklady Akad. Nauk SSSR, 141, 1413 (1961).

154. A.N. Frumkin and A. Slygin, Acta Physiocochim, U.S.S.R., 3, 791 (1935): 4, 911 (1936): 5, 819 (1936).

155. A.F. Wells, "Structural Inorganic Chemistry", Clarendon Press, 1962.

156. D.J.G. Ives and G.J. Janz, "Reference Electrodes", Academic Press, 1961.

157. E.R. Smith and J.K. Taylor, J. Res. Natl. Bureau Stds., 20, 837 (1938).